universiteit hasselt
KNOWLEDGE IN ACTION

2015 | Faculty of Sciences

DOCTORAL DISSERTATION

Modified lignin biosynthesis in field-grown *Populus tremula x alba*: Host genotype effects on the plant-associated bacterial microbiome

Doctoral dissertation submitted to obtain the degree of
Doctor of Science: Biology, to be defended by

Bram Beckers

Promoter: Prof. Dr Jaco Vangronsveld | UHasselt
Co-promoters: Prof. Dr Wout Boerjan | UGent
Dr Nele Weyens | UHasselt

D/2015/2451/28

universiteit hasselt | CMK CENTRUM VOOR MILIEUKUNDE

PhD thesis presented on the 21st of May 2015 at Hasselt University

Members of the jury

Prof. Dr K. Coninx, Hasselt University, Diepenbeek, BELGIUM, Chair
Prof. Dr J. Vangronsveld, Hasselt University, Diepenbeek, BELGIUM, Promoter
Prof. Dr W. Boerjan, Ghent University, Gent, BELGIUM, Co-promoter
Dr N. Weyens, Hasselt University, Diepenbeek, BELGIUM, Co-promoter
Prof. Dr J. Van Hamme, Thompson Rivers University, Kamloops, CANADA
Prof. Dr D. Dowling, Institute of Technology, Carlow, IRELAND
Prof. Dr J. Colpaert, Hasselt University, Diepenbeek, BELGIUM
Prof. Dr F. Rineau, Hasselt University, Diepenbeek, BELGIUM

Voorwoord

First and foremost, I would like to express my sincere gratitude to all members of the jury for the critical evaluation of my PhD thesis: Prof. Dr Jonathan Van Hamme, Prof. Dr David Dowling, Prof. Dr Jan Colpaert, Junior ;-) Prof. Dr Francois Rineau, Prof. Dr. Wout Boerjan, Dr Nele Weyens and Prof. Dr Jaco Vangronsveld.

Voilà, na deze officiële berichtgeving hierboven volgt aansluitend een korte dienstmededeling inzake de opbouw van dit voorwoord. Allereerst zou ik graag willen benadrukken dat dit voorwoord steeds integraal dient gelezen te worden aangezien sommige passages uit context mogelijk als controversieel ervaren kunnen worden. In navolging van mijn illustere ex-collega's en ex-bureaugenoten (Dhr. Kerim Schellingen en Dhr. Michiel Op De Beeck), die ik tot op heden (alsook in de toekomst) weiger aan te spreken met de titel dr. ;-), ga ik dit voorwoord zo droog en anekdote-loos mogelijk proberen te houden. Dit ook om een scherp contrast te onderhouden met onze vrouwelijke CMK-collega's waarvan de voorwoorden vaak de gedaante aannemen van een dagboek. Voor alle duidelijkheid, dit is een persoonlijke visie over het concept voorwoorden en moet op geen enkele manier geïnterpreteerd worden als kritiek op voorwoorden die een andere vorm aannemen. Zo, dat lucht op! Dit gezegd zijnde ben ik wel van mijn initiële idee afgestapt om het voorwoord in de vorm van een tabel aan te reiken, met bijhorende significantieniveaus voor personen met belangrijke bijdrages. Dit, toch wel, briljante idee vond echter geen gehoor bij sommige collega's en werd dus ook niet ten uitvoer gebracht.

Ondanks bovenstaande principiële overpeinzingen zijn er uiteraard verschillende personen die mij hebben gesteund en waarzonder mijn doctoraat nooit tot stand zou zijn gekomen. Ten eerste zou ik graag mijn promotor prof. dr. Jaco Vangronsveld willen bedanken om mij de mogelijkheid te geven onderzoek te verrichtingen aan de Universiteit Hasselt. In het bijzonder zou ik u willen bedanken voor uw intellectuele ondersteuning en het onvoorwaardelijke vertrouwen dat u in mij had en hopelijk nog steeds hebt. Bedankt voor alles! Daarnaast zou ik ook mijn co-promotor prof. dr. Wout Boerjan willen bedanken

voor de aangename samenwerking en de mogelijkheid om uitgebreide staalnames te verrichten op het proefveld van uw onderzoeksgroep. Met wat geluk vloeit er uit deze samenwerking een aantal mooie publicaties. Voorts bedank ik mijn tweede co-promotor, dr. Nele Weyens, om mij te introduceren in het plant-bacterie onderzoek als toenmalige master student. Ik denk dat het feit dat ik ben (mogen) blijven plakken na mijn masterthesis boekdelen spreekt over de manier waarop jij ons (drie masterstudenten tegelijkertijd ☺) begeleidt hebt. Bedankt voor jouw steun! Finally, I would like to direct a small word to the Junior Prof. in my PhD jury, I will write it in capitals: PROF Dr Francois Rineau. You really deserve it! I wish you all the best and hope that your research will flourish!

In wat volgt zal ik, als ultieme geste voor dr. Keunen, tevens ook een melige, zeemzoeterige alinea wijden aan al mijn huidige en ex-bureaugenoten. Den ezel op kop, of hoe zeggen ze dat ook alweer? Dus zal ik maar beginnen met Kerim dan. Heer Schellingen, dank voor alle vele leuke momenten. Samen konden we de sfeer op de bureau toch steeds luchtig houden ondanks dat deze gevuld was met enkele lichtjes mentaal gestoorde personen (de enige die zich hier niet moet aangesproken voelen is Stefanie ;-)). We hebben samen onze hele ‘carrière’ doorlopen aan de UHasselt en ik kon mij geen betere ‘wingman’ inbeelden. Veel succes gewenst met jouw nieuwe job, de bouw van jullie huis en de toekomstige gezinsuitbreiding ;-)! Voor de vrouwen die dit lezen en al meteen conclusies trekken, NEE, Julie is nog niet zwanger. Er staat duidelijk toekomstige gezinsuitbreiding. Els, ik denk dat ik wel mag zeggen dat wij de afgelopen jaren ook meer zijn geworden dan alleen maar gewoon collega’s. Van filosofische levensbeschouwingen tot het uiten van onze frustraties, wij vonden elkaar altijd in de latere uurtjes van de werkdag. Bedankt ook voor al jouw hulp de afgelopen maanden met de administratieve rompslomp die gepaard gaat met het afwerken van een doctoraat. Zonder jou was ik allang wild geworden van al die, niet nader genoemde, personen verantwoordelijk voor bijvoorbeeld de uitnodigingen ;-). Ik duim voor de goedkeuring van je FWO post-doc want als iemand het verdient dan ben jij het wel! Als laatste wil ik jou nog inprenten (voor de momenten dat ik er niet meer ga zijn) dat er geen enkele reden is om te twijfelen aan jouw capaciteiten! Ik hoop dat jouw grootste (werk-

gerelateerde) droom ooit in vervulling gaat ☺. Sarah, al een tijdje weg van de bureau maar ik ben jou nog altijd niet vergeten. Jij bent de liefste, meest onzelfzuchtige persoon die ik ken. Van konijntjes redden tot het helpen van iedereen in het labo waar je maar kon. Van jouw eerlijkheid en spontaniteit, een eigenschap waar ik zelf vaak tekortschiet, kunnen veel mensen nog iets leren, zeker diegene die daar steevast commentaar op hebben. Binnenkort ook nog mama, ik denk dat als de uitdrukking 'met je gat in de boter vallen' ergens van toepassing is, het wel voor jouw kindje is. Ik twijfel er niet aan dat jij een schitterende mama gaat worden. Veel plezier en liefde gewenst met het toekomstige baby'tje! Michiel, ik denk dat er niemand zich meer wetenschapper mag noemen dan jij. Jouw vermogen om zelf kennis te verwerven en toe te passen is onovertrefbaar. Bedankt voor al jouw hulp en de nuttige discussies over onze data alsook voor de discussies die in de verste verte niets te maken hadden met wetenschap ;-). Daarnaast heb je, ondanks jouw ruwe uiterlijk en uitstraling (wacht er komt iets positiefs eh ;-)), een enorm groot hart en betere sociale capaciteiten dan menig andere collega's, ook al wordt dat soms niet erkend. Wat ik vooral mis is jouw humor en dan voornamelijk de grofheid ervan. Sinds jouw vertrek ben ik namelijk steeds diegene die wordt bestempeld als zijnde de grofste, terwijl wij allebei weten dat jij dat bent ☺. Ik zoek meestal de grens op, terwijl jij de grens niet meer ziet liggen ☺. Gelukkig kan Stefanie soms jouw schoenen toch vullen qua grofheid. Bijkomend is de verpakking bij haar van een hogere kwaliteit, dus mij hoor je niet klagen ;-). Voor de meer feministisch ingestelde collega's die aanstoot nemen aan voorgaande opmerking, Stefanie kan hier mee lachen! Stefanie, jouw no-sense manier van communiceren is zo verfrissend dat ik het bijna mannelijk zou noemen ;-). Ik vind het ook bijzonder jammer voor jou dat je ondertussen weesje bent geworden. Eigenlijk niet alleen voor jou maar voor het hele labo...En ik denk dat deze mening gedeeld wordt door het overgrote deel van de doctoraatsstudenten, zo niet allemaal. Desalniettemin ben ik er van overtuigd dat je deze tegenslag te boven komt en een prachtig doctoraat zult afleveren! An B, ondanks dat je ons op de bureau verlaten hebt voor een, laat ons eerlijk zijn, minderwaardige bureau ;-) ben ik nog steeds fan van jouw enthousiasme! Whoop whoop! Alejandro, it was a pleasure to get to know you during the last couple of months of my PhD. Especially because you are a rarity, a Spanish guy

with flawless English, imagine that ☺! Even your Dutch skills are spectacular and improve day by day. Just try to keep your Spanish temperament in check when some results do not turn out the way you expect ;-). And thanks a lot for you help with photoshop! Jolien, mijn bureaugenoot van het eerste uur, jouw werkijver en aandacht voor kwaliteitsvol onderzoek zijn een voorbeeld voor alle doctoraatsstudenten. Ook wij konden bij elkaar terecht, vaak voor frustraties of ook wel gewoon onnozele dingen. Ik zal jouw nuchterheid en humor nooit vergeten. Thieme zal kunnen opgroeien met een lieve en ook heel toffe mama. Ook nog bedankt voor het kopen van een brooddoos voor mij ☺! Ik gebruik ze nog steeds! Het milieu dankt u. Hup se huidige en ex-bureaugenoten, check!

Daarnaast zou ik alle leden van de bacterie-groep willen bedanken voor de leuke samenwerking: Jolien, Sarah, Joke, Inge, Sascha, Wouter, Sofie, Marijke G., Jordan, Iva, Nele E., Panos. Alsook alle andere leden van het CMK voor het creëren van een aangename werksfeer.

Het laatste greintje meligheid heb ik bewaard voor iemand bijzonder. Andromeda, bedankt om gewoon jou te zijn, om mij te leren praten over dingen waar ik liever niet over praatte, om te luisteren naar mij en mij ongelijk te geven wanneer dit nodig was, ook al was dit niet vaak nodig ☺. Bedankt voor alle onzin en zever doorheen de jaren, ik had nooit gedacht dat er iemand bestond die meer onzin kan vertellen dan ik. Er zijn slechts enkele onderwerpen waarover er tussen ons weleens discussies ontstonden. Zoals over de kwaliteit van sommige films (lees Indiana Jones) en de capaciteiten van bepaalde muziekgroepen (lees The Beatles). Beide zijn niet aan mij besteed maar ik zal mij, voor één keer weliswaar, bedwingen om deze mening verder te beargumenteren. Bedankt ook om mij te tonen waar ik alle sterren aan de hemel kan terugvinden en bijkomend om dit met voldoende geduld te doen bij iemand met beperkte visuele vermogens. Als laatste zou ik eigenlijk nog twee cruciale dingen willen vragen. Als eerste, zou het mogelijk zijn om toekomstige betogen (of beter gezegd monologen) over UFO's en mogelijk ander buitenaards leven te beperken tot een lezing van pakweg 30 minuten. Ik (en ook nog wat andere mensen) danken u bij voorbaat. Voorts zal ik verder geen uitspraken doen over het al dan niet waarachtige karakter van deze verhalen ;-). Vraag 2:

wil je samen met An-Sofie misschien ooit nog eens een liedje zingen voor mij ☺? Ah, dat was ik bijna vergeten. Herinner je je nog die keer dat je bij de minivoetbal door mijn benen gespeeld hebt? Ik wil dit toch graag nogmaals, en deze keer zwart-op-wit, herhalen: dat kon enkel gebeuren met mijn toestemming ;-). Neem jij hier akte van?

Bij deze ook nog een lijstje van personen die expliciet geëist hebben om bij naam genoemd te worden in mijn voorwoord: Nicky Pieters, einde van het lijstje. Dat was maar een mopje eh Nicky ☺. Hier nog wat mooie woordjes voor jou. Als er iets is wat mij zal bijblijven is het zeker jouw gezaag…Ah nee, wacht iets positiefs…Je kent me ondertussen ook al lang genoeg, ik ben enkel grof tegen de mensen die ik echt graag heb. Dus bij deze, wees geflatteerd met voorgaande zin ;-). Over uw prachtige voiture en uw rijvaardigheid zal ik voortaan zwijgen, en dan bedoel ik inclusief de anekdote gerelateerd aan de Fitlink ;-). Ook voor jou wel een vraag: wanneer was uw house warming nu weer ☺? Ik heb nog een fles cava die ik als cadeau kan geven ;-). Tot slot nog het zelfverklaarde ‘binge drinking team’ van de vrijdagavonden met variabele samenstelling: Andromeda, Nicky P, An-Sofie, andere Nicky P, An B, Bram^2 (ook wel aanspreekbaar als BJ), Dries, Hanne en Kerim. De week afsluiten met jullie was altijd zeer aangenaam!

Als allerlaatste zou ik mij willen richten tot een bijzondere vrouw. Zij stond en staat altijd klaar voor mij en mijn zus. Zonder haar zou niets, maar dan ook echt niets, van dit alles mogelijk geweest zijn. Zij is de enige persoon die mij begrijpt zonder woorden. Mama, bedankt voor alle mogelijkheden die je ons gegeven hebt en voor jouw onvoorwaardelijke liefde en steun!

Oké, bij nader inzien heb ik mij deze keer precies niet strikt aan mijn principes gehouden inzake het concept voorwoorden. Ik kan hieruit enkel concluderen dat jullie allemaal, oké ja niet overdrijven, de meeste onder jullie heel veel voor mij betekent hebben en nog betekenen. Ik verklaar dan ook de dienstmededeling aan het begin van dit doctoraat nietig.

Bram Beckers-Mei 2015

Summary

Since their discovery and the onset of the industrial revolution, fossil fuels have powered global economical development and have been the world's primary energy source. However, the continuous depletion of the fossil energy reserves for manufacturing and transport and the accompanying side-effects (environmental ramifications and energy security) has ultimately led to an ever-increasing requirement of alternative and sustainable energy sources for our industrial economies and consumer societies. In the impending transition to a more bio-based economy, especially the need for biomass in the production of renewable energy and industrial feedstock applications is incessant and optimizing plant growth is required to ensure feed supply.

Second-generation biofuels, produced from lignocellulosic non-food feedstocks, avoid competition with food crops but their commercial viability is severely limited by the recalcitrance of lignin polymers present in the plant cell walls. Therefore genetically modified (GM) energy crops, engineered to produce less lignin or more easily degradable lignin, have been utilized to partially overcome the recalcitrance of lignocellulosic biomass and to improve the commercial viability and cost-competitiveness of second-generation biofuels. In order to reduce/modify lignin polymers to generate feedstocks with diminished recalcitrance, genes have been cloned for each of the steps of the lignin biosynthetic pathway. Gene silencing of cinnamoyl-CoA reductase (*CCR*; EC 1.2.1.44), which catalyses the conversion of feruloyl-CoA to coniferaldehyde and is considered as the first enzyme in the monolignol-specific branch of lignin biosynthesis, represents an interesting target to reduce lignin levels.

However, simultaneously gene silencing of *CCR* and by extension most of the genes silenced in the lignin biosynthesis, leads to flux changes in the phenylpropanoid and monolignol-specific pathways, most notably the accumulation of soluble phenolics (e.g. ferulic acid) and detoxicification products. In this way, the plant-associated microbiome is confronted with profound changes in the accessible carbon sources in the xylem vessels. The plant microbiome can be considered as an extension of the host genome or even as the plant's second genome. Therefore, even small changes in the host genome (ecotypes, cultivars, genetically modified genotypes, etc.) may

influence the plant microbiome, and these changes may even feed back to modulate the behaviour of the host. Furthermore, cell walls play major roles in the endophytic colonization of beneficial bacteria as well as in the resistance against pathogens. Since perturbations in the lignin biosynthesis via *CCR* downregulation lead to compositional alterations in the cell wall changes in the endophytic colonization may occur.

Therefore, the main objective of the current work was to explore the general and specific host genotype effects exerted by *CCR* gene silencing in field-grown poplar trees (*Populus tremula x alba*) on the plant bacterial microbiome (Chapter 3 and Chapter 5). Furthermore we also focussed on the microbiome niche differentiation between the different plant environments (rhizosphere, root, stem, leaf) and evaluated the potential of plant-growth promoting (PGP) bacteria to offset the negative repercussions on the biomass yield of lignin-reduced genotypes (Chapter 6).

Firstly, to reliably access the total plant bacterial microbiome and unravel plant compartment and/or host genotype effects, we optimized an approach to reduce organellar rRNA (of plastid and mitochondrial origin) co-amplification, frequently observed during 16S rRNA metabarcoding. For this purpose, we experimentally evaluated the potential of a set of 16S rRNA primers. Based on (a) low co-amplification of non-target rRNA reads, (b) high retrieval of bacterial rRNA reads and (c) low primer efficiency for pure poplar chloroplast DNA, we ultimately selected 1 primer pair to unravel the plant microbiome via 16S rRNA metabarcoding (Chapter 4).

To unravel host genotype effects associated with *CCR* downregulation and the specificity of bacterial assemblages for specific plant compartments (rhizosphere soil, root, stem, leaf) in *Populus tremula x alba* (microbiome niche differentiation) we used two different approaches: (1) evaluation of the culturable fraction of the plant microbiome via non-selective and selective isolation/enrichments techniques (i.e. introducing a metabolic selection factor) (chapter 3) and (2) evaluation of the total plant microbiome via 16S rRNA metabarcoding (454 pyrosequencing) using our optimized approach as described

in chapter 4 (Chapter 5). In general, the host genotype was found to have a profound effect on the metabolic capacities and bacterial community structure in the endosphere of *CCR* deficient poplar trees (especially the roots and stems), without perceptible effects on the rhizospheric bacterial communities. Furthermore, within the bacterial community structures, we observed strong clustering according to plant compartment whereby each compartment rendered microbiota significantly dissimilar from each other, irrespective of host genotype. In this way, our data confirm microbiome niche differentiation reports at the rhizosphere-root interface but furthermore suggest additional fine-tuning and niche differentiation of microbiota in the aerial plant organs.

Finally, we focussed on *Arabidopsis thaliana*, the model plant in lignin biosynthesis research and the biomass impairment associated with *CCR* downregulation. We evaluated the potential of several plant-growth promoting stress-reducing bacterial strains (chapter 3) to offset the biomass yield penalty associated with perturbations in the lignin biosynthesis. To test this concept we selected two T-DNA knockout mutants for *CCR*1 and inoculated the genotypes with promising bacterial strains selected based on detailed phenotypic *in vitro* screening of their metabolic range to degrade aromatic lignin-related compounds and plant growth promotion capacities. Most notably, *Norcardioides aromaticivorans* and *Microbacterium phyllosphaerae* improved leaf surface area, primary root length and lateral root development of the lignin-reduced biomass-impaired *Arabidopsis* genotypes (Chapter 6).

In conclusion, we provide evidence for the differentiation of the plant microbiome between different plant environments (chapter 3 and chapter 5), identify significant host genotype-effects instigated by the *CCR* downregulation (chapter 3 and chapter 5), optimize an efficient approach to access the plant bacterial microbiome without the co-amplification of organellar rRNA in 16S rRNA metabarcoding applications (Chapter 4) and finally prove the concept that inoculation with plant-growth promoting stress-reducing bacteria can improve the growth of lignin-reduced biomass-impaired genotypes (Chapter 6).

Samenvatting

Sinds hun ontdekking en het begin van de industriële revolutie, hebben fossiele brandstoffen wereldwijd de economische ontwikkeling aangedreven en zijn ze de primaire energiebron geworden. Echter, de voortdurende delving van de fossiele energie reserves voor de industriële productie en transport alsook de bijbehorende neveneffecten (negatieve impact op het milieu en energiezekerheid) hebben uiteindelijk geleid tot een steeds toenemende behoefte aan alternatieve en duurzame energiebronnen voor onze industriële economieën en consumptiemaatschappij. In de onafwendbare overgang naar een meer bio-gebaseerde economie is met name de nood aan biomassa in de productie van hernieuwbare energie onophoudelijk waarin de optimalisatie van de groei van gewassen een belangrijke rol speelt.

Tweede generatie biobrandstoffen, geproduceerd uit lignocellulose energiegewassen, vermijden de concurrentie met voedselgewassen maar hun commerciële levensvatbaarheid wordt ernstig beperkt door de recalcitrantie van lignine polymeren aanwezig in de celwand van de planten. Daarom bieden genetisch gemodificeerde energiegewassen, met verminderde concentraties (en/of veranderde samenstelling) van lignine, een goed alternatief om de recalcitrantie van lignocellulose biomassa te verlagen en zodoende de commerciële haalbaarheid van tweede generatie biobrandstoffen te garanderen. Om verstoringen in de lignine biosynthese teweeg te brengen en bijgevolg de concentratie aan lignine polymeren te verlagen zijn alle genen betrokken in de lignine biosynthese geïdentificeerd en gekloneerd. Voornamelijk de neerregulatie van cinnamoyl-CoA reductase (*CCR*; EC 1.2.1.44), het enzym dat de conversie katalyseert van feruloyl CoA naar coniferaldehyde en wordt beschouwd als het eerste enzym in de monolignol-specifiek tak van de lignine biosynthese, vertegenwoordigt een interessant doelwit om de concentratie aan lignine te verlagen.

Gelijktijdig zorgt de neerregulatie van *CCR* en bij uitbreiding de neerregulatie van de meeste genen in de lignine biosynthese echter ook tot ‘flux’ veranderingen in de fenylpropanoid en monolignol-specifieke biosynthese, met name de accumulatie van oplosbare fenolen (bv. ferulinezuur) en detoxificatie producten. Hierdoor wordt het plant-geassocieerde microbioom geconfronteerd

met diepgaande veranderingen in de toegankelijke koolstofbronnen in het xyleem. Het microbioom van de plant kan beschouwd worden als een uitbreiding van het gastheergenoom of zelfs als het tweede genoom van de plant. Daardoor kunnen kleine veranderingen in het gastheergenoom (ecotypes, cultivars, genetisch gemodificeerde genotypes, etc.) het microbioom beïnvloeden en deze veranderingen kunnen zelfs wederkerig het gedrag van de gastheer moduleren. Bovendien speelt de celwand van de plant een belangrijke rol in de endofytische kolonisatie van bacteriën alsook in de resistentie tegen pathogenen. Aangezien verstoringen in de lignine biosynthese via neerregulatie van *CCR* leiden tot veranderingen in de samenstelling van de celwand kunnen wijzigingen in de endofytische kolonisatie optreden.

De belangrijkste doelstelling van deze doctoraatsthesis betreft daarom het ontrafelen van de invloed van het plant genotype, meer bepaald het neerreguleren van *CCR* in populieren (*Populus tremula x alba*), op het bacterieel microbioom geassocieerd met de populieren (Hoofdstuk 3 en Hoofdstuk 5). Voorts ligt de focus van de thesis op de differentiatie van het bacterieel microbioom tussen de verschillende ecologische niches (rhizosfeer, wortel, stengel, blad) aanwezig in de plant. Als laatste wordt ook het potentieel van verschillende plantengroei-promoverende bacteriën (PGB) getest om de negatieve effecten van de genetische modificatie op de biomassa-opbrengst te compenseren (Hoofdstuk 6).

Allereerst, om een betrouwbare inschatting te kunnen maken van het bacteriële microbioom geassocieerd met populier en bijgevolg de effecten van het plant genotype en de plant niche te ontrafelen werd een aanpak geoptimaliseerd om de co-amplificatie van organellair rRNA (afkomstig van chloroplasten en mitochondriën) te verminderen tijdens 16S rDNA metabarcoding (Hoofdstuk 4). Hiervoor hebben we het potentieel geëvalueerd van een reeks veelgebruikte 16S rRNA primers. Uit deze selectie werd uiteindelijk 1 primer paar gekozen gebaseerd op (a) lage co-amplificatie van organellair rRNA, (b) efficiënte amplificatie van bacterieel 16S rRNA en (c) lage primer efficiëntie voor chloroplast DNA afkomstig van populier.

Vervolgens, om effecten van het plant genotype (*CCR* deficient) en de specificiteit van het bacteriële microbioom voor bepaalde ecologische niches te ontrafelen, werden er twee methoden gebruikt: (1) de evaluatie van de cultiveerbare fractie van het bacteriële microbioom via niet-selectieve en selectieve isolatie/aanrijking technieken (via de introductie van een metabole selectie factor) (Hoofdstuk 3) en (2) de evaluatie van het totale bacteriële microbioom via 16S rRNA metabarcoding met behulp van een geoptimaliseerde aanpak beschreven in hoofdstuk 4 (Hoofdstuk 5). In het algemeen was het plant genotype zeer bepalend voor de metabole capaciteiten en de populatie-samenstelling van het microbioom in de endosfeer van de *CCR* deficiente populieren (voornamelijk in de wortels en de stengels). Voorts werden er geen significante verschillende waargenomen in de rhizosfeer. Daarnaast toonden onze resultaten aan dat de bacteriële populaties sterk differentiëren tussen de verschillende ecologische niches, onafhankelijk van het plant genotype. Op deze manier bevestigen onze data de studies die microbioom differentiatie beschrijven tussen de rhizosfeer en wortel omgeving en suggereren ze bovendien bijkomende niche differentiatie in de bovengrondse niches van de plant (stengel en blad).

Tot slot hebben we ons gericht op *Arabidopsis thaliana*, de model plant in lignine-biosynthese onderzoek en de verminderde biomassa opbrengst geassocieerd met het neerreguleren van *CCR*. Hiervoor hebben we het potentieel geëvalueerd van verschillende plantengroei-promoverende en stress-reducerende bacteriën (Hoofdstuk 3) om de biomassa te verhogen van lignine-gereduceerde genotypes. Om dit concept te testen werd gebruik gemaakt van twee verschillende T-DNA knock-out *CCR*1 *Arabidopsis thaliana* mutanten die geïnoculeerd werden met veelbelovende bacteriestammen geselecteerd op basis van gedetailleerde fenotypische *in vitro* screening. Voornamelijk de planten geïnoculeerd met *Norcardioides aromaticivorans* en *Microbacterium phyllosphaerae* vertoonden een verbeterde groei, gekenmerkt door een verhoogde bladoppervlakte, langere primaire wortels en een meer uitgebreide ontwikkeling van de laterale wortels (Hoofdstuk 6).

Samengevat geven we (a) bewijs voor de differentiatie van het bacterieel plant microbioom tussen verschillende ecologische plant niches (Hoofdstuk 3 en hoofdstuk 5), (b) toonden we aan dat het neerreguleren van *CCR* een significant effect heeft op het bacterieel microbioom in de endosfeer omgeving (Hoofdstuk 3 en hoofdstuk 5), (c) optimaliseerden we een efficiënte aanpak om de co-amplificatie van organellair rRNA te vermijden tijdens 16S rRNA metabarcoding (Hoofdstuk 4) en tenslotte (d) bewijzen we het concept dat inoculatie met specifieke plantengroei-promoverende bacteriestammen de groei van lignine verlaagde (biomassa-gereduceerde) plant genotypes kan verhogen (Hoofdstuk 6).

Index

Voorwoord i

Summary vii

Samenvatting xi

Chapter 1: Introduction 1

1.1. Fossil fuels and the need for renewable energy sources 1

1.2. Biofuels from biomass 2

1.2.1. First-generation biofuels 3

1.2.2. Second-generation biofuels 4

1.3. Poplar as feedstock for second-generation biofuels 7

1.4. Plant cell wall and lignin molecules 8

1.4.1. Lignin: function, general composition and deposition 8

1.4.2. Monolignol biosynthesis 9

1.4.3. Monolignol transport 13

1.4.4. Polymerization: Radical formation and radical coupling 15

1.5. Lignin engineering 17

1.6. Eukaryote-Prokaryote associations 19

1.7. The plant microbiome 20

1.7.1. Bacterial microbiome in the rhizosphere environment 20

1.7.2. Bacterial microbiome in the endosphere environment 22

1.7.3. Bacterial microbiome in the phyllosphere environment 27

1.8. Determining the composition of plant microbiomes 28

1.9. Microbiome niche differentiation between plant enviroments 30

1.10. Modification of the lignin biosynthesis in poplar (gene silencing of *CCR*) versus the plant bacterial microbiome 32

1.10.1. General effects of plant host genotype on their microbiome 32

1.10.2. Specific effects of lignin-reduced host genotype 32

1.10.3. Role of secondary wall in plant resistance to pathogens 34

1.10.4. Biomass production 35

References 36

Chapter 2: Objectives 57
References 61

Chapter 3: Lignin modification of field-grown poplar trees via *CCR* gene silencing affects the metabolic capacities of the bacterial microbiome present in the endosphere 65
Abstract 65
3.1. Introduction 66
3.2. Material and Methods 68
3.2.1. Generation of *CCR* deficient poplar trees 68
3.2.2. Field trial and sampling procedure 68
3.2.3. Processing of rhizosphere soil, roots, stems and leaves samples 69
3.2.4. Bacterial isolation 70
3.2.5. Identification of bacterial strains 71
3.2.6. Univariate analysis of bacterial community structures and bacterial diversity 73
3.2.7. Respirometric metabolism analysis of pure cultures with Biolog MT2 73
3.2.8. Statistical analysis 75
3.3. Results 77
3.3.1. Selective isolation: Bacterial cell counts of WT and *CCR* deficient poplar trees 77
3.3.2. Selective enrichment: Bacterial cell counts 80
3.3.3. Bacterial community structures after selective enrichment 81
3.3.4. Univariate analyses of bacterial community structures and bacterial diversity 91
3.3.5. Respirometric metabolism analyses 93
3.3.6. OTU breakdown of Biolog respirometric responses 94
3.4. Discussion 97
3.5. Conclusion 100
References 101

Chapter 4: Performance of 16S rRNA primers in the study of rhizosphere and endosphere bacterial microbiomes in metabarcoding studies 115
Abstract 115
4.1. Introduction 116
4.2. Material & Methods 119
4.2.1. Study site description & Sampling 119
4.2.2. Processing of samples 119
4.2.3. DNA extraction 120
4.2.4. PCR amplification and 454 pyrosequencing 120
4.2.5. Sequence processing 122
4.2.6. Isolation of intact chloroplasts to extract pure chloroplast DNA 123
4.2.7. Quantitative real-time PCR 123
4.2.8. Statistical analysis 124
4.3. Results 125
4.3.1. 454 pyrosequencing 125
4.3.2. Co-amplification of non-target DNA (plastid and mitochondrial) 125
4.3.3. Primer efficiency for pure chloroplast DNA (poplar) 128
4.3.4. Sequencing depth and coverage of selected primer pairs 129
4.3.5. Parametrical comparison of selected primer pairs 130
4.3.6. Community similarity between primer pairs and description of observed communities 133
4.4. Discussion 136
4.5. Conclusion 141
References 142

Chapter 5: Gene silencing of Cinnamoyl-CoA reductase (*CCR*) in field-grown poplar trees: plant compartment and host genotype effects on the total bacterial microbiome 161
Abstract 161
5.1. Introduction 162
5.2. Material and methods 165
5.2.1. Field trial 165
5.2.2. Sampling 165
5.2.3. Processing of samples 166

5.2.4. DNA extraction....166
5.2.5. PCR amplification and 454 pyrosequencing....167
5.2.6. Sequence processing....168
5.2.7. Statistical analysis....169
5.3. Results....171
5.3.1. General analysis of 454 pyrosequencing data....171
5.3.2. Alpha rarefaction curves and alpha diversity: plant-compartment and host-genotype effects....172
5.3.3. Beta diversity: Plant compartment and host-genotype effects..176
5.3.4. Core bacterial microbiome within each plant compartment and drivers of plant compartment and host-genotype effects....185
5.4. Discussion....188
5.4.1. General analysis of the pyrosequencing data....188
5.4.2. Plant compartment effects and niche differentiation....190
5.4.3. Host-genotype effects....193
5.4.4. Drivers of plant compartment effects and host genotype effects....195
5.5. Conclusion....196
References....198

Chapter 6: Plant growth promotion of lignin-reduced, biomass impaired *Arabidopsis thaliana* genotypes....219
Abstract....219
6.1. Introduction....220
6.2. Material and methods....223
6.2.1. Metabolic range of bacteria....223
6.2.2. Processing Biolog MT2 plates....224
6.2.3. *In vitro* plant growth promotion of bacterial strains....224
6.2.4. *In vivo* growth promotion of selected bacterial strains....226
6.2.5 Statistical analysis....228
6.3. Results....229
6.3.1 Metabolic range and plant growth promotion capacities of selected bacteria....229

6.3.2. Primary root growth and leaf surface areas as evaluated with vertical agar plates (VAPs): genotype-effects....230
6.3.3. Primary root growth (end-point measurement) and leaf surface area as evaluated with vertical agar plates (VAPs): bacterium-effects 232
6.3.4. Kinetic analysis of primary root growth....234
6.3.5. Lateral root development and leaf surface area....237
6.3.6. Co-cultivation assay....242
6.4. Discussion....244
6.5. Conclusion....249
References....250

Chapter 7: General discussion and perspectives....271
7.1. Study framework....271
7.2 Accessing the total bacterial microbiome of plants via 16S rRNA metabarcoding....272
7.3 Plant compartment effects: microbiome niche differentiation....274
7.4 Host genotype effects exerted by the lignin-reduced genotype....277
7.5 Biomass production from lignin-reduced genotypes....280
7.6 Conclusion and perspectives....281
References....284

Scientific output....291
International Journals....292
Abstracts....292

Chapter 1

Introduction

1.1. Fossil fuels and the need for renewable energy sources

Fossil fuel is a general term for combustible geologic deposits of organic materials, formed from prehistoric incompletely decayed plants and animals, which were gradually buried by layers of rocks. In this way, over millions of years, the prehistoric organic materials were converted (anaerobic decomposition) to different types of fossil fuels, including crude oil, coal and natural gas by exposure to extreme heat and pressure in the Earth's crust (Berner, 2003). Since their discovery and the onset of the industrial revolution, fossil fuels have powered global economical development and have been the world's primary energy source (US Energy Information Administration (EIA), http://www.eia.gov/cfapps). However, since the last dozen years, the sustainability of fossil resources has come under severe scrutiny from economic, environmental and geopolitical point of view (Hill et al., 2006; Kerr and Service, 2005; Shafiee and Topal, 2009; Schubert, 2006). First and foremost, fossil fuels represent a non-renewable, finite energy source since they are only formed over geological time periods. Moreover, the mining efficiency of the fossil energy reserves will continuously deteriorate since more investments are required to extract less available reserves (Kerr and Service, 2005; Shafiee and Topal, 2009). From an environmental perspective, the mining and combustion of fossil fuels is a major contributor to increasing the level of CO_2 in the atmosphere, which is directly linked with global warming observed in recent decades. Fossil fuel consumption produces around a net increase of 10.65 billion tons of atmospheric CO_2 per year. CO_2, being one of the greenhouse gases, enhances radiative forcing (difference of the energy absorbed by the Earth and radiated back into space), the major cause of global warming. Moreover, the extensive use of fossil fuels leads to deterioration of air quality and water and land pollution (Solomon et al., 2009). Furthermore global geopolitical instability endangers constant energy supply. The dependency of the European Union (EU) on energy imports, particularly of oil and more recent gas, raises concerns relating to the security of energy supplies. The EU-28's imports of primary energy exceeded exports by some 922.8 million tons of oil equivalent (toe) in

2012. In recent years, Russia has maintained its position as the main supplier of crude oil (33%) and natural gas (39%) whereby much of that oil and gas travels across Ukraine. Given the on-going political instability in the country, it is not surprising that energy security has once more risen to the top of the EU agenda (Eurostat: http://ec.europa.eu/eurostat/statistics).

The continuous depletion of the fossil energy reserves for manufacturing and transport and the accompanying side-effects (environmental issues and energy security) has ultimately led to an ever-increasing requirement of alternative and sustainable energy sources for our industrial economies and consumer societies (Kerr and Service, 2005; Schubert, 2006). In the impending transition to a more bio-based economy, the need for biomass in the production of renewable energy and industrial feedstock applications is incessant and optimizing plant growth is therefore required to ensure feed supply (Yuan et al., 2008). Biomass has been a major source of energy for mankind since ancient times and presently contributes around 10–14% of the world's energy supply (Sannigrahi and Ragauskas, 2010). Biomass has the potential to be converted to different types of energy including heat, electricity, and biofuels.

1.2. Biofuels from biomass

Biofuels, besides solar radiation (Lewis, 2007) and wind energy (Lu et al., 2009), provide a potential route to avoiding the environmental and global political instability issues that arise from reliance on fossil fuels (Kerr and Service, 2005; Schubert, 2006). Biofuels comprise any fuel whose energy is obtained via a process of biological carbon fixation whereby atmospheric inorganic carbon (CO_2) is fixated and converted into organic molecules. Thereby, biofuels can be produced year after year through renewable and sustainable farming practices. Furthermore, they have the potential to reduce CO_2 emission and mitigate global warming since CO_2 released during combustion is, at least partially, offset by the CO_2 fixation during photosynthesis (Fargione et al., 2008; Naik et al., 2010; Solomon, 2010).

Biofuels are often categorized into three generations: first-generation, second-generation and third-generation. The different generations of biofuels are differentiated by the source of the feedstock used for the production of the biofuel. In general, first-generation biofuels are those mainly based on sugar, grains and/or seeds and entail relatively simple processing for fuel production. In

contrast, second-generation biofuels are generally produced from non-edible lignocellulosic biomass, including residues of crops or forestry production and whole plant biomass (e.g. energy crops). Third-generation biofuels comprise biofuels where the carbon is derived from aquatic autotrophic organisms (e.g. algae). In the following parts, we will focus on first and second-generation biofuels.

1.2.1.First-generation biofuels

First-generation biofuels are directly produced from food crops with maize (*Zea mays*) and sugar cane (*Saccharum* spp.) being the most commonly used feedstock. The biofuel is ultimately derived from the starch, sugar, animal fats, and vegetable oil that these crops provide. Currently, the largest producers of biofuel from first-generation biofuels are Brazil (sugar cane ethanol), the United States (maize ethanol), Germany (rapeseed oil biodiesel) and Malaysia (palm oil biodiesel) (Cardona et al., 2010; Hertel et al., 2010). However, the production of first-generation biofuels has not been free of controversy. Several studies and insights examined the economic viability and ecological ramifications of their production and questioned their potential to sustainably displace fossil energy (Cassman and Liska, 2007; Cassman, 2007; Naylor et al., 2007; Searchinger et al., 2008; Tilman et al., 2009.; Yuan et al., 2008). From an economic perspective, excluding government grants and subsidies, they represent an expensive option for energy security taking into account total production costs. Furthermore, the production of first-generation biofuels has been related to abrupt rises in food commodity prices sparking the ‘food-versus-fuel’ debate. For the production of energy biomass from first-generation biofuels, currently large areas of agricultural land are being used thereby endangering food supply (Cassman and Liska, 2007; Naylor et al., 2007; Weyens et al., 2009a). For decades, agricultural production and trade have continuously improved thereby steadily decreasing the price of major food commodity prices (e.g. maize, wheat, rice, sugar). However, the introduction of first-generation biofuels together with the increasing political instability of major-oil producing countries and enlarged energy demand (e.g. China), have resulted in a strong competition for land use and the resulting biomass between the food and biofuel production. This ultimately led to higher food prices (Cassman and Liska, 2007). Especially developing countries with adequate arable land, water resources and

infrastructure to support biofuel industry realized substantial economic benefits from biofuel production (e.g. sugarcane-ethanol industry accounts for 4.2 million jobs in Brazil). In contrast, urban and rural areas of countries poor in food-importing, are likely to face greater food insecurity challenges and pay much higher prices for basic food supply. Furthermore less surplus of biomass will be available for humanitarian aid to developing countries (Cassman, 2007). Besides the economical drawbacks, severe concerns have been raised about the ecological implications linked to the production of first-generation biofuels. Firstly, the net benefit in terms of greenhouse gas (GHG) emission reductions and energy balance is very limited partly due to fossil fuel utilization in the upstream processes and indirect land use change impacts (ILUC). ILUC relates to the clearance of natural lands (rainforests and grasslands), which store carbon in their soil and biomass, for the generation of biofuel farms leading to a net increase in GHG emissions. Furthermore, the cultivation of dedicated first-generation energy crops for biofuel production has been implicated in accelerated deforestation, contribution to monoculture and decreased biodiversity. Finally, in some regions first-generation biofuels compete with scarce water resources (Cassman, 2007; Fargione et al., 2008; Hertel et al., 2010; James Clive, 2013; Searchinger et al., 2008; Solomon, 2010).

For these multiple reasons, first-generation biofuels appear unsustainable for future generations and although first-generation feedstocks will provide biofuel for the foreseeable future, their importance is declining and they ultimately will give way to better alternatives such as second-generation biofuels.

1.2.2. Second-generation biofuels

Many of the problems associated with the production of first-generation biofuels can, at least partially, be alleviated by the production of second-generation biofuels. Second-generation biofuels or advanced biofuels are those produced from lignocellulosic non-food feedstocks, which avoid competition with food crops and moreover can be grown on marginal and/or contaminated soils unsuitable for food production. Generally, the production of biofuels from these feedstocks have low CO_2 emission or high green house gas reduction as well as low impacts on indirect land use change, frequently observed for first-generation biofuels. The major exploitable components of feedstocks, cellulose and hemicellulose, can be converted to sugar through a series of thermochemical

and biological processes and ultimately fermented to bioethanol (Carriquiry et al., 2011; Hinchee et al., 2009; Naik et al., 2010; Sannigrahi and Ragauskas, 2010; Solomon, 2010; Yuan et al., 2008). In general, lignocellulosic feedstocks are divided into two different categories: (1) agricultural and forest residues and (2) herbaceous and woody energy crops.

Residues from agriculture or forestry

Residue-based biofuel production comprises residues from (1) agriculture such as maize, sorghum, barley, rice, wheat and sugarcane and from (2) forestry including logging residues produced from harvest operations, fuel wood extracted from forestlands, and primary and secondary wood processing mill residues (Hill et al., 2006; Naik et al., 2010). The main advantage of using residues for biofuel production as compared to the use of dedicated energy crops is that the competition for land is completely avoided since no additional land is needed. In this way, residue-based biofuels should have minimal direct impact on food prices. Furthermore, greenhouse gas emissions associated with direct and indirect land use change are also avoided and removal of crop residues may contribute (for some crops) to enhanced disease and pest control and facilitate seed germination by increasing the soil temperature in the spring (Searchinger et al., 2008; Andrews et al. 2006). However on the other hand, crop residues also conserve the nutritional value (sequestering of nitrogen and carbon) and water status of the soils thereby maintaining and/or enhancing soil productivity. Therefore, excessive removal could have adverse effects on the soil properties, the surrounding environment and crop yield (Blanco-Canqui and Lal, 2009). The potential of logging residues is also limited by the economic costs of transportation, limited accessibility of the residues and a potential reduction of recoverability in harvest areas due to environmental considerations (Richardson, 2008).

Energy crops

The dedicated second-generation energy crops can be broadly categorized into grassy (herbaceous or forage) and woody (tree) energy crops. Perennial forage crop species such as switchgrass and *Miscanthus* sp. represent valuable feedstocks for the production of second-generation biofuels. Switchgrass (*Panicum virgatum* L.) is a perennial warm-season grass native to North America and was identified by the US Department of Energy as a model herbaceous

energy crop. Switchgrass combines several advantageous characteristics, including high productivity, suitability for marginal land quality and low water and nutritional requirements (Keshwani and Cheng, 2009). *Miscanthus* is a perennial rhizomatous grass native to Asia and a compelling herbaceous biomass feedstock for Europe mostly because of its cold tolerance and low nitrogen input requirements. The major limitation of *Miscanthus* as a bio-energy crop is the high cost related to the establishment since the propagation via rhizome cuttings takes two to three years before full production can start (Lewandowski et al., 2008). Woody (tree) energy crops also represent a valuable feedstock for second-generation biofuels primarily based on their high yield potential, wide geographical distribution, and relatively low levels of input needed when compared with annual crops (Naik et al., 2010; Smeets et al., 2007). Indeed, short-rotation, purpose-grown trees have a variety of inherent logistical benefits and economic advantages relative to other lignocellulosic energy crops. Most notably, the flexibility in the harvest time of the trees leads to reductions in storage and inventory holding costs and minimizes shrinkage or degradation losses associated with storage of annually-harvested biomass. Furthermore, they minimize environmental impacts associated with biomass production since multi-year rotations of trees allow for extended periods between harvests with limited disturbance to the land. Finally, woody (tree) energy crops provide higher economic flexibility of the feedstock as compared to other dedicated energy crops. Multiple end-use applications for these feedstocks include traditional forest products and energy products such as cellulosic ethanol for the production of biofuels, power generation through direct firing, co-firing, or wood pellet systems and applications in the pulp and paper industry (Hinchee et al., 2009; Sannigrahi and Ragauskas, 2010; Tharakan et al., 2003; Yuan et al., 2008).

In summary, woody trees dedicated as feedstock for biomass production are in general less demanding in terms of inputs, reduce erosion and improve soil properties, and provide better wildlife habitat than annual crops. However, reversely, while their yields are high and their environmental ramifications remain limited, dedicated energy crops do not entirely escape the food versus fuel debate. Complete circumvention of the food-versus-fuel debate is only achieved when these woody trees are cultivated on marginal and/or

contaminated lands unsuitable for food production (Naik et al., 2010; Nijsen et al., 2012). With increasing governmental, academic, and industrial research efforts on the production of biofuels from lignocellulosic feedstock, a few tree species have emerged as front-runners more specifically *Populus*, *Salix* and *Eucalyptus* and their respective hybrids.

1.3. Poplar as feedstock for second-generation biofuels

The genus *Populus* consists of 25-35 species of deciduous plants native to the Northern Hemisphere. Classic-breeding techniques have generated a large range of hybrids with higher biomass yield traits. These hybrid poplars are among the fastest-growing trees in the world and provide high economic flexibility with end-use applications such as biofuel production, pulp and paper and other bio-based products (chemicals and adhesives). To optimize biomass production, it is also important to consider how different clones respond to different climatic factors and to select the appropriate varieties for each region (Zalesny et al., 2009). Moreover, sequencing of the poplar genome has opened biotechnological possibilities for tailoring new clones optimized for biofuel production. The primary criterion in determining the economic viability of a lignocellulosic feedstock is the proportion of cellulose, hemicellulose and lignin. Poplar species and hybrids have cellulose contents ranging from 42 to 49%, hemicellulose from 16 to 23%, and total lignin contents from 21 to 29%. The cellulose content of poplar is higher than that of switchgrass and maize and comparable to other hardwood feedstock such as eucalyptus, making it a desirable feedstock for the production of ethanol (Sannigrahi and Ragauskas, 2010). Further desirable characteristics of poplar for use as biomass feedstock include high biomass yield on many different types of land (even marginal land), widespread growth area and considerable drought tolerance and resistance to pests and insects.

Second-generation biofuels derived from lignocellulosic biomass from dedicated energy crops (e.g. poplar), evade the “food versus fuel” debate since they can be grown on marginal land, but they present a challenge of a different nature. Lignin polymers, abundantly present in the walls of secondary thickened cells of vascular plants, represent a major hindrance in the enzymatic processing of lignocellulosic biomass to fermentable sugars (Chen and Dixon, 2007; Studer et al., 2011). Therefore genetically modified (GM) energy crops, engineered to produce less lignin or more easily degradable lignin, have been utilized to

partially overcome the recalcitrance of lignocellulosic biomass and to improve the commercial viability and cost-competitiveness of second-generation biofuels (Vanholme et al., 2012a; Wilkerson et al., 2014). Consequently, lignin molecules and by extension the complete composition of plant cell walls play important roles in the genetic engineering of feestocks.

1.4. Plant cell wall and lignin molecules

The plant cell wall constitutes an extracellular structure, which differentiates plant cells from animal cells and serves crucial functions in plant physiology. It consists of three main composing layers: primary cell wall, middle lamella and the secondary cell wall which conjointly function to provide (a) tensile strength and limited plasticity, (b) mechanical support, (c) water-proof vessels for the long-distance transport of water and nutrients, (d) protection from biotic (pathogens) and abiotic (e.g. UV radiation) stressors and (e) contribute to cell-cell communication. All plant cells that are in developmental expansion have a thin, flexible and constantly remodelling primary cell wall composed of carbohydrate-based polymers (cellulose, hemicellulose and pectin) together with lesser amounts of structural glycoproteins (hydroxyproline-rich extensins and arabinogalactan), phenolic esters (ferulic and coumaric acids), ionically and covalently bound minerals (e.g. calcium and boron), and enzymes. The middle lamella is located between the primary walls of adjacent cells. This lamella is rich in pectin and cements the cells of two adjoining cells together, which is crucial for the formation of plasmodesmata. Upon cell maturation and completion of cellular expansion, cells that have to reinforce their structure for functional reasons (e.g., to form vessel or fiber cells) generate a secondary cell wall that is mainly composed of cellulose, hemicelluloses (mostly xylans) and lignin (Cosgrove, 2005; Sarkar et al., 2009).

1.4.1. Lignin: function, general composition and deposition

Lignin molecules are, after cellulose, the second most abundant terrestrial biopolymer, accounting for approximately 30% of the organic carbon in the biosphere (Boerjan et al., 2003). Lignin evolved together with the adaptation of plants to a terrestrial environment, thereby increasing the structural integrity of the cell wall and providing the mechanical support needed for an erect growth habit. In addition, lignin imparts impermeability to the cell wall required for the transport of water and solutes through the vascular system (Weng and Chapple,

2010). Besides having multiple physiological functions during plant development, lignin molecules (as a major part of the secondary cell wall) also protect cell wall polysaccharides from microbial degradation by acting as a passive barrier. Local or extensive breakdown of the wall matrix is typically required for the progression of pathogen infections (Cantu et al., 2008; Hématy et al., 2009). Lignin molecules are defined as a large group of heterogeneous aromatic polymers formed by oxidative combinatorial coupling of 4-hydroxy-phenylpropanoid monomeric units termed monolignols. They are predominantly deposited in the walls of secondary thickened cells (xylem, sclerenchyma) of vascular plants and represent approximately 25% of the dry weight of wood (Boerjan et al., 2003; Vanholme et al., 2010). However, recent studies have also detected secondary wall and apparent lignin in the marine red alga *Calliarthron*, which diverged from vascular plants 1 billion years ago, suggesting convergent evolution (Martone et al., 2009). From a developmental point of view, lignification is generally initiated in the primary cell wall of xylem elements (middle lamella/cell corners) at the start of secondary cell wall formation, although cell-/tissue-specific differences in the developmental pattern can occur (Boerjan et al., 2003). Besides developmental initiation of lignin deposition, biotic- and/or abiotic-stresses can also induce lignification in cell walls that, under non-stress conditions, do not normally lignify. Stressors with the ability to induce lignification include wounding, metabolic stress, pathogen infections and perturbations in the cell wall structure (Srivastava et al., 2007; Wang et al., 2013). For example, lignin biosynthetic genes that are up-regulated (or activated) after mechanical injury suggest that stress lignification is a tightly controlled phenomenon. Reversely, expression of monolignol biosynthesis genes is not always correlated with the presence of the lignin polymer since a wide range of non-lignin products (e.g. phenol esters) are also produced by the phenylpropanoid pathway (Wang et al., 2013).

1.4.2. Monolignol biosynthesis

The formation of lignin polymers is the result of oxidative coupling of phenolic monomeric units termed monolignols. The main monolignols composing lignin polymers are the hydroxycinnamyl alcohols: sinapyl alcohol, coniferyl alcohol with typically minor amounts of p-coumaryl alcohol, which differ in their degree of methoxylation. The monolignols are, when ultimately incorporated in the

lignin polymer, termed respectively sinapyl (S), guaiacyl (G) and p-hydroxyphenyl (H) units (Boerjan et al., 2003; Hisano et al., 2009; Ralph et al., 2004).

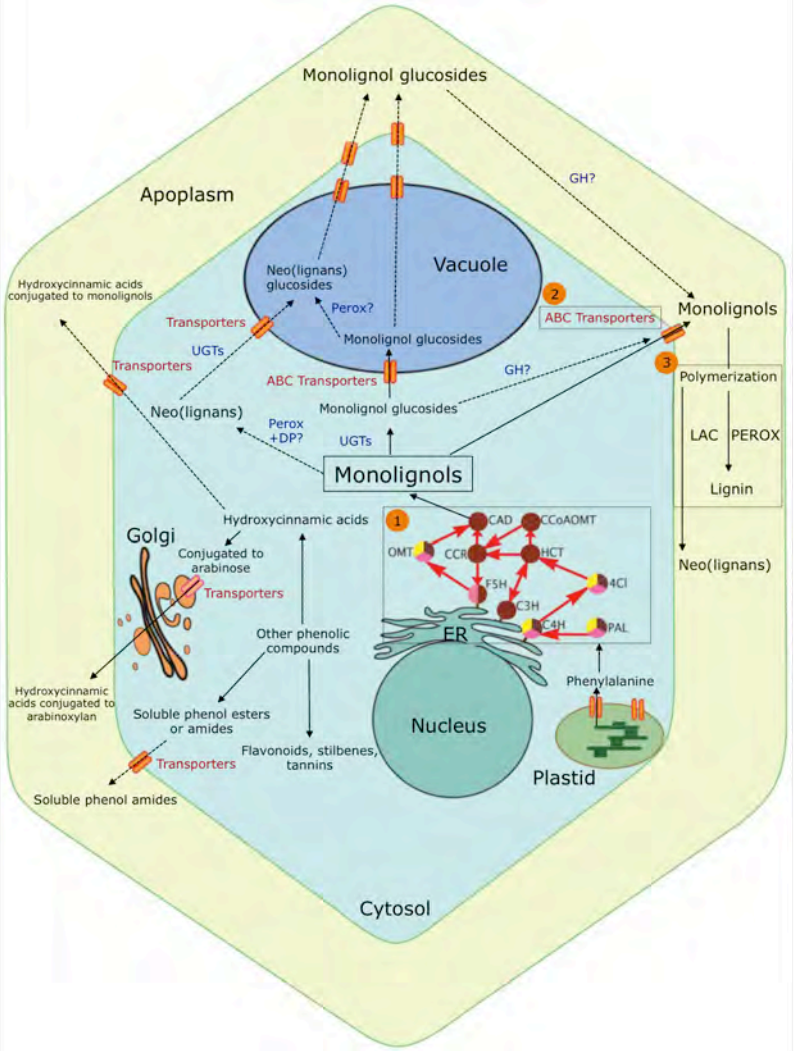

Figure 1.1. General view of the monolignol biosynthetic pathway, transport and polymerization (adapted from Wang et al., 2013). The main steps are indicated in orange circles. The biosynthesis of monolignols from phenylalanine involves cytosolic (PAL, HCT, 4CI, CCR, CAD, CCoAOMT, and OMT) and ER membrane-anchored (the cytochrome P450 enzymes F5H, C3H, and C4H) enzymes (Step 1). Monolignols may be conjugated by UGTs and then transported to the vacuole or directly transported to the cell wall (Step 2) for oxidative cross-linking by apoplastic peroxidases and laccases into lignins (Step 3).

Figure 1.1.(continued). The dashed lines delineate putative pathways and full lines delineate known routes. Enzymes of the monolignol-specific pathway are represented by circles. The brown color indicates involvement of the enzyme in the monolignol pathway; yellow indicates involvement in the flavonoid pathway; and pink indicates involvement in the sinapate ester pathway. PAL, phenylalanine ammonia lyase; C4H, cinnamic acid 4-hydroxylase; 4CL, 4-hydroxycinnamoyl-CoA ligase; HCT, hydroxycinnamoyl-CoA:shikimate hydroxycinnamoyl transferase; C3H, p-coumaroyl shikimate 3′-hydroxylase; CCoAOMT, caffeoyl-CoA O-methyltransferase; CCR, hydroxycinnamoyl-CoA reductase; F5H, ferulic acid 5-hydroxylase; COMT, caffeic acid/5-hydroxyferulic acid O-methyltransferase; CAD, cinnamyl alcohol dehydrogenase; UGT, UDP-glycosyltransferase; GH, beta-glucosidase; PEROX, peroxidase; LAC, laccase; DPs, dirigent proteins; BAHD, hydroxycinnamic acid transferase; ER, endoplasmic reticulum.

The biosynthesis of the monolignols is initiated from the general phenylpropanoid pathway with phenylalanine, derived from the shikimate biosynthetic pathway in the plastid, as the major starting point (Figure 1.1: Step 1). The synthesis of monolignols from phenylalanine via the general phenylpropanoid and the monolignol-specific pathways occurs in the cytosol and involves several cytosolic enzymes: phenylalanine ammonia-lyase (*PAL*), shikimate hydroxycinnamoyl transferase (*HCT*), 4-coumarate-CoA ligase (*4CL*), cinnamoyl-CoA reductase (*CCR*), cinnamyl alcohol dehydrogenase (*CAD*), caffeoyl-CoA 3-O-methyltransfer- ase (*CCoAOMT*), caffeic acid/5-hydroxyferulic acid O-methyltransferase (*COMT*) and endoplasmatic reticulum (ER) membrane-anchored enzymes: ferulate 5- hydroxylase (*F5H*), coumarate 3- hydroxylase (*C3H*), and cinnamate 4-hydroxylase (*C4H*) (Boerjan et al., 2003; Vanholme et al., 2010; Wang et al., 2013). The general phenylpropanoid pathway starts with the deamination of phenylalanine to cinnamic acid by PAL, followed by hydroxylation of the aromatic ring which leads to p-coumaric acid, a reaction catalyzed by *C4H*. Activation of the acid to a thioester by 4CL yields p-coumaroyl-CoA, which is subsequently transesterified to its quinic or shikimic acid ester derivative (*HCT*), hydroxylated (*C3H*) and then transesterified again by *HCT* to produce caffeoyl-CoA. Further methylation of the 3-hydroxyl group by *CCoAOMT* yields feruloyl-CoA. From this general phenylpropanoid pathway various pathways branch off including the pathways towards flavonoids, benzenoids, coumarins, sinapate and ferulate esters as well as the monolignol-specific pathway. The monolignol-specific pathway includes (a) reduction of

feruloyl-CoA to coniferaldehyde by cinnamoyl-CoA reductase (*CCR*), (b) hydroxylation of coniferaldehyde by *F5H* to produce 5-hydroxyconiferaldehyde, and (c) methylation of 5-hydroxyconiferaldehyde by *COMT* to provide sinapaldehyde. Further reduction to their corresponding alcohols, coniferyl alcohol and sinapyl alcohol, is catalyzed by *CAD*. p-coumaryl alcohol, the third major monolignol is enzymatically produced from p-coumaroyl CoA via *CCR* and *CAD* (Figure 1.1: Step 1 and Figure 1.2) (Boerjan et al., 2003; Vanholme et al., 2010; Wang et al., 2013). Upstream of the genes encoding these enzymes are several transcription factors, belonging to NAC and MYB gene families, which have shown key roles in regulating gene expression during lignin biosynthesis (Guillaumie et al., 2010; Rogers and Campbell, 2004; Zhou et al, 2009).

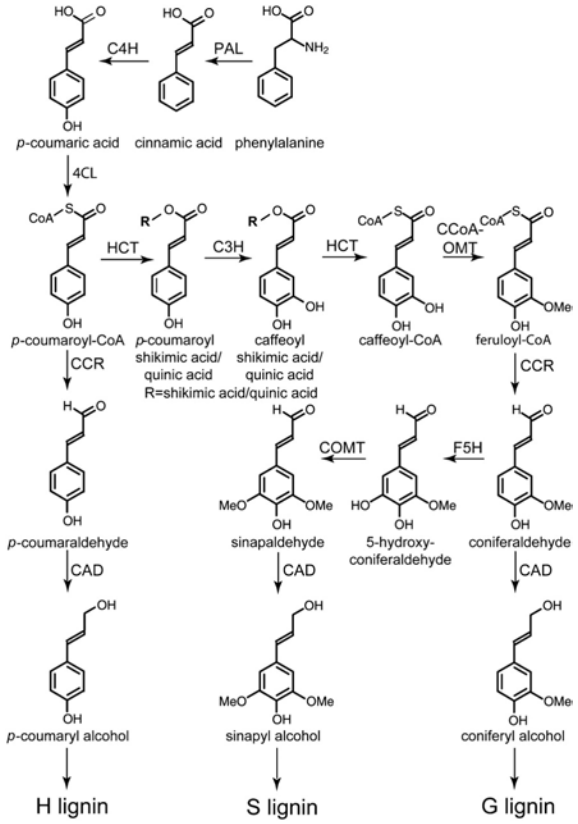

Figure 1.2.. The main biosynthetic route toward the monolignols p-coumaryl, coniferyl, and sinapyl alcohol (Boerjan et al., 2003). Full names of enzymes are listed in Figure 1.1. and in the main text.

The monolignols produced by the monolignol-specific pathway are ultimately used for at least three different product classes: monolignol 4-O-hexosides, (neo)lignans and oligolignols/lignin. The biological role of 4-O-glucosylated monolignols (e.g. coniferin and syringin) has not been completely determined, but they could serve as storage forms for their aglycones (Vanholme et al., 2012a). Lignans are optically active phenylpropanoid dimers formed by the initial stereospecific β-β coupling of two monolignol radicals and are believed to be involved in defense responses and some may also have hormonal functions (Davin, 1997; Umezawa, 2003). However, in the following we will focus on monolignols dedicated for the production of lignin polymers.

1.4.3. Monolignol transport

After their synthesis in the cytosol, monolignols are translocated to the cell wall for subsequent polymerization into lignin molecules (Figure 1.1.: Step 2 and Figure 1.3) Different hypotheses concerning the mechanisms of monolignol transport have been suggested including passive diffusion of coniferyl and sinapyl alcohols across the plasma membrane lipid bilayer, vesicular trafficking with the involvement of Golgi-derived vesicles (exocytosis), simple release of monolignols after cell death (vacuole lysis) and active translocation via direct plasma membrane pumping by ABC transporters (Figure 1.3) (Alejandro et al., 2012; Liu et al., 2011; Liu, 2012; Miao and Liu, 2010). Recently, most of the evidence is building towards the role of active transport via ATP-binding cassette (ABC) transporters. Miao and Liu (2010) demonstrated that the glycosylation status determines monolignol transport and subcellular compartmentation. Via the use of plasma membrane and tonoplast-derived vesicles (prepared from *Arabidopsis* and poplar cells), they proved that coniferyl alcohol (the aglycone form) was transported across the plasma membrane in an ATP-dependant process by an ABC-transporter whereas coniferin (the glycosylated form) was transported into the vacuole for storage; suggesting that glucoconjugation is a prerequisite for selective import into the vacuole. Furthermore, Alejandro et al. (2012) recently reported genetic confirmation of the involvement of ABC transporters in monolignol transport into the cell wall. Via co-expression and protein fusion studies in *Arabidopsis,* they identified an ABCG transporter gene (AtABCG29), which was co-regulated with phenylpropanoid gene expression and was localized in the plasma membrane.

The ABCG transporter showed active transportation of the monolignol p-coumaryl alcohol across the plasma membrane with also minor activity toward sinapyl alcohol. The transportation mechanisms for sinapyl and coniferyl alcohol remain to be identified and characterized but plant genomes contain large ABC transporter gene families (e.g. 130 genes in *Arabidopsis*). However, AtABCG29 is part of the PDR subfamily of ABC transporters, which has 12 members in *Arabidopsis*, at least six of which are located in the plasma membrane representing promising candidates for other monolignol pumps (Dunkley et al., 2006; Sibout and Höfte, 2012; Wang et al., 2013).

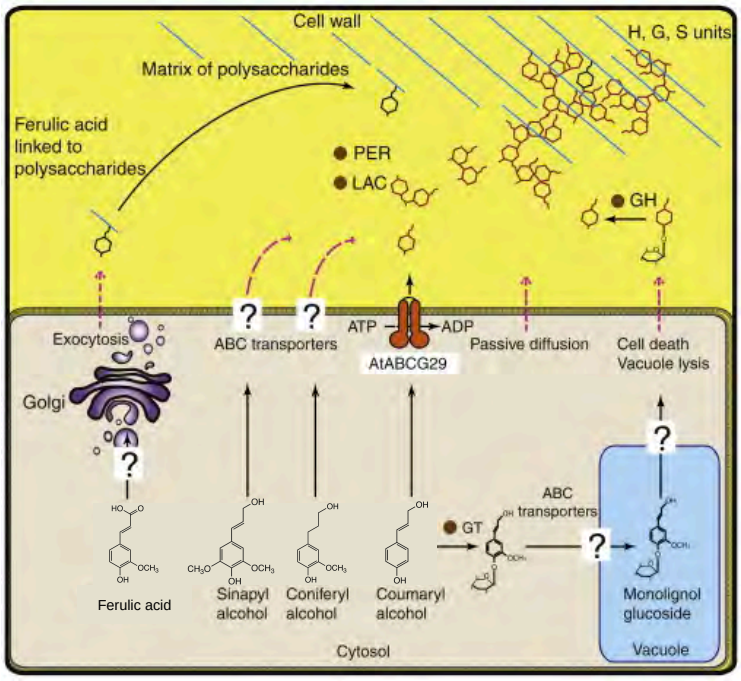

Figure 1.3. Monolignol transport (Sibout and Höfte, 2012). The monolignols (p-coumaryl alcohol, coniferyl alcohol and sinapyl alcohol), synthetized in the cytosol are transported to different locations: the cell wall for oxidative cross linking into lignins by apoplastic peroxidases (PER) and laccases (LAC); the vacuole for storage as glucoconjugates and, for ferulic acid, into the Golgi apparatus for incorporation into polysaccharides (pectins or arabinoxylans). Transport routes may include passive diffusion, active transport through membrane transporters, through Golgi-derived vesicles or simply by release from dying cells. p-coumaryl alcohol is exported across the plasma membrane by the AtABCG29 transporter whereas free coniferyl alcohol and sinapyl alcohol are exported probably by other unknown ABC transporters. Monolignols are selectively imported into the vacuole as glucoconjugates by unknown ABC transporters.

1.4.4. Polymerization: Radical formation and radical coupling

After transportation of the monolignols into the cell wall, lignin polymerization starts with oxidative radicalization of the phenols (dehydrogenation) followed by combinatorial radical coupling (Boerjan et al., 2003; Ralph et al., 2004; Vanholme et al., 2010) (Figure 1.1: Step 3 and Figure 1.4). The oxidative capacity required for the first step, monolignol dehydrogenation, is provided by peroxidases (type III) and/or laccases, which play pivotal roles in lignification. Peroxidases use H_2O_2 as co-substrate (probably provided by combined action of NADPH oxidase or germin-like proteins) whereas laccases use oxygen to oxidize their metal centre to enable catalytic phenol oxidation (Figure 1.4). Both type of enzymes belong to large multigene families, whereof individual members display overlapping activities, making the clarification of the biological role of each member and the *in planta* mechanisms difficult to study. Due to gene redundancy, knockouts may have little to no effects on lignification (McCaig et al., 2005; Welinder et al., 2002). Furthermore, peroxidases generally show low and differential substrate specificities; recent studies show that some peroxidase isoforms exclusively accept coniferyl alcohol whereas other are highly specific for toward sinapyl alcohol (Gómez Ros et al., 2007; Marjamaa et al. 2009). Recently, direct evidence was also provided that laccases are involved in monolignol polymerization by the characterization of *Arabidopsis lac4-lac17* double mutants (Berthet et al., 2011).

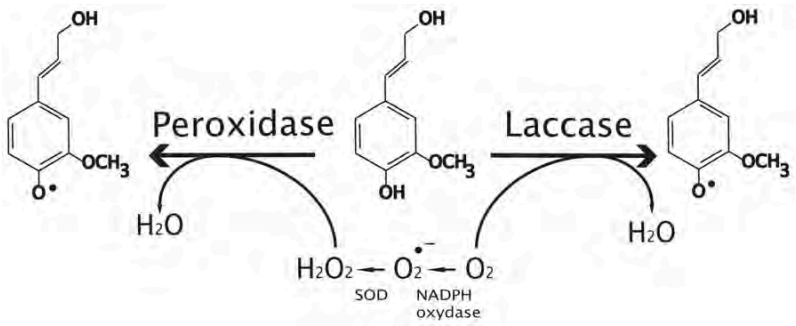

Figure 1.4. Radical formation by peroxidase and laccases. Peroxidases use H_2O_2 as co-substrate whereas laccases use oxygen to oxidize their metal centre to enable catalytic phenol oxidation. Radicals are resonance-stabilized by having various sites of enhanced single-electron density in the molecule.

The formation of monolignol radicals by peroxidases and laccases upon entry of monolignols in the cell wall matrix is followed by combinatorial radical coupling. Mutual coupling of monolignol radicals (dimerization) will proceed via the formation of covalent bonds between resonance-stabilized radicalized subunits. Since monolignols favour coupling at their β-position, three inter-unit linkages dominate lignin structure more specifically β-O-4 (β-aryl esters), β-β (resinols) and β-5 linkages (phenylcoumarans). After dimerization, the resulting dimer is once more dehydrogenated (radicalized) where after coupling to another monomer radical occurs. In this way the lignin polymers grow via endwise coupling one monomer at a time (Boerjan et al., 2003; Ralph et al., 2004; Vanholme et al., 2012a, 2010). The average length of a linear lignin chain in poplar is estimated to be between 13 to 20 monomeric units (Stewart et al., 2009). Recently, Demont-Caulet and colleagues (2010) argued that endwise polymerization mechanisms might co-exist with bulk polymerization mechanisms in *Arabidopsis thaliana* whereby different oligomers are linked together at the same time after total consumption of monomers.

The final composition of lignin polymers, i.e. the ratio of different composing units (S-, G-, H-units), depends largely on the taxon of the plant. Lignin polymers from gymnosperms are composed almost exclusively of G-units with minor amounts of H-units (no S-units) whereas angiosperm dicot lignin molecules are comprised of both G- and S-units with only traces of H-units and lignin from monocot grasses contain G- and S-units with modest levels of H-units (typically less than 5%). In general, lignin unit composition is highly variable, not only between species, but also between tissues and cell types and moreover even within a single cell wall (Boerjan et al., 2003; Vanholme et al., 2010). Furthermore, besides the major composing monomeric units (S-, G-, H-units), any phenolic compound entering the cell wall region has the potential to be oxidized and ultimately incorporated in the lignin polymers. Indeed, all lignins contain traces of alternative monomers from apparently incomplete monolignol biosynthesis such as hydroxycinnameldehydes and other (side-) reactions that occur during biosynthesis. For example, traditional monolignols are often acetylated at their γ-position acetate, p-hydroxybenzoate and p-coumarate. Such acylated units and others like dihydro-hydroxycinnamyl alcohols, hydroxybenzaldehydes and hydroxycinnamic acids are found in wild type plants

(Boerjan et al., 2003; Lu and Ralph, 2008; Morreel et al., 2004; Ralph et al., 2006).

1.5. Lignin engineering and consequences

Lignin molecules, as a major component of the secondary plant cell walls, serve crucial physiological roles and were even essential in the evolution of vascular land plants to grow in a gravitropic environment and to transport water and nutrients in their vascular system (Vanholme et al., 2012a; Weng and Chapple, 2010). However, in the transition to a more bio-based economy, lignin has a far-reaching impact on agriculture and industry. Lignin polymers represent the major limiting factor in lignocellulosic biomass recalcitrance since they block the enzymatic hydrolysis of polysaccharides to monosaccharides (saccharification) by immobilizing cellulases (and associated enzymes). As a consequence, expensive mechanical, thermal and chemical pretreatments are required to disrupt cell wall structure and render the polysaccharides more accessible. Therefore considerable research interest has been devoted to reducing and/or modifying lignin content via genetic engineering, a strategy that would reduce the input of chemicals and energy during the pre-treatment reactions (Chen and Dixon, 2007; Himmel et al., 2007; Vanholme et al., 2012b; Vanholme et al., 2008; Weng et al., 2008). In order to reduce/modify lignin polymers to generate feedstocks with diminished recalcitrance, genes have been cloned for each of the enzymatically catalysed steps of the lignin biosynthetic pathway and the impact on lignin amount and composition has been studied through mutants or reverse genetics in various species including Arabidopsis (*Arabidopsis thaliana*), maize (*Zea mays*), alfalfa (*Medicago sativa*), poplar (*Populus spp.*) and tobacco (*Nicotiana tabacum*)(Vanholme et al., 2012a, 2010). *Arabidopsis thaliana* is widely considered to be the model plant for understanding lignin biosynthesis, deposition and function while *Populus* spp. are one of the model systems for extrapolation to lignocellulosic biofuel crops (Leplé et al., 2007; Mir Derikvand et al., 2008; Ruel et al., 2009; Van Acker et al., 2013, 2014). Taken together, all these studies revealed the individual roles of the monolignol biosynthetic genes and in general concluded that down-regulation of *PAL*, *C4H*, *4CL*, *HCT*, *C3H*, *CCoAOMT*, *CCR*, and to a lesser extent *CAD,* lowers lignin amounts in the cell wall to varying extents, depending on the gene, the species, and the level of gene redundancy. Furthermore, reduced lignin levels are typically associated

with dramatic changes in the soluble phenolic pools, and different species accumulate various storage and detoxification products (Leplé et al., 2007; Mir Derikvand et al., 2008; van der Rest et al., 2006). And when lignin levels become too low, plant growth and development are also affected (Leplé et al., 2007; Mir Derikvand et al., 2008). Specifically, gene silencing of cinnamoyl-CoA reductase (*CCR*; EC 1.2.1.44) which catalyzes the conversion of feruloyl-CoA to coniferaldehyde and is considered as the first enzyme in the monolignol-specific branch of lignin biosynthesis (Boerjan et al., 2003; Vanholme et al., 2010), represents an interesting target to reduce lignin levels (Chabannes et al., 2001; Leplé et al., 2007; Mir Derikvand et al., 2008; Ruel et al., 2009; Van Acker et al., 2014; van der Rest et al. 2006). Gene silencing of *CCR* and by extension most of the genes silenced in the lignin biosynthesis, leads to flux changes in the phenylpropanoid and monolignol-specific pathways (Leplé et al., 2007). In 2007, Leplé and colleagues generated *CCR*-downregulated poplar trees via *Agrobacterium tumefaciens* transformations. Out of 10 homologous *CCR* genes present in the poplar genome, Leplé et al. (2007) selected and cloned one specific *CCR* gene, which was strongly expressed in developing poplar xylem. Multi-level phenotyping of these trees revealed complex effects on cell wall development as well as improved pulping and bioconversion performance of these down-regulated trees. They reported that in young developing xylem, scraped from 3-month-old greenhouse-grown wild-type and *CCR*-down-regulated poplars, (a) the concentrations of ferulic and sinapic acids had increased relative to those of coniferaldehyde and sinapaldehyde in the *CCR*-down-regulated lines and (b) strong accumulation of the phenolic glucosides O^4-b-D-glucopyranosyl sinapic acid (GSA) and O^4-b-D-glucopyranosyl vanillic acid (GVA) (glucosylated detoxification products of ferulic acid) occurred in the *CCR*-dowregulated lines. Furthermore, transciptome and metabolome analysis revealed an altered hemicellulose and pectin metabolism and an alteration in the general carbohydrate metabolism (decreased amounts of glucose, mannose, and myo-inositol in the metabolite pools) in the *CCR*-down-regulated lines. All together these changes in the xylem metabolome deliver substantially different conditions for the plant-associated microbiome. Recently, a field trial, using the *CCR*-down-regulated lines contructed by Leplé and colleagues (2007), was

conducted by the VIB (Flemish Institute for Biotechnology, Ghent) (Custers, 2009; Van Acker et al., 2014).

1.6. Eukaryote-Prokaryote associations

Inter-organismal associations between eukaryotic and prokaryotic cells are one of the most studied research areas in recent years with numerous studies covering a large range of eukaryotic-prokaryotic associations: from the human microbiome (Human Microbiome Project Consortium, 2012) and host-genotype associations therein (Koch, 2014; Spor et al., 2011), gut microfauna of insects (Dillon and Dillon, 2004; Hansen and Moran, 2014; Sudakaran et al., 2012) to microbiota associated with plants (Bonito et al., 2014; Bulgarelli et al. 2013; Compant et al. 2010; Haichar et al., 2008; Hallman and Berg, 2007; Ryan et al. 2008). Moreover, the single most important evolutionary event during the development of the eukaryotic cell was the incorporation of prokaryotic endosymbionts, which would ultimately evolve to the mitochondria and chloroplasts (photosynthetic capacity of plants), providing the cells with compartmentalized bioenergetic and biosynthetic capacities (Dyall et al., 2004; Raven, 1970). From this point onward, eukaryotic and prokaryotic organisms have been intertwined. Indeed, most eukaryotes maintain close mutualistic relationships with microorganisms providing a plethora of advantages: (1) improved nutrient acquisition via the breakdown of dietary products and the production of essential nutrients (animal gut) (Derrien et al., 2010; Fagundes et al., 2012) or increased nutrient availability and/or uptake (rhizosphere of plants) (Bais et al., 2006; van der Heijden et al, 2008); (2) preventing the colonization by pathogens via the competition for (micro)-nutrients and the production of inhibitory/antibiotic compounds (Doornbos et al. 2011; Fagundes et al., 2012; Lugtenberg and Kamilova, 2009) and (3) modulation of the host immune system via priming of the intestinal mucosa in the human gut (Bron et al., 2012; Fagundes et al., 2012; Ichinohe et al., 2011) or via induced systemic resistance (ISR) in plants (Pieterse et al., 2009; Van der Ent et al., 2009). Reciprocal advantages for the microbiome include stabile abiotic conditions and a steady supply of carbon in the form of mucins (human gut) (Derrien et al., 2010) or root exudates (and other rhizodeposits) in the association with plants (Bais et al., 2006; Compant et al., 2010; Haichar et al., 2008).

Plant-microbiota interactions are of specific interest, not only to get a better understanding of their role during plant growth and development but also for the exploitation of the plant-microbe associations in phytoremediation applications, sustainable crop production and the production of secondary metabolites (Brader et al. 2014; Hardoim et al., 2008; Weyens et al. 2009a, 2009b).

1.7. The plant microbiome

Plants are colonized by an astounding number of microorganisms and collectively, consistent with the terminology used for microorganisms colonizing the human body (Gevers et al., 2012; Qin et al., 2010; Zhao, 2010), communities of plant-associated microorganisms are referred to as the plant microbiome or as the plants' other genome. The plant microbiome is one of the key determinants of plant health and productivity and has received substantial attention in recent years. They help plants to suppress diseases, to stimulate growth, to occupy space that would otherwise be available to pathogens, to promote stress resistance, and influence crop yield and quality by nutrient mobilization and transport (Bakker et al., 2013; Berendsen et al., 2012; Berg et al., 2014; Mendes et al., 2013; Turner et al., 2013).

In the following we will focus on the bacterial microbiome of plants. Virtually all tissues of a plant host bacterial communities: at the soil-plant interface (rhizosphere environment) (Bakker et al., 2013; Berendsen et al., 2012; Bulgarelli et al., 2013; Compant et al., 2010), inside the plant tissues (endosphere environment harbouring the endophytes) (Bulgarelli et al., 2013; Compant et al., 2010; Hardoim et al., 2008; Ryan et al., 2008; Weyens et al, 2009a) and at the air-plant interface (phyllosphere environment)(Delmotte et al., 2009; Lindow and Brandl, 2003; Vorholt, 2012). To a lesser extent we can also distinguish the bacterial colonization of the anthosphere (flower) (Shade et al., 2013; Compant et al., 2008), the spermosphere (seeds) (Nelson, 2004; Truyens et al., 2014), and the carposphere (fruit) (Compant et al. 2011). All these microenvironments provide specific biotic and abiotic conditions for the residing bacterial communities. Here we will focus on the rhizosphere, endosphere and phyllosphere environment.

1.7.1. Bacterial microbiome in the rhizosphere environment

More than a century ago, Lorenz Hiltner defined the rhizosphere as root-surrounding soil, which is influenced by the release of root exudates (Hartmann

et al., 2007). Due to the importance of the soil habitat of plants, the majority of research now focuses on the rhizosphere environment (Bakker et al., 2013; Berendsen et al., 2012; Mendes et al., 2013). The rhizosphere is a hot spot for numerous organisms and is considered as one of the most complex ecosystems on Earth (Hinsinger et al., 2009; Jones and Hinsinger, 2008; Raaijmakers et al. 2008). Organisms found in the rhizosphere include bacteria, fungi, oomycetes, nematodes, protozoa, algae, viruses, archaea, and arthropods, which recently had led to the emergence of the term 'rhizosphere zoo' (Bonkowski et al., 2009; Buée et al., 2009; Raaijmakers et al., 2008; Turner et al., 2013). Specifically, the rhizosphere microbiome is of central importance not only for plant nutrition and health but also contributes substantially to microorganism-driven carbon sequestration, which has an important role in ecosystem functioning and nutrient cycling in terrestrial ecosystems (Berg et al., 2014; Mendes et al., 2013; Philippot et al., 2008). In contrast to non-rooted bulk soil, the rhizosphere is characterized by much higher bacterial abundances and activities, collectively termed as "the rhizosphere effect" (Bais et al., 2006; Hartmann et al., 2008; Walker et al., 2003). The major driving force in the regulation of the microbial diversity and activity in the rhizosphere soil and rhizoplane (external root surface) and ultimately the formation of distinctive rhizosphere microbiota from soil biomes is the deposition of large amounts of organic carbon by the plant roots in a process termed rhizodeposition (Bertin et al., 2003; Dennis et al., 2010; Jones et al., 2009).

Rhizodeposition comprises the release of (1) soluble root exudates by rhizodermis cells, (2) insoluble mucilage by the root cap, (3) root cap and border cells and (4) carbon to root-associated symbionts and death and lysis of root cells. Soluble root exudates contain a variety of compounds, predominantly organic acids and sugars but also inorganic acids, amino acids, phytosiderophores, fatty acids, vitamins, growth factors, hormones, purines, nucleoside and antimicrobial compounds (Jones et al., 2009). Together these root exudates are key determinants of rhizosphere microbiome structure (Badri, et al., 2013; Bais et al., 2006; Shi et al., 2011). The composition of the plant root exudates is highly variable between plant species, cultivars and moreover with plant age and developmental stage resulting in specific bacterial communities (Cavaglieri et al., 2009; Chaparro et al., 2013; DeAngelis et al.,

2009; Haichar et al., 2008; Inceoğlu et al., 2010; Mark et al., 2005; Micallef et al., 2009). It now appears that in addition to carbohydrates and even amino acids, which act as general chemical determinants in the rhizosphere, secondary metabolites such as plant-specific flavonoids also play a role in the development of plant-specific microbial communities in the rhizosphere (Badri et al., 2013; Weston and Mathesius, 2013).

Most authors consider the process of rhizodeposition as active plant-microbe signalling, at significant carbon cost, whereby plants may modulate the rhizosphere microbiome to their benefit by selectively stimulating microorganisms with traits that are beneficial to plant growth and health. However, others have argued that exudates are passively 'released' as over-flow/waste products of the plant (Dennis et al., 2010; Hartmann et al., 2008; Jones et al., 2009). Since rhizodeposition accounts for around 11% of the net photosynthetically fixed carbon and 10-16% of total plant nitrogen, varying greatly depending on plant species and plant age (Jones et al., 2009), defining the process as waste products seems highly unlikely. However, root exudation is not a unidirectional flux and plant roots can take up a range of exuded compounds from the rhizosphere into the roots and transfer them again to shoots (Jones et al., 2009). In any case, soil microorganisms are chemo-tactically attracted to the plant root rhizodeposits, after which rhizosphere/rhizoplane competent bacteria proliferate in this carbon rich environment and form distinctive rhizosphere communities (Lugtenberg and Kamilova, 2009).

1.7.2. Bacterial microbiome in the endosphere environment

In addition to bulk soil and rhizosphere communities, large and diverse bacterial populations live inside plants without causing detrimental effects or cellular damage to the plant, collectively termed endophytes. Bacterial endophytes have been isolated from virtually all plant species studied including a number of potential bioenergy crops. For a long time, endophytes were ignored and/or considered as contaminants but many endophytic inhabitants of plants are now often recognized as having unique, intimate and crucial interactions with the plant (Bulgarelli et al., 2013; Hardoim et al., 2008; Hirsch and Mauchline, 2012; Mitter et al., 2013; Rosenblueth and Martínez-Romero, 2006; Ryan et al., 2008; Turner et al., 2013; Weyens et al., 2009a). Endophytic bacteria reside for at

least part of their lives within plant tissues and can be considered to sit at the benign end of the spectrum between mutualists and pathogens (Compant et al., 2010). However, they also include latent pathogens, which depending on environmental conditions and/or host genotype can cause diseases (James and Olivares, 1998; Monteiro et al., 2012; Sessitsch et al., 2012). The majority of endophytes are widely considered as being a sub-population of the rhizosphere microbiome, since their primary colonization route are the plant roots (Compant et al., 2010; Hardoim et al., 2008; Turner et al., 2013). However, endophytes also display characteristics distinct from rhizospheric bacteria suggesting that not all rhizospheric bacteria can enter plants and/or that after colonization of their host plant, endophytes have the potential to modulate their metabolism and become adapted to their internal environment (Ferrara et al., 2011; Monteiro et al., 2012; Sessitsch et al., 2012). In order to transition from the soil to the plant, free-living soil-borne bacteria must first demonstrate rhizosphere and/or rhizoplane (external root surface) competence, i.e. having the ability to colonize the rhizosphere and/or rhizoplane during an extended period in an environment characterized by strong microbial competition where after establishment in the host plant can follow (Compant et al., 2010). Rhizosphere/rhizoplane competence is predominantly determined by the ability of soil bacteria to approach plant roots via chemotaxis-induced motility to plant root rhizodeposits (Compant et al., 2010; Haichar et al., 2008; Jones et al., 2009). Mutant *Pseudomonas fluorescens* strains, which lacked the *cheA* gene (encoding a chemotaxis response regulator) showed reduced movement towards root exudates in the tomato rhizosphere and also decreased root colonization (de Weert et al., 2002). Furthermore, Mark et al. (2005) studied the transcriptome of *Pseudomonas aeruginosa* strain PAO1 in response to exudates of two cultivars of sugar beet and genes responsive to the exudates included genes known to be involved in recognition and chemotaxis towards plant root exudates as well as genes involved in aromatic compound catabolism, energy generation and amino biosynthesis and metabolism, type III secretion and various hypothetical proteins. In addition to chemotaxis towards exudates, mucilage and other rhizodeposits characteristics like bacterial flagella, quorum sensing as well as the production of specific compounds/enzymes are involved in the rhizosphere/rhizoplane colonization process (Böhm et al., 2007; Cho et al.,

2007; Turnbull et al., 2001). Furthermore since root exudates and mucilage-derived nutrients attract a myriad of organisms to the rhizosphere environment (Buée et al., 2009; Mendes et al., 2013; Raaijmakers et al., 2008), beneficial plant-associated bacteria have to be highly competitive to successfully colonize the root zone (Compant et al., 2010). The production of secondary metabolites involved in biocontrol (such as siderophores, lytic enzymes and antibiotics) provide some bacteria a selective and competitive advantage against other microorganisms, thereby contributing to their rhizocompetence (Lugtenberg and Kamilova, 2009; Raaijmakers et al., 2008).

After rhizoplane colonization, endophytic competence, i.e. the ability to successfully colonize the host plant involves several specific characteristics (Compant et al., 2010). Most evidence suggests that endophytic bacteria enter their host plant at naturally occurring cracks in the roots and/or root tips such as those found at root emergence sites (lateral root junctions) or those created by deleterious microorganisms (James and Olivares, 1998; James et al., 2002; Monteiro et al., 2012; Reinhold-Hurek and Hurek, 2011). The colonization process does not necessarily involve active mechanisms and thus all rhizosphere bacteria can be expected to be endophytic at one stage of their life (Hardoim et al., 2008). Especially the progression from the rhizoplane to the root cortex may occur via passive mechanisms at natural breaks in root and/or root tips. However, further endophytic colonization, crossing barriers such as the endodermis and pericycle in the root cortex, is unlikely to be an entirely passive process (Compant et al., 2010; Gregory, 2006). Although the endodermal cell layer is often disrupted by the formation of secondary roots (which derive from the pericycle) (Casimiro et al., 2003) or the action of deleterious bacteria, many endophytic bacteria express cell-wall-degrading enzymes (CWDEs), albeit generally in lower concentrations than expressed by plant pathogens (Monteiro et al., 2012). Genome analysis of the non-nodulating endophyte *Azoarcus* sp. BH72 revealed the presence of genes encoding CWDEs such as cellulases and polygalactorunases (Krause et al., 2006). Moreover, few endophytic bacteria (*Herbaspirillum* sp.) have been shown to posses Type-3-secretion systems (T3SS), which are the route of exit for excreted plant CWDEs (Sessitsch et al., 2012). Fouts et al. (2008) reported additional genes involved in endophytic competence based on the genome analysis of *Klebsiella pneumoniae* Kp342.

More specifically genes involved in chemotaxis, the formation of flagella and pili but also various metabolic pathways (catabolism of plant-derived polysaccharides) and transport systems were observed. After passing through the endodermis barrier, endophytic bacteria have to penetrate the pericycle to further reach the root xylem vessels of their hosts and spread systematically inside the plant colonizing the stems and leafs (Compant et al., 2010; Hardoim et al., 2008). Endophyte numbers are generally lower in aerial parts than in roots, which suggests that although there is some upward movement of endophytes within their hosts, supported through the plant transpiration stream, this movement is limited, and may only be possible for bacteria that express CWDEs and/or T3SS (Compant et al., 2010; Monteiro et al., 2012). In addition, amongst others lipopolysaccharides, flagella, pili, and twitching motility have been shown to affect endophytic colonization and bacterial mobility within host plants (Böhm et al., 2007; Dörr et al., 1998; Duijff et al., 1997).

Endophytic competence and the active mechanisms associated with colonization (e.g. secretion of CWDEs) require intricate interplay between the endophyte microbiome and the plant innate immune system (Jones and Dangl, 2006). Plants have evolved an elaborate innate immune system consisting of two classes of immune receptors that detect the presence of non-self molecules both inside and on the surface of host cells: (1) transmembrane pattern recognition receptors (PRRs) that respond to slowly evolving microbial- or pathogen-associated molecular patterns (MAMPs or PAMPs) such as flagellin, the translocation elongation factor Tu, bacterial liposaccharide or fungal chitin (Boller and Felix, 2009; Boller and He, 2009) and (2) polymorphic NB-LRR protein products (encoded by most resistance(R)-genes) named after their characteristic nucleotide binding (NB) and leucine rich repeat (LRR) domains (Bent and Mackey, 2007), which act largely inside the cell and recognize pathogen effectors from diverse kingdoms where after they activate similar defence responses (Jones and Dangl, 2006). The plant response includes production of reactive oxygen species, strengthening of the cell wall, activation of signalling and defence genes and the accumulation of antimicrobials in healthy tissues (Turner et al., 2013). Plant defence signalling is coordinated by pathogen-specific hormonal regulation (Bari and Jones, 2009). Salicylic acid is produced in response to attack by biotrophic pathogens (pathogens that colonize

living plant tissue and obtain nutrients from living host cells) (Iniguez et al., 2005) whereas jasmonate controls responses to insect herbivores and necrotrophic pathogens (pathogens that infect and kill host tissue and extract nutrients from the dead host cells) (Miché et al., 2006; Van der Ent et al., 2009). Furthermore ethylene is also produced in response to herbivores, necrotrophic pathogens, and environmental and developmental signals and moreover has the potential to modulate the jasmonate and salicylic acid signalling pathways (Turner et al., 2013). The elaborate plant innate immune system and the identification of an increasing number of pattern recognition receptors on the plant cell surface seems difficult to reconcile with endophytic colonization of soil-derived bacteria (Bulgarelli et al., 2013). Indeed some endophytic bacteria have been known to produce defence mechanisms in plants (James et al., 2002). However, genomic responses from several studies suggest that the response of the plant immune system is very different to their reactions to phytopathogens (Monteiro et al., 2012). The best-studied systems have been those involving the inoculation of sugarcane and rice by defined strains of endophytic and/or rhizospheric bacteria, particularly *Azospirillum*, *Burkholderia*, *Gluconacetobacter* and *Herbaspirillum* spp (Brusamarello-Santos et al., 2011; Cavalcante et al., 2007; Vinagre et al., 2006). Inoculation of the sugar cane variety B4362 with *Herbaspirillum seropedicae* (non-pathogenic endophyte) resulted in significantly decreased expression of the LRR-rich receptor-like kinase SHR5 as compared to the inoculation with the phytopathogenic relative *Herbaspirillum rubrisubalbicans* (Monteiro et al., 2012; Vinagre et al., 2006). Furthermore, in sugar cane ethylene response transcription factors (ERFs), which were repressed after inoculation with endophytic bacteria, were strongly upregulated when challenged with phytopathogens such as *Leifsonia xyli* and sugarcane mosaic virus (Brusamarello-Santos et al., 2011; Cavalcante et al., 2007). Possible mechanisms for the evasion of the plant immune system by the endophytic bacteria include: (1) immune response interception as demonstrated by some pathogenic microbes (Boller and He, 2009), (2) effective MAMP camouflage mechanisms to escape immune receptor detection, (3) limited secretion of different compounds and secondary metabolites (James et al., 2002). Reversely, the plant immune system may control endophytic populations by inducing mild defence reactions, thereby limiting endophyte multiplication

and keeping endophytes titers well below those of pathogenic bacteria (Bulgarelli et al., 2013).

1.7.3 Bacterial microbiome in the phyllosphere environment

The phyllosphere environment, i.e. the aerial outer surface of a plant with the bulk of this surface provided by green leaves, is thought to represent one of the largest microbial habitats on Earth (Lindow and Brandl, 2003; Vorholt, 2012). The phyllosphere embodies an environment much more dynamic than the rhizosphere where buffered fluctuations of abiotic conditions prevail. Resident microbes are subjected to large fluctuations in temperature, moisture and UV light radiation throughout the day/night and moreover face limited access to nutrients (Hirano, 2000). Unlike root exudation, which releases significant amounts of photosynthetically fixed carbon into rhizosphere, no mechanism exists for the constant supply of soluble organic compounds to leaf and/or stem surfaces. Microbial colonization of leaves is not homogenous but is affected by leaf structures such as veins, hairs and stomata and microbial phyllosphere communities are highly variable (intraspecies and temporal) with reduced complexity (Lindow and Brandl, 2003; Redford et al., 2010). A few bacterial genera, including *Pseudomonas*, *Sphingomonas*, *Methylobacterium*, *Bacillus*, *Massilia*, *Arthrobacter* and *Pantoea*, appear to compose the core of phyllosphere communities (Delmotte et al., 2009). The low-complexity phyllosphere communities may originate from several sources: (1) air and its aerosols, which flow around the leaves and moreover abundant sequences assigned to *Sphingomonas* and *Pseudomonas* were identified in clone libraries of several aerosol samples (Fahlgren et al., 2010); (2) neighbouring plants and plant debris; (3) water, as reported by Delmotte et al. (2009) in a meta-proteogenomics approach to compare the phyllosphere communities of paddy-field-grown rice (*Oryza sativa*) plants in relation to the flooding water of the paddy field. Recently proteogenomic analyses of various phyllosphere microbiomes have revealed differential adaptation strategies to the leaf environment (Delmotte et al., 2009). These analyses revealed species that assimilate plant-derived ammonium, amino acids and simple carbohydrates, implicating these compounds as primary nitrogen and carbon sources in the phyllosphere. These studies also observed that *Methylobacterium* spp., a widely abundant phyllosphere microbe, expresses proteins for the active assimilation

and metabolism of methanol, a by-product of plant cell wall metabolism derived from pectin. These bacteria seem to adapt to the phyllosphere via a specific methylotrophic one-carbon metabolism. Reversely, *Sphingomonas* spp. contained multiple transport proteins (e.g. TonB-dependent receptors) indicating a large substrate spectrum as adaptation strategy to low-nutrient availability.

1.8. Determining the composition of plant microbiomes

Although healthy plants are associated with an astounding number of bacteria in the soil immediately adjacent to and under the influence of the root system (rhizosphere), in their internal tissues (endosphere) and at the air-plant interface (phyllosphere), it has been challenging to define the absolute composition of plant microbiomes.

Two major approaches can be distinguished to investigate plant microbiomes: cultivation-dependent and cultivation-independent characterization. For decades, plant-microbiota research relied on cultivation-based methods to characterize plant-associated bacterial communities (Compant et al., 2010; Hardoim et al., 2008; Turner et al., 2013). Culture-dependent studies provide (a) detailed information about specific, readily isolated bacteria, (b) isolated pure bacterial cultures suited for genome sequencing and the unravelling of genes responsible for e.g. efficient rhizospheric and endophytic colonization and/or genes responsible for plant-growth promotion mechanisms (Fouts et al., 2008; Krause et al., 2006) and (c) collections of phenotypically screened bacterial strains (e.g. plant growth promotion characteristics, metal resistance, potential to degrade organic pollutants) which can be exploited for example to improve biomass production and/or phytoremediation (Weyens et al., 2009a, 2009b) or for the production of secondary metabolites (Brader et al., 2014). In contrast to their advantages, culture-dependent studies also entail some inherent drawbacks including: (a) giving an incomplete view of microbiomes and lacking the sensitivity to detect small shifts in community compositions and (b) introducing significant bias in the taxa they identify and drastically limiting community diversity estimates (Lebies et al., 2014).

More recently, the development and implementation of massive parallel sequencing technologies (next-generation sequencing) and their corresponding bioinformatics tools have revolutionized the methods for studying microbial

ecology by enabling high-resolution community profiling (Margulies et al., 2005; Metzker, 2010; Shendure and Ji, 2008; Sogin et al., 2006).

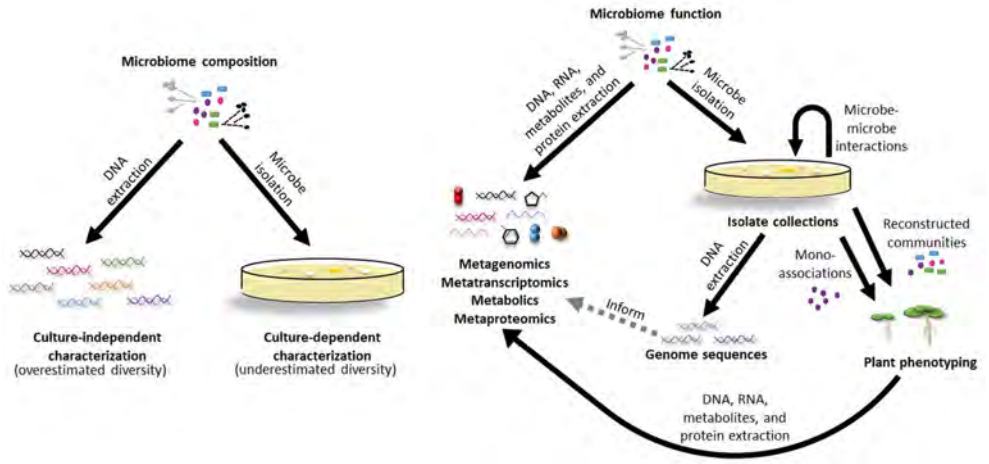

Figure 1.5. Methods for characterization of plant microbiome composition and function (Lebeis et al., 2014). (A) *Culture-dependent and culture-independent methods are the two major approaches used to determine the microbial make-up of plant microbiomes with each having its own limitations in identifying community composition. (B) Proposed pipelines to integrate the data from culture-independent and culture-dependent methods together to address functions of plant microbiomes and the individual types of microbes found within them.*

These sequencing technologies are the cornerstones of the culture-independent characterization of plant microbiomes. They perform a survey of all 16S rRNA sequences (after DNA extraction and PCR amplification) and give a detailed picture in terms of diversity and community composition. These technologies use miniaturized, spatially separated clonal amplification to sequence, rather than individual Sanger sequencing reactions, with various chemistries including: pyrosequencing (e.g. 454), reverse dye terminator (e.g. Illumina), phospholinked fluorescent nucleotides (e.g., PacBio), and proton detection (e.g. Ion Torrent). Each platform has unique platform-specific up-stream preparations and down-stream analyses, but they all hold great potential for use in plant-microbiota research. Although these next-generation sequencing technologies have unearthed insights beyond the information provided by individual microbes, they still represent only a projection of microbial communities and are not

exempt from drawbacks. For example, they do not differentiate live from dead cells, potentially contain sequencing errors that lead to misinterpretations of the data, including diversity overestimations, and are subject to primer biases (Berry et al., 2011; Kennedy et al., 2014; Claesson et al., 2010). Nonetheless, studies using massive parallel sequencing have defined plant-associated microbial communities for a wide variety of plant species from *Arabidopsis thaliana* (Bulgarelli et al., 2012; Lundberg et al., 2012) to poplar (Gottel et al., 2011) and potato (Inceoğlu et al. 2010). Although it is difficult to infer general conclusions from all these results due to various up-stream and down-stream variations in the sequencing protocols used, differentiation of the bacterial microbiome between the external rhizosphere and internal root bacterial communities is very clear (microbiome niche differentiation).

1.9. Microbiome niche differentiation between plant environments

Within plant-microbiota research, intra-plant niche differentiation (or compartmentalization) within the available ecological niches in plants (rhizosphere/rhizoplane, root, stem and leaf endosphere) of the bacterial microbiomes has been sporadically evaluated. Niche differentiation at the rhizosphere soil-root interface has been reported in a limited amount of studies (Bulgarelli et al., 2012; Gottel et al., 2011; Inceoğlu et al. 2010; Lundberg et al., 2012; Weinert et al., 2011). Gottel et al. (2011) compared the bacterial (and fungal) microbiota of mature poplar (*Populus deltoides*) trees growing at two natural sites using 16S rRNA gene pyrosequencing and revealed strikingly different root endophytic bacterial communities as compared with the surrounding rhizosphere. Root endophyte microbiota were differentiated by an order-of-magnitude reduction in richness and were dominated by members of Proteobacteria whereas Acidobacteria dominated rhizosphere assemblages. Qualitatively similar observations were reported in two independent studies on the bacterial root microbiota of *Arabidopsis.* Both studies encountered remarkably different microbiota in the root tissues as compared to the rhizosphere or unplanted soil as evaluated by reduced richness of the root-inhabiting communities and concomitant increases in the abundance of Actinobacteria, Bacteroidetes, and Proteobacteria (Bulgarelli et al., 2012; Lundberg et al., 2012). Recently, Bulgarelli et al. (2013) inferred some general principles concerning niche differentiation from the available literature. In the

bulk soil biomes, edaphic factors determine the structure of the bacterial communities where after the first differentiation step, rhizodeposits (and the resulting chemo-tactic effects) and host cell wall features of the plant roots fuels a substrate-driven community shift to form distinctive rhizosphere microbiomes. Subsequently, host genotype-dependent selection, with the plant innate immune system as main driving factor, of communities thriving on the rhizoplane leads to differentiation of the endophytic microbiota within the plant roots. Further, niche differentiation in the aerial plant compartments (stem and leaf endosphere) was suggested by Bulgarelli et al. (2013) but is yet to be validated by experimental data.

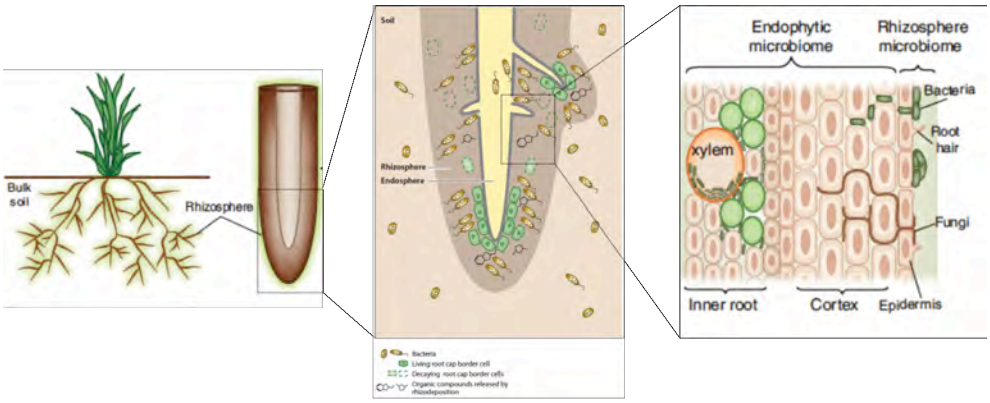

Figure 1.6. Microbiome niche differentiation at the root-soil interface (Adapted from Bulgarelli et al. (2013) and Hirsch and Mauchline (2012)). From outside to inside, the habitats are the bulk soil, rhizosphere, and endosphere. Rhizodeposits generated from root cap border cells and the rhizodermis provoke a shift in the soil biome. Cellular disjunction of the root surface during lateral root emergence provides a potential entry gate for the rhizosphere microbiota into the root interior. The rhizosphere microbiome includes bacteria and fungi that are recruited from bulk soil and colonize the root surface. The endophytic microbiome includes species that infiltrate the root cortex and live as endophytes until their release back into the soil upon root senescence.

1.10. Modification of the lignin biosynthesis in poplar (gene silencing of *CCR*) versus the plant bacterial microbiome

1.10.1. General effects of plant host genotype on their microbiome

The microbiome can be considered as an extension of the host genome or even as the plant's second genome. The interactions between a plant and its microbiome are highly complex and dynamic, as described above, involving multiple reciprocal signalling mechanisms and intricate interplay between bacteria and the plant's innate immune system. Therefore, even small changes in the host genome (ecotypes, cultivars, genetically modified genotypes, etc.) may influence the plant microbiome, and these changes may even feed back to modulate the behaviour of the host. However, only few studies have explored the magnitude of host genotype–dependent variation on bacterial root microbiota profiles. Recently, Lundberg et al. (2012) and Bulgarelli et al. (2012) evaluated the host genotype-dependent effect of several *Arabidopsis* ecotypes in a similar approach and revealed significant but weak host genotype–dependent effects act in the selection of *Arabidopsis* root-inhabiting bacterial communities. Lundberg et al. (2012) identified a total of 12 OTUs (operational taxonomic units) exhibiting host genotype–dependent quantitative enrichment in the root endophyte compartment among 778 measurable OTUs in eight *Arabidopsis* ecotypes whereas Bulgarelli et al. (2012) only identified one OTU differentially abundant in the roots of two *Arabidopsis* ecotypes. Furthermore Wienert et al. (2011) used Phylochip, a high-density 16S rRNA gene probe array that can detect up to 8,741 known OTUs, to examine the root endophytes of three field-grown potato cultivars and revealed quantitative cultivar dependence for 9% of the OTUs detected (2432). Moreover, studies in other organisms, particular in the human gut, have revealed strong host genotype effects and even single host genes which affect the microbiota (such as *MEFV*, encoding pyrin)(Spor et al., 2011).

1.10.2. Specific effects of lignin-reduced host genotype

Modification of the lignin biosynthesis in poplar, via gene silencing of cinnamoyl-CoA reductase (*CCR*), the first enzyme in the monolignol-specific branch of lignin biosynthesis, leads to several specific host genotype-dependent alterations in the plant cells, which have the potential to interfere with the plant microbiome.

Firstly, gene silencing of *CCR* and by extension most of the genes silenced in the lignin biosynthesis, leads to flux changes in the phenylpropanoid and monolignol-specific pathways (see 1.5 lignin engineering and consequences). Briefly, in poplar *CCR*-down-regulation increased the concentrations of ferulic and sinapic acids relative to those of coniferaldehyde and sinapaldehyde and strong accumulation of the phenolic glucosides O^4-b-D-glucopyranosyl sinapic acid (GSA) and O^4-b-D-glucopyranosyl vanillic acid (GVA) occurred, as well as an altered hemicellulose and pectin metabolism and an alteration in the general carbohydrate metabolism. In general, the *CCR*-down-regulation resulted in a differential accumulation of several carbon sources in developing xylem, most notably soluble phenolics. Substrate-driven selection in the rhizosphere of bacterial communities in response to rhizodeposition is a well-documented phenomenon (Bais et al., 2006; Haichar et al., 2008; Shi et al., 2011). Compositional changes in the root exudates of plant species, genotypes, cultivars, plant growth stages result in the selective attraction of rhizobacterial assemblages (Cavaglieri et al., 2009; Chaparro et al., 2013; DeAngelis et al., 2009; Haichar et al., 2008; Inceoğlu et al., 2010; Mark et al., 2005; Micallef et al., 2009). Furthermore, several studies have indicated that once inside their hosts endophytic bacteria change their metabolism and become adapted to their internal environment (de Santi Ferrara et al., 2011; Monteiro et al., 2012; Sessitsch et al., 2012). Indeed, redirection of the fluxes in the phenylpropanoid and monolignol-specific pathways leads to the accumulation of soluble phenolics in the xylem vessels. As these xylem vessels have been frequently reported as a route for spreading and residence of endophytic bacteria, direct contact between the endophytes and the accumulated soluble phenolics can be ensured. Moreover, phenolic-related compounds have been implicated in the modulation of the rhizosphere microbiome in *Arabidopsis thaliana* (Badri et al., 2013), underlining their potential to affect bacterial communities.

Secondly, perturbations in the lignin biosynthesis via *CCR*-down-regulation lead to compositional alterations in the cell wall. Most notably, the cell walls have looser structures due to lower lignin contents and alternative monomers (such as ferulic acid in poplar) may be incorporated in the lignin polymers (Leplé et al., 2007). Cell wall features play important roles during endophytic colonization. Endophytic competence and active colonization mechanisms by soil-derived

bacteria predominantly rely on the secretion of cell-wall degrading enzymes (CWDEs) (Compant et al., 2010; Hardoim et al., 2008). Cell walls with more loose structures could be more easily accessible and passive entry mechanisms may play a more substantial role during colonization. This could allow soil-derived bacteria, which otherwise would not have the ability to penetrate the plant tissues, to adapt to an endophytic lifestyle. This could also have implications for pathogen colonization (see 1.10.3). Moreover, cell walls may serve as carbon sources in nutrient-poor environments such as the leaf endosphere and fully differentiated xylem vessels, indicating that the incorporation of alternative monomers in the lignin polymers may also exert selective pressure on the plant-associated bacterial communities. And finally, Bulgarelli et al. (2012) reported that cell wall features can serve as sufficient assembly (colonization) cues in root microbiota of *Arabidopsis thaliana.* Therefore, compositional alterations in the cell walls may result in changes in the bacterial colonization of the *CCR*-down-regulated trees.

1.10.3. Role of secondary wall in plant resistance to pathogens

Plants have evolved a myriad of resistance mechanisms, which are either constitutively present or induced after pathogen attack, to resist the continuous threat of biotic stresses caused by pathogenic bacteria, fungi, viruses and oomycetes (Jones and Dangl, 2006). Plant cell walls, with lignin as major component, also play important roles in preventing pathogen invasion. They act as passive barriers, provide a reservoir for antimicrobial compounds and are a source of signalling molecules that trigger immune responses (Cantu et al., 2008; Hématy et al. 2009). Perturbations in the lignin biosynthesis needed for improved industrial processing of the biomass could conflict with the principal biological roles of the cell wall as a supportive and protective structure. Miedes et al. (2014) recently reviewed detailed aspects of the role of secondary cell wall in plant resistance to pathogens. Contra-intuitively, gene silencing of essential genes involved in the lignin biosynthesis and reducing the lignin content does not automatically lead to enhanced susceptibility to pathogens. Indeed some studies report the occurrence of enhanced susceptibility of lignin-reduced genotypes to pathogens (such as the reduction of *PAL* in tobacco (Maher et al., 1994)) whereas for example in hybrid poplar (*Populus tremula* × *Populus alba*) no increased disease incidence was observed in field-grown antisense *COMT* and

CAD lines relative to that observed in wild-type trees (Halpin et al., 2006; Pilate et al., 2002).

1.10.4. Biomass production

Perturbations in the lignin biosynthesis often affect plant growth and development. Indeed, *CCR*-down-regulation causes the development of dwarf phenotypes in *Arabidopsis thaliana* (Mir Derikvand et al., 2008; Ruel et al., 2009; Van Acker et al., 2013) and reduced biomass production in *Populus tremula x alba* (Leplé et al., 2007; Van Acker et al., 2014), thereby countervailing, at least to some extent, the improved processing efficiency of these genetically engineered plants by reducing the total biomass yield.

Beneficial plant-associated bacteria, collectively termed plant growth promoting bacteria (PGPB), can play a key role in supporting and/or enhancing plant health and growth (Compant et al., 2010; Hardoim et al., 2008). There is a great potential for optimizing biomass production through the application of plant-associated bacteria as evidenced by a 55% biomass increase in poplar cuttings 17 weeks after inoculation with *Enterobacter* sp.strain 638 (Rogers et al., 2012). PGBs are diverse in their modes of action, including nitrogen fixation by diazotrophic bacteria, mobilisation/solubilisation of highly unavailable nutrients (e.g. iron, phosphorus, etc.), production of phytohormones (auxins, cytokinins, gibberelins) and the suppression of stress ethylene production by 1-aminocyclopropane-1-carboxylic acid (ACC) deaminase activity (Bloemberg and Lugtenberg, 2001; Bulgarelli et al., 2013; Zhang et al., 2007).

The selection and inoculation of specific bacterial strains in lignin-reduced biomass-impared genotypes could contribute to the generation of plants with (a) high processing efficiency due to lower lignin levels and (b) optimized biomass production through the inoculation with PGPBs.

References

Alejandro, S., Lee, Y., Tohge, T., Sudre, D., Osorio, S., Park, J., Bovet, L., Lee, Y., Geldner, N., Fernie, A. and Martinoia, E. (2012). AtABCG29 is a monolignol transporter involved in lignin biosynthesis. *Current Biology : CB*, *22*, 1207–1212.

Andrews, S.S. (2006). Crop Residue Removal for Biomass Energy Production: Effects on Soils and Recommendations. USDA-NRCS

Badri, D. V, Chaparro, J. M., Zhang, R., Shen, Q. and Vivanco, J. M. (2013). Application of natural blends of phytochemicals derived from the root exudates of Arabidopsis to the soil reveal that phenolic-related compounds predominantly modulate the soil microbiome. *The Journal of Biological Chemistry*, *288*, 4502–4512.

Bais, H. P., Weir, T. L., Perry, L. G., Gilroy, S. and Vivanco, J. M. (2006). The role of root exudates in rhizosphere interactions with plants and other organisms. *Annual Review of Plant Biology*, *57*, 233–266.

Bakker, P. A. H. M., Berendsen, R. L., Doornbos, R. F., Wintermans, P. C. A. and Pieterse, C. M. J. (2013). The rhizosphere revisited: root microbiomics. *Frontiers in Plant Science*, *165*, 1-7.

Bari, R. and Jones, J. D. G. (2009). Role of plant hormones in plant defence responses. *Plant Molecular Biology*, *69*, 473–488.

Bent, A. F. and Mackey, D. (2007). Elicitors, effectors, and R genes: the new paradigm and a lifetime supply of questions. *Annual Review of Phytopathology*, *45*, 399–436.

Berendsen, R. L., Pieterse, C. M. J. and Bakker, P. A. H. M. (2012). The rhizosphere microbiome and plant health. *Trends in Plant Science*, *17*, 478–486.

Berg, G., Grube, M., Schloter, M. and Smalla, K. (2014). Unraveling the plant microbiome: looking back and future perspectives. *Frontiers in Microbiology*, *5*, 148, 1-7.

Berner, R. A. (2003). The long-term carbon cycle, fossil fuels and atmospheric composition. *Nature*, *426*, 323–326.

Berry, D., Mahfoudh, K. B., Wagner, M. and Loy A. Barcoded Primers used in Multiplex Amplicon Pyrosequencing Bias Amplification. Applied and Environmental Microbiology, *77*, 7846-7849.

Berthet, S., Demont-Caulet, N., Pollet, B., Bidzinski, P., Cézard, L., Le Bris, P., Borrega, N., Hervé, J., Blondet, E., Balzergue, S., Lapierre, C. and Jouanin, L. (2011). Disruption of LACCASE4 and 17 results in tissue-specific alterations to lignification of Arabidopsis thaliana stems. *The Plant Cell*, *23*, 1124–1137.

Bertin, C., Yang, X. and Weston, L. A. (2003). The role of root exudates and allelochemicals in the rhizosphere. *Plant and Soil*, *256*, 67–83.

Blanco-Canqui, H. and Lal, R. (2009). Crop Residue Removal Impacts on Soil Productivity and Environmental Quality. *Critical Reviews in Plant Sciences*, *28*, 139–163.

Bloemberg, G. V and Lugtenberg, B. J. (2001). Molecular basis of plant growth promotion and biocontrol by rhizobacteria. *Current Opinion in Plant Biology*, *4*, 343–350.

Boerjan, W., Ralph, J., and Baucher, M. (2003). Lignin biosynthesis. *Annual Review of Plant Biology*, *54*, 519–546.

Böhm, M., Hurek, T. and Reinhold-Hurek, B. (2007). Twitching motility is essential for endophytic rice colonization by the N2-fixing endophyte Azoarcus sp. strain BH72. *Molecular Plant-Microbe Interactions*, *20*, 526–533.

Boller, T. and Felix, G. (2009). A renaissance of elicitors: perception of microbe-associated molecular patterns and danger signals by pattern-recognition receptors. *Annual Review of Plant Biology*, *60*, 379–406.

Boller, T. and He, S. Y. (2009). Innate immunity in plants: an arms race between pattern recognition receptors in plants and effectors in microbial pathogens. *Science*, *324*, 742–744.

Bonito, G., Reynolds, H., Robeson, M. S., Nelson, J., Hodkinson, B. P., Tuskan, G., Schadt, C. and Vilgalys, R. (2014). Plant host and soil origin influence fungal and bacterial assemblages in the roots of woody plants. *Molecular Ecology*, *23*, 3356–3370.

Bonkowski, M., Villenave, C. and Griffiths, B. (2009). Rhizosphere fauna: the functional and structural diversity of intimate interactions of soil fauna with plant roots. *Plant and Soil*, *321*, 213–233.

Brader, G., Compant, S., Mitter, B., Trognitz, F. and Sessitsch, A. (2014). Metabolic potential of endophytic bacteria. *Current Opinion in Biotechnology*, *27*, 30–37.

Bron, P. A., van Baarlen, P. and Kleerebezem, M. (2012). Emerging molecular insights into the interaction between probiotics and the host intestinal mucosa. *Nature Reviews. Microbiology*, *10*, 66–78.

Brusamarello-Santos, L. C. C., Pacheco, F., Aljanabi, S. M. M., Monteiro, R. A., Cruz, L. M., Baura, V. A., Pedrosa, F. O., Souza, E. M. and Wassem, R. (2011). Differential gene expression of rice roots inoculated with the diazotroph Herbaspirillum seropedicae. *Plant and Soil*, *356*, 113–125.

Buée, M., De Boer, W., Martin, F., van Overbeek, L. and Jurkevitch, E. (2009). The rhizosphere zoo: An overview of plant-associated communities of microorganisms, including phages, bacteria, archaea, and fungi, and of some of their structuring factors. *Plant and Soil*, *321*, 189–212.

Bulgarelli, D., Rott, M., Schlaeppi, K., Ver Loren van Themaat, E., Ahmadinejad, N., Assenza, F., Rauf, P., Huettel, B., Reinhardt, R., Schmelzer, E., Perlies, J., Gloeckner, F. O., Amann, R., Eickhorst, T. and Schulze-Lefert, P. (2012). Revealing structure and assembly cues for Arabidopsis root-inhabiting bacterial microbiota. *Nature*, *488*, 91–95.

Bulgarelli, D., Schlaeppi, K., Spaepen, S., Ver Loren van Themaat, E. and Schulze-Lefert, P. (2013). Structure and functions of the bacterial microbiota of plants. *Annual Review of Plant Biology*, *64*, 807–838.

Cantu, D., Vicente, A. R., Labavitch, J. M., Bennett, A. B. and Powell, A. L. T. (2008). Strangers in the matrix: plant cell walls and pathogen susceptibility. *Trends in Plant Science*, *13*, 610–617.

Cardona, C. A., Quintero, J. A. and Paz, I. C. (2010). Production of bioethanol from sugarcane bagasse: Status and perspectives. *Bioresource Technology*, *101*, 4754–4766.

Carriquiry, M. A., Du, X. and Timilsina, G. R. (2011). Second-generation biofuels: Economics and policies. *Energy Policy*, *39*, 4222–4234.

Casimiro, I., Beeckman, T., Graham, N., Bhalerao, R., Zhang, H., Casero, P., Sandberg, G., and Bennett, M. J. (2003). Dissecting Arabidopsis lateral root development. *Trends in Plant Science*, *8*, 165–171.

Cassman, K. G. (2007). Climate change, biofuels, and global food security. *Environmental Research Letters*, *2*, 1-3.

Cassman, K. G. and Liska, A. J. (2007). Food and fuel for all : realistic or foolish ? *Biofuels, Bioproducts and Biorefining*, *1*, 18–23.

Cavaglieri, L., Orlando, J. and Etcheverry, M. (2009). Rhizosphere microbial community structure at different maize plant growth stages and root locations. *Microbiological Research*, *164*, 391–399.

Cavalcante, J. J. V, Vargas, C., Nogueira, E. M., Vinagre, F., Schwarcz, K., Baldani, J. I., Ferreira, P. C. G., Hemerly, A. S. (2007). Members of the ethylene signalling pathway are regulated in sugarcane during the association with nitrogen-fixing endophytic bacteria. *Journal of Experimental Botany*, *58*, 673–686.

Chabannes, M., Barakate, A., Lapierre, C., Marita, J. M., Ralph, J. and Pean, M. (2001). Strong decrease in lignin content without significant alteration of plant development is induced by simultaneous down-regulation of cinnamoyl CoA reductase (*CCR*) and cinnamyl alcohol dehydrogenase (*CAD*) in tobacco plants, *28*, 257–270.

Chaparro, J. M., Badri, D. V, Bakker, M. G., Sugiyama, A., Manter, D. K., and Vivanco, J. M. (2013). Root exudation of phytochemicals in Arabidopsis follows specific patterns that are developmentally programmed and correlate with soil microbial functions. *PloS One*, *8*, e55731.

Chen, F. and Dixon, R. A. (2007). Lignin modification improves fermentable sugar yields for biofuel production. *Nature Biotechnology*, *25*, 759–761.

Cho, H.-S., Park, S.-Y., Ryu, C.-M., Kim, J. F., Kim, J.-G. and Park, S.-H. (2007). Interference of quorum sensing and virulence of the rice pathogen Burkholderia glumae by an engineered endophytic bacterium. *FEMS Microbiology Ecology*, *60*, 14–23.

Claesson, M., Wang, Q., O'Sullivan O., Greene-Diniz, R., Cole, J. R., Ross, R. P. and O'Toole P. W. (2010). Comparison of two next-generation sequencing technologies for resolving highly complex microbiota composition using tandem variable 16S rRNA gene regions. *Nucleic acids research*, *38*, e200.

Compant, S., Clément, C. and Sessitsch, A. (2010). Plant growth-promoting bacteria in the rhizo- and endosphere of plants: Their role, colonization, mechanisms involved and prospects for utilization. *Soil Biology and Biochemistry*, *42*, 669–678.

Compant, S., Kaplan, H., Sessitsch, A., Nowak, J., Ait Barka, E. and Clément, C. (2008). Endophytic colonization of Vitis vinifera L. by Burkholderia phytofirmans strain PsJN: from the rhizosphere to inflorescence tissues. *FEMS Microbiology Ecology*, *63*, 84–93.

Compant, S., Mitter, B., Colli-Mull, J. G., Gangl, H. and Sessitsch, A. (2011). Endophytes of Grapevine Flowers, Berries and Seeds: Identification of cultivable bacteria, comparison with other plant parts and visualisation of niches of colonization. *Microbial Ecology*, *62*, 188-197.

Cosgrove, D. J. (2005). Growth of the plant cell wall. *Nature Reviews. Molecular Cell Biology*, *6*, 850–861.

Custers, R. (2009). First GM trial in Belgium since 2002. *Nature Biotechnology*, 27, 506.

Davin, L. B. (1997). Stereoselective Bimolecular Phenoxy Radical Coupling by an Auxiliary (Dirigent) Protein Without an Active Center. *Science*, *275*, 362–367.

Demont-Caulet N., Lapierre C., Jouanin L., Baumberger S. and Méchin V. (2010). Arabidopsis peroxidase-catalyzed copolymerization of coniferyl and sinapyl alcohols: Kinetics of an endwise process. *Phytochemistry*, 71, 1673-1683.

De Santi Ferrara, F. I., Oliveira, Z. M., Gonzales, H. H. S., Floh, E. I. S. and Barbosa, H. R. (2011). Endophytic and rhizospheric enterobacteria isolated from sugar cane have different potentials for producing plant growth-promoting substances. *Plant and Soil*, *353*, 409–417.

De Weert, S., Vermeiren, H., Mulders, I. H. M., Kuiper, I., Hendrickx, N., Bloemberg, G. V, Vanderleyden, J., De Mot, R. and Lugtenberg, B. J. J. (2002). Flagella-driven chemotaxis towards exudate components is an important trait for tomato root colonization by Pseudomonas fluorescens. *Molecular Plant-Microbe Interactions*, *15*, 1173–1180.

DeAngelis, K. M., Brodie, E. L., DeSantis, T. Z., Andersen, G. L., Lindow, S. E. and Firestone, M. K. (2009). Selective progressive response of soil microbial community to wild oat roots. *The ISME Journal*, *3*, 168–178.

Delmotte, N., Knief, C., Chaffron, S., Innerebner, G., Roschitzki, B., Schlapbach, R., von Mering, C. and Vorholt, J. A. (2009). Community proteogenomics reveals insights into the physiology of phyllosphere bacteria. *Proceedings of the National Academy of Sciences of the United States of America*, *106*, 16428–16433.

Dennis, P. G., Miller, A. J. and Hirsch, P. R. (2010). Are root exudates more important than other sources of rhizodeposits in structuring rhizosphere bacterial communities? *FEMS Microbiology Ecology*, *72*, 313–327.

Derrien, M., van Passel, M. W., van de Bovenkamp, J. H., Schipper, R. G., de Vos, W. M. and Dekker, J. (2010). Mucin-bacterial interactions in the human oral cavity and digestive tract. *Gut Microbes*, *1*, 254–268.

Dillon, R. J. and Dillon, V. M. (2004). The gut bacteria of insects: nonpathogenic interactions. *Annual Review of Entomology*, *49*, 71–92.

Doornbos, R. F., van Loon, L. C. and Bakker, P. A. H. M. (2011). Impact of root exudates and plant defense signaling on bacterial communities in the rhizosphere. A review. *Agronomy for Sustainable Development*, *32*, 227–243.

Dörr, J., Hurek, T. and Reinhold-Hurek, B. (1998). Type IV pili are involved in plant-microbe and fungus-microbe interactions. *Molecular Microbiology*, *30*, 7–17.

Duijff, B. J., Gianinazzi-Pearson, V. and Lemanceau, P. (1997). Involvement of the outer membrane lipopolysaccharides in the endophytic colonization of tomato roots by biocontrol Pseudomonas fluorescens strain WCS417r. *New Phytologist*, *135*, 325–334.

Dunkley, T. P. J., Hester, S., Shadforth, I. P., Runions, J., Weimar, T., Hanton, S. L., Griffin, J. L., Bessant, C., Brandizzi, F., Hawes, C., Watson, R. B., Dupree, P. and Lilley, K. S. (2006). Mapping the Arabidopsis organelle proteome. *Proceedings of the National Academy of Sciences of the United States of America*, *103*, 6518–6523.

Dyall, S. D., Brown, M. T. and Johnson, P. J. (2004). Ancient invasions: from endosymbionts to organelles. *Science*, *304*, 253–257.

Fagundes, C. T., Amaral, F. A., Teixeira, A. L., Souza, D. G. and Teixeira, M. M. (2012). Adapting to environmental stresses: the role of the microbiota in controlling innate immunity and behavioral responses. *Immunological Reviews*, *245*, 250–264.

Fahlgren, C., Hagström, A., Nilsson, D. and Zweifel, U. L. (2010). Annual variations in the diversity, viability, and origin of airborne bacteria. *Applied and Environmental Microbiology*, *76*, 3015–3025.

Fargione, J., Hill, J., Tilman, D., Polasky, S. and Hawthorne, P. (2008). Land clearing and the biofuel carbon debt. *Science*, *319*, 1235–1238.

Ferrara, F. I. D., Oliveira, Z. M., Gonzales, H. H. S., Floh, E. I. S., Barbosa, H. R. (2012). Endophytic and rhizopsheric enterobacteria isolated from sugarcane have different potentials for producing plant growth-promoting substances. *Plant Soil*, 353, 409-417.

Fouts, D. E., Tyler, H. L., DeBoy, R. T., Daugherty, S., Ren, Q., Badger, J. H., Durkin, A. S., Huot, H., Shrivastava, S., Kothari, S., Dodson, R. J., Mohamoud, Y., Khouri, H., Roesch L. F. W., Krogfelt, K. A., Struve, C., Triplett, E. W. and Methé, B. A. (2008). Complete genome sequence of the N2-fixing broad host range endophyte Klebsiella pneumoniae 342 and virulence predictions verified in mice. *PLoS Genetics*, *4*, e1000141.

Gevers, D., Knight, R., Petrosino, J. F., Huang, K., McGuire, A. L., Birren, B. W., Nelson, K. E., White, O., Methé B. A. and Huttenhower, C. (2012). The Human Microbiome Project: a community resource for the healthy human microbiome. *PLoS Biology*, *10*, e1001377.

Gómez Ros, L. V, Gabaldón, C., Pomar, F., Merino, F., Pedreño, M. A. and Barceló, A. R. (2007). Structural motifs of syringyl peroxidases predate not only the gymnosperm-angiosperm divergence but also the radiation of tracheophytes. *The New Phytologist*, *173*, 63–78.

Gottel, N. R., Castro, H. F., Kerley, M., Yang, Z., Pelletier, D. A., Podar, M., Karpinets, T., Tuskan, G. A., Vilgalys, R., Mitchel, J., Schadt, C. W., Uberbacher, E. and Doktycz, M. J. (2011). Distinct Microbial Communities within the Endosphere and Rhizosphere of Populus deltoides Roots across Contrasting Soil Types. *Applied and Environmental Microbiology*, 77, 5934-5944.

Gregory, P.J. (2006). Plant Roots: Growth, Activity and Interaction with Soils. Blackwell Publishing, Oxford, 318 pp.

Guillaumie, S., Mzid, R., Méchin, V., Léon, C., Hichri, I., Destrac-Irvine, A., Trossat-Magnin, C., Delrot, S. and Lauvergeat, V. (2010). The grapevine transcription factor WRKY2 influences the lignin pathway and xylem development in tobacco. *Plant Molecular Biology*, *72*, 215–234.

Haichar, F. E. Z., Marol, C., Berge, O., Rangel-Castro, J. I., Prosser, J. I., Balesdent, J., Heulin, T. and Achouak, W. (2008). Plant host habitat and root exudates shape soil bacterial community structure. *The ISME Journal*, *2*, 1221–1230.

Hallmann, J. and Berg, B. (2006). Spectrum and population dynamics of bacterial root endophytes. In B. J. E. Schulz, C. J. C. Boyle, and T. N. Sieber (Eds.), *Microbial Root Endophytes* (pp. 15–31). Berlin, Heidelberg: Springer.

Halpin, C., Thain, S. C., Tilston, E. L., Guiney, E., Lapierre, C. and Hopkins, D. W. (2006). Ecological impacts of trees with modified lignin. *Tree Genetics and Genomes*, *3*, 101–110.

Hansen, A. K. and Moran, N. A. (2014). The impact of microbial symbionts on host plant utilization by herbivorous insects. *Molecular Ecology*, *23*, 1473–1496.

Hardoim, P. R., van Overbeek, L. S. and Van Elsas, J. D. (2008). Properties of bacterial endophytes and their proposed role in plant growth. *Trends in Microbiology*, *16*, 463–471.

Hartmann, A., Rothballer, M. and Schmid, M. (2007). Lorenz Hiltner, a pioneer in rhizosphere microbial ecology and soil bacteriology research. *Plant and Soil*, *312*, 7–14.

Hartmann, A., Schmid, M., Tuinen, D. van, and Berg, G. (2008). Plant-driven selection of microbes. *Plant and Soil*, *321*, 235–257.

Hématy, K., Cherk, C. and Somerville, S. (2009). Host-pathogen warfare at the plant cell wall. *Current Opinion in Plant Biology*, *12*, 406–413.

Hertel, T. W., Golub, A. A., Jones, A. D., O'Hare, M., Plevin, R. J., and Kammen, D. M. (2010). Effects of US Maize Ethanol on Global Land Use and Greenhouse Gas Emissions: Estimating Market-mediated Responses. *BioScience*, *60*, 223–231.

Hill, J., Nelson, E., Tilman, D., Polasky, S. and Tiffany, D. (2006). Environmental , economic , and energetic costs and benefits of biodiesel and ethanol biofuels. *Proceedings of the National Academy of Sciences of the United States of America*, *103*, 11206-11210.

Himmel, M. E., Ding, S.-Y., Johnson, D. K., Adney, W. S., Nimlos, M. R., Brady, J. W. and Foust, T. D. (2007). Biomass recalcitrance: engineering plants and enzymes for biofuels production. *Science*, *315*, 804–807.

Hinchee, M., Rottmann, W., Mullinax, L., Zhang, C., Chang, S., Cunningham, M., Pearson, L., Nehra, N. (2009). Short-rotation woody crops for bioenergy and biofuels applications. *In Vitro Cellular and Developmental Biology, 45*, 619–629.

Hinsinger, P., Bengough, A. G., Vetterlein, D. and Young, I. M. (2009). Rhizosphere: biophysics, biogeochemistry and ecological relevance. *Plant and Soil*, *321*, 117–152.

Hirano, S. S. (2000). Bacteria in the Leaf Ecosystem with Emphasis on Pseudomonas syringae — a Pathogen , Ice Nucleus , and Epiphyte, *64*, 624–653.

Hirsch, P.R. and Mauchline, T. H. (2012) Who's who in the plant root microbiome. Nature Biotechnology, *30*, 961-962.

Hisano, H., Nandakumar, R. and Wang, Z.-Y. (2009). Genetic modification of lignin biosynthesis for improved biofuel production. *In Vitro Cellular and Developmental Biology* , *45*, 306–313.

Ichinohe, T., Pang, I. K., Kumamoto, Y., Peaper, D. R., Ho, J. H., Murray, T. S. and Iwasaki, A. (2011). Microbiota regulates immune defense against respiratory tract influenza A virus infection. *Proceedings of the National Academy of Sciences of the United States of America*, *108*, 5354–5359.

Inceoğlu, O., Salles, J. F., van Overbeek, L. and Van Elsas, J. D. (2010). Effects of plant genotype and growth stage on the betaproteobacterial communities associated with different potato cultivars in two fields. *Applied and Environmental Microbiology*, *76*, 3675–3684.

Iniguez, A. L., Dong, Y., Carter, H. D., Ahmer, B. M. M., Stone, J. M. and Triplett, E. W. (2005). Regulation of enteric endophytic bacterial colonization by plant defenses. *Molecular Plant-Microbe Interactions*, *18*, 169–178.

James Clive. (2013). Global Status of Commercialized Biotech/GM Crops. *The International Service for the Acquisition of Agri-Biotech Applications (ISAAA) Brief*, *46*.

James, E. K., Gyaneshwar, P., Mathan, N., Barraquio, W. L., Reddy, P. M., Iannetta, P. P. M., Olivares, F., L. and Ladha, J. K. (2002). Infection and colonization of rice seedlings by the plant growth-promoting bacterium Herbaspirillum seropedicae Z67. *Molecular Plant-Microbe Interactions*, *15*, 894–906.

James, E. K. and Olivares, F. L. (1998). Infection and Colonization of Sugar Cane and Other Graminaceous Plants by Endophytic Diazotrophs. *Critical Reviews in Plant Sciences*, *17*, 77–119.

Jones, D. L. and Hinsinger, P. (2008). The rhizosphere: complex by design. *Plant and Soil*, *312*, 1–6.

Jones, D. L., Nguyen, C. and Finlay, R. D. (2009). Carbon flow in the rhizosphere: carbon trading at the soil–root interface. *Plant and Soil*, *321*, 5–33.

Jones, J. D. G. and Dangl, J. L. (2006). The plant immune system. *Nature*, *444*, 323–329.

Kennedy, K., Hall, M. W., Lynch, M. D. J., Moreno-Hagelsieb, G. and Neufeld, J. D. (2014). Evaluating bias of illumina-based bacterial 16S rRNA gene profiles. *Applied and Environmental Microbiology*, *80*, 5717–5722.

Kerr, R. A. and Service, R. F. (2005). What can replace cheap oil and when? *Science*, *309*, 101.

Keshwani, D. R. and Cheng, J. J. (2009). Switchgrass for bioethanol and other value-added applications: a review. *Bioresource Technology*, *100*, 1515–1523.

Koch, L. (2014). Metagenomics: Shaping the gut microbiome. *Nature Reviews. Genetics*, *16*, 2-3.

Krause, A., Ramakumar, A., Bartels, D., Battistoni, F., Bekel, T., Boch, J., Böhm, M., Friedrich, F., Hurek, T., Krause, L., Linke, B., McHardy, A. C., Sarkar, A., Schneiker, S., Syed A. A., Thauer, R., Vorhölter, F., Weidner, Pühler, A., Reinhold-Hurek, B., Kaiser, O. and Goesmann, A. (2006). Complete genome of the mutualistic, N2-fixing grass endophyte Azoarcus sp. strain BH72. *Nature Biotechnology*, *24*, 1385–1391.

Lebies, S. L. (2014). The potential for give and take in plant-microbiome relationships. *Frontiers in Plant Science*, *5*, 1-6.

Leplé, J.-C., Dauwe, R., Morreel, K., Storme, V., Lapierre, C., Pollet, B., Naumann A., Kang, K., Kim, H., Ruel, K., Lefèbvre, A., Joseleau, J., Grima-Pettenati, J., De Rycke, R., Andersson-Gunnerås, S., Erban, A., Fehrle A., Petit-Conil, M., Kopka, J., Polle, A., Messens, E., Sundberg, B., Mansfield, S., Ralph, J., Pilate, G. and Boerjan, W. (2007). Down-regulation of cinnamoyl-coenzyme A reductase in poplar: multiple-level phenotyping reveals effects on cell wall polymer metabolism and structure. *The Plant Cell*, *19*, 3669–3691.

Lewandowski, I., Clifton-brown, J. C., Scurlock, J. M. O. and Huisman, W. (2008). Miscanthus : European experience with a novel energy crop. *Biomass and Bioenergy*, *19*, 209–227.

Lewis, N. S. (2007). Toward cost-effective solar energy use. *Science*, *315*, 798–801.

Lindow, S. E. and Brandl, M. T. (2003). Microbiology of the Phyllosphere. Applied and Environmental Microbiology, *69*, 1875–1883

Liu, C.-J. (2012). Deciphering the enigma of lignification: precursor transport, oxidation, and the topochemistry of lignin assembly. *Molecular Plant*, *5*, 304–317.

Liu, C.-J., Miao, Y.-C. and Zhang, K.-W. (2011). Sequestration and transport of lignin monomeric precursors. *Molecules*, *16*, 710–727.

Lu, F. and Ralph, J. (2008). Novel tetrahydrofuran structures derived from beta-beta-coupling reactions involving sinapyl acetate in Kenaf lignins. *Organic and Biomolecular Chemistry*, *6*, 3681–3694.

Lu, X., McElroy, M. B. and Kiviluoma, J. (2009). Global potential for wind-generated electricity. *Proceedings of the National Academy of Sciences of the United States of America*, *106*, 10933–10938.

Lugtenberg, B. and Kamilova, F. (2009). Plant-growth-promoting rhizobacteria. *Annual Review of Microbiology*, *63*, 541–556.

Lundberg, D. S., Lebeis, S. L., Paredes, S. H., Yourstone, S., Gehring, J., Malfatti, S., Tremblay, J., Engelbrektson, A., Kunin, V., del Rio, T. G., Edgar, R. C., Eickhorst, T., Ley, R. E., Hugenholtz, P., Tringe, S. G. and Dangl, J. L. (2012). Defining the core Arabidopsis thaliana root microbiome. *Nature*, *488*, 86–90.

Maher, E. A., Bate, N. J., Nit, W., Elkindt, Y., Dixont, R. A. and Lamb, C. J. (1994). Increased disease susceptibility of transgenic tobacco plants with suppressed levels of preformed phenylpropanoid products, *91*, 7802–7806.

Margulies, M., Egholm, M., Altman, W. E., Attiya, S., Bader, J. S., Bemben, L. A., et al. (2005). Genome sequencing in microfabricated high-density picolitre reactors. *Nature*, *437*, 376–380.

Marjamaa, K., Kukkola, E. M. and Fagerstedt, K. V. (2009). The role of xylem class III peroxidases in lignification. *Journal of Experimental Botany*, *60*, 367–376.

Mark, G. L., Dow, J. M., Kiely, P. D., Higgins, H., Haynes, J., Baysse, C., Abbas, A., Foley, T., Franks, A., Morrissey, J. and O'Gara, F. (2005). Transcriptome profiling of bacterial responses to root exudates identifies genes involved in microbe-plant interactions. *Proceedings of the National Academy of Sciences of the United States of America*, *102*, 17454–17459.

Martone, P. T., Estevez, J. M., Lu, F., Ruel, K., Denny, M. W., Somerville, C. and Ralph, J. (2009). Discovery of lignin in seaweed reveals convergent evolution of cell-wall architecture. *Current Biology*, 19, 169-175.

McCaig, B. C., Meagher, R. B. and Dean, J. F. D. (2005). Gene structure and molecular analysis of the laccase-like multicopper oxidase (LMCO) gene family in Arabidopsis thaliana. *Planta*, *221*, 619–636.

Mendes, R., Garbeva, P. and Raaijmakers, J. M. (2013). The rhizosphere microbiome: significance of plant beneficial, plant pathogenic, and human pathogenic microorganisms. *FEMS Microbiology Reviews*, *37*, 634–663.

Metzker, M. L. (2010). Sequencing technologies - the next generation. *Nature Reviews. Genetics*, *11*, 31–46.

Miao, Y.-C. and Liu, C.-J. (2010). ATP-binding cassette-like transporters are involved in the transport of lignin precursors across plasma and vacuolar membranes. *Proceedings of the National Academy of Sciences*, *107*, 22728–22733.

Micallef, S. A., Channer, S., Shiaris, M. P. and Colón-Carmona, A. (2009). Plant age and genotype impact the progression of bacterial community succession in the Arabidopsis rhizosphere. *Plant Signaling and Behavior*, *4*, 777–780.

Miché, L., Battistoni, F., Gemmer, S., Belghazi, M. and Reinhold-Hurek, B. (2006). Upregulation of jasmonate-inducible defense proteins and differential colonization of roots of Oryza sativa cultivars with the endophyte Azoarcus sp. *Molecular Plant-Microbe Interactions*, *19*, 502–511.

Miedes, E., Vanholme, R., Boerjan, W. and Molina, A. (2014). The role of the secondary cell wall in plant resistance to pathogens. *Frontiers in Plant Science*, *5*, 358.

Mir Derikvand, M., Sierra, J. B., Ruel, K., Pollet, B., Do, C.-T., Thévenin, J., Buffard, D., Jouanin, L. and Lapierre, C. (2008). Redirection of the phenylpropanoid pathway to feruloyl malate in Arabidopsis mutants deficient for cinnamoyl-CoA reductase 1. *Planta*, *227*, 943–956.

Mitter, B., Petric, A., Shin, M. W., Chain, P. S. G., Hauberg-Lotte, L., Reinhold-Hurek, B., Nowak, J. and Sessitsch, A. (2013). Comparative genome analysis of Burkholderia phytofirmans PsJN reveals a wide spectrum of endophytic lifestyles based on interaction strategies with host plants. *Frontiers in Plant Science*, *4*, 120.

Monteiro, R. A., Balsanelli, E., Wassem, R., Marin, A. M., Brusamarello-Santos, L. C. C., Schmidt, M. A., Tadra-Sfeir, M. Z., Pankievicz, V. C. S., Cruz, L. M., Chubatsu, L., S., Pedrosa, F. O. and Souza, E. M. (2012). Herbaspirillum-plant interactions: microscopical, histological and molecular aspects. *Plant and Soil*, *356*, 175–196.

Morreel, K., Ralph, J., Lu, F., Goeminne, G., Busson, R., Herdewijn, P., Goeman, J. L., Van Der Eycken, J., Boerjan, W. and Messens, E. (2004). Phenolic Profiling of Caffeic Acid O -Methyltransferase-Deficient Poplar Reveals Novel Benzodioxane Oligolignols 1, *136*, 4023–4036.

Naik, S. N., Goud, V. V., Rout, P. K. and Dalai, A. K. (2010). Production of first and second-generation biofuels: A comprehensive review. *Renewable and Sustainable Energy Reviews*, *14*, 578–597.

Naylor, R. L., Liska, A. J., Burke, M. B., Falcon, W. P., Gaskell, J. C., Rozelle, S. D. and Cassman, K. G. (2007). The Ripple Effect: Biofuels, Food Security, and the Environment. *Environment: Science and Policy for Sustainable Development*, *49*, 30–43.

Nelson, E. B. (2004). Microbial dynamics and interactions in the spermosphere. *Annual Review of Phytopathology*, *42*, 271–309.

Nijsen, M., Smeets, E., Stehfest, E. and Vuuren, D. P. (2012). An evaluation of the global potential of bioenergy production on degraded lands. *GCB Bioenergy*, *4*, 130–147.

Philippot, L., Hallin, S., Börjesson, G. and Baggs, E. M. (2008). Biochemical cycling in the rhizosphere having an impact on global change. *Plant and Soil*, *321*, 61–81.

Pieterse, C. M. J., Leon-Reyes, A., Van der Ent, S. and Van Wees, S. C. M. (2009). Networking by small-molecule hormones in plant immunity. *Nature Chemical Biology*, *5*, 308–16.

Pilate, G., Guiney, E., Holt, K., Petit-Conil, M., Lapierre, C., Leplé, J.-C., Pollet, B., Mila, I., Webster, E. A., Marstorp, H., G., Hopkins, D. W., Jouanin, L., Boerjan, W., Schuch, W., Cornu, D. and Halpin, C. (2002). Field and pulping performances of transgenic trees with altered lignification. *Nature Biotechnology*, *20*, 607–12.

Qin, J., Li, R., Raes, J., Arumugam, M., Burgdorf, K. S., Manichanh, C., Nielsen, T., Pons, N., Levenez, F., Yamada, T., Mende, D. R., Li, J., Xu, J., Li, S., Li, D., Cao, J., Wang, B., Liang, H., Zheng, W., Xie, Y., Tap, J. et al. (2010). A human gut microbial gene catalogue established by metagenomic sequencing. *Nature*, *464*, 59–65.

Raaijmakers, J. M., Paulitz, T. C., Steinberg, C., Alabouvette, C. and Moënne-Loccoz, Y. (2008a). The rhizosphere: a playground and battlefield for soilborne pathogens and beneficial microorganisms. *Plant and Soil*, *321*, 341–361.

Ralph, J., Akiyama, T., Kim, H., Lu, F., Schatz, P. F., Marita, J. M., Ralph, S., A., Reddy, M., S., S., Chen, F. and Dixon, R. A. (2006). Effects of coumarate 3-hydroxylase down-regulation on lignin structure. *The Journal of Biological Chemistry*, *281*, 8843–8853.

Ralph, J., Lundquist, K., Brunow, G., Lu, F., Kim, H., Schatz, P. F., Marita, J., M., Hatfield, R., D., Ralph, S., A, Christensen, J., H. and Boerjan, W. (2004). Lignins: Natural polymers from oxidative coupling of 4-hydroxyphenyl- propanoids. *Phytochemistry Reviews*, *3*, 29–60.

Raven, P. H. (1970). A Multiple Origin for Plastids and Mitochondria: Many independent symbiotic events may have been involved in the origin of these cellular organelles. *Science*, *169*, 641–646.

Redford, A. J., Bowers, R. M., Knight, R., Linhart, Y. and Fierer, N. (2010). The ecology of the phyllosphere: geographic and phylogenetic variability in the distribution of bacteria on tree leaves. *Environmental Microbiology*, *12*, 2885–2893.

Reinhold-Hurek, B. and Hurek, T. (2011). Living inside plants: bacterial endophytes. *Current Opinion in Plant Biology*, *14*, 435–443.

Richardson, J. (2008). Production of biomass for energy from sustainable forestry systems: Canada and Europe. In: Proceedings of the Short Rotation Crops International Conference.

Rogers, A., McDonald, K., Muehlbauer, M. F., Hoffman, A., Koenig, K., Newman, L., Taghavi, S. and van der Lelie, D. (2012). Inoculation of hybrid poplar with the endophytic bacterium Enterobacter sp. 638 increases biomass but does not impact leaf level physiology. *GCB Bioenergy*, *4*, 364–370.

Rogers, L. A. and Campbell, M. M. (2004). The genetic control of lignin deposition during plant growth and development. *New Phytologist*, *164*, 17–30.

Rosenblueth, M. and Martínez-Romero, E. (2006). Bacterial endophytes and their interactions with hosts. *Molecular Plant-Microbe Interactions*, *19*, 827–837.

Ruel, K., Berrio-sierra, J., Derikvand, M. M., Pollet, B., Thévenin, J., Lapierre, C., Jouanin, L. and Joseleau, J. (2009). Impact of *CCR*1 silencing on the assembly of lignified secondary walls in Arabidopsis thaliana. *The New Phytologist, 184*, 99–113.

Ryan, R. P., Germaine, K., Franks, A., Ryan, D. J. and Dowling, D. N. (2008). Bacterial endophytes: recent developments and applications. *FEMS Microbiology Letters*, *278*, 1–9.

Sannigrahi, P. and Ragauskas, A. J. (2010). Poplar as a feedstock for biofuels: A review of compositional characteristics. *Biofuels, Bioproducts and Biorefining*, *4*, 209–226.

Sarkar, P., Bosneaga, E. and Auer, M. (2009). Plant cell walls throughout evolution: towards a molecular understanding of their design principles. *Journal of Experimental Botany*, *60*, 3615–3635.

Schubert, C. (2006). Can biofuels finally take center stage? *Nature Biotechnology*, *24*, 777–784.

Searchinger, T., Heimlich, R., Houghton, R. A., Dong, F., Elobeid, A., Fabiosa, J., Tokgoz, S., Hayes, D. and Yu, T.-H. (2008). Use of U.S. croplands for biofuels increases greenhouse gases through emissions from land-use change. *Science*, *319*, 1238–40.

Sessitsch, A., Hardoim, P., Döring, J., Weilharter, A., Krause, A., Woyke, T., Mitter, B., Hauberg-Lotte L., Friedrich, F., Rahalkar, M., Hurek, T., Sarkar, A., Bodrossy, L., van Overbeek, L., Brar, D., van Elsas, J. D. and Reinhold-Hurek, B. (2012). Functional characteristics of an endophyte community colonizing rice roots as revealed by metagenomic analysis. *Molecular Plant-Microbe Interactions*, *25*, 28–36.

Shade, A., McManus, P. S. and Handelsman, J. (2013). Unexpected Diversity during Community Succession in the Apple Flower Microbiome. *mBio*, *4*, 1–12.

Shafiee, S. and Topal, E. (2009). When will fossil fuel reserves be diminshed? *Energy policy*, *37*, 181-189.

Shendure, J. and Ji, H. (2008). Next-generation DNA sequencing. *Nature Biotechnology*, *26*, 1135–1145.

Shi, S., Richardson, A. E., O'Callaghan, M., DeAngelis, K. M., Jones, E. E., Stewart, A., Firestone, M., K. and Condron, L. M. (2011). Effects of selected root exudate components on soil bacterial communities. *FEMS Microbiology Ecology*, *77*, 600–610.

Sibout, R., and Höfte, H. (2012). Plant cell biology: the ABC of monolignol transport. *Current Biology, 22*, 533-535.

Smeets, E., Faaij, A., Lewandowski, I. and Turkenburg, W. (2007). A bottom-up assessment and review of global bio-energy potentials to 2050. *Progress in Energy and Combustion Science*, *33*, 56–106.

Sogin, M. L., Morrison, H. G., Huber, J. A, Mark Welch, D., Huse, S. M., Neal, P. R., Arrieta, J. M. and Herndl, G. J. (2006). Microbial diversity in the deep sea and the underexplored "rare biosphere". *Proceedings of the National Academy of Sciences of the United States of America*, *103*, 12115–12120.

Solomon, B. D. (2010). Biofuels and sustainability. *Annals of the New York Academy of Science*, *1185*, 119–134.

Solomon, S., Plattner, G.-K., Knutti, R. and Friedlingstein, P. (2009). Irreversible climate change due to carbon dioxide emissions. *Proceedings of the National Academy of Sciences of the United States of America*, *106*, 1704–1709.

Spor, A., Koren, O. and Ley, R. (2011). Unravelling the effects of the environment and host genotype on the gut microbiome. *Nature Reviews. Microbiology*, *9*, 279–290.

Srivastava, V., Schinkel, H., Witzell, J., Hertzberg, M., Torp, M., Srivastava, M. K., Karpinska, B., Melzer, M. and Wingsle, G. (2007). Down-regulation of high-isoelectric-point extracellular superoxide dismutase mediates alterations in the metabolism of reactive oxygen species and developmental disturbances in hybrid aspen. *The Plant Journal : For Cell and Molecular Biology*, *49*, 135–148.

Stewart, J. J., Akiyama, T., Chapple, C., Ralph, J. and Mansfield, S. D. (2009). The effects on lignin structure of overexpression of ferulate 5-hydroxylase in hybrid poplar. *Plant Physiology*, *150*, 621–35.

The Human Microbiome Project Consortium. Structure, function and diversity of the healthy human microbiome. (2012). *Nature*, *486*, 207–14.

Studer, M. H., Demartini, J. D., Davis, M. F., Sykes, R. W., Davison, B. and Keller, M. (2011). Lignin content in natural Populus variants affects sugar release. *Proceedings of the National Academy of Sciences of the United States of America*, *108*, 6300-6305.

Sudakaran, S., Salem, H., Kost, C. and Kaltenpoth, M. (2012). Geographical and ecological stability of the symbiotic mid-gut microbiota in European firebugs, Pyrrhocoris apterus (Hemiptera, Pyrrhocoridae). *Molecular Ecology*, *21*, 6134–6151.

Tharakan, P. J., Volk, T. a., Abrahamson, L. P. and White, E. H. (2003). Energy feedstock characteristics of willow and hybrid poplar clones at harvest age. *Biomass and Bioenergy*, *25*, 571–580.

Tilman, D., Socolow, R., Foley, J. A., Hill, J., Larson, E., Lynd, L., Pacala, S., Reilly, J., Searchinger, T., Somerville, C. and Williams, R. (2009). Beneficial Biofuels—The Food, Energy, and Environment Trilemma, *325*, 270–271.

Truyens, S., Weyens, N., Cuypers, A. and Vangronsveld, J. (2014). Bacterial seed endophytes: genera, vertical transmission and interaction with plants. *Environmental Microbiology Reports*, *7*, 40-50.

Turnbull, G. A., Morgan, J. A. W., Whipps, J. M. and Saunders, J. R. (2001). The role of bacterial motility in the survival and spread of Pseudomonas fluorescens in soil and in the attachment and colonisation of wheat roots. *FEMS Microbiology Ecology*, *36*, 21–31.

Turner, T. R., James, E. K. and Poole, P. S. (2013). The plant microbiome. *Genome Biology*, *14*, 1-10.

Turner, T. R., Ramakrishnan, K., Walshaw, J., Heavens, D., Alston, M., Swarbreck, D., Osbourn, A., Grant, A. and Poole, P. S. (2013). Comparative metatranscriptomics reveals kingdom level changes in the rhizosphere microbiome of plants. *The ISME Journal*, *7*, 2248–58.

Umezawa, T. (2003). Diversity in lignan biosynthesis. *Phytochemistry Reviews*, *2*, 371–390.

Van Acker, R., Leplé, J.-C., Aerts, D., Storme, V., Goeminne, G., Ivens, B., Légée, F., Lapierre, C., Piens, K., Van Montagu, M., C., E., Santoro, N., Foster, C., E., Ralph, J., Soetaert, W., Pilate, G. and Boerjan, W. (2014). Improved saccharification and ethanol yield from field-grown transgenic poplar deficient in cinnamoyl-CoA reductase. *Proceedings of the National Academy of Sciences of the United States of America*, *111*, 845–50.

Van Acker, R., Vanholme, R., Storme, V., Mortimer, J. C., Dupree, P. and Boerjan, W. (2013). Lignin biosynthesis perturbations affect secondary cell wall composition and saccharification yield in Arabidopsis thaliana. *Biotechnology for Biofuels*, *6*, 1-17.

Van der Ent, S., Van Hulten, M., Pozo, M. J., Czechowski, T., Udvardi, M. K., Pieterse, C. M. J. and Ton, J. (2009). Priming of plant innate immunity by rhizobacteria and beta-aminobutyric acid: differences and similarities in regulation. *The New Phytologist*, *183*, 419–31.

Van der Ent, S., Van Wees, S. C. M. and Pieterse, C. M. J. (2009). Jasmonate signaling in plant interactions with resistance-inducing beneficial microbes. *Phytochemistry*, *70*, 1581–1588.

Van der Heijden, M. G. A., Bardgett, R. D. and van Straalen, N. M. (2008). The unseen majority: soil microbes as drivers of plant diversity and productivity in terrestrial ecosystems. *Ecology Letters*, *11*, 296–310.

Van der Rest, B., Danoun, S., Boudet, A.-M. and Rochange, S. F. (2006). Down-regulation of cinnamoyl-CoA reductase in tomato (Solanum lycopersicum L.) induces dramatic changes in soluble phenolic pools. *Journal of Experimental Botany*, *57*, 1399–1411.

Vanholme, R., Demedts, B., Morreel, K., Ralph, J. and Boerjan, W. (2010). Lignin biosynthesis and structure. *Plant Physiology*, *153*, 895–905.

Vanholme, R., Morreel, K., Darrah, C., Oyarce, P., Grabber, J. H., Ralph, J. and Boerjan, W. (2012a). Metabolic engineering of novel lignin in biomass crops. *The New Phytologist*, *196*, 978–1000.

Vanholme, R., Morreel, K., Ralph, J. and Boerjan, W. (2008). Lignin engineering. *Current Opinion in Plant Biology*, *11*, 278–85.

Vanholme, R., Storme, V., Vanholme, B., Sundin, L., Christensen, J. H., Goeminne, G., Halpin, C., Rohde, A., Morreel, K. and Boerjan, W. (2012b). A Systems Biology View of Responses to Lignin Biosynthesis Perturbations in Arabidopsis. *The Plant Cell*, *24*, 3506–3529.

Vinagre, F., Vargas, C., Schwarcz, K., Cavalcante, J., Nogueira, E. M., Baldani, J. I., Ferreira, P., C., G. and Hemerly, A. S. (2006). SHR5: a novel plant receptor kinase involved in plant-N2-fixing endophytic bacteria association. *Journal of Experimental Botany*, *57*, 559–69.

Vorholt, J. A. (2012). Microbial life in the phyllosphere. *Nature Reviews. Microbiology*, *10*, 828–40.

Walker, T. S., Bais, H. P., Grotewold, E. and Vivanco, J. M. (2003). Update on Root Exudation and Rhizosphere Biology Root Exudation and Rhizosphere Biology. *Plant Physiology*, *132*, 44–51.

Wang, Y., Chantreau, M., Sibout, R. and Hawkins, S. (2013). Plant cell wall lignification and monolignol metabolism. *Frontiers in Plant Science*, *4*, 220.

Weinert, N., Piceno, Y., Ding, G.-C., Meincke, R., Heuer, H., Berg, G., Schloter, M., Andersen, G. and Smalla, K. (2011). PhyloChip hybridization uncovered an enormous bacterial diversity in the rhizosphere of different potato cultivars: many common and few cultivar-dependent taxa. *FEMS Microbiology Ecology*, *75*, 497–506.

Welinder, K. G., Justesen, A. F., Kjaersgård, I. V. H., Jensen, R. B., Rasmussen, S. K., Jespersen, H. M. and Duroux, L. (2002). Structural diversity and transcription of class III peroxidases from Arabidopsis thaliana. *European Journal of Biochemistry*, *269*, 6063–6081.

Weng, J.-K. and Chapple, C. (2010). The origin and evolution of lignin biosynthesis. *The New Phytologist*, *187*, 273–85.

Weng, J.-K., Li, X., Bonawitz, N. D. and Chapple, C. (2008). Emerging strategies of lignin engineering and degradation for cellulosic biofuel production. *Current Opinion in Biotechnology*, *19*, 166–72.

Weston, L. A. and Mathesius, U. (2013). Flavonoids: their structure, biosynthesis and role in the rhizosphere, including allelopathy. *Journal of Chemical Ecology*, *39*, 283–97.

Weyens, N., van der Lelie, D., Taghavi, S., Newman, L. and Vangronsveld, J. (2009a). Exploiting plant–microbe partnerships to improve biomass production and remediation. *Trends in Biotechnology*, *27*, 591–598.

Weyens, N., van der Lelie, D., Taghavi, S., and Vangronsveld, J. (2009b). Phytoremediation: plant-endophyte partnerships take the challenge. *Current Opinion in Biotechnology*, *20*, 248–54.

Wilkerson, C. G., Mansfield, S. D., Lu, F., Withers, S., Park, J.-Y., Karlen, S. D., Gonzales-Vigil, E., Padmakshan, D., Unda, F., Rencoret, J. and Ralph, J. (2014). Monolignol ferulate transferase introduces chemically labile linkages into the lignin backbone. *Science*, *344*, 90–93.

Yuan, J. S., Tiller, K. H., Al-Ahmad, H., Stewart, N. R. and Stewart, C. N. (2008). Plants to power: bioenergy to fuel the future. *Trends in Plant Science*, *13*, 421–9.

Zalesny, R., Hall, R. B., Zalesny, J. A., McMahon, B. G., Berguson, W. E., Stanosz, G. R. (2009). Biomass and Genotype × Environment Interactions of *Populus* Energy Crops in the Midwestern United States. *Bioenergy Research*, 2, 106-122.

Zhang, H., Kim, M.-S., Krishnamachari, V., Payton, P., Sun, Y., Grimson, M., Farag, M., Ryu, C., Allen, R., Melo, I. S. and Paré, P. W. (2007). Rhizobacterial volatile emissions regulate auxin homeostasis and cell expansion in Arabidopsis. *Planta*, *226*(4), 839–851.

Zhao, L. (2010). Genomics: The tale of our other genome. *Nature*, *465*, 879–80.

Zhou, J., Lee, C., Zhong, R. and Ye, Z.-H. (2009). MYB58 and MYB63 are transcriptional activators of the lignin biosynthetic pathway during secondary cell wall formation in Arabidopsis. *The Plant Cell*, *21*, 248–66.

Chapter 2

Objectives

In the search of renewable and sustainable energy sources to reduce the reliance on fossil fuels, the production of biofuels from biomass represents a vital component in the transition to a more bio-based economy. Second-generation biofuels derived from lignocellulosic biomass in dedicated energy crops (e.g. poplar) provide considerable advantages over first-generation biofuels, which directly originate from food crops (e.g. maize, sugar cane). Most notably, second-generation biofuels evade the “food versus fuel” debate since they can be grown on marginal lands (contaminated and/or nutrient poor soils unsuitable for the food production). However, the main drawback in the industrial processing of lignocellulosic plant biomass to fermentable sugars is the recalcitrance of lignin polymers present in the plant cell walls. Therefore, the generation of feedstocks with reduced or more easily degradable lignin polymers has attracted significant research attention. Gene silencing of cinnamoyl-CoA reductase (*CCR*, E.C.1.2.1.44), the first enzyme in the monolignol-specific branch of lignin biosynthesis (Boerjan et al., 2003; Vanholme et al., 2010), typically results in reduced lignin content, altered cell wall metabolism and/or improved pulping characteristics, higher saccharification and ethanol yield in for example tobacco plants, *Arabidopsis thaliana* (Mir Derikvand et al., 2008; Ruel et al., 2009; Van Acker et al., 2013) and poplar (Leplé et al., 2007; Van Acker et al., 2014). However, simultaneously gene silencing of CCR and by extension most of the genes silenced in the lignin biosynthesis, leads to flux changes in the phenylpropanoid and monolignol-specific pathways, most notably the accumulation of soluble phenolics (e.g. ferulic acid). Ultimately this results in differential accumulation of a wide range of carbon sources in developing xylem accessible for the endophytic bacteria. Furthermore, perturbations in the lignin biosynthesis via *CCR*-down-regulation lead to compositional alterations in the cell wall resulting in looser cell wall structure and the incorporation of alternative monomers in the lignin polymers (Leplé et al., 2007). Cell walls play major roles in the endophytic colonization of beneficial bacteria (Compant et al., 2010;

Hardoim et al., 2008) as well as in the resistance against pathogens (Miedes et al. 2014)

Together all these factors lead to our general hypothesis: modification of the lignin biosynthesis (via *CCR* down-regulation) in field-grown poplar trees and the accompanying changes in the host genotype, most notably (a) the xylem metabolome and (b) compositional alterations in the cell-wall, has profound effects on colonization capacity, the structural composition and the metabolic capacities of the plant-associated bacterial microbiome. Therefore, the main objective of the current work was to explore the general and specific host genotype effects exerted by *CCR* gene silencing in field-grown poplar trees (*Populus tremula x alba*) on the plant bacterial microbiome. Furthermore we also focussed on the microbiome niche differentiation between the different plant environments (rhizosphere, root, stem, leaf) and evaluated the potential of plant-growth promoting (PGP) bacteria to offset the negative repercussions on the biomass yield of lignin-reduced genotypes.

To this end, four research questions have been put forward in the outline of this study:

1. How can we access the total bacterial microbiome associated with plants via 16S rRNA metabarcoding without the co-amplification of organellar 16S rRNA?

A first challenge was to optimize an approach to reliably access the total plant microbiome and determine plant compartment and host genotype-dependent effects via 16S rRNA metabarcoding (Chapter 4). Accessing the plant microbiome using 16S rDNA metabarcoding represents significant challenges, exclusively due to the mixed presence of eukaryotic cells, prokaryotic cells and eukaryotic plant organelles with a prokaryotic lineage (chloroplasts and mitochondria). We experimentally evaluated the performance of a set of 16S rRNA primers (7 primer pairs) based on (a) low co-amplification of non-target rRNA reads (b) high retrieval of bacterial 16S rRNA sequences and (c) low primer efficiency for pure poplar chloroplast DNA. Ultimately, this optimization ensured the selection of a specific primer pair, which was used in the evaluation of plant compartment and host genotype effects on the total bacterial plant microbiome (Chapter 5).

2. Is microbiome niche differentiation, frequently reported at the rhizosphere soil-root interface, continued in the aerial plant compartments (stem and leaf)?

Niche differentiation of the plant microbiome at the rhizosphere soil-root interface has been reported in a limited number of studies (Bulgarelli et al., 2012; Gottel et al., 2011; Inceoğlu et al. 2010; Lundberg et al., 2012; Weinert et al., 2011). However, each microenvironment (rhizosphere, root, stem and leaf) provides specific biotic and abiotic conditions for microbial life. Indeed, recently Bulgarelli et al., (2013) suggested the possibility of additional fine-tuning and niche differentiation of microbiota in the aerial plant organs. However, experimental validation of this concept is still lacking. Via 16S rRNA metabarcoding as well as evaluating the culturable bacterial fraction, we studied the microbiome niche differentiation in *Populus tremula x alba* across rhizosphere, root, stem and leaf samples (Chapter 3 and Chapter 5).

3. What is the magnitude of host genotype effects, i.e. modification of the lignin biosynthesis (*CCR* down-regulation), on the bacterial microbiota?

Few studies have explored possible host genotype-dependent effects (ecotypes, cultivars, genetically modified genotypes) on the bacterial assemblages. Most of them have focussed on *Arabidopsis thaliana* (Bulgarelli et al., 2012; Lundberg et al., 2012) and potato cultivars (Inceoğlu et al., 2010; van Overbeek & van Elsas, 2008; Weinert et al., 2011) as well as on other organisms such as the human gut microbiome (Spor et al., 2011). To determine host genotype-dependent effects exerted by the lignin-reduced (*CCR* deficient) poplar genotype on bacterial microbiomes, we compared the total bacterial microbiome of wild type and *CCR* deficient poplar trees using 16S rRNA metabarcoding (Chapter 5). Furthermore, we evaluated the metabolic capacities present in the culturable bacterial populations of *CCR*-down-regulated and wild type poplar trees via selective isolation/enrichments experiments (Chapter 3)

4. What is the potential of plant-growth promoting stress-reducing bacteria to enhance the plant growth of lignin-reduced biomass-impared genotypes?

Perturbations in the lignin biosynthesis often affect plant growth and developmental effects. *CCR*-down-regulation causes the development of dwarf phenotypes in *Arabidopsis thaliana* (Mir Derikvand et al., 2008; Ruel et al., 2009; Van Acker et al., 2013) and reduced biomass production in *Populus tremula x alba* (Leplé et al., 2007; Van Acker et al., 2014). Since beneficial plant-associated bacteria can play a key role in supporting and/or enhancing plant health and growth through several direct and indirect mechanisms, we explored the following concept: can we improve the plant growth of biomass-impaired lignin-reduced *Arabidopsis* genotypes by exploiting the metabolic and plant growth promotion capacities of selected bacterial strains and thereby reduce the biomass penalty associated with *CCR* down-regulation?

References

Boerjan, W., Ralph, J., & Baucher, M. (2003). Lignin biosynthesis. *Annual Review of Plant Biology*, *54*, 519–46.

Bulgarelli, D., Rott, M., Schlaeppi, K., Ver Loren van Themaat, E., Ahmadinejad, N., Assenza, F., Rauf, P., Huettel, B., Reinhardt, R., Schmelzer, E., Perlies, J., Gloeckner, F. O., Amann, R., Eickhorst, T. and Schulze-Lefert, P. (2012). Revealing structure and assembly cues for Arabidopsis root-inhabiting bacterial microbiota. *Nature*, *488*, 91–95.

Compant, S., Clément, C. and Sessitsch, A. (2010). Plant growth-promoting bacteria in the rhizo- and endosphere of plants: Their role, colonization, mechanisms involved and prospects for utilization. *Soil Biology and Biochemistry*, *42*, 669–678.

Gottel, N. R., Castro, H. F., Kerley, M., Yang, Z., Pelletier, D. A., Podar, M., Karpinets, T., Tuskan, G. A., Vilgalys, R., Mitchel, J., Schadt, C. W., Uberbacher, E. and Doktycz, M. J. (2011). Distinct Microbial Communities within the Endosphere and Rhizosphere of Populus deltoides Roots across Contrasting Soil Types. *Applied and Environmental Microbiology*, 77, 5934-5944.

Hardoim, P. R., van Overbeek, L. S. and Van Elsas, J. D. (2008). Properties of bacterial endophytes and their proposed role in plant growth. *Trends in Microbiology*, *16*, 463–471.

Inceoğlu, O., Salles, J. F., van Overbeek, L. and Van Elsas, J. D. (2010). Effects of plant genotype and growth stage on the betaproteobacterial communities associated with different potato cultivars in two fields. *Applied and Environmental Microbiology*, *76*, 3675–3684.

Leplé, J.-C., Dauwe, R., Morreel, K., Storme, V., Lapierre, C., Pollet, B., Naumann A., Kang, K., Kim, H., Ruel, K., Lefèbvre, A., Joseleau, J., Grima-Pettenati, J., De Rycke, R., Andersson-Gunneråas, S., Erban, A., Fehrle A., Petit-Conil, M., Kopka, J., Polle, A., Messens, E., Sundberg, B., Mansfield, S., Ralph, J., Pilate, G. and Boerjan, W. (2007). Down-regulation of cinnamoyl-coenzyme A reductase in poplar: multiple-level phenotyping reveals effects on cell wall polymer metabolism and structure. *The Plant Cell*, *19*, 3669–3691.

Lundberg, D. S., Lebeis, S. L., Paredes, S. H., Yourstone, S., Gehring, J., Malfatti, S., Tremblay, J., Engelbrektson, A., Kunin, V., del Rio, T. G.,

Edgar, R. C., Eickhorst, T., Ley, R. E., Hugenholtz, P., Tringe, S. G. and Dangl, J. L. (2012). Defining the core Arabidopsis thaliana root microbiome. *Nature*, *488*, 86–90.

Miedes, E., Vanholme, R., Boerjan, W. and Molina, A. (2014). The role of the secondary cell wall in plant resistance to pathogens. *Frontiers in Plant Science*, *5*, 358.

Mir Derikvand, M., Sierra, J. B., Ruel, K., Pollet, B., Do, C.-T., Thévenin, J., Buffard, D., Jouanin, L. and Lapierre, C. (2008). Redirection of the phenylpropanoid pathway to feruloyl malate in Arabidopsis mutants deficient for cinnamoyl-CoA reductase 1. *Planta*, *227*, 943–956.

Ruel, K., Berrio-sierra, J., Derikvand, M. M., Pollet, B., Thévenin, J., Lapierre, C., Jouanin, L. and Joseleau, J. (2009). Impact of *CCR*1 silencing on the assembly of lignified secondary walls in *Arabidopsis thaliana. The New Phytologist, 184*, 99–113.

Spor, A., Koren, O. and Ley, R. (2011). Unravelling the effects of the environment and host genotype on the gut microbiome. *Nature Reviews. Microbiology*, *9*, 279–290.

Van Acker, R., Leplé, J.-C., Aerts, D., Storme, V., Goeminne, G., Ivens, B., Légée, F., Lapierre, C., Piens, K., Van Montagu, M., C., E., Santoro, N., Foster, C., E., Ralph, J., Soetaert, W., Pilate, G. and Boerjan, W. (2014). Improved saccharification and ethanol yield from field-grown transgenic poplar deficient in cinnamoyl-CoA reductase. *Proceedings of the National Academy of Sciences of the United States of America*, *111*, 845–50.

Van Acker, R., Vanholme, R., Storme, V., Mortimer, J. C., Dupree, P. and Boerjan, W. (2013). Lignin biosynthesis perturbations affect secondary cell wall composition and saccharification yield in Arabidopsis thaliana. *Biotechnology for Biofuels*, *6*, 1-17.

Van Overbeek, L. and van Elsas, J. D. (2008). Effects of plant genotype and growth stage on the structure of bacterial communities associated with potato (*Solanum tuberosum* L.). *FEMS Microbiology Ecology*, *64*(2), 283–296.

Vanholme, R., Demedts, B., Morreel, K., Ralph, J. and Boerjan, W. (2010). Lignin biosynthesis and structure. *Plant Physiology*, *153*, 895–905.

Weinert, N., Piceno, Y., Ding, G.-C., Meincke, R., Heuer, H., Berg, G., Schloter, M., Andersen, G. and Smalla, K. (2011). PhyloChip hybridization uncovered an enormous bacterial diversity in the rhizosphere of different potato cultivars: many common and few cultivar-dependent taxa. *FEMS Microbiology Ecology*, *75*, 497–506.

Chapter 3

Lignin modification of field-grown poplar trees via *CCR* gene silencing affects the metabolic capacities of the bacterial microbiome present in the endosphere

Abstract

Cinnamoyl-CoA reductase (*CCR*), the first enzyme in the monolignol-specific branch of lignin biosynthesis represents an efficient target to reduce lignin levels in poplar and thereby decrease biomass recalcitrance. However, gene silencing of *CCR* also results in flux changes of the general and monolignol-specific pathways ultimately leading to differential accumulation of carbon sources in the xylem vessels, which are accessible for the associated microbiota. Therefore, we hypothesize that the poplar-associated bacteria are dependent on the host genotype and *CCR* deficient poplar trees (and the accompanying changes in the xylem metabolome) influence the metabolic capacities present of the bacterial microbiome. To unravel the host genotype effects of *CCR* down-regulation in field-grown poplar trees *(Populus tremula x alba)* on the metabolic capacities of the culturable fraction of the poplar-associated microbiome, we used selective isolation and enrichments techniques. Specific carbon sources (e.g. ferulic acid) shown to be up-regulated in *CCR* deficient poplars were used to isolate bacterial cells from the rhizosphere, roots, stems and leaves of wild type and *CCR* deficient poplars.

Selective isolation and selective enrichment revealed significant host genotype effects on the bacterial metabolisms as well as the bacterial community structures. These effects were exclusively found in the endosphere environment without perceptible effects on the rhizospheric bacterial communities.

Keywords:

Populus tremula x alba, *CCR* down-regulation, bacterial microbiome, metabolism analysis

3.1 Introduction

Second-generation biofuels, derived from lignocellulosic biomass from dedicated energy crops represent a vital component in the impending transition to a more bio-based economy (Solomon, 2010; Yuan et al., 2008). The major limiting factor in the industrial processing of lignocellulosic plant biomass to fermentable sugars is the recalcitrance of lignin polymers, which are profusely present in the secondary thickened cell walls of vascular plants (Chen & Dixon, 2007; Studer et al., 2011). Accordingly, considerable attention has been focused on exploring genetic engineering to tailor lignin content and composition to generate feedstocks with reduced recalcitrance and improved commercial viability (Leplé et al., 2007; Van Acker et al., 2014; Vanholme et al., 2012; Vanholme et al., 2008; Wilkerson et al., 2014). Gene silencing of cinnamoyl-CoA reductase (*CCR*), the first enzyme in the monolignol-specific branch of lignin biosynthesis (Boerjan et al., 2003; Vanholme et al, 2010), typically results in reduced lignin levels (Ruel et al., 2009). *CCR*-down-regulated poplar trees (*Populus tremula* x *Populus alba*) grown in the greenhouse and in field trials in Belgium (Ghent) and France (Orléans), repeatedly displayed lower lignin levels (Leplé et al., 2007; Van Acker et al., 2014). Simultaneously, *CCR* gene silencing in poplar leads to the accumulation of various extractable phenolic compounds in the xylem (Leplé et al., 2007). Hence, the carbon sources available for the associated microbiota are profoundly different between wild type and *CCR* deficient genotypes.

The interactions between a plant and its microbiome are highly complex and dynamic involving multiple reciprocal signalling mechanisms and intricate interplay between bacteria and the plant's innate immune system. Therefore, even small changes in the host genome (ecotypes, cultivars, genetically modified genotypes, etc.) may influence the plant microbiome, and these changes may even feed back to modulate the behaviour of the host (Bulgarelli et al, 2013; Compant et al., 2010; Hardoim et al., 2008; Weyens et al., 2009). Furthermore, several studies have indicated that once inside their hosts endophytic bacteria change their metabolism and become adapted to their internal environment (de Santi Ferrara et al., 2011; Monteiro et al., 2012; Sessitsch et al., 2012). Moreover, phenolic-related compounds, such as these accumulating in *CCR* deficient trees, have been implicated in the modulation of the rhizosphere microbiome in *Arabidopsis thaliana* (Badri et al., 2013),

underlining their potential to affect bacterial communities. Furthermore, perturbations in the lignin biosynthesis via *CCR* down-regulation lead to compositional alterations in the cell wall. Cell wall features play important roles during endophytic colonization regulating endophytic competence (Compant et al., 2010; Hardoim et al., 2008). And finally, Bulgarelli et al. (2012) reported that cell wall features serve as sufficient assembly (colonization) cues in root microbiota of *Arabidopsis thaliana.* Therefore, compositional alterations in the cell wall may result in changes in the bacterial colonization of the *CCR*-down-regulated trees.

We hypothesized that the poplar-associated bacteria are dependent on the host genotype and that the differential accumulation of compounds in the xylem of *CCR* deficient poplar trees influences the metabolic capacities present of the bacterial microbiome. *CCR* deficient poplar trees are, except for the T-DNA construct, isogenic with the wild type poplar trees making them prime candidates to investigate host-genotype effects and the direct causality of the *CCR* gene silencing on the plant-associated bacterial communities. Moreover, studies in other organisms, particular in the human gut, have revealed strong host genotype effects and even single host genes which affect the microbiota (such as *MEFV*, encoding pyrin) (Spor et al., 2011).

3.2. Material and Methods

3.2.1. Generation of *CCR* deficient poplar trees

CCR deficient poplar clones, down-regulated for cinnamoyl-coA reductase (CCR; EC 1.2.1.44), were produced as previously described in Leplé et al. (2007). Briefly, a full-length *CCR* cDNA, with strong expression in developing poplar xylem, was cloned from a xylem cDNA library of poplar (*Populus trichocarpa* cv Trichobel) (Leplé et al., 1998). From this *CCR* cDNA sequence sense and antisense constructs, under the control of the cauliflower mosaic virus (CaMV) 35S promotor, were designed for downregulation of *CCR* expression (Leplé et al. 2007). Sense and antisense constructs were used to genetically modify the female poplar clone number 717-1-B4 (*Populus tremula* x *Populus alba*) from the Institut National de la Recherche Agronomique via an *Agrobacterium tumefaciens* procedure (Leplé et al., 1992).

3.2.2. Field trial and sampling procedure

The study site is a field trial established in April 2009 by the VIB with 240 *CCR* deficient (CCR^-) trees and 120 wild type (WT) poplar trees (*Populus tremula* x *Populus alba*). Both CCR^- and WT poplar trees were simultaneously micropropagated *in vitro*, acclimatized in a greenhouse and 6-month-old greenhouse-grown poplars (2 meters in height) were pruned and transferred to the field after 10 days. The trees were planted in a randomized block design (5 x 4 trees per block, for a total of 20 trees per block) in a density of 15.000 trees per hectare and an inter-plant distance of 0.75m. A border of wild type poplar trees surrounded the field to reduce environmental effects on tree growth (Custers, 2009; Van Acker et al., 2014). The full field layout can be found in Van Acker et al. (2014).

Poplar trees (wild type and *CCR* deficient) were sampled (in October 2011) after approximately 2.5 years of growth. Twelve biologically independent replicates (individual trees) were sampled for the wild type and for the *CCR* deficient poplar trees. Samples were spread, as much as possible, between different randomized blocks taking into account general appearance and preliminary data of *CCR* down-regulation (Prof. Dr. Boerjan; Personal communication). Since our main interest was the influence of the genetic modification (*CCR* down-regulation) of poplar on the plant-associated bacterial communities, we sampled poplar trees with the highest *CCR* down-regulation. Gene silencing of *CCR* is

associated with a visible phenotype (red-brown xylem coloration), which allowed us to sample according to phenotype, and thereby somewhat bypass unequal levels of gene silencing. Samples included rhizosphere soil, roots, stems and leaves.

Root samples were collected at a depth of 5-10 cm below ground level. Per poplar individual, a minimum of 10 g of roots was sampled. Root samples were placed into 50 mL plastic tubes containing 20 mL of sterile 10 mM phosphate saline buffer (PBS; 130 mM NaCl, 7 mM Na_2HPO_4, 3 mM NaH_2PO_4, pH 7.4). Soil particles adhering to the roots were collected as rhizosphere soil. For the stem and leaves samples, one complete offshoot of every poplar individual was collected. To standardize and maximize reproducibility of stem samples, several small stem 'cores' with bark (5-7, 1cm each) where collected from each offshoot from the base to the top of the offshoot to represent the stem compartment. Further, we specifically selected stem cores with high red coloration indicating high *CCR* down-regulation. For the leaf samples, all leaves from the sampled offshoot were collected to represent the leaf compartment.

3.2.3. Processing of rhizosphere soil, roots, stems and leaves samples

Rhizosphere soil was strictly defined as soil in the immediate vicinity of the roots. Therefore root samples were washed in 10 mM PBS buffer for 10 min on a shaking platform (120 rpm) and then transferred to new 50 mL plastic tubes. The soil particles directly dislodged from the roots represented the rhizosphere samples. Plastic tubes were pre-weighted to correct bacterial cell counts to colony forming units. Since our study focuses on rhizospheric and endophytic bacteria colonizing the internal tissues of plants, the epiphytic bacteria were removed from the surface of the plant tissues by sequential washing with (a) sterile Millipore water (30 sec), (b) followed by immersion in 70% (vol/vol) ethanol (2 min), (c) sodium hypochlorite solution (2.5 % active Cl^-, 5 min) supplemented with 0.1% Tween 80, (d) 70% (vol/vol) ethanol (30 sec) and finalized by washing the samples five times with sterile Millipore water. To confirm the absence of epiphytic bacteria on the surface of the plant tissues, aliquots (100µl) of the final rinse water were spread on solid 869 rich medium (Mergeay et al., 1985) containing per liter of deionised water: 10 g tryptone, 5 g yeast extract, 5 g NaCl, 1 g D-glucose and 0.345 g $CaCl_2.2H_2O$ (pH 7). The plates were examined for bacterial growth after 3 days of incubation at 30°C.

Plant samples were portioned into small fragments using a sterile scalpel and were subsequently macerated in sterile PBS buffer (10 mM) using a Polytron PR1200 mixer (Kinematica A6) in cycles of 2 min (4x) with cooling of the mixer on ice between cycles to reduce heating of the samples.

Finally, to counter biological and microbiological variation inherently present in the *CCR* deficient trees, the resulting homogenates (rhizosphere soil, root, stem, leaf) from three trees were pooled resulting in four independent biological replicates derived from twelve poplar individuals. Additionally, for every biological replicate a technical replicate was added to all experimental set-ups.

3.2.4. Bacterial isolation

Bacterial cells were isolated from the resulting homogenates of rhizosphere soil, root, stem and leaf tissues via (a) a direct non-selective and selective isolation technique with respectively a standard carbon source mix and specific phenolic lignin precursors as sole carbon sources and (b) a selective enrichment technique.

Direct isolation of bacterial cells (selective & non-selective)

In this approach bacterial cells were isolated by directly plating serially diluted aliquots (100µl) of the prepared homogenates on inorganic culture solution (containing per liter of deionised water: 6.06 g Tris–HCl, 4.68 g NaCl, 1.49 g KCl, 1.07 g NH_4Cl, 0.43 g Na_2SO_4, 0.2 g $MgCl_2 \cdot 6H_2O$, 0.03 g $CaCl_2 \cdot 2H_2O$, 40 mg $Na_2HPO_4 \cdot 2H_2O$, 10 ml 1.8 mM Fe (III) NH_4 citrate solution and 1 ml of trace element solution SL7 (pH7) supplemented with either 1mM p-coumaric acid, 1mM ferulic acid or 1mM sinapic acid (Sigma-Aldrich) as sole carbon source for the selective isolation. To control for normal baseline bacterial cell counts between wild type and *CCR* deficient poplars, bacterial cells were also non-selectively isolated using the same inorganic culture solution but supplemented with a carbon source mix (per liter deionised water: 0.52 g glucose, 0.66 g gluconate, 0.54 g fructose, 0.81 g succinate and 0.35 g lactate) optimized to accommodate a large range of bacterial carbon-source requirements. Bacterial cultures (selective and non-selective) were incubated (30°C, 7 days) after which the colony forming units (CFU) per g of rhizosphere soil and per g of fresh plant tissues were determined.

Selective enrichment of bacterial cells

The direct selective isolation of rhizospheric and endophytic bacteria with ferulic acid as sole carbon source provided the best results, therefore the selective enrichment of the bacterial cultures was performed using ferulic acid as sole carbon source. Briefly, bacterial cultures were enriched using the same liquid inorganic culture solution as described above supplemented with 2.5 mM ferulic acid. Culture media were inoculated with 2 mL of the prepared homogenates of rhizosphere soil, roots, stems and leaf tissues. Enrichments cultures were incubated for 5 weeks (36 days) on a shaking platform (120 rpm) at 30°C and diluted every 12 days with fresh inorganic culture medium. After 5 weeks of incubation, serially diluted aliquots (100µl) of the cultures were spread on solidified inorganic culture medium (10 g l^{-1} agar) with 1mM ferulic acid as sole carbon source. Plates were incubated for 7 days at 30°C and bacterial cell counts were determined for all samples (rhizosphere soil, roots, stems and leaves) of wild type and *CCR* deficient poplar trees. Bacterial strains were grouped based on morphology to create provisional OTUs (operational taxonomic units), which were validated using 16S-rRNA sequencing. Abundance data (cell counts) for each OTU were also determined. Subsequently, all morphologically different strains were purified in fivefold and subsequently stored at -70°C in a glycerol solution [15% (w:v) glycerol; 0.85% (w:v) NaCl] for genomic DNA extraction. In total 1820 isolates were stored across all compartments and genotypes.

3.2.5. Identification of bacterial strains

DNA extraction, PCR amplification and sequencing of bacterial amplicons

Total genomic DNA was extracted from all purified morphologically different bacterial strains in triplicate using the DNeasy® Blood and Tissue kit (Qiagen, Valencia, CA, USA). Bacterial DNA concentrations and purity were evaluated with a Nanodrop ND-1000 Spectro-photometer (Isogen Life Sciences, Temse, Belgium). PCR amplification of bacterial small-subunit ribosomal RNA genes (16S) was performed using approximately 50 ng μl^{-1} of bacterial DNA with the 26F/1392R (*E. coli* numbering) primer pair. The bacteria-specific 26F primer (5'-AGAGTTTGATCCTGGCTCAG-3', targeting 16S–23S internal transcribed spacer regions) and the universal 1392R primer (5'-ACGGGCGGTGTGTRC-3', targeting 16S bp 1392-1406) span the hypervariable V1-V9 regions (amplicon size:

±1366bp). The sequence variability and phylogenetic content of these amplicons allow for highly reliable and reproducible identification of bacterial cultures at a species level. The mastermix consisted of the following components: 1.8 mM high fidelity PCR buffer, 1.8 mM $MgCl_2$, 0.2 mM dNTPs, 0.4 µM 26F, 0.4 µM 1392R and 1.25U high fidelity Taq polymerase (Invitrogen, Ghent, Belgium). PCR cycling conditions were: initial denaturation step at 95°C for 5 min, followed by 30 cycles of 94°C for 1 min, 52°C for 30s and 72°C for 3 min, and completed with a final elongation step of 10 min at 72 °C (Techne TC 5000 PCR Thermal Cycler). PCR amplicons were purified with the QIAquick PCR Purification Kit (Qiagen, Valencia, CA, USA) and bi-directionally sequenced by Macrogen Inc. (Amsterdam, the Netherlands) using BigDyeTM terminator cycling conditions (Applied Biosystems (ABI) 3730XL).

16S rDNA sequence processing and taxonomic assignment

Partial 16S rRNA gene sequences were obtained from Macrogen Inc., Amsterdam, The Netherlands. Forward and reverse sequences were assembled to construct a 16S rDNA consensus sequence for each bacterial strain using the Geneious package (Biomatters Ltd., Auckland, New Zealand). All consensus sequences were queried against GREENGENES (DeSantis et al., 2006) and the National Center for Biotechnology Information (NCBI BLAST). Subsequently, consensus sequences were manually clustered into OTUs based on BLAST homology (97% sequence similarity). Based on previously determined bacterial cell counts and taxonomies of OTUs, abundance data for OTUs at specific taxonomic ranks (species, genus, family, order, class and phylum) were calculated for all plant compartments (rhizosphere soil, roots, stems, leaves) and genotypes (wild type and *CCR* deficient poplar trees). Subsequently, the OTU abundance data were used to construct taxonomic rank-specific matrices for the analysis of the bacterial community structures (see statistical analysis: multivariate). Finally, the consensus sequences were aligned using the MUSCLE (MUltiple Sequence Comparison by Log-Expectation) algorithm in Unipro UGENE and taxonomic dendograms were generated with the PHYLIP Neighbor-Joining algorithm (Unipro UGENE). In order to assess branch supports, bootstrap values were calculated with 2,000 pseudoreplicates.

3.2.6. Univariate analysis of bacterial community structures and bacterial diversity

Univariate community measures (species richness, species evenness & species diversity) reduce the great amount of species information into single summary indexes. These methods are less robust and sensitive than multivariate analyses (NMDS, canonical analyses) at detecting changes in bacterial communities but represent a valuable addition to the multivariate analysis by providing a higher level of visualization and interpretability. Species richness was calculated using Margalef's richness index: $D_{mg} = (S-1)/\ln(N)$, where S represents the number of OTUs in the samples and N the total number of clones in the samples. Species evenness was calculated using Pielou's evenness index: $J = H'/\ln(S)$ where H' represents the Shannon-Weiner diversity index ($H' = -\Sigma\ p_i \ln p_i$) and S the number of OTUs in the samples. Species diversity was calculated using the Inverse Simpson Index: $D = 1/\Sigma\ p_i^2$, where p_i is the proportion of clones in the i^{th} OTU.

3.2.7. Respirometric metabolism analysis of pure cultures with Biolog MT2

To quantify the ferulic acid degradation capacity of each isolated bacterial strain and thereby evaluate the effect of the *CCR* deficient poplar trees (and the resulting change in xylem composition and available carbon sources) on the individual bacterial metabolisms, all isolated bacterial strains were semi-quantitatively evaluated using Biolog MT2 plates (Biolog Inc., Hayward, CA, USA). Biolog MT2 plates utilize redox-chemistry to semi-quantitatively assess the degradation of externally added carbon sources. Each well of the Biolog MT2 microplates (96 well) contains tetrazolium violet redox dye, which is highly sensitive to bacterial respiration, and a buffered nutrient medium optimized for a wide variety of bacteria. Bacterial respiration, *e.g.* degradation of the added carbon source, results in the reduction of tetrazolium violet to formazan, which can be spectrophotometrically quantified at 595nm.

For the Biolog MT2 respirometric assay, pure bacterial cultures were grown in liquid 869 rich medium overnight (18h, 30°C, 120 rpm). Subsequently, the exponentially growing cultures were washed twice (4000 rpm, 20 min) with sterile 10 mM PBS buffer and the optical density of all bacterial suspensions was adjusted to 0.200 (600nm) with sterile 10 mM PBS buffer. Finally, the cultures

were incubated at 30°C on a shaking platform (120 rpm) for 18h to deplete residual carbon nutrient content. Each well of the biolog MT2 plates was filled with (a) 5 mM ferulic acid (30 µl) and (b) 115 µl of the designated bacterial suspension at optical density$_{600nm}$ = 0.20, resulting in a final concentration of approximately 1mM ferulic acid per well. Each bacterial strain was tested in triplicate. Positive control wells (3) were filled with 5 mM of D-glucose and 3 different bacterial strains. Negative control wells (3) were inoculated with 5 mM ferulic acid (30 µl) and 115 µl of sterile deionised H_2O. Inoculated plates were placed in self-sealing plastic bags (VWR) containing a water-soaked paper towel to minimize evaporation from the wells and incubated at 30°C. Absorbance was measured at 595 nm using an OMEGA plate reader (Fluorostar) immediately after inoculation (0 h) and at 3, 6, 18, 24, 48, 72, and 144 h. Actively respiring bacterial strains, *e.g.* those that degrade the added ferulic acid as sole carbon source, instigate the reduction of tetrazolium violet to formazan, which can be quantified spectroscopically at 595 nm.

Raw absorbance data for all bacterial strains from each time point (3, 6, 18, 24, 48, 72 and 144 h) were collected and individually standardized by subtracting the corresponding absorbance value measured immediately after inoculation (0 h) (reaction-independent absorbance). Furthermore, to semi-quantitatively evaluate the degradation capacity of each bacterial strain in the kinetic Biolog data set, the net area under the absorbance versus time curve was calculated according to the trapezoidal approximation (Guckert et al., 1996).

$$\text{Formula: } \sum_{i=1}^{4} ((v_i + v_{i=1})/2)*(t_i + t_{i=1}) = 50$$

The resulting value calculated via the trapezoidal approximation summarizes different aspects of the measured respirometric reaction including differences in the lag phases, rates of increase, maximum optical densities, etc. (Guckert et al., 1996). Finally the average respirometric responses of all bacterial strains, indicating the ferulic acid degradation capacity, were calculated for the rhizosphere soil, root, stem and leaf samples of wild type and *CCR* deficient poplar trees and displayed using box-whisker plots.

3.2.8. Statistical analysis

Univariate analysis

Statistical analyses were performed in R 2.15.1 (The R Foundation for Statistical Computing, Vienna, Austria). Normal distributions of the data were checked with the Shapiro-Wilkes test and homoscedasticity of variances was analysed using either Bartlett's or the Fligner-Killeens test. Significant differences in the variance of parameter were evaluated, depending on the distribution of the estimated parameters, either with ANOVA or the Kruskal Wallis Rank Sum Test. Post-hoc comparisons were conducted by either the Tukey's Honest Significant Differences tests or Pairwise Wilcoxon Rank Sum Tests.

Multivariate analysis of bacterial community structures and bacterial diversity

Statistical analysis of the multivariate ecological data included, in accordance with the recommendations of Anderson and Willis (2003) and most recently implemented by Hartmann et al. (2012), the following components:

(1) Robust unconstrained ordination: The OTU abundance data were square-root transformed (to down weight quantitatively abundant OTUs) and similarities in the bacterial community structures were displayed using nonmetric multi-dimensional scaling (NMDS) with Bray-Curtis distances. NMDS has been identified as particularly robust and useful for ecological data (Anderson & Willis, 2003). NMDS analyses were performed using R (package "Vegan") with 10,000 permutations. Comparisons between the different tissues within each genotype (wild type and *CCR* deficient) were displayed as well as pairwise comparisons between wild type and *CCR* deficient poplar trees for rhizosphere soil, root, stem and leaf samples. All the ordinations were plotted using R.

(2) Rigorous statistical test of the hypothesis: Differences between the *a priori* defined groups (Wild type and *CCR* deficient poplar trees) were evaluated using permutation-based hypothesis tests: analysis of similarities (ANOSIM), an analogue of univariate ANOVA and permutational multivariate analysis of variance (*adonis*). Both ANOSIM and *adonis* were run in R (package "Vegan") with 10,000 permutations (Table 2).

(3) Indicator species analysis: To evaluate the degree of preference of each species for the *a priori* defined groups (Wild type and *CCR* deficient poplar trees) a species-genotype association analysis was used. Correlations were calculated

using the multipat() function of the indicspecies package (version 1.7.1; Cáceres & Legendre, 2009). in R with 10,000 permutations.

3.3. Results

3.3.1. Selective isolation: Bacterial cell counts of WT and *CCR* deficient poplar trees

In a first approach, we directly isolated bacterial cells from the rhizosphere soil and surface-sterilized plant tissues (root, stem, leaf) of WT and *CCR* deficient poplar trees (Figure 3.1). Bacterial cell counts were expressed as colony forming units (CFU) per gram and analysed using a two-way ANOVA per block of added carbon source (Figure 3.1A, B, C, D) to allow for comparison between different host genotypes (WT, *CCR*$^-$) and sampled compartments (rhizosphere soil, root, stem, leaf). Firstly to compare the total number of bacterial cell counts, we directly isolated bacterial cells from rhizosphere soil and surface-sterilized plant compartments of WT and *CCR*$^-$ poplar trees using a non-selective approach with a carbon source mix, optimized to accommodate a large range of bacterial metabolisms. (Figure 3.1A). Bacterial cell counts (CFU g^{-1}) were highly comparable between WT and *CCR*$^-$ poplars across all compartments. For both host genotypes, the numbers of bacterial cells (CFU g^{-1}) recovered from the rhizosphere soil and roots were significantly higher compared to the numbers isolated from the stem and leaf samples ($P < 0.05$). In fact, the abundance of bacterial cells (CFU g^{-1}) consistently declined from the rhizosphere soil (WT: $7.13 \times 10^7 \pm 1.16 \times 10^7$, *CCR*$^-$: $6.17 \times 10^7 \pm 1.39 \times 10^7$) over the root samples (WT: $3.50 \times 10^7 \pm 9.14 \times 10^7$, *CCR*$^-$: $2.65 \times 10^7 \pm 5.86 \times 10^6$) to the stem samples (WT: $1.41 \times 10^4 \pm 4.23 \times 10^3$, *CCR*$^-$: $1.53 \times 10^4 \pm 7.12 \times 10^3$) within each genotype, with a small, not significant, increase in cell counts in the leaf samples (WT: $2.39 \times 10^4 \pm 6.39 \times 10^3$, *CCR*$^-$: $1.73 \times 10^4 \pm 1.16 \times 10^4$) as compared to the stem samples.

To relate the influence of *CCR* gene silencing (and resulting changes in the poplar xylem composition) to changes in the metabolic capacities of the bacterial communities, we selectively isolated bacterial cells from all 4 compartments (WT and *CCR*$^-$ trees) using specific phenylpropanoids (ferulic acid, sinapic acid and p-coumaric acid) as sole carbon sources in the nutrient medium (Figure 3.1B, C, D). Of these, ferulic and sinapic acid, and derivatives thereof, were previously shown to be upregulated in the *CCR*$^-$ poplar (Leplé et al, 2007), and ferulic acid was even incorporated into the lignin polymer.

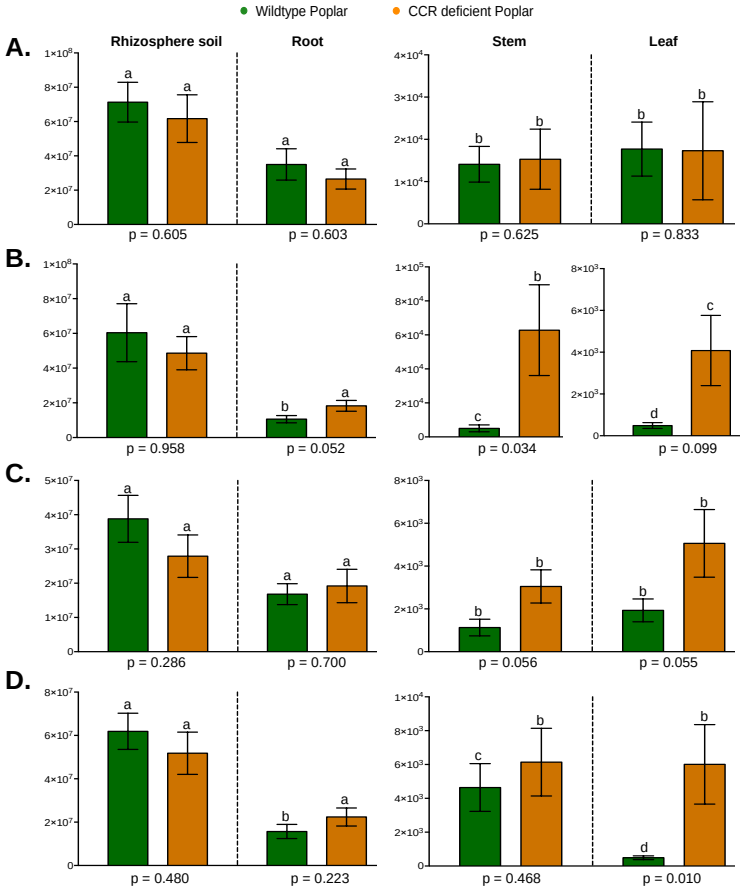

Figure 3.1. Bacterial cell counts (abundance) expressed as colony forming units (CFU) per gram soil (rhizosphere soil) or per gram fresh plant tissue (root, stem, leaf). A. Baseline cell counts from different compartments for both genotypes. Cells were non-selectively isolated using a standard carbon source mix optimized to accommodate a large range of bacterial carbon-source requirements. B. Selective isolation of bacterial cells using ferulic acid as sole carbon source. C. Selective isolation of bacterial cells using sinapic acid as sole carbon source. D. Selective isolation of bacterial cells using p-coumaric acid as sole carbon source. Colony forming units values are averages of at least 8 replicates ± standard error. Pairwise comparisons were conducted with Tukey's honest Significant Difference tests or Pairwise Wilcoxon Rank Sum test. Significant differences (P < 0.05) between the different plant compartments within each genotype are indicated with lower cased letters. P-values of pairwise comparisons between wildtype and CCR deficient poplars within each compartment are indicated below each graph.

In contrast to the non-selective isolation, selective isolation of bacteria with specific phenolic compounds as sole carbon source did reveal significant differences between WT and *CCR*$^{-}$ poplars. These significant differences between genotypes were exclusively found inside the plant (root, stem and leaf samples). In the rhizosphere soil, *i.e.* outside the plant, pairwise comparison of the bacterial cell counts between the genotypes revealed highly comparable bacterial abundances across the different phenolic carbon sources (Figure 3.1B, C, D). In the endosphere environment, the results were particularly consistent throughout the different compartments and different phenolic carbon sources. For all conditions, compartments and carbon sources, bacterial cell counts were notably higher in the WT poplar trees as compared to the *CCR*$^{-}$ poplars. Significant differences were most pronounced with the use of ferulic acid as sole carbon source with significantly higher bacterial abundances in the roots ($P = 0.05$), stems ($P = 0.03$) and leaves ($P = 0.10$) of *CCR*- poplars (Figure 3.1B). The use of sinapic acid as sole carbon source also revealed significant differences in the stems ($P = 0.06$) and the leaves ($P = 0.06$) in the pairwise comparisons between both genotypes (Figure 3.1C). Finally when using p-coumaric acid as sole carbon source, a significant difference was only observed in the leaves ($p < 0.01$) but the overall trend of higher bacterial cell counts in the *CCR*- poplars persisted in the root and stem tissues (Figure 3.1D). In accordance with the non-selective isolation, bacterial cell counts decreased gradually from the rhizosphere soil to the leaves across the different used phenolic carbon sources (Figure 3.1B, C, D).

These findings represent the first indication that the genetic modification had an effect on the plant-associated bacterial communities but also that the effect remained restricted to the inside of the plant since only significant differences could be revealed at the level of the endophytes. To further explore this effect in more depth, bacterial cells were selectively enriched with ferulic acid as sole carbon source and bacterial cell counts were assessed and compared between genotypes. Furthermore, the species composition were evaluated and compared between genotypes.

3.3.2. Selective enrichment: Bacterial cell counts

To complement the selective isolation experiments, we selectively enriched bacterial cells (using ferulic acid as sole carbon source) from the rhizosphere soil and surface-sterilized plant tissues (root, stem, leaf) of WT and *CCR* deficient poplar trees. Bacterial cell counts were determined as well as the bacterial community structures (16S rRNA sequencing), which were analysed using multivariate and univariate ecological analyses. We determined and compared bacterial cell counts (CFU g^{-1}) (Figure 3.2) as well as the bacterial community structures (Figure 3.3 and 3.4).

Bacterial cell counts were expressed as colony forming units (CFU) per gram of soil or plant tissue and analysed using a one-way ANOVA per compartment (rhizosphere soil, roots, stems, leaves) to allow for pairwise comparison between the different host genotypes (Figure 3.2). Interestingly, the results from the bacterial cell counts of the selective isolation were confirmed by the selective enrichment experiments. In accordance with the selective isolation from the rhizosphere soil, highly similar numbers of bacterial cells (CFU g^{-1} ± standard deviation) were obtained from the *CCR*$^{-}$ poplars ($8.33 \times 10^7 \pm 1.44 \times 10^7$) as compared to the WT ($9.16 \times 10^7 \pm 1.93 \times 10^7$) ($P = 0.96$) (Figure 3.2A). However, bacterial abundances inside roots ($p < 0.01$), stems ($P = 0.02$) and leaves ($p < 0.001$) of *CCR* deficient trees were consistently higher (Figure 3.2B, C, D). Further, considerably more variation was observed in the bacterial cell counts from the *CCR*$^{-}$ trees as compared to those from the WT (Figure 3.2). This discrepancy can be attributed to variation of the *CCR* genotype in the levels of gene silencing that are reflected by different intensities of the red xylem coloration associated with *CCR* down-regulation and the associated variation in the xylem composition, thereby potentially influencing the plant-associated bacterial community.

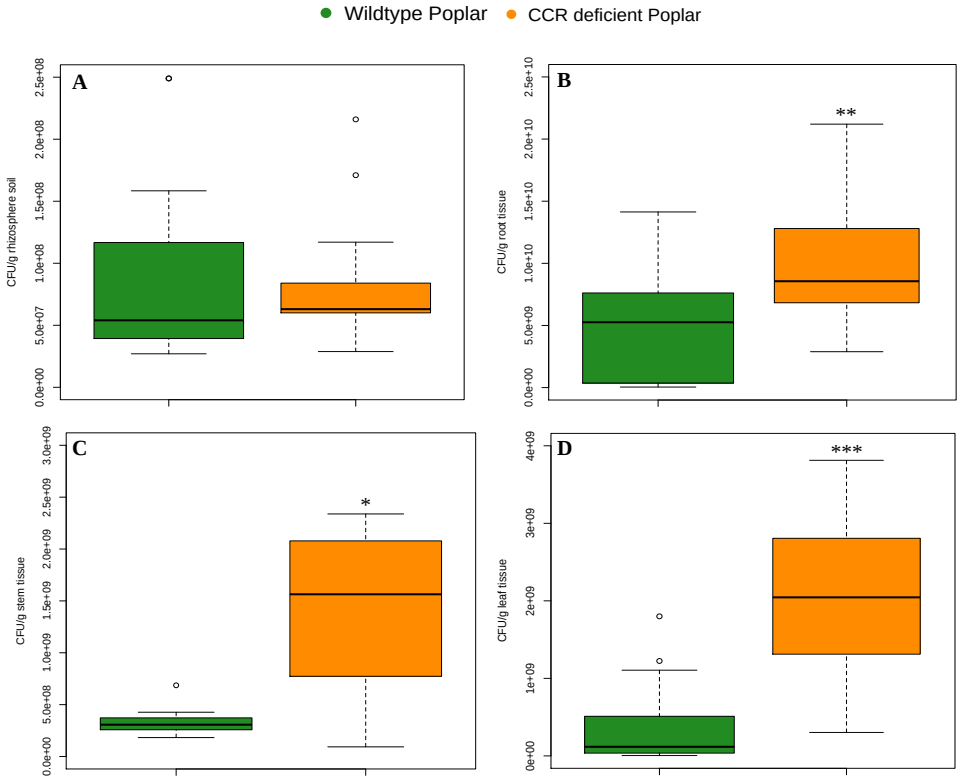

*Figure 3.2. Bacterial cell counts of the selective enrichment expressed as colony forming units (CFU) per gram of soil for the rhizosphere soil (A) or per gram root (B), stem (C) and leaf (D) for the plant tissues. Box-plots display the first (25%) and third (75%) quartile, the median (bold line), maximum and minimum observed values (without outliers). Outliers (more or less than 3/2 of the upper/lower quartile) are displayed as open circles. Cell counts were statistically analysed using an one-way ANOVA. P-values of pairwise comparisons between WT and CCR deficient poplars within each tissue are indicated on the graphs (P < 0.05: *, P < 0.01: **, P < 0.001: ***).*

3.3.3. Bacterial community structures after selective enrichment

Multivariate analysis

To compare species composition within the different sampled compartments and genotypes, we grouped all isolated bacterial strains based on their morphology to create provisional operational taxonomic units (OTUs), which were validated using 16S-rRNA Sanger sequencing and we determined abundance data (cell counts) for each bacterial OTU. OTU abundance data were square-root transformed and similarities were displayed using nonmetric multi-dimensional

scaling (NMDS) with Bray-Curtis distances. NMDS analyses were performed using R (package “Vegan”) with 10,000 permutations (Figure 3.3 and 3.4).

For both genotypes, NMDS analyses revealed strong clustering of the bacterial communities according to the different plant compartments (rhizosphere soil, root, stem, leaf) (Figure 3.3). To statistically support the visual clustering of the bacterial communities in the NMDS analyses, the different compartments were compared using permutation-based hypothesis tests: analysis of similarities (ANOSIM) and permutational multivariate analysis of variance (*adonis*). ANOSIM is routinely used in multivariate ecological data analysis but is often considered as less robust than *adonis*. Therefore both statistical methods were used in parallel. Both ANOSIM and *adonis* indicated highly significant differences between the bacterial communities of the different compartments for WT poplars and *CCR*- poplars. A graphical representation of the ANOSIM analyses is provided in Supplementary Figure 3.1 For both genotypes, the variation within each group was considerably lower than the variation between the different groups, resulting in significant differences between the compartments for the WT poplars ($R = 0.82$, $P < 0.01$) and the *CCR*- poplars ($R = 0.76$, $P < 0.01$). This illustrates that all compartments rendered microbiota significantly dissimilar from each other.

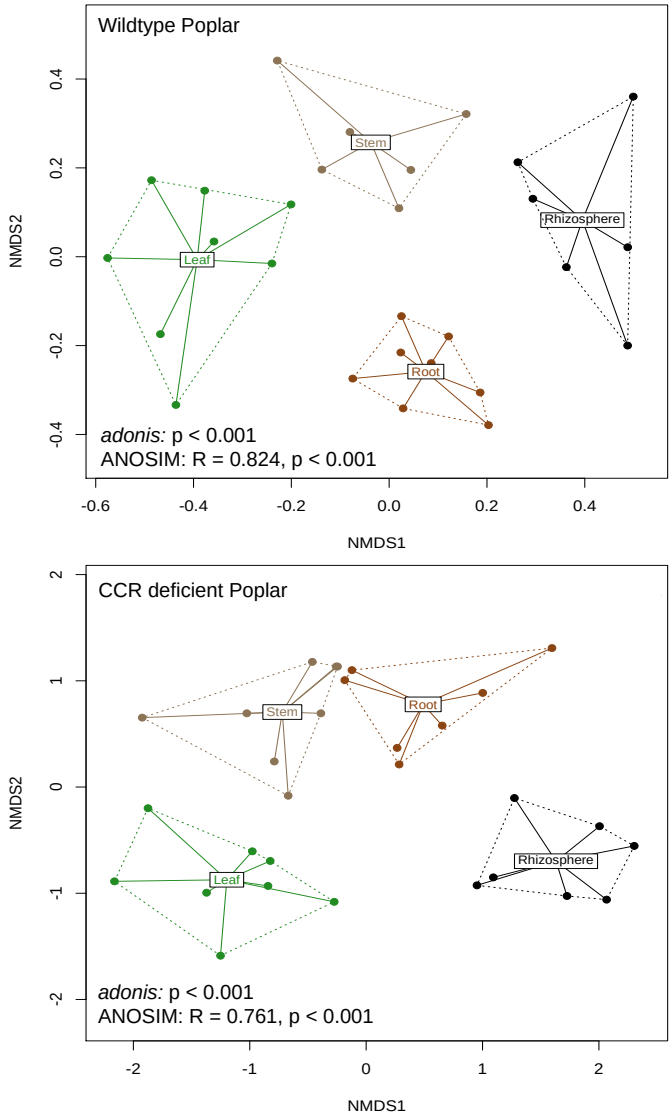

Figure 3.3. NMDS analyses of bacterial communities isolated from the different plant compartments (rhizosphere soil, root, stem, leaf) for each genotype (WT and CCR-). NMDS analyses contain at least 6 replicates per plant compartment and were run as routine in R (package 'Vegan') with 10,000 permutations. Statistical support for the NMDS clustering is provided using the permutation-based hypothesis tests analysis of similarities (ANOSIM) and permutational multivariate analysis of variance (adonis). Results from both hypothesis tests are indicated below each graph.

To determine the influence of the genotype (WT versus *CCR*$^-$) on the bacterial communities, pairwise comparisons were made between the genotypes within each compartment and displayed using NMDS with Bray-Curtis distances (Figure 3.4). Furthermore, pairwise comparisons within each compartment were statistically tested using ANOSIM and *adonis*. In the rhizosphere soil, bacterial communities showed no relevant clustering according to the genotype as visually apparent by the NMDS analysis (Figure. 4A). NMDS analyses showed a high overlap between the bacterial communities of wild type and *CCR* deficient poplar trees. Both ANOSIM and *adonis* statistically confirmed that the bacterial communities of both genotypes were highly comparable within the rhizosphere (ANOSIM: $R < 0.01$, $P = 0.41$, *adonis*: $P = 0.43$) (Figure 3.4A). However, in contrast to the rhizosphere soil, we noted significant differences between the poplar genotypes at the level of the endophytes. Moreover these differences were highly consistent throughout the different compartments (roots, stems and leaves). NMDS analyses of the bacterial communities in the roots, stems and leaves revealed strong clustering according to the genotype (Figure 3.4B-D). Most pronounced clustering, according to genotype, was observed in the stems, where no visual overlap was observed between the bacterial communities (Figure 3.4B). In the roots and leaves, the clustering according to genotype persisted with small visual overlaps between WT and *CCR*$^-$ poplar trees. Pairwise statistical analysis of the genotypes within the compartments confirmed the significance of the visually observed differences with NMDS. Most pronounced significant differences, in conjunction with the visual interpretation, were found in the stems (Figure 3.4C, ANOSIM: $R = 0.51$, $P < 0.01$, adonis: $P < 0.01$). However, results in the roots and leaves were also significant at the 95% significance level (Figure 3.4B, D). ANOSIM results of the pairwise comparisons are graphically visualized in Supplementary Figure 3.2. For the endosphere compartments (root, stem and leaf), the variation within the genotypes is considerably lower than the variation between the groups illustrating the differentiation of the host genotypes within these plant compartments.

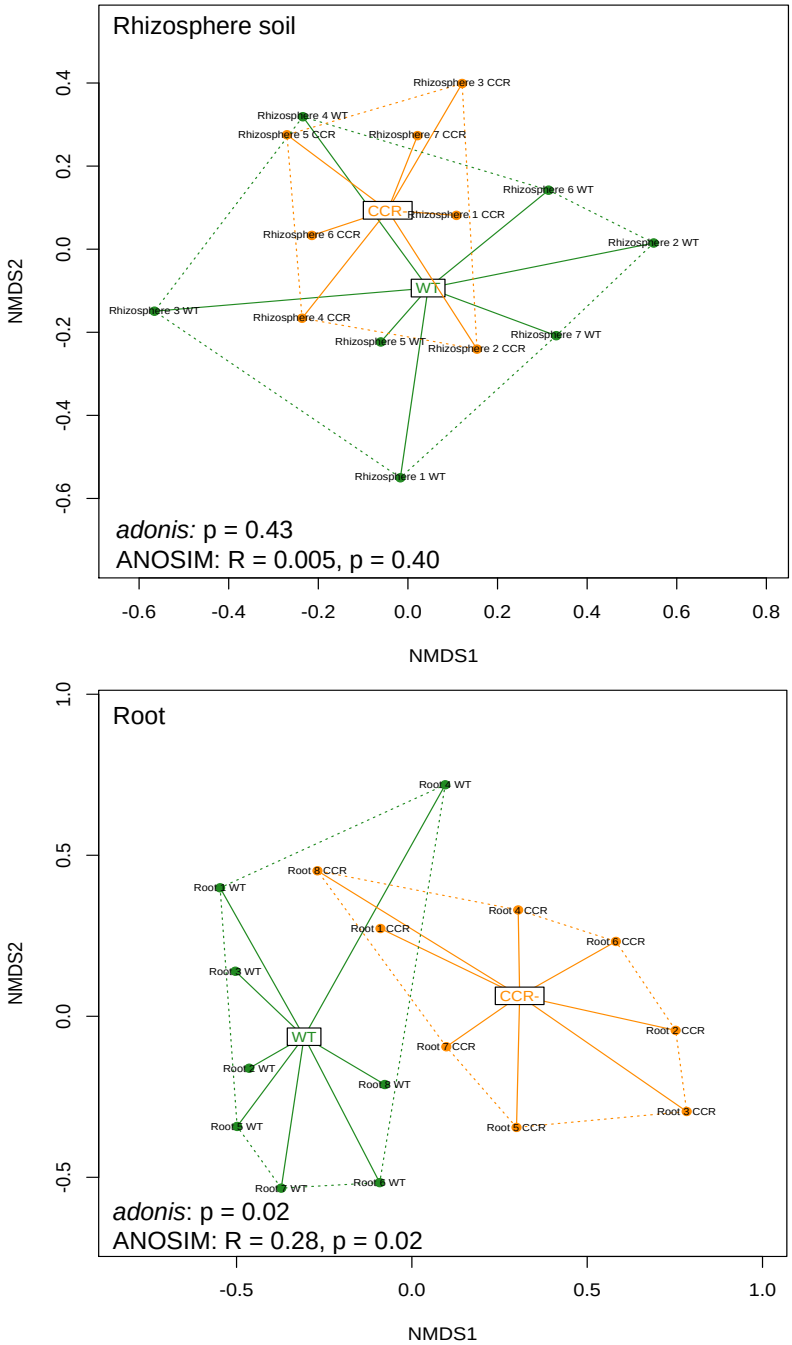

Figure 3.4: Nonmetric multi-dimensional scaling (NMDS) with Bray-Curtis distances of pairwise comparisons between wildtype and CCR deficient poplar trees within each compartment (rhizosphere soil, root, stem, leaf).

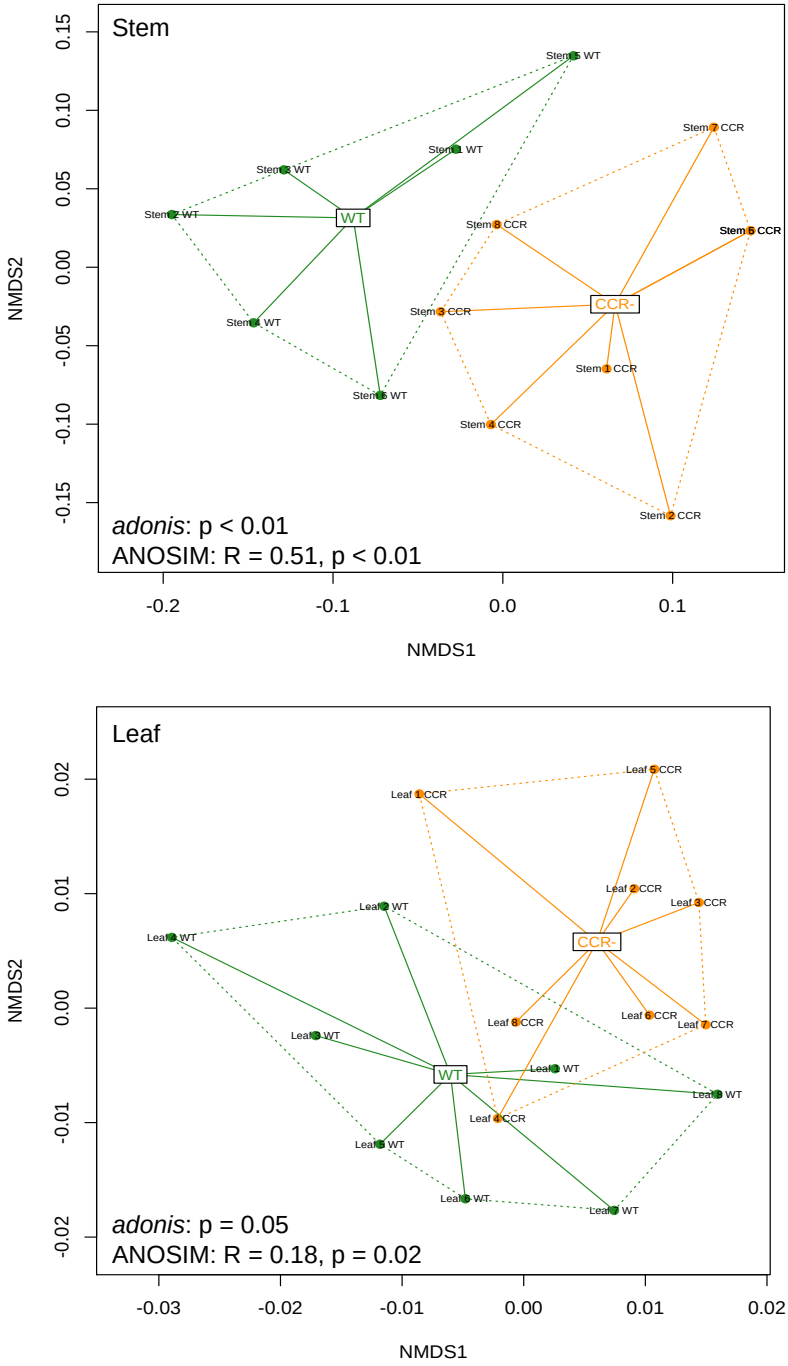

Figure 3.4. (Continued) Nonmetric multi-dimensional scaling (NMDS) with Bray-Curtis distances of pairwise comparisons between wildtype and CCR deficient poplar trees within each compartment (rhizosphere soil, root, stem, leaf). NMDS analyses contain at least 6

replicates per plant compartment and were run as routine in R (package 'Vegan') with 10,000 permutations. Statistical support for the NMDS clustering is provided using the permutation-based hypothesis tests analysis of similarities (ANOSIM) and permutational multivariate analysis of variance (adonis). Results from both hypothesis tests are indicated below each graph.

In depth taxonomic composition (species breakdown)

Consensus sequences within each compartment were aligned (MUSCLE) and taxonomic dendograms were generated (Unipro UGENE) (Okonechnikov et al., 2012) and displayed using Itol (Letunic & Bork, 2011). OTU abundance data for both genotypes were mapped onto the dendograms (Supplementary Figure 3.3-3.6). Sequence clustering across all compartments and genotypes generated a total of 93 OTUs. The taxonomic composition within each compartment and genotype was determined and significant associations between species abundance and compartment or genotype were determined using an indicator species analysis.

Overall, in the rhizosphere samples, the predominant phyla were Proteobacteria (WT= 73.8%, *CCR*- = 96.7%), Actinobacteria (WT= 22.3%, *CCR*- = 2.8%) and Firmicutes (WT= 3.53%, *CCR*- = 0.56%). Among the Proteobacteria, the class Alphaproteobacteria accounted for 30.7% in the WT poplar trees and 37.7% in the *CCR* deficient poplar trees, the class Betaproteobacteria for 5.14% (WT) and 2.78% (*CCR*-). Finally the class Gammaproteobacteria represented 37.9% of the proteobacterial abundance in the WT poplar trees and 56.2% in the *CCR*- poplar trees. At the species level, the culturable rhizospheric communities of both poplar genotypes are dominated by *Rhodanobacter lindaniclasticus* representing 28.4% (WT) and 37.9% (*CCR*-) of the respectively total rhizospheric community. Complete species composition presented in supplementary figure 3.3.

In the roots, the dominance of the Proteobacteria persisted in both genotypes (WT= 77.2%, *CCR*-= 89.04%) with Actinobacteria (WT= 17.1%, *CCR*- = 8.0%) and Firmicutes (WT= 5.65%, *CCR*-= 2.96%) representing the minor contributing phyla. Within the Proteobacteria, the class Alphaproteobacteria accounted for 44.7% of the bacterial abundance in the WT poplar trees and for 13.4% in the WT poplar trees. The class Betaproteobacteria accounted for respectively 21.9% (WT poplar) and 22.7% (*CCR*- poplar) of the bacterial abundance. Finally, the class Gammaproteobacteria represented 10.7% (WT poplar) and 10.7%, (*CCR*-

poplar) of the bacterial abundance. At the species level, both genotypes showed clear differences in species composition and abundance. WT poplar trees were dominated by *Variovorax paradoxus* (14.7%), *Mesorhizobium plurifarium* (12.1%) and *Ensifer adhaerens* (11.2%) whereas *CCR* deficient poplars trees were dominated by *Pseudomonas putida* (26.3%), *Stenotrophomonas rhizophila* (21.6%) and *Achromobacter denitrificans* (13.4%). Complete species composition presented in supplementary figure 3.4.

In the stems, even a more obvious divergence between the genotypes appeared. The dominant phylum in the WT poplar trees was Actinobacteria (WT = 62.8%, *CCR*- = 3.02%) whereas in the *CCR*- poplar trees Proteobacteria remained the predominant phylum (WT = 93.8%, *CCR*- = 24.4%). At the species level, stems of WT poplar trees showed a high dominance of *Plantibacter flavus* (49.1%) whereas stems of the *CCR* deficient poplars were highly dominated by *Pseudomonas putida* (75.9%) and to a lesser extent *Stenotrophomonas rhizophila* (9.8%). Complete species composition and abundance data are presented in supplementary figure 3.5.

In the leaves, the predominant phyla were Actinobacteria (WT = 61.9%, *CCR*- = 47.7%), Proteobacteria (WT = 37.9%, *CCR*- = 47.7%) and to a lesser extent in the CCR- poplar trees Firmicutes (*CCR*- = 4.1%). Among the Proteobacteria, the class Alphaproteobacteria accounted for 36.0% in the WT poplars and for 41.3% in the *CCR*- poplar trees. The class Gammaproteobacteria represented 1.9% and 6.83% respectively in the WT and *CCR*- poplar trees. No representatives of the class Betaproteobacteria were detected in the leaf samples. At the species level, WT poplar trees were dominated by *Plantibacter flavus* (22.0%), *Bosea robinae* (16.9%) and *Rhodococcus cercidyphylli* (9.7%). In contrast, *CCR*- poplar trees showed a high dominance of *Brevundimonas diminuta* (20.8%), *Microbacterium testaceum* (16.8%) and *Curtobacterium flaccumfaciens* (10.6%). Complete species composition and abundance data can be found in supplementary figure 3.6.

Influence of compartment on species composition

Furthermore, to investigate the association between species abundance and the plant compartment (rhizosphere soil, root, stem and leaf) or the host genotype (WT and *CCR*- poplar trees), an indicator species analysis was performed. For

each identified bacterial species (OTU) maximum association strength (R: indicator value) and the significance of the association were calculated using an Indicator species analysis (the multipat() function of the indicspecies package R) (Table 3.1 and 3.2).

To identify significant associations between species abundance and compartment (rhizosphere soil, root, stem, leaf), an indicator species analysis was performed within each genotype (Table 3.1). For the WT poplar trees, 62 bacterial species were identified across the different compartments. Among these 62 identified bacterial species, 2 species were strongly associated with the rhizosphere soil, 7 species were associated with the roots, and finally 2 species were associated with the stems and leaves.

Table 1.1. Indicator species analysis evaluating significant associations between species abundance and the plant compartment (rhizosphere soil, root, stem and leaf)

Wild type Poplar				
OTU	Associated with	Indicator value	p-value	Relative abundance (%)
Rhodanbacter lindaniclasticus	Rhizosphere	0.71	<0.01	28.43
Arthrobacter sp.	Rhizosphere	0.57	<0.01	8.23
Variovorax paradoxus	Root	0.50	<0.01	14.74
Stenotrophomonas rhizophila	Root	0.75	<0.01	9.15
Mesorhizobium huakii	Root	0.62	<0.01	12.12
Achromobacter sp.	Root	0.62	<0.01	7.11
Microbacterium phyllosphaerae	Root	0.63	<0.01	8.25
Staphylococcus caprae	Root	0.48	0.03	3.6
Rhizobium huatlense	Root	0.38	0.04	3.51
Plantibacter flavus	Stem	0.52	<0.01	49.2
Bacillus subtilis	Stem	0.33	0.04	3.46
Rhodococcus cercidyphylli	Leaf	1.00	<0.01	9.72
Methylobacterium extorquens	Leaf	0.50	<0.01	2,07

CCR deficient Poplar				
OTU	Associated with	Indicator value	p-value	Relative abundance (%)
Rhodanbacter lindaniclasticus	Rhizosphere	0.86	<0.01	37.85
Ochrobactrum intermedium	Rhizosphere	0.57	<0.01	3.15
Rhodococcus jostii	Rhizosphere	0.29	0.04	0.74
Dokdonella fugitiva	Rhizosphere	0.29	0.02	8.35
Stenotrophomonas rhizophila	Root	0.60	<0.01	21.60
Mesorhizobium huakii	Root	0.59	0.02	4.54
Xanthomonas sp.	Root	0.50	<0.01	4.72
Microbacterium phyllosphaerae	Root	0.50	<0.01	5.72
Bosea robinae	Root	0.50	<0.01	4.26
Achromobacter denitrificans	Root	0.50	0.01	13.37
Bacillus subtilis	Stem	0.37	0.05	9.76
Pseudomonas putida	Stem	0.52	0.02	75.90
Rhodococcus cercidyphylli	Leaf	0.82	<0.01	4.92
Methylobacterium extorquens	Leaf	0.88	<0.01	4.70
Pseudomonas syringae	Leaf	0.63	0.01	1.98
Plantibacter flavus	Leaf	0.57	<0.01	10.52
Sphingomonas sp.	Leaf	0.38	0.05	6.88
Pseudomonas graminis	Leaf	0.38	0.04	0.48

Indicator value (R): association strength

For the *CCR*- poplar trees, 69 bacterial species were identified across the different compartments. Among these 69 identified bacterial species, 4 species were strongly associated with the rhizosphere soil, 7 species were associated with the roots, and finally 1 species and 6 were associated with respectively the stems and leaves. For both genotypes (WT and *CCR*- poplar trees) we found bacterial species strongly associated with each matrix compartment (rhizosphere soil, root, stem, leaf) illustrating the specificity of each compartment (Table 3.1).

Influence of genotype on species composition

To identify significant associations between species abundance and genotype (WT and *CCR*- poplar trees) an indicator species analysis was performed within each compartment for both genotypes (Table 3.2).

Table 3.2. Species indicator analysis indicating species significantly correlated to WT poplar or CCR deficient poplars within each tissue. Correlations were calculated using the Dufrene-Legendre Indicator Species Analysis routine (Indval) in R with 10,000 permutations.

		Wild type Poplar		
Plant compartment	OTU	Indicator value	p-value	Relative abundance (%)
Rhizosphere soil	NA			
Root	NA			
Stem	*Plantibacter flavus*	0.01	0.73	49.2
Leaf	NA			
		CCR deficient Poplar		
Plant compartment	OTU	Indicator value	p-value	Relative abundance (%)
Rhizosphere soil	*Mesorhizobium plurifarium*	0.71	0.04	26.53
Root	*Pseudomonas putida*	0.71	0.01	26.30
Stem	*Pseudomonas putida*	0.95	<0.01	75.90
Leaf	*Methylobacterium extorquens*	0.80	0.02	4.70

NA: No significant association found

In the rhizosphere soil no bacterial species showed a significant association with the WT poplar trees. In contrast, *Mesorhizobium plurifarium* (R = 0.84, P = 0.04) was associated with the *CCR*- poplar trees. For the roots in the WT poplars, we again found no significant association for any bacterial species whereas in the *CCR*- poplar trees a strong association was found for *Pseudomonas putida* (R=0.85, P < 0.01). In the stems, the association of *Pseudomonas putida* with the *CCR*- poplars trees persisted (R=0.98, P < 0.01).

Interestingly, for the WT poplar trees a completely different association was found for *Plantibacter flavus* (R = 0.85, P = 0.01). Finally in the leaves, no significant associations were found for the WT poplar trees and for the *CCR* deficient poplar trees we found a significant association for *Methylobacterium extorquens* (R = 0.80, P = 0.02) (Table 3.2).

3.3.4. Univariate analyses of bacterial community structures and bacterial diversity

Univariate ecological measures represent a valuable addition to multivariate analyses and provided direct interpretability between conditions. Margalef's richness, Pielou's evenness and the Inverse Simpson Diversity were calculated based on OTU abundances (Table 3.4). Indices were statistically compared using a two-way ANOVA within each ecological index. Furthermore, total endophytic richness, evenness and diversity, calculated as the average of roots, stems and leaves, were statistically compared with the rhizospheric richness, evenness and diversity using a two-way ANOVA.

For all ecological indices (richness, evenness and diversity) the average values were highly similar between WT and *CCR*- poplar trees in the rhizosphere soil (P-values: richness = 0.82, evenness = 0.86 and diversity = 0.85). However, in contrast to the rhizosphere soil, at the level of the endophytes the results showed a consistent trend throughout the different indices. OTU richness, evenness and diversity were notably and consistently lower in the *CCR*- poplar trees as compared to the WT poplars with the exception of the OTU richness in the leaves. High variation in the indices reduced the significance of the results but borderline significant differences were found in the OTU evenness in the roots (P = 0.095) and the stems (P = 0.075). Within each genotype, the OTU richness consistently declined from the rhizosphere soil (WT: 0.329 ± 0.044, *CCR*-: 0.346 ± 0.044), over the roots (WT: 0.248 ± 0.025, *CCR*-: 0.195 ± 0.024), to the stems (WT: 0.180 ± 0.011, *CCR*-: 0.130 ± 0.038) and the leaves (WT: 0.128 ± 0.011, *CCR*-: 0.138 ± 0.012). A single exception to this constant decline is the difference between the stems and leaves of the *CCR* deficient poplar trees (stems: 0.130 ± 0.038 vs. leaves: 0.138 ± 0.012). Similar differences between the different compartments were obtained for the evenness and the inverse Simpson diversity index where the values persistently declined from the rhizosphere soil up to the leaves within each genotype. Significant

differences between the compartments in the different ecological indices within each genotype are indicated in table 3.4.

Table 3.4. Univariate ecological measures of the bacterial communities based upon OTU abundance with (A) Margalef's richness, (B) Shannon's evenness, (C) Inverse Simpson diversity.

A. Margalef's richness	Rhizosphere	Root	Stem	Leaf	Endophytic richness
Wild type	0.329 ± 0.044 a	0.248 ± 0.025 a,b	0.180 ± 0.011 b,c	0.128 ± 0.011 c	0.157 ± 0.012*
CCR deficient	0.346 ± 0.042 a	0.195 ± 0.024 b	0.130 ± 0.038 b	0.138 ± 0.012 b	0.148 ± 0.011*
p-value WT vs. CCR	0.816	0.160	0.176	0.639	0.459
B. Shannon's evennness	Rhizosphere	Root	Stem	Leaf	Endophytic evenness
Wild type	0.776 ± 0.086 a	0.664 ± 0.040 a,b	0.544 ± 0.078 b,c	0.447 ± 0.028 c	0.503 ± 0.026*
CCR deficient	0.783 ± 0.104 a	0.560 ± 0.043 b	0.338 ± 0.086 c	0.390 ± 0.029 c	0.417 ± 0.026 *
p-value WT vs. CCR	0.863	0.095	0.075	0.167	0.023
C. Inverse Simpson Diversity	Rhizosphere	Root	Stem	Leaf	Endophytic diversity
Wild type	3.451 ± 0.358 a	3.860 ± 3.126 a	2.718 ± 0.249 a,b	2.239 ± 0.129 b	2.607 ± 0.160*
CCR deficient	3.345 ± 0.420 a	3.126 ± 0.289 a	2.415 ± 0.214 a,b	2.050 ± 0.112 b	2.33 ± 0.113*
p-value WT vs. CCR	0.850	0.201	0.303	0.282	0.177

Values are averages of at least 8 biological independent replicates ± standard deviation. Indices were statistically compared using a two-way ANOVA per block (A, B, C). Significant differences between the different plant compartments within each genotype are indicated with letters (P < 0.05). P-values of pairwise comparisons between host genotypes within each tissue are indicated below each block. Significant differences between the rhizospheric and total endophytic compartment are indicated with an asterisk (P < 0.05).

Lastly, total endophytic richness, evenness and diversity (calculated as the average of the roots, stems and leaves) were significantly lower than the rhizospheric richness, evenness and diversity for both genotypes (P < 0.05). Pairwise comparison between WT and *CCR*- poplar trees revealed a significant decrease in the total endophytic evenness (P = 0.023) of the *CCR*- poplars as compared to the WT poplars. The same trends were also visible for the total endophytic richness and diversity, but these trends were not statistically significant (Table 3.4).

3.3.5. Respirometric metabolism analyses

The results above clearly indicated changes in the bacterial populations between WT poplars and *CCR*- poplars. To obtain a clear view on the extent of the effect of the genetic modification on the individual metabolisms of the isolated bacterial strains, all strains were evaluated for their ferulic acid degradation capacity using Biolog MT2 plates (Biolog Inc.). Raw absorbance data were standardized and the net area under the absorbance versus time curve was calculated according to the trapezoidal approximation. Finally, respirometric responses of the bacterial strains were averaged within each compartment (rhizosphere soil, root, stem, leaf) and genotype (WT and *CCR*- poplars) and displayed using box-whisker plots (Figure 3.5.). Biolog data sets were statistically analysed with a parametric one-way analysis of variance ANOVA.

Interestingly, the results of the respirometric analysis supported the results at the population level. In the rhizosphere soil, the average ferulic acid degradation capacity, as measured by Biolog, was highly similar between WT and *CCR*- poplar trees ($P = 0.56$). In contrast, the bacterial metabolisms within the endophytic communities were significantly different between both genotypes. The respirometric response was significantly higher in the bacterial endophytes isolated from the *CCR*- poplars in the roots ($P < 0.001$), in the stems ($P < 0.01$) and in the leaves ($P < 0.05$) as compared to the WT poplars indicating a higher ferulic acid degradation capacity of the bacterial endophytes present in the *CCR*- poplars.

Furthermore, to evaluate whether or not the significant differences observed in the average respirometric responses were not solely attributable to limited number of bacterial strains (with high responses and in that way skewing the general average to higher values) but were definitely a population response, we also assessed the metabolism evenness of the bacterial strains within each compartment and genotype. For all compartments the evenness values were highly comparable, except in the stem tissues. In the stem tissues, the community metabolic evenness of the *CCR*- poplar trees was significantly lower than the WT poplar trees ($P < 0.05$) indicating that the higher respirometric response is limited to specific strains (Supplementary fig. 3.7.).

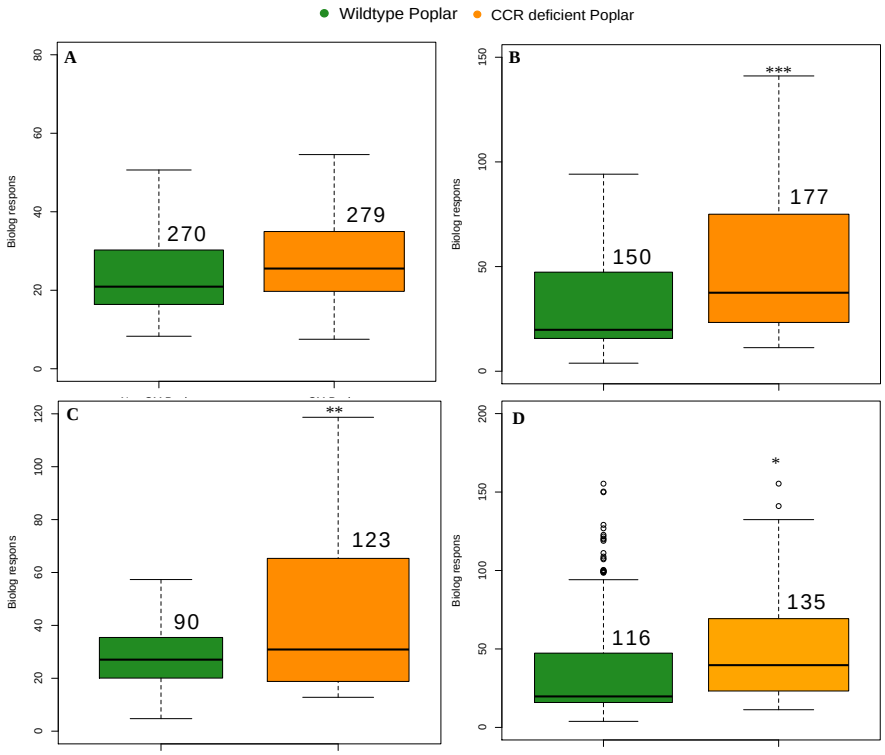

*Figure 3.5. Respirometric metabolism analyses using BIOLOG with 1mM ferulic acid. Average respirometric responses of all bacterial strains isolated from the different plant compartments per host genotype (A. Rhizosphere, B. Root, C. Stem and D. Leaf). Box-plots display the first (25%) and third (75%) quartile, the median (bold line), maximum and minimum observed values (without outliers). Outliers (more or less than 3/2 of the upper/lower quartile) are displayed as open circles. Biolog responses for each individual bacterial strain are calculated using the net area under the absorbance versus time curve according to the trapezoidal approximation. Averages were calculated per compartment and compared between genotypes. P-values of pairwise comparisons between wildtype and CCR deficient poplars within each plant compartment are indicated on the graphs (P < 0.05: *, P < 0.01: **, P < 0.001: ***). Numbers in boxplots represent the amount of isolates included in the analysis.*

3.3.6. OTU breakdown of Biolog respirometric responses

Further, we evaluated the individual respirometric response of each identified OTU (Figure 3.6, Supplementary Figure 3.8) within each compartment and genotype, to relate OTU abundance to the respirometric response to ferulic acid.

Pseudomonas putida isolated from the roots and stems of the *CCR*$^{-}$ poplar clearly possessed the highest degradation capacity for ferulic acid (Figure 3.6).

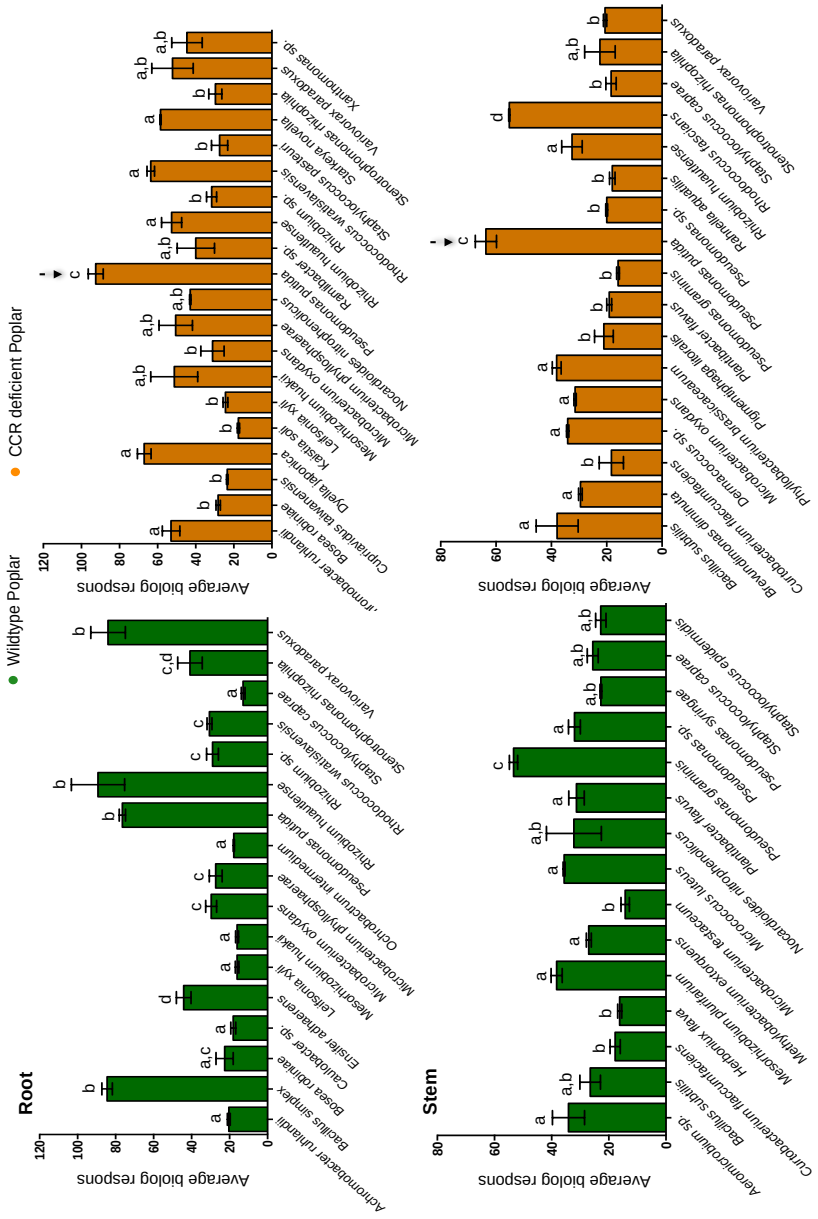

Figure 3.6. Respirometric metabolism analyses using BIOLOG with 1mM ferulic acid. Species-level OTU breakdown of respirometric responses (individual bacterium responses) for the root and stem compartment. Significant differences in variances of parameters at the 95% significance level are indicated with lower cased letters (P < 0.05).

The high relative OTU abundance of *P. putida* in roots (26.3%) and stems (75.9%) of the *CCR*$^{-}$ trees can therefore be attributed to their efficient degradation of ferulic acid (Figure 3.6). In the roots of WT poplar trees *Pseudomonas putida* also displayed high degradation capacity for ferulic acid, however this was not reflected in high relative abundance (1.54%). In the stems of WT poplar trees, *Pseudomonas graminis* displayed the highest capacity to degrade ferulic acid, but again this was not reflected in high relative abundance (3.90%). In the WT trees, no clear relation between OTU abundance and ferulic acid degradation capacity was observed in the roots and stems. In the rhizosphere and leaf samples, also little to no correlation was observed between OTU abundance and respirometric responses to ferulic acid.

3.4. Discussion

To our knowledge, this study represents the first in depth assessment of the influence of a genetic modification in plants, growing under field conditions, on the metabolic capacities of the plant-associated rhizospheric and endophytic bacterial communities. We specifically evaluated the influence of downregulation in Cinnamoyl-CoA reductase (*CCR*) in poplar on the rhizospheric and endophytic colonization, the bacterial community structures within each genotype and the present bacterial metabolisms.

WT and *CCR*- (*CCR* deficient) poplar trees were sampled simultaneously, after approximately 2.5 years of growth on a field site, thereby bypassing genotype x field and genotype x time effects. Firstly, to control for normal baseline bacterial cell counts, bacterial cells were directly isolated from the rhizosphere soil and plant tissues using a non-selective approach (Figure 3.1). Bacterial cell counts (CFU g^{-1}) were highly comparable between WT and *CCR*- poplar trees across all compartments. No significant differences were found between the genotypes indicating that the *CCR* down-regulation does not affect rhizospheric and endophytic colonization and stable establishment of bacterial communities. Furthermore within each genotype, the abundance of bacterial cells (CFU g^{-1}) consistently declined from the rhizosphere soil over the root samples to the stem samples. These results are consistent with what is generally reported concerning the colonization pattern of plant-associated bacteria (Compant et al., 2010; Hardoim et al., 2008). Most endophytic bacteria originate from the rhizosphere soil and progressively colonize the roots, stems and leaves (Chi et al., 2005; Sessitsch et al., 2002). Soil-residing bacteria will initially colonize the rhizosphere and rhizoplane, largely driven by chemo-attraction to photosynthetic root exudates (carbohydrates, amino acid, etc.) released into the root zone by plants (Bais et al. 2006; Lugtenberg & Dekkers, 1999; Lugtenberg & Kamilova, 2009; Walker et al. 2003). Following rhizosphere and rhizoplane colonization only certain soil-borne bacteria can, through passive or active mechanisms, cross the physical barriers (endodermis, pericycle) needed to reach the xylem vessels and further colonize the roots, stems and leaves (Compant et al., 2010;Hardoim et al., 2008), thereby directly affecting the number of bacterial cells recovered from the plant tissues. Higher bacterial cell counts observed in the leaves as compared to the stems is, most likely, attributed to endophytic

colonization via the stomata (Hardoim et al., 2008; McCully, 2001). Lastly, bacterial cell counts recovered from the different compartments in both genotypes were highly consistent with literature. Rhizospheric bacterial populations generally range from 10^7-10^9 CFU g^{-1} rhizosphere soil and endophytic subpopulations from 10^5-10^7 CFU g^{-1} of fresh weight (Hallmann & Berg, 2007; Hallmann, 2001).

The numbers of bacterial cells that could be isolated on selective medium with specific carbon sources (ferulic acid, sinapic acid and p-coumaric acid) was, in general, higher in the *CCR*- poplar trees as compared the wild type trees (Figure 3.1B, C, D). Interestingly, we observed the largest differences between the host genotypes when bacterial cells were selectively isolated with ferulic acid as sole carbon source (Figure 3.1B). Ferulic and derivatives thereof, were previously shown to be up-regulated in the *CCR*$^-$ poplar (Leplé et al, 2007), and ferulic acid was even incorporated into the lignin polymer. Furthermore selective enrichment of bacterial cells (sole carbon source: ferulic acid) from all compartments did reveal significant differences in bacterial abundance (Figure 3.2) and community structure between WT and *CCR*- poplars (Figure 3.4). Interestingly, all observed differences between the genotypes were exclusively found inside the plant (root, stem and leaf samples) at the level of the endophytes. In the rhizosphere soil, *i.e.* outside the plant, we found highly comparable bacterial abundances (Figure 3.1 and 3.2), community structures (Figure 3.4A, P = 0.40) and bacterial metabolic capacities (Figure 3.5, P = 0.51) between both genotypes. Rhizospheric bacterial communities in both genotypes were dominated by *Rhodanobacter lindaniclasticus,* originally described as a soil bacterium capable of degrading lindane (γ-hexachlorocyclohexane) (Nalin et al., 1996; Thomas et al., 1996), which illustrates its extensive degradation capacity for complex organic compounds. These results clearly indicate that the effects of *CCR* down-regulation in poplar trees on the bacterial communities remain confined within the plants. Danielsen et al. (2013) already reported that transgenic poplar lines modified in the biosynthesis of lignin show a normal capacity to form ectomycorrhiza (EM) and variations in EM community structure between different poplar genotypes were similar to intra-specific variation in commercial poplar clones (Danielsen et al., 2013).

In contrast, at the level of the endophytes, bacterial cell counts were consistently higher in the *CCR*- poplar trees (Figure 3.1 and Figure 3.2B, C, D), bacterial community structures were significantly different (Figure 3.4B, C, D) as well as the bacterial metabolic capacities (Figure 3.5). Within the endosphere of the *CCR* deficient poplars, the higher variation in bacterial cell counts (Figure 3.2), bacterial community structures (Figure 3.4) and bacterial metabolisms (Figure 3.5) is, most likely, attributed to the unequal levels of gene silencing which not only leads to a distinct phenotype of the *CCR*- poplar trees (red-brown coloration) but also results in variable xylem compositions and variations in the accessible carbon sources for the endophytes (Leplé et al., 2007; Ralph et al., 2008; Van Acker et al., 2014). Within the endosphere, we found the most pronounced differences between the genotypes in the stems of the poplar trees. Secondary thickening of the cell walls and lignin deposition, being the final stage of the xylem cell differentiation, is the highest in the xylem cells of the stems tissues (Boerjan et al., 2003). Most pronounced effects of gene silencing in *CCR* and changes in xylem composition are therefore found in the stems of poplar trees (Leplé et al., 2007). Moreover lumen colonization of xylem vessels by bacterial endophytes has been frequently reported as a route for bacterial dispersal to vegetative plant parts, ensuring direct contact between endophytes and nutrients available in the xylem cells (Compant et al., 2010; McCully, 2001). Endophytic root and stem bacterial communities in the *CCR*- poplar trees were dominated by *Pseudomonas putida,* which is known for its diverse metabolic capacities and adaptation to various ecological niches including the ability to thrive in soils and sediments with high concentrations of toxic metals and complex organic contaminants (Marques & Ramos, 1993; Wu et al., 2011). Furthermore, *Pseudomonas putida* strains are routinely found as plant growth promoting rhizospheric and endophytic bacteria (Taghavi et al., 2009; Weyens et al., 2009). The genetic modification, *i.e. CCR* down-regulation, results in changes in the accessible carbon and energy sources in the xylem vessels, most notably the phenolic compounds (e.g. upregulation of ferulic acid) (Leplé et al., 2007), and thereby exerts selective pressure on the metabolisms of the endophytic bacteria which favours species capable of using these phenolic compounds as carbon sources, such as *Pseudomonas putida*. Indeed, several degradation pathways for ferulic acid have been identified in *P. putida* strains

such as the ferulate catabolic pathway in *Pseudomonas putida* WCS358 (Venturi et al., 1989) and the protocatechuate 4,5-cleavage pathway (Harwood & Parales, 1996). Moreover, we proved that the high relative abundance of *Pseudomonas putida* in the roots and stems of *CCR* deficient trees was related to high degradation capacity for ferulic acid (Figure 3.6).

Finally, comparison of the bacterial community structures of each compartment (rhizosphere soil, roots, stems, leaves) within the genotypes also revealed unique rhizospheric and endophytic communities within each compartment (Figure 3.3). This is not surprising since every plant compartment represents an unique ecological niche with specific available nutrients (McCully, 2001) and active systemic colonization originating from the rhizosphere is limited to specific endophytic strains (Compant et al., 2010).

3.5. Conclusion

In conclusion, we identified host genotype effects, which are reminiscent of the host genotype-dependent associations shaping the human microbiome (Spor et al., 2011; Koch et al., 2014). The host genotype was found to have a profound effect on the metabolic capacities and bacterial species in the endosphere of *CCR* deficient poplar trees, without perceptible effects on the rhizospheric bacterial communities. Of particular interest was *Pseudomonas putida*, which showed high relative abundance in the roots and stems of *CCR* deficient poplar trees correlated with high ferulic acid degradation capacities. This indicates that gene silencing of *CCR* has the potential to influence the metabolic capacities present in the endosphere. Further exploration of the *CCR* deficient poplar-bacteria interaction with next-generation sequencing will provide more detailed knowledge concerning the effects of *CCR* gene silencing on the total bacterial populations.

References

Anderson, M. J., & Willis, T. J. (2003). Canonical analysis of principal coordinates: A useful method of constrained ordination for ecology. *Ecology*, *84*, 511–525.

Badri, D. V, Chaparro, J. M., Zhang, R., Shen, Q. and Vivanco, J. M. (2013). Application of natural blends of phytochemicals derived from the root exudates of Arabidopsis to the soil reveal that phenolic-related compounds predominantly modulate the soil microbiome. *The Journal of Biological Chemistry*, *288*, 4502–4512.

Bais, H. P., Weir, T. L., Perry, L. G., Gilroy, S. and Vivanco, J. M. (2006a). The role of root exudates in rhizosphere interactions with plants and other organisms. *Annual Review of Plant Biology*, *57*, 233–266.

Boerjan, W., Ralph, J., & Baucher, M. (2003). Lignin biosynthesis. *Annual Review of Plant Biology*, *54*, 519–546.

Bulgarelli, D., Schlaeppi, K., Spaepen, S., Ver Loren van Themaat, E. and Schulze-Lefert, P. (2013). Structure and functions of the bacterial microbiota of plants. *Annual Review of Plant Biology*, *64*, 807–838.

Cáceres, M. D. and Legendre, P. (2009). Associations between species and groups of sites: indices and statistical inference. *Ecology*, *90*, 3566–3574.

Chen, F. and Dixon, R. A. (2007). Lignin modification improves fermentable sugar yields for biofuel production. *Nature Biotechnology*, *25*, 759–761.

Chi, F., Shen, S., Cheng, H., Jing, Y., Yanni, Y. G. and Dazzo, F. B. (2005). Ascending Migration of Endophytic Rhizobia , from Roots to Leaves , inside Rice Plants and Assessment of Benefits to Rice Growth Physiology. Applied and Environmental Microbiology, *71*, 7271-7278.

Compant, S., Clément, C. and Sessitsch, A. (2010). Plant growth-promoting bacteria in the rhizo- and endosphere of plants: Their role, colonization, mechanisms involved and prospects for utilization. *Soil Biology and Biochemistry*, *42*, 669–678.

Custers, R. (2009). First GM trial in Belgium since 2002. *Nature Biotechnology*, 27, 506.

Danielsen, L., Lohaus, G., Sirrenberg, A., Karlovsky, P., Bastien, C., Pilate, G. and Polle, A. (2013). Ectomycorrhizal colonization and diversity in relation to tree biomass and nutrition in a plantation of transgenic poplars with modified lignin biosynthesis. *PloS One*, *8*, e59207.

De Santi Ferrara, F. I., Oliveira, Z. M., Gonzales, H. H. S., Floh, E. I. S. and Barbosa, H. R. (2011). Endophytic and rhizospheric enterobacteria isolated from sugar cane have different potentials for producing plant growth-promoting substances. *Plant and Soil*, *353*, 409–417.

DeSantis, T. Z., Hugenholtz, P., Larsen, N., Rojas, M., Brodie, E. L., Keller, K., Huber, T., Dalevi, D., Hu, P. and Andersen, G. L. (2006). Greengenes, a chimera-checked 16S rRNA gene database and workbench compatible with ARB. *Applied and Environmental Microbiology*, *72*, 5069–72.

Guckert, J. B., Carr, G. J., Johnson, T. D., Hamm, B. G., Davidson, D. H. and Kumagai, Y. (1996). Community analysis by Biolog: curve intergation for statistical analysis of activated sludge microbial habitats. *Journal of Microbiological Methods*, *27*, 183–197.

Hallmann, J. (2001). Plant Interactions with endophytic bacteria. In M. J. Jeger & Spence N J (Eds.), *Biotic Interaction in Plant-Pathogen Associations* (pp. 87–119). Wallingford, United Kingdom: Cabi Publishing.

Hallmann, J. and Berg, B. (2007). Spectrum and population dynamics of bacterial root endophytes. In B. J. E. Schulz, C. J. C. Boyle, & T. N. Sieber (Eds.), *Microbial Root Endophytes* (pp. 15–31). Berlin, Heidelberg: Springer.

Hardoim, P. R., van Overbeek, L. S. and Van Elsas, J. D. (2008). Properties of bacterial endophytes and their proposed role in plant growth. *Trends in Microbiology*, *16*, 463–471.

Hartmann, M., Howes, C. G., VanInsberghe, D., Yu, H., Bachar, D., Christen, R., Nilsson, R. H., Hallam, S. J., and Mohn W. W. (2012). Significant and persistent impact of timber harvesting on soil microbial communities in Northern coniferous forests. *The ISME Journal*, 6, 2199-2218.

Harwood, C. S. and Parales, R. E. (1996). The β-ketoadipate pathway and the biology of self-identity. *Annual Review of Microbiology*, *50*, 553–590.

Koch, L. (2014). Metagenomics: Shaping the gut microbiome. *Nature Reviews. Genetics*, *16*, 2-3.

Leplé, J.-C., Brasileiro, A. C. ., Michel, M. F., Delmotte, F. and Jouanin, L. (1992). Expression of chimeric genes using four different constructs. *Plant Cell Reports*, 11, 137–141.

Leplé, J.-C., Dauwe, R., Morreel, K., Storme, V., Lapierre, C., Pollet, B., Naumann A., Kang, K., Kim, H., Ruel, K., Lefèbvre, A., Joseleau, J., Grima-Pettenati, J., De Rycke, R., Andersson-Gunnerås, S., Erban, A., Fehrle A., Petit-Conil, M., Kopka, J., Polle, A., Messens, E., Sundberg, B., Mansfield, S., Ralph, J., Pilate, G. and Boerjan, W. (2007). Downregulation of cinnamoyl-coenzyme A reductase in poplar: multiple-level phenotyping reveals effects on cell wall polymer metabolism and structure. *The Plant Cell*, *19*, 3669–3691.

Leplé, J.-C., Grima-Pettenati, J., Van Montagu, M. and Boerjan, W. (1998). A cDNA encoding cinnamoyl-CoA reductase from Populus trichocarpa Title. *Plant Physiology*, 117, 1126.

Letunic, I. and Bork, P. (2011). Interactive Tree Of Life v2: online annotation and display of phylogenetic trees made easy. *Nucleic Acids Research*, *39*, 475–478.

Lugtenberg, B. and Dekkers, L. C. (1999). What makes Pseudomonas bacteria rhizosphere competent . *Environmental Microbiology*, *1*, 9–13.

Lugtenberg, B. and Kamilova, F. (2009). Plant-growth-promoting rhizobacteria. *Annual Review of Microbiology*, *63*, 541–556.

Marques, S. and Ramos, J. L. (1993). Transcriptional control of the Pseudomonas putida TOL plasmid catabolic pathways. *Molecular Microbiology*, *9*, 923–929.

McCully, M. E. (2001). Niches for bacterial endophytes in crop plants: a plant biologist's view. *Australian Journal of Plant Physiology*, *28*, 983–990.

Mergeay, M., Nies, L. D., Schlegel, H. G., Gerits, J., Charles, P. and Gijsegem, F. V. A. N. (1985). Alcaligenes eutrophus CH34 Is a Facultative Chemolithotroph with Plasmid-Bound Resistance to Heavy Metals. *Journal of Bacteriology*, *162*, 328–334.

Monteiro, R. A., Balsanelli, E., Wassem, R., Marin, A. M., Brusamarello-Santos, L. C. C., Schmidt, M. A., Tadra-Sfeir, M. Z., Pankievicz, V. C.

S., Cruz, L. M., Chubatsu, L., S., Pedrosa, F. O. and Souza, E. M. (2012). Herbaspirillum-plant interactions: microscopical, histological and molecular aspects. *Plant and Soil*, *356*, 175–196.

Nalin, R., Simonet, P., Voge, T. M. and Normandl, P. (1996). Rhodanobacter lindaniclasticus. International Journal of Systematic Bacteriology, *49*, 19–23.

Okonechnikov, K., Golosova, O. and Fursov, M. (2012). Unipro UGENE: a unified bioinformatics toolkit. *Bioinformatics*, 28, 1166–1167.

Ralph, J., Kim, H., Lu, F., Grabber, J. H., Leplé, J.-C., Berrio-Sierra, J., Derikvand, M. M., Jouanin, L., Boerjan, W. and Lapierre, C. (2008). Identification of the structure and origin of a thioacidolysis marker compound for ferulic acid incorporation into angiosperm lignins (and an indicator for cinnamoyl CoA reductase deficiency). *The Plant Journal : For Cell and Molecular Biology*, *53*, 368–79.

R Development Core Team (2011). R: A language and environment for statistical computing. R Foundation for Statistical Computing, Vienna, Austria. ISBN 3-900051-07-0, URL http://www.R-project.org/.

Ruel, K., Berrio-sierra, J., Derikvand, M. M., Pollet, B., Thévenin, J., Lapierre, C., Jouanin, L. and Joseleau, J. (2009). Impact of CCR1 silencing on the assembly of lignified secondary walls in *Arabidopsis thaliana*. *The New Phytologist, 184*, 99–113.

Sessitsch, A., Hardoim, P., Döring, J., Weilharter, A., Krause, A., Woyke, T., Mitter, B., Hauberg-Lotte L., Friedrich, F., Rahalkar, M., Hurek, T., Sarkar, A., Bodrossy, L., van Overbeek, L., Brar, D., van Elsas, J. D. and Reinhold-Hurek, B. (2012). Functional characteristics of an endophyte community colonizing rice roots as revealed by metagenomic analysis. *Molecular Plant-Microbe Interactions*, *25*, 28–36.

Sessitsch, A., Reiter, B., Pfeifer, U. and Wilhelm, E. (2002). Cultivation-independent population analysis of bacterial endophytes in three potato varieties based on eubacterial and Actinomycetes-specific PCR of 16S rRNA genes. *FEMS Microbiology Ecology*, *39*, 23–32.

Solomon, B. D. (2010). Biofuels and sustainability. *Annals of the New York Academy of Science*, *1185*, 119–134.

Spor, A., Koren, O. and Ley, R. (2011). Unravelling the effects of the environment and host genotype on the gut microbiome. *Nature Reviews. Microbiology*, *9*, 279–290.

Studer, M. H., Demartini, J. D., Davis, M. F., Sykes, R. W., Davison, B. and Keller, M. (2011). Lignin content in natural Populus variants affects sugar release. *Proceedings of the National Academy of Sciences of the United States of America*, *108*, 6300-6305.

Taghavi, S., Garafola, C., Monchy, S., Newman, L., Hoffman, A., Weyens, N., Barac, T., Vangronsveld, J. and van der Lelie, D. (2009). Genome survey and characterization of endophytic bacteria exhibiting a beneficial effect on growth and development of poplar trees. *Applied and Environmental Microbiology*, *75*, 748–757.

The Human Microbiome Project Consortium. Structure, function and diversity of the healthy human microbiome. (2012). *Nature*, *486*, 207–14.

Thomas, J. C., Berger, F., Jacquier, M., Bernillon, D., Baud-Grasset, F., Truffaut, N., Normand, Vogel, T. M. and P., Simonet, P. (1996). Isolation and characterization of a novel gamma-hexachlorocyclohexane-degrading bacterium. *Journal of Bacteriology*, *178*, 6049–6055.

Van Acker, R., Leplé, J.-C., Aerts, D., Storme, V., Goeminne, G., Ivens, B., Légée, F., Lapierre, C., Piens, K., Van Montagu, M., C., E., Santoro, N., Foster, C., E., Ralph, J., Soetaert, W., Pilate, G. and Boerjan, W. (2014). Improved saccharification and ethanol yield from field-grown transgenic poplar deficient in cinnamoyl-CoA reductase. *Proceedings of the National Academy of Sciences of the United States of America*, *111*, 845–50.

Vanholme, R., Demedts, B., Morreel, K., Ralph, J. and Boerjan, W. (2010). Lignin biosynthesis and structure. *Plant Physiology*, *153*, 895–905.

Vanholme, R., Morreel, K., Darrah, C., Oyarce, P., Grabber, J. H., Ralph, J. and Boerjan, W. (2012). Metabolic engineering of novel lignin in biomass crops. *The New Phytologist*, *196*, 978–1000.

Vanholme, R., Morreel, K., Ralph, J. and Boerjan, W. (2008). Lignin engineering. *Current Opinion in Plant Biology*, *11*, 278–85.

Venturi, V., Zennaro, F., Degrassi, G., Okeke, B. C., & Bruschi, C. V. (1989). Genetics of ferulic acid bioconversion to protocatechuic acid in plant-growth-promoting. *Microbiology*, *144*, 965–973.

Walker, T. S., Bais, H. P., Grotewold, E. and Vivanco, J. M. (2003). Update on Root Exudation and Rhizosphere Biology Root Exudation and Rhizosphere Biology. *Plant Physiology*, *132*, 44–51.

Weyens, N., van der Lelie, D., Taghavi, S., & Vangronsveld, J. (2009). Phytoremediation: plant-endophyte partnerships take the challenge. *Current Opinion in Biotechnology*, *20*, 248–54.

Wilkerson, C. G., Mansfield, S. D., Lu, F., Withers, S., Park, J.-Y., Karlen, S. D., Gonzales-Vigil, E., Padmakshan, D., Unda, F., Rencoret, J. and Ralph, J. (2014). Monolignol ferulate transferase introduces chemically labile linkages into the lignin backbone. *Science*, *344*, 90–93.

Wu, X., Monchy, S., Taghavi, S., Zhu, W., Ramos, J. and van der Lelie, D. (2011). Comparative genomics and functional analysis of niche-specific adaptation in Pseudomonas putida. *FEMS Microbiology Reviews*, *35*, 299–323.

Yuan, J. S., Tiller, K. H., Al-Ahmad, H., Stewart, N. R. and Stewart, C. N. (2008). Plants to power: bioenergy to fuel the future. *Trends in Plant Science*, *13*, 421–9.

Supplementary Information

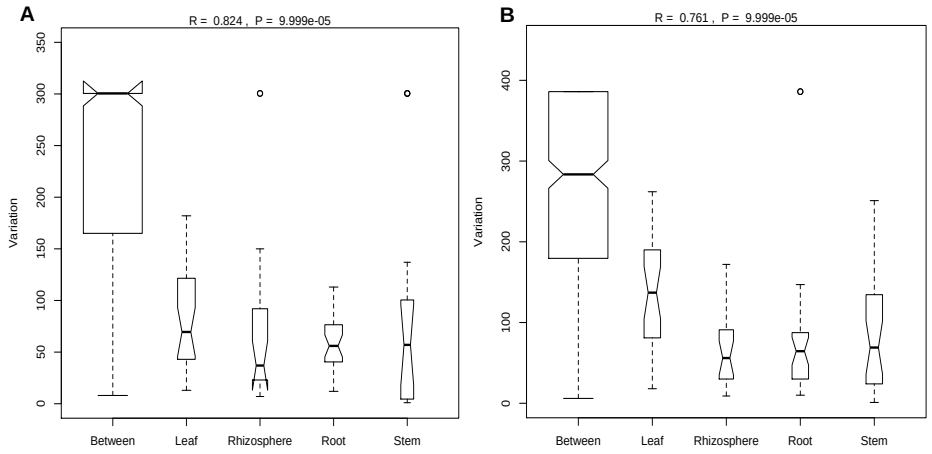

Supplementary Figure 3.1. Graphical representation of analysis of similarity (ANOSIM) of a priori defined groups (rhizosphere, root, stem and leaf) within each host genotype (A. Wild type and B. CCR deficient poplar trees). Variation of each a priori defined group is compared with the 'between' variation which represents the observed variation between the different groups. R-values and p-values are depicted on top of each graph. Box-plots display the first (25%) and third (75%) quartile, the median (bold line), maximum and minimum observed values (without outliers). Outliers (more or less than 3/2 of the upper/lower quartile) are displayed as open circles.

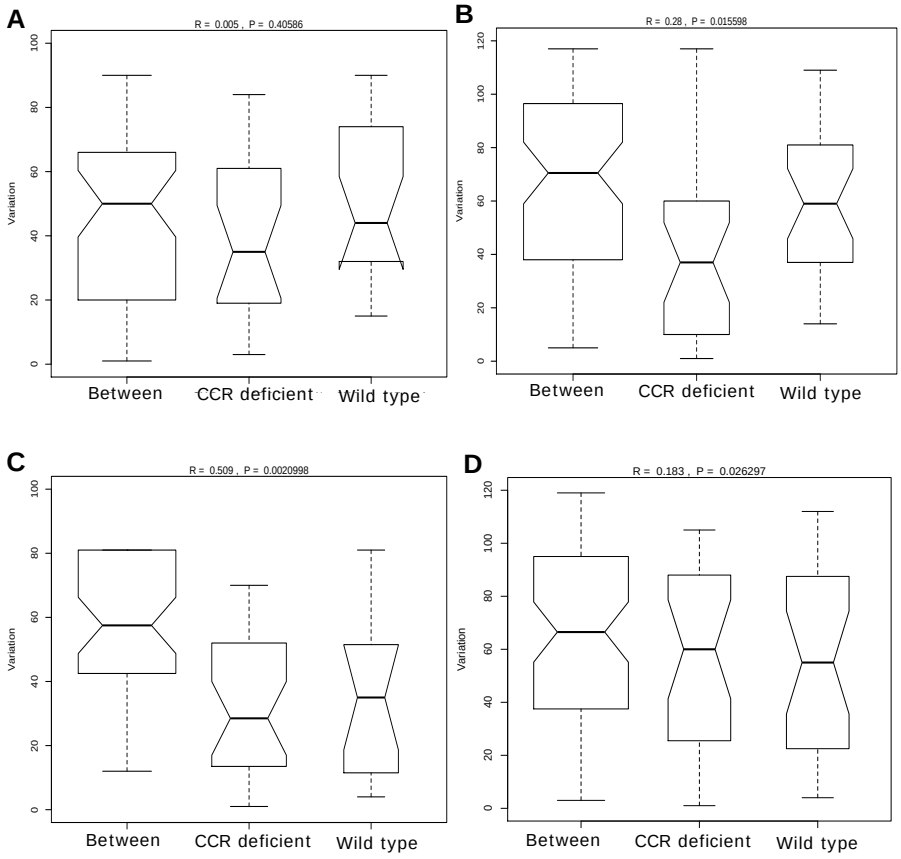

Supplementary Figure 3.2. Graphical representation of analysis of similarity (ANOSIM) of a priori defined groups (WT and CCR deficient poplar trees) within each plant compartment (A. Rhizosphere, B. Root, C. Stem, D. Leaf). Variation of each a priori defined group is compared with the 'between' variation which represents the observed variation between the different groups. R-values and p-values are depicted on top of each graph. Box-plots display the first (25%) and third (75%) quartile, the median (bold line), maximum and minimum observed values (without outliers). Outliers (more or less than 3/2 of the upper/lower quartile) are displayed as open circles.

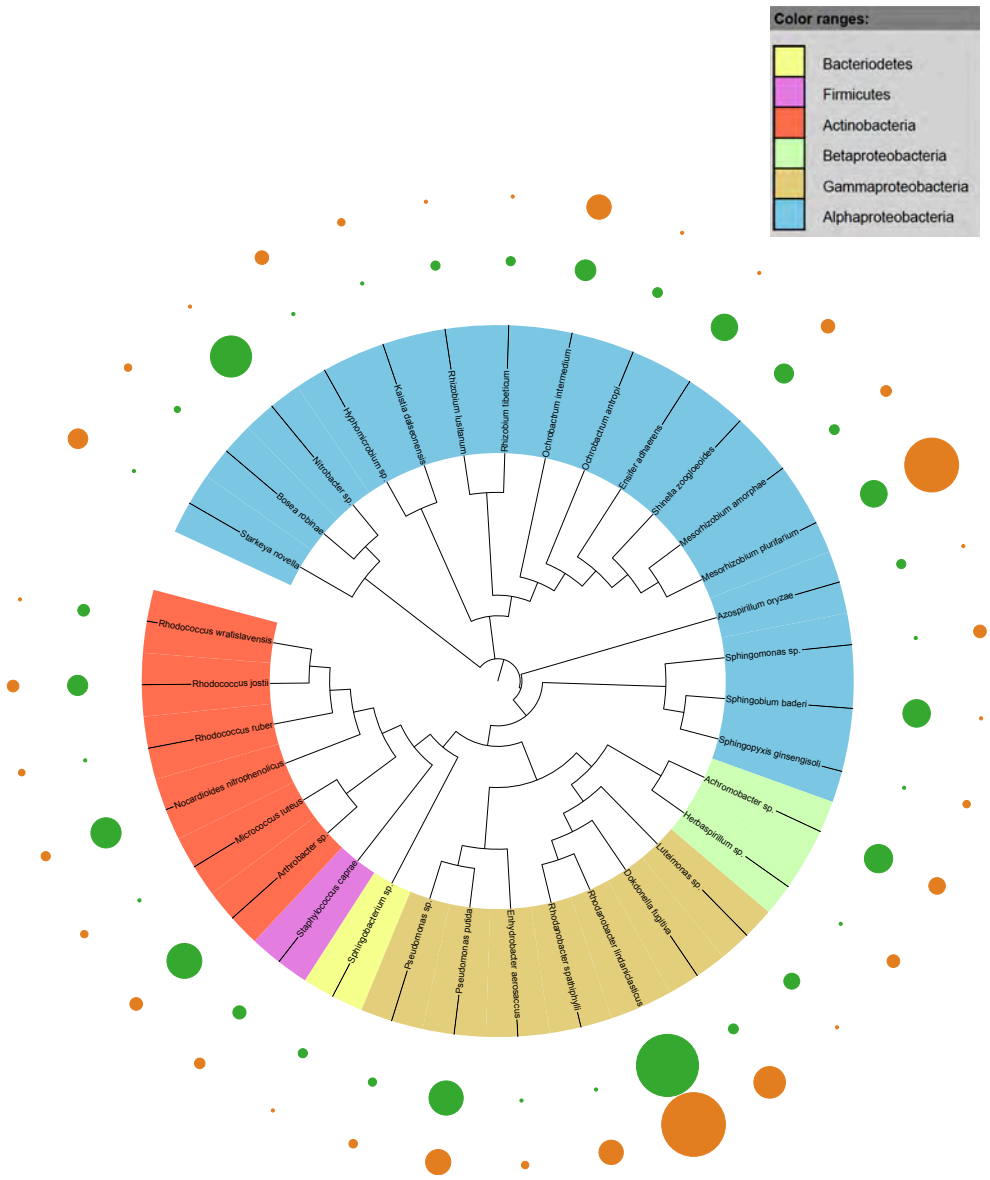

Supplementary figure 3.3 Taxonomic dendogram showing the taxonomy of all bacterial species isolated from the rhizosphere of WT (green) and CCR deficient poplar trees (orange). Color ranges identify phyla within the tree. Legend colors refer to circles. Diameters of the circles represent the square-root transformed abundance of the corresponding species in the overall community. Taxonomic dendrogram was generated with Unipro UGENE and displayed using Itol (Letunic and Bork, 2011).

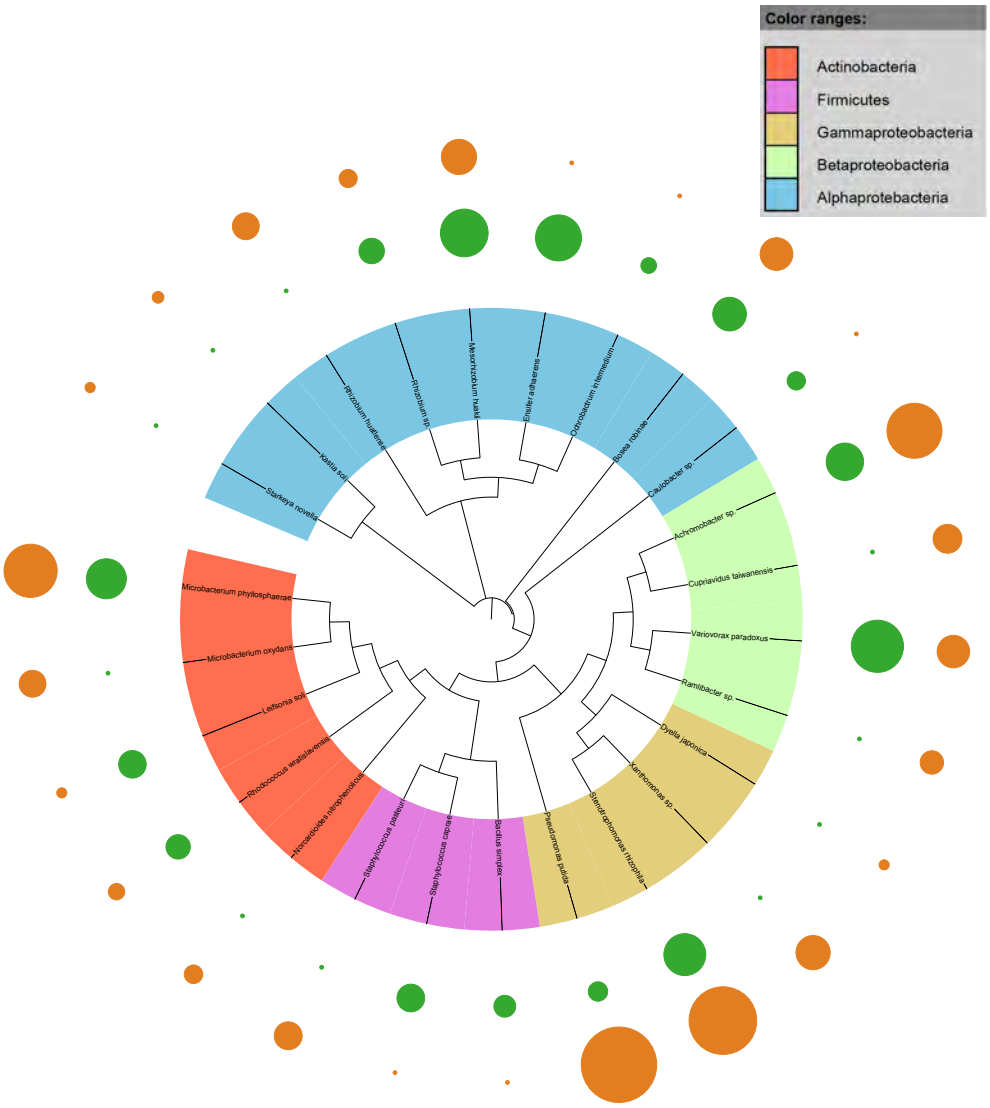

Supplementary Figure 3.4: Taxonomic dendogram showing the taxonomy of all bacterial species isolated from the roots of WT (green) and CCR deficient poplar trees (orange). Color ranges identify phyla within the tree. Legend colors refer to circles. Diameters of the circles represent the square-root transformed abundance of the corresponding species in the overall community. Taxonomic dendrogram was generated with Unipro UGENE and displayed using Itol (Letunic and Bork, 2011).

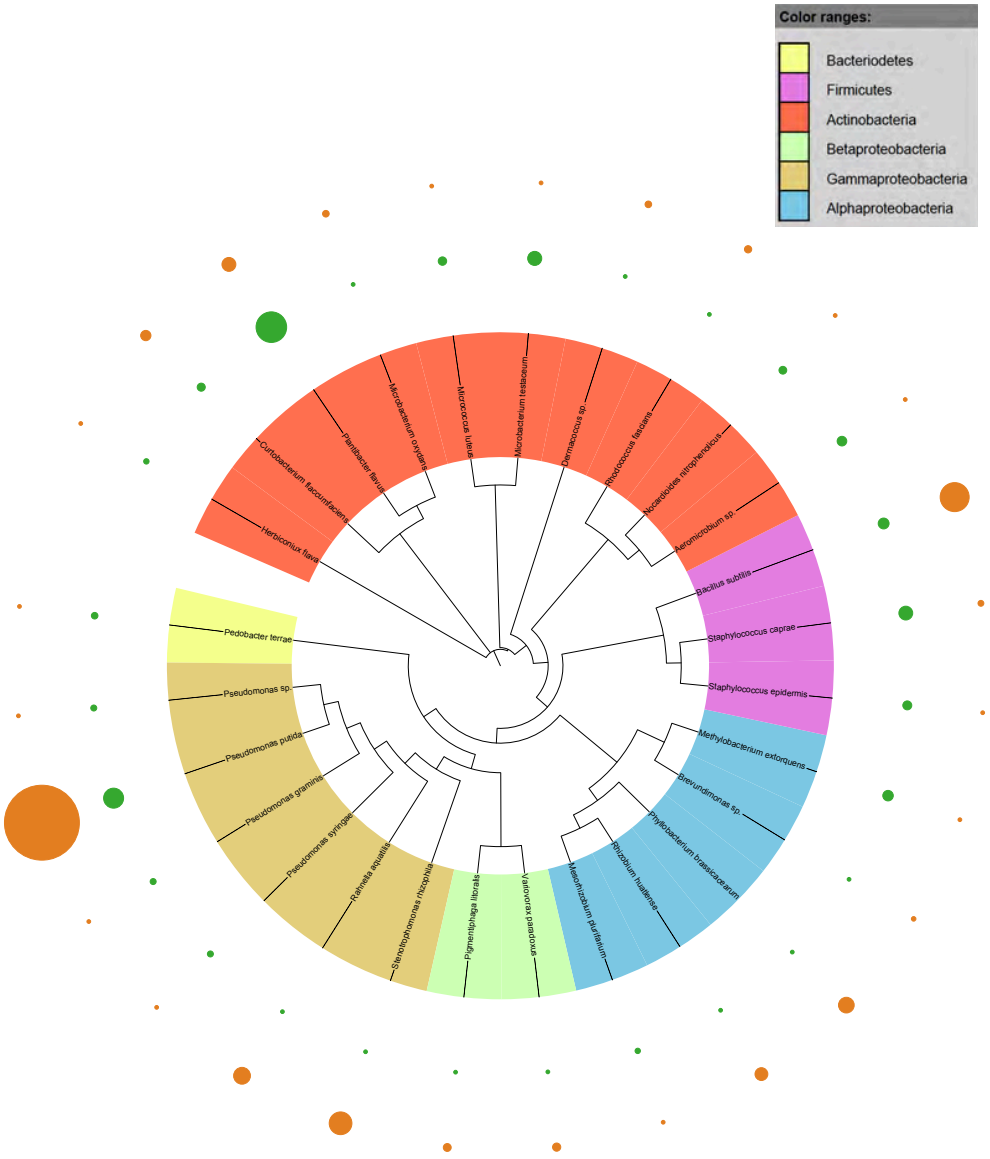

Supplementary Figure 3.5. Taxonomic dendogram showing the taxonomy of all bacterial species isolated from the stems of WT (green) and CCR deficient poplar trees (orange). Color ranges identify phyla within the tree. Legend colors refer to circles. Diameters of the circles represent the square-root transformed abundance of the corresponding species in the overall community. Taxonomic dendrogram was generated with Unipro UGENE and displayed using Itol (Letunic and Bork, 2011).

Supplementary figure 3.6. Taxonomic dendogram showing the taxonomy of all bacterial species isolated from the leaves of WT (green) and CCR deficient poplar trees (orange). Color ranges identify phyla within the tree. Legend colors refer to circles. Diameters of the circles represent the square-root transformed abundance of the corresponding species in the overall community. Taxonomic dendrogram was generated with Unipro UGENE and displayed using Itol (Letunic and Bork, 2011).

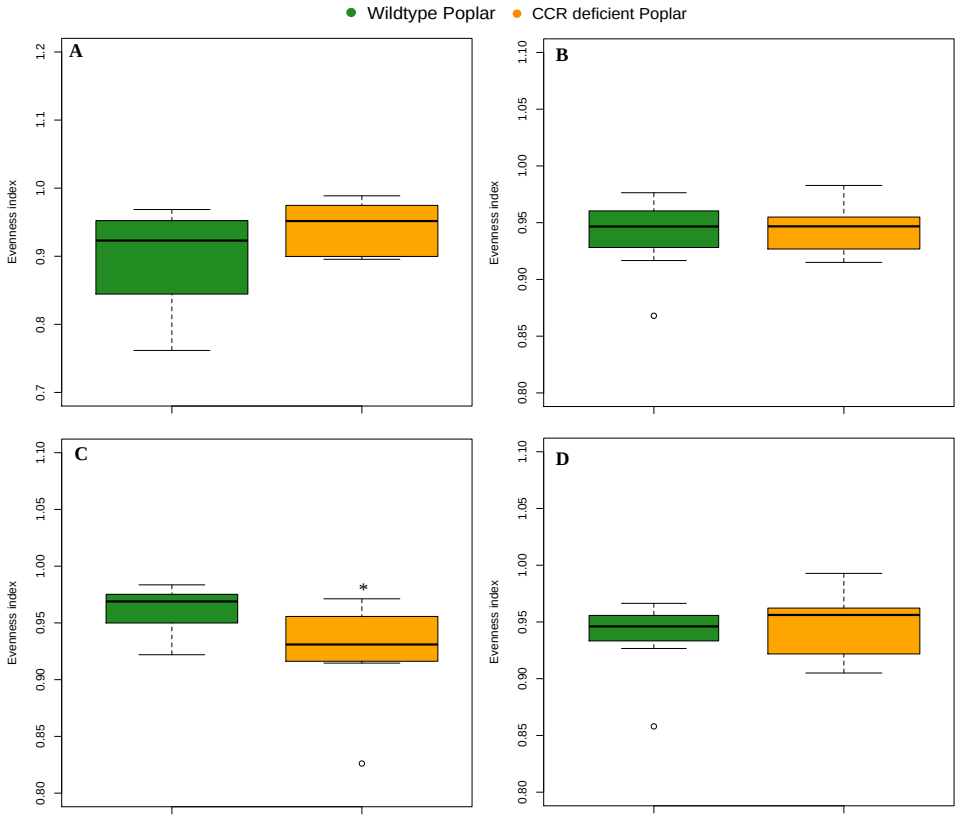

Supplementary Figure 3.7. Metabolic evenness of respirometric responses in rhizosphere (A), roots (B), stems (C) and leaves (D) of wildtype (green) and CCR deficient (orange) poplar trees. Evenness was calculated according to Pielou : J'=H'/LN S) where H' is the number derived from the Shannon Diversity index and S is the total number of species in the community. Pielou's evenness is constrained between 0 and 1. Box-plots display the first (25%) and third (75%) quartile, the median (bold line), maximum and minimum observed values (without outliers). Outliers (more or less than 3/2 of the upper/lower quartile) are displayed as open circles. Evenness indices were analysed using an one-way ANOVA and statistically significant differences are indicated on the box-plots (P < 0.05:).*

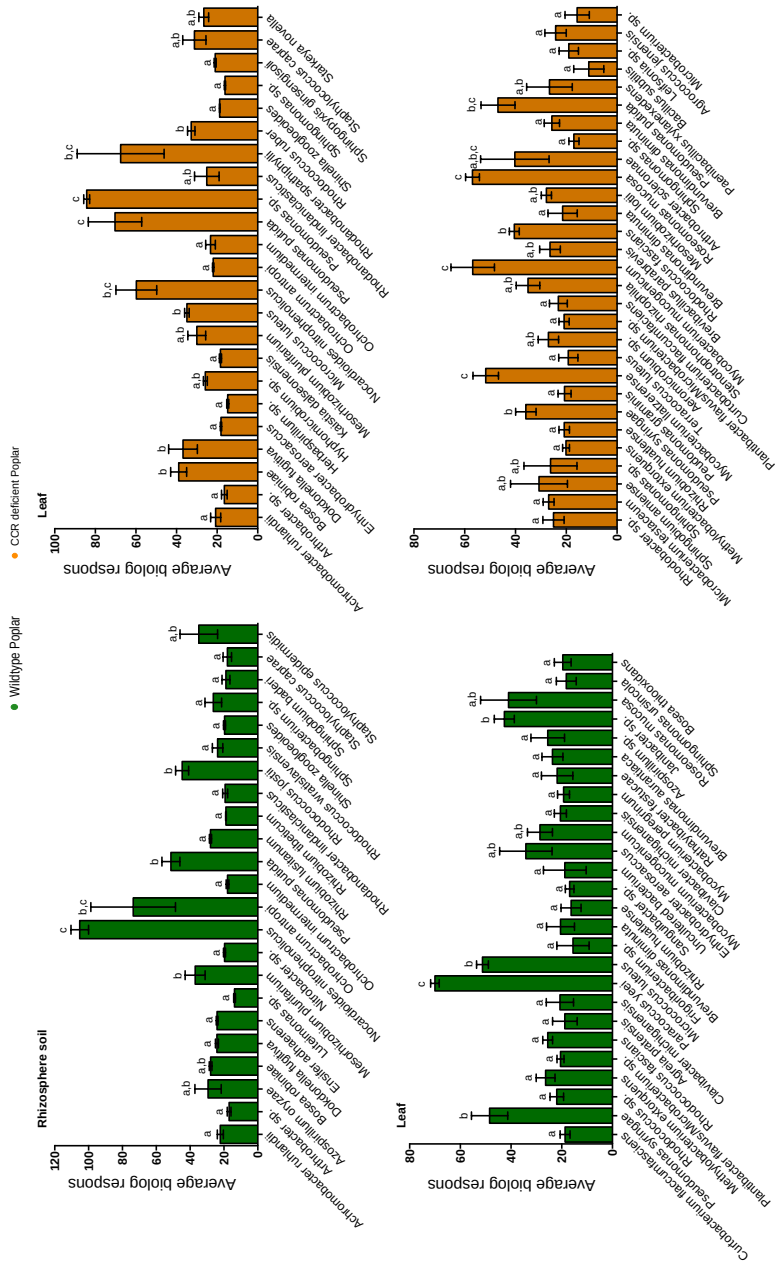

Supplementary Figure 8: Respirometric metabolism analyses using BIOLOG with 1mM ferulic acid. Species-level OTU breakdown of respirometric responses (individual bacterium responses) for the rhizosphere and leaf compartment. Significant differences in variances of parameters at the 95% significance level are indicated with lower cased letters (P < 0.05).

Chapter 4

Performance of 16s rRNA primer pairs in the study of rhizosphere and endosphere bacterial microbiomes in metabarcoding studies

Abstract

Next-generation sequencing technologies have revolutionized the methods for studying microbial ecology by enabling high-resolution community profiling. The use of these next-generation techniques (e.g. 454 pyrosequencing) to unravel the plant microbiome with 16S rRNA metabarcoding is challenging. Indeed, many bacterial 16S rRNA primer pairs also exhibit high affinity for non-target rRNA such as chloroplast 16S rRNA and mitochondrial 18S rRNA. Several studies have routinely encountered high levels of plastid contamination. Therefore, we experimentally tested a series of commonly used primers for the analysis of plant-associated bacterial communities using 454 pyrosequencing. Our selection included, amongst others, primers 799F and 783Rabc, containing mismatches with the poplar chloroplast 16S rRNA. We tested all selected primer pairs in the study of the bacterial microbiomes present in the rhizosphere soil, roots, stems and leaves of poplar trees (*Populus tremula x Populus alba*). The following parameters were used to evaluate the performance of the primer pairs: (a) co-amplification of non-target rRNA, low amplification efficiency for pure chloroplast DNA (real-time PCR (qPCR) set-up), (b) high retrieval of bacterial 16S rRNA and (c) high operational taxonomic unit (OTU) richness and Simpson Diversity.

Results indicate that experimental evaluation of primers provide valuable information that could contribute in the selection of suitable primer pairs for 16S rRNA metabarcoding studies in plant-microbiota research. Furthermore, we show that primer pair 799F-1391R outperforms all other primer pairs in terms of (a) low amplification of non-target rRNA sequences, (b) retrieval of bacterial 16S rRNA sequences and (c) retrieval of genus-level OTUs. Therefore, we propose primer pair 799F-1391R as highly suitable for 16S rRNA metabarcoding studies in plant-microbiota research.

Keywords:

16S rRNA metabarcoding, 454 pyrosequecing, chloroplast 16S rRNA, endophytes

4.1. Introduction

The development and implementation of next-generation sequencing technologies and their corresponding bioinformatics tools have revolutionized the methods for studying microbial ecology by enabling high-resolution community profiling (Gottel et al., 2011; Hartmann et al., 2012; Margulies et al., 2005; Metzker, 2010; Shendure & Ji, 2008; Sogin et al., 2006). However unravelling the plant microbiome using DNA metabarcoding (amplification of barcode regions using taxon-specific primers) (Hajibabaei et al. 2007; Taberlet & Coissac, 2012) still represents significant challenges. The mixed presence of eukaryotic cells, prokaryotic cells and eukaryotic plant organelles with a prokaryotic lineage, more specifically chloroplasts and mitochondria leads to specific difficulties in 16S rRNA metabarcoding studies of plant-associated endophytic bacteria, and to a lesser extent of bacterial communities of folivorous insects (Dyall et al. 2004; Raven, 1970). Engulfment of mitochondria and plastids (endosymbiont theory) were crucial events in the evolution of the eukaryote cell, providing it with bioenergetic and biosynthetic capacities (Dyall et al., 2004). However, the homology between bacterial 16S rRNA, chloroplast 16S rRNA and mitochondrial 18S rRNA leads to significant challenges in the selection of appropriate primer pairs to study plant-microbe interactions.

For the study of maize roots, Chelius and Triplett (2001) developed the first primer (799F), which was able to amplify bacterial 16S rRNA sequences while simultaneously avoiding the amplification of chloroplast 16S rRNA sequences. Their primer design was centred on the two base pair mismatches at positions 798-799 (*E coli.* numbering) and two additional base pair mismatches at positions 783 and 784, which exist in the chloroplast 16S rRNA genes. It is well recognized that a primer-to-target mismatch at the 3' end of the primer blocks efficient amplification of the target sequence (Klindworth et al., 2013; Nossa et al., 2010). Primer 799F has been used with varying success in several plant systems (Bodenhausen et al., 2013; Bulgarelli et al., 2012; Shade et al., 2013; Sagaram et al., 2009). Further, Sakai *et al.* (2004) modified primer 799F into primer 783Rabc, in an attempt to access the hypervariable regions V3-V4 of the bacterial 16S rRNA genes in the study of the rhizobacterial communities of wheat and spinach. Indeed hypervariable regions V3 and V4 have been the preferred target of the 16S rRNA in studying soil and rhizosphere assemblages

and databases are more exhaustive for these regions. These primers were all developed before the onset of next-generation DNA sequencing studies and have so far been used without further exploration of their experimental performance.

Additionally, numerous studies have evaluated the *in silico* performance of primer pairs. Most notably, Klindworth et al. (2012) evaluated 512 selected primer pairs for next-generation based diversity studies. For 454 pyrosequencing applications, Klindworth et al. (2012) proposed 341F-785R as the ideal primer pair with a high overall coverage and large phylum spectrum. Although *in silico* analyses provide valuable technical information and indicate the theoretical optimal performance of primer pairs, they fail to capture the true experimental potential and are expected to result in an incomplete picture of how primers will perform during PCR amplification (Op De Beeck et al., 2014). Indeed, most environmental samples contain high concentrations of non-target DNA and/or contaminants (e.g. humic acids) after DNA extraction (Kosch & Summers, 2013). Particularly in the studies of plant-bacteria interactions, extracting DNA from plant tissues results in high levels of plant DNA, containing chloroplast 16S rRNA and mitochondrial 18S rRNA with high homology with the bacterial 16S rRNA (Bodenhausen et al., 2013; Dyall et al., 2004; Lundberg et al., 2012; Raven, 1970).

Experimental evaluation of the amplification efficiency and robustness of selected primer pairs in metabarcoding plant-bacteria interaction studies is essential to assess their behaviour in these specific conditions. Since minor differences in primer efficiency may result in strong PCR biases, thereby potentially influencing current views on plant-associated bacterial communities. Furthermore, selecting primer pairs with high co-amplification of organellar rRNA potentially will reduce the actual sequencing depth of metabarcoding studies. By combining *in silico* analyses (coverage and phylum spectrum) of selected primer pairs, with experimentally gathered data, optimal primer pairs can be selected to reduce organellar rRNA amplification. For this reason, we experimentally tested a set of commonly used primers for the analysis of plant-associated bacterial communities using 454 pyrosequencing (Table 4.1). Our selection included primers 799F and 783Rabc (Chelius & Triplett, 2001; Sakai et al. 2004), containing mismatches with the chloroplast 16S rRNA. Based on *in silico* analysis and taking into account amplicon length, both primers were matched with two

primers to produce four primer pairs, respectively 799F-1391R, 799F-1193R, 341F-783R and 68F-783R. Further, we included primer pair 341F-785R, as described by Klinworth et al. (2012), to evaluate the performance of the mismatch primer sets with the ideal primer pair for 16S rRNA metabarcoding studies with 454 applications. We tested all selected primer pairs in the study of plant-associated bacterial communities in rhizosphere, roots, stems and leaves of poplar trees (*Populus tremula x Populus alba*). The different amounts of chloroplast 16S rRNA input of these plant compartments, ranging from virtually no plastid input (rhizosphere soil) to very high input (leaves) will allow us to evaluate the performance of the selected primer sets in specific conditions.

4.2. Material & Methods

4.2.1. Study site description & Sampling

A poplar (*Populus tremula* x *Populus alba)* field trial located in Ghent, Belgium (property of the Flemish Institute for Biotechnology, VIB) was selected to acquire samples for this study (Custers, 2009). The field trial was established in April 2009 and contains wild type and genetically modified (GM) female poplar clones (cv '717-1-B4': *Populus tremula* x *Populus alba*) (Leplé et al., 2007) in a density of 15,000 trees per hectare and an inter-plant distance of 0.75 m. Wild type and GM poplar clones, down-regulated for cinnamoyl-CoA reductase (*CCR*; EC 1.2.1.44), were recently evaluated for their saccarification efficiency and ethanol yield by Van Acker et al. (2014). For this study, only wild type poplar trees were sampled as described by Beckers et al (2015) (Chapter 3). Briefly, poplar trees were sampled after approximately 3.5 years of growth in October 2012. We collected samples from rhizosphere, roots, stems and leaves of three biologically independent poplar individuals. Per poplar individual, we collected (a) 10 g of roots at a depth of 5-10 cm below ground in 50 mL plastic tubes, (b) one complete offshoot for the stem and leaf samples. To standardize and maximize reproducibility of stem samples, several small 'cores' with bark (5-7 cores, each about 1 cm) were collected from each offshoot. Finally all leaves of each offshoot were gathered and placed in sealed plastic bags for transportation.

4.2.2. Processing of samples

Poplar root samples were shaken for 10 min on a shaking platform (100 rpm) and soil particles dislodged from the roots were collected as rhizosphere soil. Rhizosphere soil was sieved using a 2 mm sieve for homogenization and removal of residual roots and debris. Subsequently the samples were stored at -80°C until DNA was extracted.

Epiphytes (microbes living on the plant surface) were removed from all plant samples (roots, stems and leaves) via surface-sterilization under aseptic conditions. Samples were sequentially washed with a) sterile Millipore water (30 sec), (b) followed by immersion in 70% (v/v) ethanol (2 min), (c) sodium hypochlorite solution (2.5 % active Cl^-, 5 min) supplemented with 0.1% Tween 80, (d) 70% (v/v) ethanol (30 sec) and finalized by washing the samples five times with sterile Millipore water. Finally plant samples (approximately 5 g of each compartment per sample) were homogenized by (a) portioning the

samples into small fragments using a sterile scalpel and (b) macerating them in sterile 10 mM phosphate saline (PBS) buffer (130 mM NaCl, 7 mM Na_2HPO_4, 3 mM NaH_2PO_4, pH 7.4) using a Polytron PR1200 mixer (Kinematica A6) in four cycles of 2 min with cooling of the mixer on ice between cycles to reduce heating of the samples. Finally, quadruplicate aliquots of each sample (1.5 mL) of the homogenized plant material (root, stem and leaf) were stored for al poplar individuals at -80°C until DNA was extracted.

4.2.3. DNA extraction

DNA from rhizosphere, roots, stems and leaves (further denoted as “plant compartments”) was extracted in quadruplicate from three biologically independent poplar individuals to minimize DNA extraction bias (Feinstein et al. 2009; Op De Beeck et al., 2014). In total, DNA was extracted from 48 samples (3 poplar individuals x 4 plant compartments x 4 quadruplicate extractions per sample).

Approximately 250 mg of rhizosphere soil was used for each individual DNA extraction. DNA extraction was performed with the Power Soil DNA Isolation Kit following the protocol provided by the manufacturer (MoBio, Carlsbad, CA, USA). For the plant compartments (roots, stems, leaves), aliquots (1.5 mL) of homogenized plant material were first centrifuged (13.400 rpm, 30 min) to collect all cells. Supernatants were discarded and DNA extractions were performed on pelleted plant material. The performance of three different commercially available DNA extractions kits (Qiagen DNeasy Plant Mini Kit, Invitek Invisorb Spin Plant Mini Kit and the Mobio Powerplant DNA Isolation Kit) to extract bacterial DNA from plant tissue was tested (Supplementary Figure 4.1). Quantity and quality of extracted DNA was evaluated for each kit using a Nanodrop ND-1000 Spectrophotometer (Isogen Life Sciences, Temse, Belgium), as well as the bacterial product delivered after 16S rRNA PCR amplification (data not shown). In accordance with these results (Supplementary Figure 4.1), DNA was extracted from the plant samples using the Invisorb Spin Plant Mini Kit according to the manufacturer’s protocol (Stratec Biomedical AG, Birkenfeld, Germany).

4.2.4. PCR amplification and 454 pyrosequencing

For the PCR amplification, we selected seven different primer pairs to evaluate their performance in metabarcoding studies for rhizospheric and endophytic

bacteria (Table 4.1). Primer pairs covered all hyper-variable regions from V1 until V7 of the 16S rRNA gene and included, amongst others, primer 799F (5'-AACMGGATTAGATACCCKG-3')(Chelius & Triplett, 2001) and primer 783R (5'-CTACC*AGGGTATCTAATCC*TG) (Sakai et al., 2004), which theoretically minimize chloroplast contamination by providing considerable mismatches with the poplar plastid DNA (3-4 mismatches). All primers and their sequences are listed in Table 4.1. Except for primer pair 68F-518R, all forward primers were fused to the Roche 454 pyrosequencing adaptor A including a sample-specific 10bp barcode (multiplex identifiers, MIDs) and all reverse primers were fused to adaptor B (Roche Applied Science, Mannheim, Germany). For primer pair 68F-518R, the reverse primer was fused to adaptor A and the forward primer was fused to adaptor B.

DNA samples (n = 48) were individually amplified using a Techne TC-5000 thermocycler (Bibby Scientific Limited, Staffordshire, UK) with the seven different primer pairs. Since the concentration of bacterial DNA in comparison with the plant DNA is low, we chose a nested PCR strategy to amplify all samples and thereby minimize the formation of primer dimers. A first round of PCR amplification was conducted using primers without the Roche 454 pyrosequencing adaptors and sample-specific barcode. Each 25µl PCR reaction contained approximately 10 ng of DNA and was carried out using the FastStart High Fidelity PCR System (Roche Applied Science, Mannheim, Germany). Each reaction contained 2.75 µl FastStart 10 x reaction buffer, 1.8 mM $MgCl_2$, 0.2 mM dNTP mix, 0.4 µM of each primer and 2 U FastStart HiFi polymerase. Cycling conditions included: initial denaturation at 94°C for 3 min, followed by 35 cycles of denaturation at 94°C for 1 min, annealing at 53°C for 1 min and extension at 72°C during 1 min; a final extension phase was performed at 72°C during 10 min. PCR amplicon pools were cleared from residual primers and primer dimers by separating the PCR products on a 1.5% agarose gel. Bacterial amplicons were excised from the gels using the QIAQuick gel extraction kit (Qiagen Benelux N.V., Venlo, The Netherlands). Mitochondrial products produced by primers 799F-1391R and 799F-1193R of respectively 1000 bp and 800 bp were also eliminated via the gel purification (Supplementary Figure 4.2). Following the first round of PCR amplification and gel-purification of the PCR products, a second round of PCR amplification was carried out for all seven primer pairs with the

sample-specific barcode. Amplicon length of sequences produced by primer pairs 799F-1391R and 68F-783R was reduced by amplifying the samples with 967F-1391 and 68F-518R in the second round. PCR cycling conditions were identical as previously described, with the exception of the number of PCR cycles, which was lowered to 25.

Subsequently, quadruplicate PCR amplicon pools from the corresponding samples were pooled together to end up with twelve samples from four different compartments (rhizosphere, root, stem, leaf) of three biologically independent poplar individuals. PCR amplicon pools were purified to remove PCR primers and primer dimers using the QIAquick PCR purification kit (Qiagen Benelux B.V., Venlo, the Netherlands). Following purification, the quality of the amplicon pools was evaluated using an Agilent 2100 Bioanalyzer system (Agilent Technologies, Diegem, Belgium) according to the manufacturer's protocol. Finally, purified amplicon libraries were quantified with the Quant-iT PicoGreen dsDNA Assay Kit (Invitrogen, Carlsbad, CA, USA) and a Fluostar Omega plate reader (BMG Labtech, Ortenberg, Germany) and pooled in equimolar concentrations. The resulting seven amplicon pools (one for each primer pair), each of them containing 12 samples, were sequenced on one eighth of a Pico Titer Plate on a Roche Genome Sequencer FLX+ using Titanium chemistry (Roche Applied Science, Mannheim, Germany) by LGC Genomics (Berlin, Germany).

4.2.5. Sequence processing

Sequencing generated seven individual Standard Flowgram Format (SFF) files, which were analysed separately using the software package mothur (version 1.33.2) following the Standard Operating Procedure outlined in http://www.mothur.org/wiki/Schloss_SOP (Schloss et al., 2009). Briefly, sequencing errors were reduced by denoising (shhh.flows, mothur implementation of Amplicon Noise algorithm) and quality trimming, which removed reads shorter than 200 bases, reads with homopolymers longer than 8 bases and reads containing ambiguous bases. Unique sequences were identified, whilst archiving the abundance data of the unique sequences, and aligned using align.seqs with the SILVA reference alignment (Release 119) (Pruesse et al., 2007). Within the unique sequences, chimeric sequences were identified using the Uchime tool (Edgar, 2011) followed by their removal from the dataset. Sequences matching "Chloroplast" and "Mitochondria" were identified using

classify.seqs and abundance data of these sequences were used to compare the performance of all primer pairs (Table 4.2). Subsequently these sequences were removed from the data set. Finally, genus-level OTUs (Operational Taxonomic Unit) were defined based on a 97% sequence similarity level. Complete parametrical evaluation was conducted with primer pairs 799F-1391R, 799F-1193R and 341F-783R based on low co-amplification of non-target rRNA and high retrieval of bacterial reads. Because these selected primer pairs resulted in differential amounts of reads per sample, the number of reads per sample were rarefied to 417 reads per sample. Samples for which fewer than 417 reads were obtained, were removed from the data set. Only for primer pair 341F-783R, we removed 3 samples, all belonging to the stem compartment. Rarefaction curves were assembled based on 10,000 permutations and intra-sample richness, diversity and Good's coverage estimates which were calculated in mothur (version 1.33.2) based on 10,000 iterations.

4.2.6. Isolation of intact chloroplasts to extract pure chloroplast DNA

Intact chloroplasts were isolated from *Populus tremula x alba* leaves following a method described by Cortleven et al., 2011. Briefly, fresh leaves (approximately 10g) were harvested and homogenized in 100 mL ice-cold grinding buffer (2.0 mM NaEDTA; 1.0 mM MgCl2; 1.0 mM MnCl2; 50.0 mM Hepes/KOH, pH 7.5; 0.33 M sorbitol; 5.0 mM sodium ascorbate) using a Braun MX-32 mixer. The resulting homogenate was filtered through four layers of Miracloth (pore size: 22-25 µm) and centrifuged (1400 g, 5 min). The pellet was resuspended in 1 mL of grinding buffer whereafter the suspension was loaded on a continuous 10-80% Percoll gradient (3% PEG 6000; 1% Ficoll; 1% BSA) and centrifuged (8000 g, 20 min). Finally, intact chloroplasts were collected after centrifugation (lower band), washed twice with 5 volumes of grinding buffer and stored at -70°C until chloroplast DNA was extracted. DNA was extracted from intact chloroplasts using the Invisorb Spin Plant Mini Kit following the manufacturer's instructions.

4.2.7. Quantitative real-time PCR

To evaluate the primer efficiency of the selected primer pairs amplifying pure chloroplast DNA (*Populus tremula x alba*), we tested all primer pairs in a qPCR set-up. From five chloroplast DNA samples, we made a 2 fold dilution series (1:2 up to 1:64). qPCR cycling conditions included: initial denaturation at 94°C for 3 min, followed by 35 cycles of denaturation at 94°C for 1 min, annealing at 53°C

for 1 min and extension at 72°C during 1 min; a final extension phase was performed at 72°C during 10 min. Finally, a dissociation curve was generated to verify amplification efficiency. Each reaction contained 2 µl of template DNA, 5 µl 2 x Fast SYBR Green Master Mix (Applied Biosystems, Foster City, CA, USA), 0.3 µl forward and reverse primer (0.3 µM each) and 2.4 µl nuclease-free water in a total volume of 10 µl. PCR efficiencies (E) were calculated as $E=(10^{-1/slope}-1) \times 100$.

4.2.8. Statistical analysis

Statistical analyses were performed in R 2.15.1 (The R Foundation for Statistical Computing, Vienna, Austria). Normal distributions of the data were checked with the Shapiro-Wilk test and homoscedasticity of variances was analysed using either Bartlett's or the Fligner-Killeens test. Significant differences in the variance of parameter were evaluated, depending on the distribution of the estimated parameters, either with ANOVA or the Kruskal Wallis Rank Sum Test. Post hoc comparisons were conducted by either the Tukey's Honest Significant Differences tests or Pairwise Wilcoxon Rank Sum tests. Poisson corrections were used for abundance data and distributions of ratios were compared with Pearson's Chi-squared tests. Non-metric multi-dimensional scaling (NMDS) was performed using the Vegan 2.0 – 8 package in R (Oksanen et al., 2013).

4.3. Results

4.3.1. 454 pyrosequencing

We analysed 12 samples derived from four different plant compartments of poplar (*Populus tremula x alba*) (rhizosphere, roots, stems and leaves) with seven selected bacterial 16S rRNA primer pairs (Table 4.1). Each amplicon library (one for each primer pair) was sequenced on 1/8 of a 454-picotiter plate. Sequencing of the amplicon libraries generated a total of 799,429 reads with an average of (± standard deviation) 114,204 (± 12013) reads. No more than one erroneous base in the MIDs and no more than two erroneous bases in the primer sequence were allowed for the assignment of the reads to a sample. The average length (± standard deviation) of the reads assigned to primer pairs 799F-1391R, 967F-1391R, 799F-1193R, 68F-783F, 68F-518, 341F-785, 341F-783R prior to quality checking and trimming was respectively 405 (± 96), 401 (± 101), 364 (± 105), 348 (± 139), 349 (± 105), 392 (± 105) and 361 (± 129).

Table 4.1. Summary of primers used in the current study

Primer pairs [1]	Primer Sequence (5'-3')	Hypervariable region of 16S rRNA operon	3' mismatch (%)	Chloroplast mismatch	Reference
799F	AACMGGATTAGATACCCKG	V5-V6-V7	3.99	4	Chelius et al. (2001)
1391R	GACGGGCGGTGWGTRCA		4.45	0	Walker et al. (2007)
967F	CAACGCGAAGAACCTTACC	V6-V7	0.20	0	Sogin et al. (2006)
1391R	GACGGGCGGTGWGTRCA		4.45	0	Walker er al. (2007)
799F	AACMGGATTAGATACCCKG	V5-V6-V7	3.99	4	Chelius et al. (2001)
1193R	ACGTCATCCCCACCTTCC		0.36	0	Bodenhausen et al. (2013)
341F	CCTACGGGNGGCWGCAG	V3-V4	0.37	0	Klindworth et al. (2012)
785R	GACTACHVGGGTATCTAATCC		0.37	0	Klindworth et al. (2012)
68F	TNANACATGCAAGTCGRRCG	V1-V4	2.75	0	McAllister et al. (2011)
783R	CTACC*AGGGTATCTAATCC*TG		36.7	3	Sakai et al. (2004)
68F	TNANACATGCAAGTCGRRCG	V1-V3	2.75	0	Mc Allister et al. (2011)
518R	WTTACCGCGGCTGCTGG		0.98	0	Lee et al. (2010)
341F	CCTACGGGNGGCWGCAG	V3-V4	0.37	0	Klindworth et al. (2012)
783R	CTACC*AGGGTATCTAATCC*TG		36.7	3	Sakai et al. (2004)

**Primer 783R is a primer mix: (a) 5'-CTACCAGGGTATCTAATCCTG-3', (b) 5'-CTACCGGGGTATCTAATCCCG-3' and (c) 5'- CTACCCGGGTATCTAATCCGG-3'*

(1) Primers are indicated as forward (F) or reverse (R)

4.3.2. Co-amplification of non-target DNA (plastid and mitochondrial)

During sequence processing in mothur, we identified all non-target rRNA reads (using classify.seqs) obtained by each primer pair within all plant compartments. The number of sequences identified as chloroplast or mitochondrial sequences were averaged across the three poplar individuals (within each plant compartment) and listed in Table 4.2.

As expected, practically no chloroplast or mitochondrial sequences were obtained from the rhizosphere samples by any of the studied primer pairs. Only primer pairs 967F-1391R, 341F-785R and 341F-783R amplified minute fractions of chloroplast sequences (<0.1 % of total sequences retrieved) and primer pair 799F-1193R obtained a small number of mitochondrial sequences (1.5% of total sequences retrieved).

Table 4.2. Co-amplification of non-target rRNA sequences by primer pairs

A. Chloroplast	799F-1391R	967F-1391R	799F-1193R	341F-785R	68F-783R	68F-518R	341F-783R
Rhizosphere soil	0^{a} (0)	0.3 ± 0.6^{a} (<0.1)	0^{a} (0)	2.3 ± 3.2^{a} (<0.1)	0^{a} (0)	0^{a} (0)	0.3 ± 0.6^{a} (<0.1)
Root	0^{a} (0)	2022 ± 165^{b} (76)	0^{a} (0)	2528 ± 492^{b} (85)	1824 ± 225^{b} (72)	3398 ± 503^{c} (97)	705 ± 327^{d} (26)
Stem	6 ± 8^{a} (0.2)	$2496 \pm 164^{b,c}$ (99)	0^{a} (0)	3173 ± 334^{d} (96)	2054 ± 388^{a} (99)	3406 ± 627^{d} (99)	1670 ± 60^{a} (80)
Leaf	0^{a} (0)	2174 ± 130^{b} (90)	0^{a} (0)	$2386 \pm 196^{b,c}$ (91)	1754 ± 87^{c} (89)	3206 ± 352^{d} (98)	885 ± 110^{e} (52)
B. Mitochondrial	799F-1391R	967F-1391R	799F-1193R	341F-785R	68F-783R	68F-518R	341F-783R
Rhizosphere soil	0^{a} (0)	0^{a} (0)	0.3 ± 0.6^{a} (1.5)	0^{a} (0)	0^{a} (0)	0^{a} (0)	0^{a} (0)
Root	0^{a} (0)	0^{a} (0)	16 ± 2^{a} (2.3)	127 ± 26^{b} (4)	35 ± 9^{a} (1)	14 ± 1^{a} (0.4)	343 ± 41^{c} (13)
Stem	0^{a} (0)	0^{a} (0)	$48 \pm 36^{a,b}$ (0.7)	114 ± 9^{b} (3)	11 ± 5^{a} (0.6)	3 ± 1^{a} (0.1)	359 ± 53^{c} (17)
Leaf	0^{a} (0)	0^{a} (0)	26 ± 4^{a} (<0.1)	179 ± 30^{b} (7)	40 ± 28^{a} (2)	17 ± 3^{a} (0.5)	325 ± 76^{c} (19)
C. Total non-target rRNA	799F-1391R	967F-1391R	799F-1193R	341F-785R	68F-783R	68F-518R	341F-783R
Rhizosphere soil	0^{a} (0)	0^{a} (0)	0.3 ± 0.6^{a} (1.5)	2.3 ± 3.2^{a} (<0.1)	0^{a} (0)	0^{a} (0)	0.3 ± 0.6^{a} (<0.1)
Root	0^{a} (0)	2022 ± 165^{b} (76)	16 ± 2^{a} (2.3)	$2655 \pm 466^{b,c}$ (89)	1860 ± 217^{b} (73)	3412 ± 504^{c} (97)	1048 ± 337^{d} (39)
Stem	6 ± 8^{a} (0.2)	$2496 \pm 164^{b,c}$ (99)	48 ± 36^{a} (0.7)	$3287 \pm 344^{b,d}$ (99)	2066 ± 384^{c} (99)	3410 ± 628^{d} (99)	2029 ± 7^{c} (97)
Leaf	0^{a} (0)	$2174 \pm 130^{b,c}$ (90)	26 ± 4^{a} (<0.1)	2565 ± 168^{b} (98)	1794 ± 114^{c} (91)	3223 ± 350^{d} (99)	1211 ± 34^{e} (71)

Average number of chloroplast (A), mitochondrial (B) and total non-target rRNA sequences (C, sum of chloroplast and mitochondrial sequences) obtained from each plant compartment by the selected primer pairs. Values are averages of three biologically independent replicates ± standard deviation. Values between brackets represent the average percentage (%) of chloroplast/mitochondrial sequences as compared to the total number of sequences obtained per sample. Sequence counts were statistically analysed using a two-way ANOVA per block (A, B, C). Differences at the 95% significance level are indicated with lower cased letters ($P < 0.05$).

In the root samples, we found a clear difference in performance of the selected primer pairs. Both primer pairs 799F-1391R and 799F-1193R completely avoided co-amplification of chloroplast sequences in the root samples. Primer pair 68F-518R amplified the highest number of chloroplast sequences in the root samples (3398 ± 503, $P < 0.05$) accounting for 97% of the total sequences obtained. Primer pairs 967F-1391R, 341F-785R and 68F-783R retrieved on average (± standard deviation) 2022 (± 165), 2528 (± 492), and 1824 (± 225) chloroplast sequences respectively accounting for 76%, 85% and 72% of the total

sequences. Primer pair 341F-783R retrieved significantly less ($P < 0.05$) chloroplast sequences from the root samples, more specifically 705 (± 327) representing 26% of the total sequences. No noteworthy amounts of mitochondrial sequences were obtained from the root samples by any of the primer pairs, except by primer pairs 341F-785R (127 ± 26) and 341F-783R (343 ± 41) accounting for respectively 4% and 13% of the total sequences.

In the stem and leaf samples, the performance of the primer pairs was highly comparable to those of the root samples. Primer pairs 799F-1391R and 799F-1193R showed no amplification of chloroplast sequences, with the exception of a single stem sample with primer pair 799F-1391R which amplified 15 chloroplast sequences (average: 6 ± 8). Primer pair 68F-518R consistently retrieved the highest numbers of chloroplast sequences from the stem (3406 ± 627, $P < 0.05$) and leaf samples (3206 ± 352, $P < 0.05$) accounting for 99% and 98% of the total sequences obtained. Primer pairs 967F-1391R, 341F-785R and 68F-783R also obtained high amounts of chloroplast sequences from the stem and leaf samples representing up to 99% of the total sequences (Table 4.2). Primer pair 341F-783R again retrieved significantly less ($P < 0.05$) chloroplast sequences from the stem and leaf samples with respectively 1670 ± 60 and 885 ± 110 sequences accounting for 80% and 52% of the total sequences. Large amounts of mitochondrial sequences in the stem and leaf samples were obtained by primer pairs 341F-785R and 341F-783R. Primer pair 341F-785R retrieved 114 ± 9 and 179 ± 30 from the stem and leaf samples accounting for 3% and 7% of the total sequences. Primer pair 341F-783R, on the other hand, co-amplified 359 ± 53 (stem) and 325 ± 76 (leaf) mitochondrial sequences representing 17% and 19% of the total sequences. Minute fractions of mitochondrial sequences were obtained by the other primers pairs in the stem and leaf samples, except for primer pairs 799F-1391R and 967F-1391R, which did not co-amplify any mitochondrial sequences. Complete sequence counts for the chloroplast and mitochondrial sequences as well the total non-target rRNA sequence count and statistical differences are presented in Table 4.2.

After filtering of the non-target rRNA sequences, we calculated the number of bacterial 16S rRNA sequences for each primer pair within each plant compartment (Table 4.3)

4.3.3. Primer efficiency for pure chloroplast DNA (poplar)

We tested the amplification efficiency of all primer pairs with pure poplar chloroplast DNA as template in a qPCR set-up to evaluate their affinity for non-bacterial chloroplast rRNA present in the plant samples. A 2-fold dilution series (1:1 to 1:64) was used to amplify the chloroplast DNA with all 16S rRNA primer pairs (Figure 4.1).

The average PCR efficiencies (as calculated by $E=(10^{-1/slope}-1) \times 100$) divided all primer pairs into three separate groups. For 967F-1391R, 341F-785R and 68F-518R, PCR efficiencies (± standard error) were calculated to be respectively 94.5% (± 0.1%), 91.1% (± 0.7%) and 95.3% (± 3.2%). For 68F-783R and 341F-783R, containing 783R with chloroplast mismatches, we found a significantly lower PCR efficiency at the 95% significance level. PCR efficiencies were 67.3% (± 3.2%) for 68F-783R and 50.3% (± 4.8%) for 341F-783F. Finally, 799F-1391R and 799F-1193R showed very low affinities for pure chloroplast DNA with PCR efficiencies of 9.2% (± 2.4%) and 17.4% (± 10.50%) ($P < 0.05$).

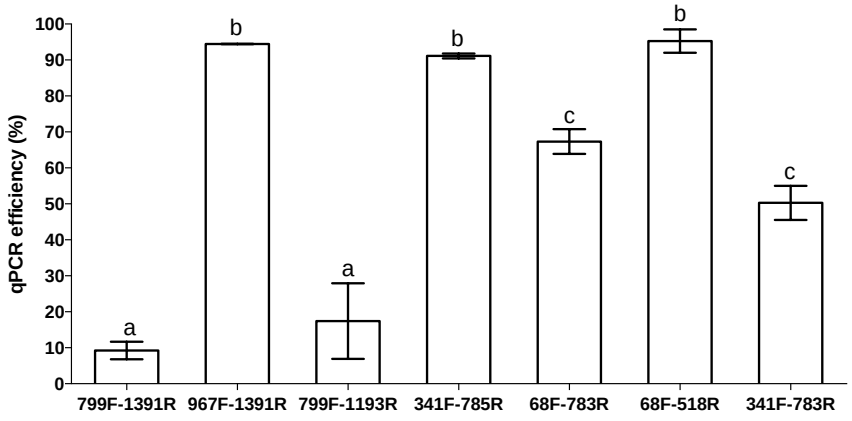

Figure 4.1. Average PCR amplification efficiency of selected 16S rRNA primers for pure chloroplast DNA (poplar) using quantitative real-time PCR. Values are averages of five biologically independent replicates ± standard error. PCR efficiencies were compared using an one-way ANOVA. Differences at the 95% significance level are indicated with lower cased letters ($P < 0.05$).

4.3.4. Sequencing depth and coverage of selected primer pairs

Based on low co-amplification levels of chloroplast and mitochondrial sequences and consequently high retrieval of bacterial rRNA reads (Table 4.3), we selected primer pairs 799F-1391R, 799F-1193R and 341F-783R for further parametrical analysis. Rarefaction curves were assembled showing the numbers of observed OTUs, defined at a 97% sequence similarity, relative to the number of total identified bacterial rRNA sequences (Figure 4.2). Good's coverage estimates were calculated in mothur based on 10,000 iterations (Figure 4.2).

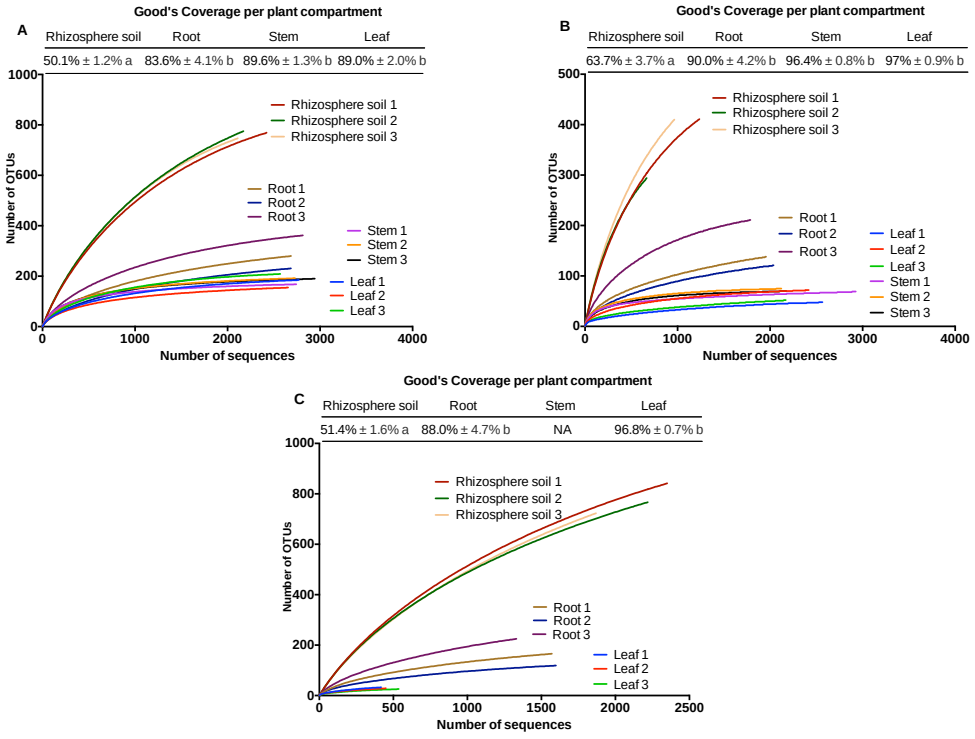

Figure 4.2. Good's coverage estimates and rarefaction curves of the different replicates from each plant compartment (rhizosphere soil, root, stem and leaf) for each primer pair including (A) 799F-1391R, (B) 799F-1193R and (C) 341F-783R. Good's coverage estimates were calculated in mothur based on 10,000 iterations. Differences at the 95% significance level between the plant compartments are indicated with lower cased letters ($P < 0.05$). Rarefaction curves were assembled showing the number of observed OTUs, defined at a 97% sequence similarity cut-off, relative to the total number of identified bacterial rRNA sequences.

For the root, stem and leaf samples, rarefaction curves of all primer pairs tended towards saturation demonstrating that the sequencing effort was sufficient to obtain the most abundant bacterial OTUs. Good's coverage estimates ranged from 83.6% to up to 97%. However, the rarefaction curves of the rhizosphere samples showed little to no saturation for all primer pairs indicating that the sequencing depth for these samples was insufficient and OTUs may have remained undetected. This is also reflected in the low Good's coverage estimate for these samples with 50.1% (± 1.2%), 63.7% (± 3.7%) and 51.4% (± 1.6%) for respectively primer pairs 799F-1391R, 799F-1193R and 341F-783R.

4.3.5. Parametrical comparison of selected primer pairs

To compare primer pair performance, the numbers of sequences per sample were rarefied to the minimum number of sequences in a single sample (417 sequences). Averages of the number of bacterial rRNA sequences were calculated across replicates within each plant compartment (rhizosphere, root, stem, leaf) (Table 4.3).

Table 4.3. Bacterial 16S rRNA sequences retrieved by each primer pair

Plant Compartment	799F-1391R	967F-1391R	799F-1193R	341F-785R	68F-783R	68F-518R	341F-783R
Rhizosphere soil	2235 ± 165^{a,b}	2550 ± 673^{a,c}	956 ± 285^{d}	1958 ± 117^{a,b}	3346 ± 454^{c}	1519 ± 216^{b,d}	2196 ± 316^{a,b}
Root	2728 ± 74^{a}	555 ± 212^{b}	1927 ± 128^{c}	261 ± 93^{b,d}	624 ± 236^{b}	76 ± 35^{d}	1500 ± 147^{c}
Stem	2804 ± 120^{a}	5.7 ± 6.3^{b}	2407 ± 450^{a}	11 ± 6^{b}	2.5 ± 2.1^{b}	2 ± 4^{b}	51 ± 25^{b}
Leaf	2665 ± 100^{a}	228 ± 58^{b}	2384 ± 201^{a}	55 ± 35^{c}	166 ± 72^{b}	34 ± 20^{c}	467 ± 62^{b}

Average number of bacterial rRNA sequences obtained from each compartment by the selected primer pairs after quality trimming and removal of non-target rRNA sequences (chloroplast/mitochondrial). Values are averages of three biologically independent replicates ± standard deviation. Sequence counts were statistically analysed using an one-way ANOVA per compartment. Differences at the 95% significance level are indicated with lower cased letters.

In the rhizosphere, the average number of reads per sample obtained by 799F-1193R after quality trimming was significantly lower ($P < 0.05$) than for primer pairs 799F-1391R and 341F-783R. Primer pair 799F-1193R yielded on average (± standard deviation) 956 (± 285) high quality reads per sample as compared to 799F-1391R and 341F-783R which obtained respectively 2235 (± 165) and 2196 (± 316) bacterial reads per sample. In the roots, primer pair 799F-1391R

amplified on average 2728 (± 74) reads as compared to primer sets 799F-1193R and 341F-783R which amplified significantly less reads per sample ($p<0.05$) with respectively 1927 (± 128) and 1500 (± 147) bacterial reads per sample. In the stem and leaf compartments, primer pair 799F-1391R amplified on average respectively 2804 (± 120) and 2665 (± 100) reads per sample. Primer set 799F-1193R retrieved consistently less reads per sample, although not statistically significant with 1927 (± 128) reads in the stems and 2384 (± 201) reads in the leaves amplified respectively. Due to co-amplification of chloroplast and mitochondrial sequences, primer pair 341F-783R performed very poorly in the stems and leaves with on average (± standard deviation) respectively 51 (± 25) and 467 (± 62) bacterial reads per sample respectively.

To further compare primer pair performance, the numbers of reads per sample was rarefied to 417 reads and the average numbers of OTUs at a 97% sequence similarity threshold (observed OTU richness) were calculated across replicates and within each compartment (Figure 4.3).

In the rhizosphere (Figure 4.3A), we observed the highest OTU richness for primer pairs 799F-1391R and 341F-783R, which yielded on average the same amount of OTUs ($P = 0.80$) with 277 OTUs (min = 271; max = 281) and 270 OTUs (min = 265; max = 276) per sample respectively. For primer pair 799F-1193R, OTU richness was significantly lower ($P < 0.01$) with on average 236 OTUs (min = 227; max = 252) per sample (Figure 4.3A). In the roots (Figure 4.3B), all primer pairs yielded comparable OTUs richness estimates. Primer pair 799F-1391R obtained on average 115 OTUs (min = 93; max = 143) per sample, primer set 799F-1193 retrieved 79 OTUs (min = 58; max = 111) per sample and finally primer pair 341F-783R yielded 87 OTUs (min = 62; max = 117). However, in the stem and leaves (Figure 4.3C, D), we consistently observed the highest OTU richness for primer pair 799F-1391R ($P < 0.01$). In the stem (Figure 4.3C), primer pair 799F-1391R retrieved on average 109 OTUs (min = 107; max = 110). In contrast, primer set 799F-1193R only obtained 47 OTUs (min = 45; max = 51) per sample in the stems. For primer pair 341F-783R, OTU richness could not be determined in the stem samples (nd) as a consequence of very low amplification of bacterial rRNA reads (Table 4.2 and 4.3). In the leaves (Figure 4.3D), primer pair 799F-1391R yielded on average 90 OTUs (min = 80; max = 102) whereas primer sets 799F-1193 and 341F-783R retrieved

significantly less (P < 0.01) OTUs with respectively 29 OTUs (min = 22; max = 39) and 28 OTUs (min = 23; max = 33) per sample.

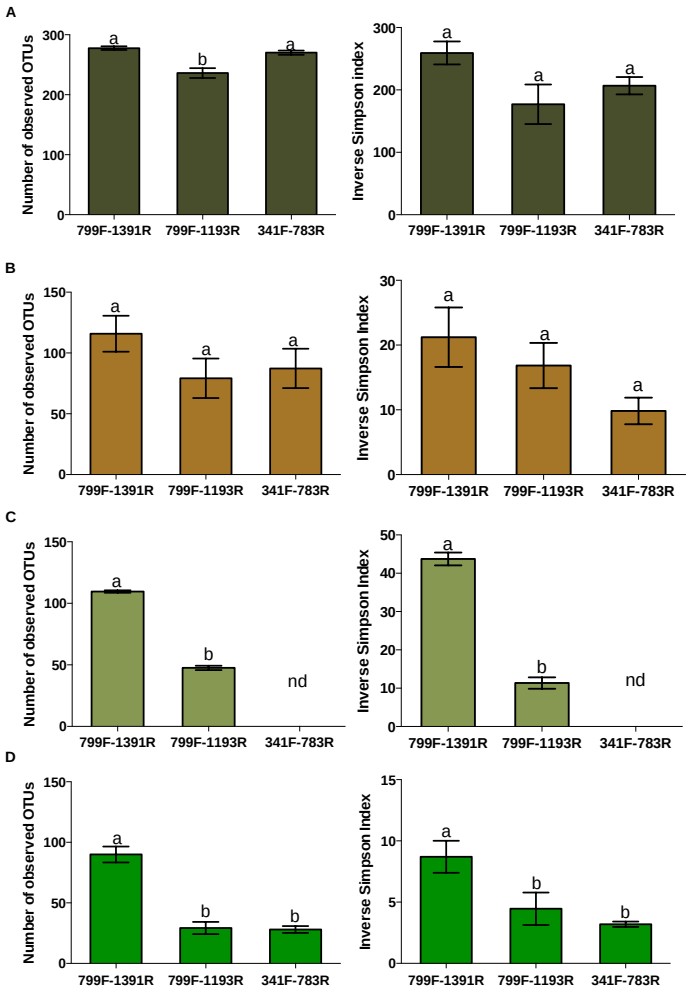

Figure 4.3. Comparison of parametrical alpha diversity between selected 16S rRNA primer pairs (799F -1391R, 799F-1193R and 341F-783R) for all sampled plant compartments (A. Rhizosphere soil, B. Root, C. Stem, D. Leaf). All averages were calculated across three biologically independent poplar individuals for each primer pair. Left panels: average number of operational taxonomic units (OTUs) observed based on a 97% sequence similarity cutoff (richness) and right panels: Inverse Simpson diversity indices. OTU counts and Inverse Simpson indices were statistically analysed using a one-way ANOVA per plant compartment. Differences at the 95% significance level are indicated with lower cased letters (P < 0.05).

Finally, diversity was estimated using the inverse Simpson index (Figure 4.3A, B, C, D). In the rhizosphere and the root samples, we observed statistically comparable diversity estimates for all primer pairs. However in the stems and leaves, primer pair 799F-1391R consistently showed a higher diversity as compared to primer pairs 799F-1193R and 341F-783R ($P < 0.01$). Diversity indeces could not be calculated for primer pair 341F-783R in the stem samples due to low amplification of bacterial reads.

4.3.6. Community similarity between primer pairs and description of observed communities

To compare the bacterial community structures retrieved by each selected primer pair (799F-1391R, 799F-1193R and 341F-783R) at the phylum and genus level, relative frequency distributions of the obtained genus-level OTUs and phyla were analysed with chi-squared tests for the three primer pairs, based on average abundances across replicate samples. At the phylum and genus-level, differences were observed ($P < 0.05$) for all three primer pairs within all plant compartments.

At the phylum level (Figure 4.4), the majority of the OTUs in the rhizosphere soil (Figure 4.4A) identified by all primer pairs were assigned to Proteobacteria (37% to 60%), Actinobacteria (14% to 25%), Acidobacteria (3% to 21%) and Bacteriodetes (3% to 9%). In the roots (Figure 4.4B), we observed a strong dominance of Proteobacteria (78% to 91%) with a minority of the identified OTUs belonging to Bacteriodetes (2% to 11%), Actinobacteria (2% to 4%) and TM7 (1% to 4%). In the stems (Figure 4.4C), the dominance of phylum Proteobacteria (48% to 97%) persisted although it was slightly less pronounced for the analyses on primer pairs 799F-1391R (61%) and 799F-1193R (48%) compared to primer pair 341F-783R (97%). For the analyses based on primer pairs 799F-1391R and 799F-1193R, the rest of the identified OTUs mainly belonged to Actinobacteria (respectively 11% and 19%) and Deinococcus-Thermus (respectively 6% and 27%). Finally in the leaves, the majority of the OTUs were also identified as Proteobacteria (82% to 96%). A minority of the OTUs found in the leaves belonged to Actinobacteria lineages (3% to 11%) (Figure 4.4D).

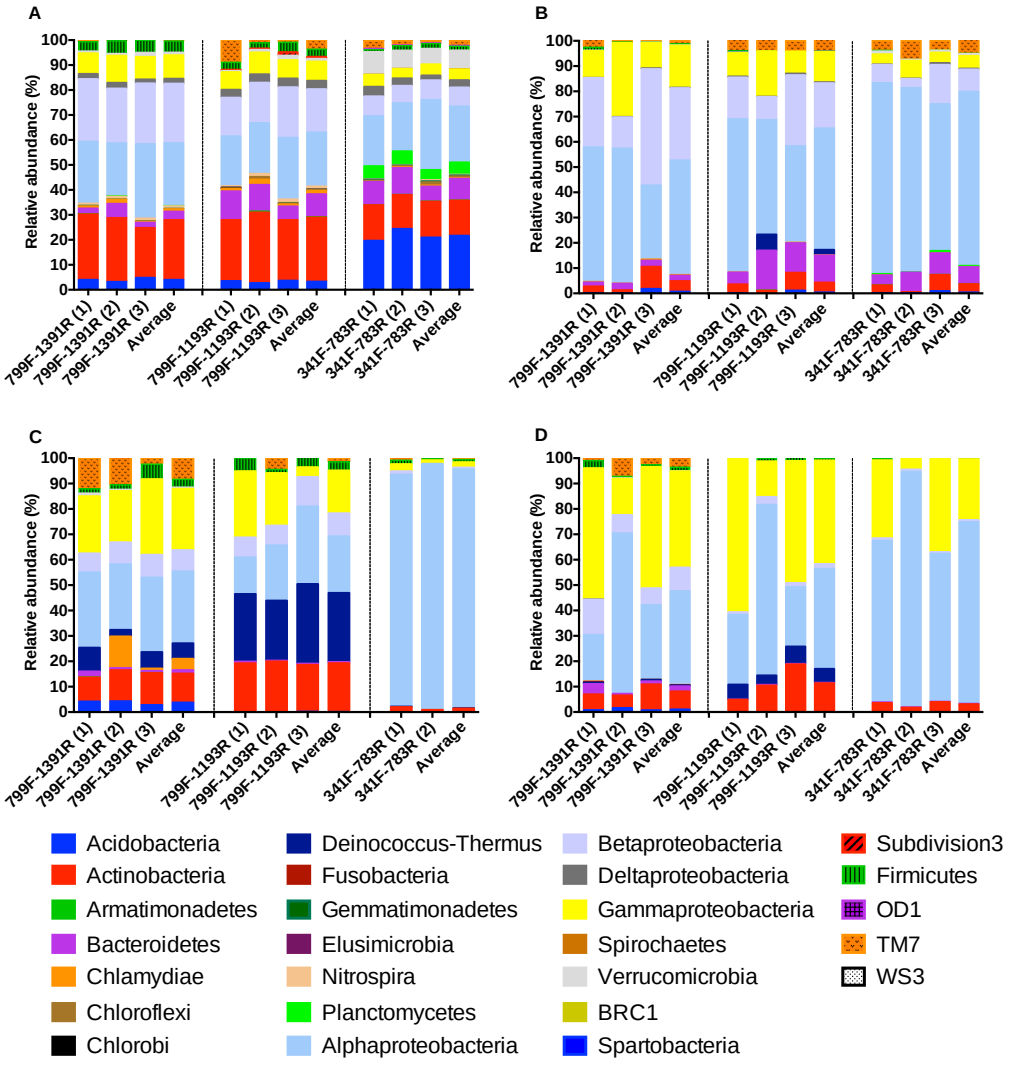

Figure 4.4. Relative sequence abundance of bacterial phyla associated with different plant compartments (A. Rhizosphere soil, B. Root, C. Stem, D. Leaf) identified by the three selected primer pairs (799F-1391R, 799F-1193R and 341F-783R). Proteobacteria OTU has been replaced by 4 OTUs at the subclass level (alpha, beta, gamma, delta). Replicates are displayed in separate bars and also are averaged per primer pair.

To give an idea of the bacterial communities at the genus level, we defined the core bacterial community, described by each primer pair, as the ten most abundant genus-level OTUs per compartment. This resulted in 21 OTUs for the rhizosphere, 18 OTUs for the roots and 23 OTUs for the stem and leaf samples

(Supplementary Table 4.1A, B, C, D). The percentage of sequences represented by these 10 most abundant OTUs for each primer pair and plant compartment are listed in Supplementary Table 4.1A, B, C, D. For all plant compartments, and in particular the rhizosphere soil, we observed long-tailed rank-abundance curves characteristic of microbial communities (Hartmann et al., 2012). Worth noting here is that for all compartments, except for the leaves, the most abundantly identified OTU was different for each primer pair. This demonstrates emphasizing the major effect of primer choice on the observed bacterial communities. In the rhizosphere, *Actinomycetales* (9.9 %, 799F-1391R), *Rhizobiales* (11.3%, 799F-1193R) and *Acidobacteria_Gp6* (15.7, 341F-783R) were the dominant OTUs. In the roots, *Pseudomonas* (11.9%, 799F-1391R), *Rhizobium* (15.9%, 799F-1193R) and *Rhizobiales* (38.9%, 341F-783R) constituted the major identified OTUs. In the stems, *Pseudomonas* (12.9%, 799F-1391R), *Deinococcaceae* (18.2%, 799F-1193R) and *Sphingomonadaceae* (34.2%, 341F-783R) were the most observed OTUs. Finally, in the leaves, *Pseudomonas* dominated bacterial communities regardless of the primer pair used.

Further, to explore the specificity and robustness of the selected primer pairs, we compared phylum and genus-level OTU abundances of samples for each primer pair within every plant compartment (rhizosphere, root, stem, leaf) using non-metric multi-dimensional scaling (NMDS) with Bray-Curtis dissimilarities (Supplementary Figure 4.3A and B). In general, samples from each primer pair grouped closely together at phylum level (Supplementary Figure 4.3A) and genus level (Supplementary Figure 4.3B). Hence, the primer pairs deliver reproducible results and the choice of primer pair shapes the bacterial community observed in metabarcoding analyses. Finally, we compared the bacterial communities (NMDS) retrieved per plant compartment within each primer pair (Supplementary figure 4.4A and B). In general, for all selected primer pairs, samples from each compartment clustered closely together at the phylum level (Supplementary figure 4.4A) and genus level (Supplementary figure 4.4B), clearly illustrating the specific niche differentiation of plant-associated bacteria.

4.4. Discussion

Plant organelles of prokaryotic origin (chloroplasts and mitochondria) represent specific problems during 16S rRNA metabarcoding of bacterial communities associated with host plant species and folivorous insects. High homology between bacterial 16S rRNA genes, chloroplast 16S rRNA genes, plant nuclear and mitochondrial 18S rRNA genes (Dyall et al., 2004; Raven, 1970) and the high abundance of chloroplast 16S rRNA genes in these environments lead to significant challenges in selecting suitable primer pairs and ultimately undesired co-amplification of non-target sequences (Bodenhausen et al., 2013; Bulgarelli et al., 2012; Gottel et al., 2011; Lundberg et al., 2012). This issue is widespread in insect and plant samples but, until now, it remained under investigated. Although primers have been developed to theoretically minimize chloroplast contamination (799F and 783R) (Chelius & Triplett, 2001; Sakai et al., 2004), they are used without first evaluating their experimental phylum spectrum and performance for next generation sequencing studies. Especially in specific heterogeneous environments, such as plants, *in silico* PCR analyses provide a valuable basis for primer selection but should be complemented with the actual experimental performance of the primers (Klindworth et al., 2013; Op De Beeck et al., 2014). For this purpose, we experimentally evaluated the potential of a series of commonly used primers to eliminate the amplification of non-target DNA, e.g. chloroplast and mitochondrial sequences, and to optimize retrieval of bacterial rRNA reads in metabarcoding studies of rhizospheric and endophytic bacterial communities.

Firstly, we evaluated the co-amplification of non-target DNA, e.g. chloroplast and mitochondrial DNA, by all primer pairs in the different plant compartments (Table 4.2). In the rhizosphere, some of the selected primer pairs retrieved minute fractions of chloroplast (967F-1391R, 341F-785R, 341F-783R) and mitochondrial (799F-1193R) sequences. Retrieval of plastid and mitochondrial 16 rRNA from soil and rhizosphere samples is surprising but most likely trace amounts of decaying root, stem or leaf tissue, present in the soil during DNA extraction, could have contributed to the retrieval of these sequences. Moreover root cap border cells have been shown to remain alive (for a week or longer) after desquamation from the root corpus into soil (Hawes et al., 2000; Vermeer & McCully, 1982). As a result, rhizosphere soil is inevitably contaminated with

live and dead root cap border cells (Bulgarelli et al., 2013). In the plant compartments, we found significant differences in performance of the primer pairs for co-amplification of non-target DNA (Table 4.2). As expected, interference of non-target DNA was significantly reduced by the primer pairs containing a forward or reverse primer with incorporated mismatches with chloroplast DNA, e.g. primers 799F and 783R (only in combination with 341F). Primer pairs 799F-1391R and 799F-1193R completely eliminated the co-amplification of chloroplast sequences in the root, stem and leaf samples. Indeed, primer 799F and variations thereof have been used in the literature to minimize chloroplast contamination in plant samples with varying success and mostly resulting in considerable co-amplification of chloroplast 16S rRNA (Bodenhausen et al., 2013; Bulgarelli et al., 2012; Lundberg et al., 2012; Shade, 2013; Sagaram et al., 2009). However, although primer 783R (Sakai et al., 2004) displayed 3 mismatches with poplar 16S rRNA during *in silico* analyses (data not shown), in an experimental set-up it failed to efficiently eliminate chloroplast 16S rRNA amplification (Table 4.2). Primer pair combination 341F-783R performed reasonably well in the root samples (26% of chloroplast 16S rRNA) but higher chloroplast input from stems and leaf samples resulted in significant co-amplification of chloroplast 16S rRNA (Table 4.2). In this case, *in silico* analyses portrayed an incorrect image of the primer potential and endorse that the position of the mismatches are crucial for their effectiveness in PCR amplification (Ayyadevara et al., 2000; Klindworth et al., 2013; Lefever et al., 2013).

Interestingly, we consistently retrieved more chloroplast sequences from the stem samples as compared to the leaf samples for all primer pairs (except 799F-1193R). Although absolute chloroplast DNA concentration is clearly higher in the leaf samples (being the major photosynthetic organ) than the stem samples, the balance between endophytic bacterial DNA and chloroplast DNA seems to play a more important role. Poplar stems are highly lignified and consist of a high proportion of dead cells (xylem vessels) (Leplé et al., 2007; Leplé et al., 1998; Vanholme et al. , 2010) with low nutrient content and therefore most likely harbour fewer total bacterial cells than the leaf samples thereby skewing the balance towards the chloroplast 16S rRNA.

To assess whether or not the observed differences in the amplification of chloroplast sequences in the plant-bacteria DNA extracts during 16S rRNA metabarcoding would correlate with PCR amplification efficiency of the selected primer pairs for pure chloroplast DNA, a qPCR experiment was conducted. To this end, we isolated pure chloroplast DNA from the intact chloroplasts of 5 poplar leaf samples (Cortleven et al., 2011) and amplified the pure chloroplast DNA with the selected primer pairs (Figure 4.1). We observed a strong correlation between the qPCR set-up and the pyrosequencing results. Primer pairs 799F-1391F and 799F-1193R showed very low affinity for pure chloroplast 16S rRNA (efficiency of respectively 9.2% and 17.4%) resulting in virtually no amplification of chloroplast 16S rRNA in the pyrosequencing set-up. Medium affinity for chloroplast 16S rRNA was observed for primer pairs 68F-783R (67.3%) and 341F-783R (50.3%) resulting in differential amplification of chloroplast 16S rRNA (specifically for 341F-783R) depending on the chloroplast input (root versus stem and leaf) in the pyrsequencing set-up. The other primer pairs 967F-1391 (94.5%), 341F-785R (91.1%) and 68F-518R (95.3%) displayed very high PCR amplification efficiencies and indeed resulted in high co-amplification of chloroplast 16S rRNA during metabarcoding (Table 4.2).

We selected primer pairs 799F-1391R, 799F-1193R and 341F-783R, based on high retrieval of bacterial 16S rRNA sequences, for further parametrical analysis. Rarefaction curves and Good's coverage indicated that our sampling effort (regardless of primer pair) for the rhizospheric samples was inadequate (ranging from 50.1% to 63.7%) to fully capture the bacterial communities (Figure 4.2). Indeed, rarefaction curves from other studies using rhizosphere soil only tend towards saturation after 5000-6000 sequenced reads (Gottel et al., 2011). However, the comparison of the selected primer pairs revealed higher OTU retrieval (richness) of primer pairs 799F-1391R and 341F-783 as compared to primer pair 799F-1193R (Figure 4.3). Inverse Simpson diversity estimates were comparable for all primers (Figure 4.3). In the roots, the performance (OTU richness and Inverse Simpson) of all primer pairs was also comparable with a slight trend towards higher estimates for primer pair 799F-1391R. Gottel et al. (2011) reported high variability in the OTU retrieval isolated from the roots of poplar trees in mature, natural ecosystems (83 OTUs per sample ± 78). We obtained comparable OTU counts for all primer pairs (Figure 4.3). Primer pair

799F-1391R attained on average 115 OTUs (min = 93; max = 143) per sample, primer set 799F-1193 retrieved 79 OTUs (min = 58; max = 111) per sample and finally primer pair 341F-783R yielded 87 OTUs (min = 62; max = 117). However, important to mention, is that we rarefied our samples to 417 sequences per sample, thereby reducing the amounts of OTUs retrieved. Indeed much higher OTUs richness counts were observed in the roots and leaves of *Arabidopsis thaliana* (Bodenhausen et al., 2013; Bulgarelli et al., 2012; Lundberg et al., 2012). Finally in the stems and leaves, samples with the highest chloroplast input, the performance of primerpair 799F-1391R was significantly higher when evaluating the OTU richness and Inverse Simpson diversity (Figure 4.3).

Remarkably, we also found a clear difference in the numbers of reads that could not be unambiguously classified at the phylum level in the V6-V7 region (799F-1391R, 799F-1193R) as compared to the V3-V4 region (341F-783R) in the rhizosphere samples. This is indicative of an insufficient database representation of the biodiversity of soil-borne bacteria and an underrepresentation of the hypervariable V6-V7 region (Bulgarelli et al., 2012; Gans et al., 2005). Indeed, V3-V4 has been the preferred region for next-generation studies (Klindworth et al., 2013). Therefore, at least for the time being, for the study of plant-associated bacteria a trade-off enforces itself to choose for the V6-V7, with the availability of primers to avoid co-amplification of organellar 16 rRNA but with an underrepresentation of sequences in this region in the databases.

Further, to explore the specificity and robustness of the selected primer pairs, we compared phylum and genus-level OTU abundances of samples for each primer pair within every plant compartment (rhizosphere, root, stem, leaf) (Supplementary Figure 4.3A and 4.3B). Samples from all plant compartments displayed strong clustering according to the primer pairs, indicating that the primers deliver reproducible results. This observation also demonstrates that the choice of primer pair shapes the bacterial communities observed in 16S rRNA metabarcoding studies (primer bias) (Klindworth et al., 2012).

Finally, we also obtained a first look at the rhizospheric and endophytic bacterial communities associated with the different plant compartments of poplar trees (*Populus tremula x Populus alba)* in the studied field trial. For all primer pairs, we observed close clustering of samples (both at the phylum level and genus

level) according to the different plant compartments (Supplementary Figure 4.4A and 4.4B). We previously observed the same niche differentiation in the isolation of cultivable bacteria from poplar trees in the same field study (Beckers et al., 2015, Chapter 3). Niche differentiation between the rhizosphere and root endophyte microbiome has been described for mature poplar trees growing in natural ecosystems (*Populus deltoides*) (Gottel et al., 2011) and for *Arabidopsis thaliana* (Bulgarelli et al., 2012; Lundberg et al., 2012). Recently, Bulgarelli *et al*. (2013) proposed a two-step selection model for root microbiota differentiation from the rhizosphere where rhizodeposition and host genotype-dependent fine-tuning converge to select specific endophytic assemblages. Although we used a limited amount of biological replicates (3), our data indicates additional fine-tuning and niche differentiation of the microbiota in the aerial plant organs, with the stem and leaf bacterial communities being remarkably dissimilar from the root and rhizosphere (Supplementary Figure 4.4A and 4.4B) Indeed, each of these microenvironments (rhizosphere soil, root, stem and leaf) provide very specific abiotic conditions such as availability of soluble organic compounds (Bulgarelli et al., 2013; Lindow & Brandl, 2003; McCully, 2001).

Taking a closer look at the phylum level, in the rhizosphere we predominantly identified *Proteobacteria*, *Acidobacteria* and *Actinobacteria*, irrespective of the selected primer pair. The ratio of *Proteobacteria* to *Acidobacteria* in rhizosphere bacterial communities has previously been shown to be an indicator of the trophic level of soils where *Proteobacteria* were linked to nutrient-rich soils and *Acidobacteria* to nutrient-poor soils (Gottel et al., 2011; Castro et al. 2010; Smit et al. 2001). Endophytic communities were, for the most part dominated by *Proteobacteria* suggesting substantial overlap in key community members across host species (Bodenhausen et al., 2013; Bulgarelli et al., 2012; Gottel et al., 2011; Lundberg et al., 2012; Romero, Marina, & Pieckenstain, 2014). At genus-level, most remarkable is the efficiency of the endophytic colonization of *Pseudomonas* as indicated by all studied primer pairs. (Supplementary Table 4.1A, B, C, D). A low relative abundance of *Pseudomonas* in the rhizosphere soil (0.3% to 1.9%) is contrasted by its dominance in the leaf samples (33.9% to 40.1 %). Leaf colonization may occur via the rhizosphere where most endophytic bacteria should originate from and/or via leaf stomatal colonization

since aerosol samples were found to harbour abundant *Pseudomonas* sequences (Chi et al., 2005; Fahlgren et al. 2010; Sessitsch et al. 2002). Finally, important to mention with the interpretation of community studies with next generation sequencing platforms, as argued by Bodenhausen et al. (2013), is the 16S rRNA operon copy number. This copy number may vary, depending on species, from 1 to 15, introduces significant bias and distort views on bacterial communities (Crosby et al. 2003; Lee et al. 2009).

4.5. Conclusion

We experimentally evaluated the performance of seven 16S rRNA primers pairs in 16S rRNA metabarcoding studies of endophytic and rhizospheric bacterial communities. From our selection, primer pairs 799F-1391R, 799F-1193R and 341F-783R reduced, with varying success, co-amplification of non-target rRNA in root, stem and leaf samples. Specifically, primer pair 799F-1391R displayed very low amplification of non-target rRNA across all sampled plant compartments. Furthermore, parametrical comparison (OTU richness and Simpson diversity) of the three primer pairs revealed that primerpair 799F-1391R retrieved the highest number of OTUs as well exhibited the highest Simpson diversity, especially in the plant compartments with high chloroplast input (stem and leaf samples). Therefore, we propose primer pair 799F-1391R as best suited for 16S rRNA metabarcoding studies of rhizospheric and endophytic bacterial microbiomes.

References

Ayyadevara, S., Thaden, J. J. and Shmookler Reis, R. J. (2000). Discrimination of primer 3'-nucleotide mismatch by taq DNA polymerase during polymerase chain reaction. *Analytical Biochemistry*, *284*, 11–18.

Bodenhausen, N., Horton, M. W. and Bergelson, J. (2013). Bacterial communities associated with the leaves and the roots of Arabidopsis thaliana. *PloS One*, *8*, e56329.

Bulgarelli, D., Rott, M., Schlaeppi, K., Ver Loren van Themaat, E., Ahmadinejad, N., Assenza, F., Rauf, P., Huettel, B., Reinhardt, R., Schmelzer, E., Perlies, J., Gloeckner, F. O., Amann, R., Eickhorst, T. and Schulze-Lefert, P. (2012). Revealing structure and assembly cues for Arabidopsis root-inhabiting bacterial microbiota. *Nature*, *488*, 91–95.

Bulgarelli, D., Schlaeppi, K., Spaepen, S., Ver Loren van Themaat, E. and Schulze-Lefert, P. (2013). Structure and functions of the bacterial microbiota of plants. *Annual Review of Plant Biology*, *64*, 807–838.

Castro, H. F., Classen, A. T., Austin, E. E., Norby, R. J. and Schadt, C. W. (2010). Soil microbial community responses to multiple experimental climate change drivers. *Applied and Environmental Microbiology*, *76*, 999–1007.

Chelius, M. K. and Triplett, E. W. (2001). The Diversity of Archaea and Bacteria in Association with the Roots of Zea mays L. *Microbial Ecology*, *41*, 252–263.

Chi, F., Shen, S., Cheng, H., Jing, Y., Yanni, Y. G. and Dazzo, F. B. (2005). Ascending Migration of Endophytic Rhizobia , from Roots to Leaves , inside Rice Plants and Assessment of Benefits to Rice Growth Physiology. *Applied and Environmental Microbiology*, *71*, 7271-7278.

Cortleven, A., Noben, J.-P. and Valcke, R. (2011). Analysis of the photosynthetic apparatus in transgenic tobacco plants with altered endogenous cytokinin content: a proteomic study. *Proteome Science*, *9*, 1-14.

Crosby, L. D., Criddle, C. S. (2003). Understanding Bias in Microbial Community Analysis Techniques due to rrn Operon Copy Number Heterogeneity. *Biotechniques*, *34*, 1-9.

Custers, R. (2009). First GM trial in Belgium since 2002. *Nature Biotechnology*, 27, 506.

Dyall, S. D., Brown, M. T. and Johnson, P. J. (2004). Ancient invasions: from endosymbionts to organelles. *Science*, *304*, 253–257.

Edgar, R. C., Haas, B. J., Clemente, J. C., Quince, C. and Knight, R. (2011). UCHIME improves sensitivity and speed of chimera detection. *Bioinformatics*, *27*, 2194–2200.

Fahlgren, C., Hagström, A., Nilsson, D. and Zweifel, U. L. (2010). Annual variations in the diversity, viability, and origin of airborne bacteria. *Applied and Environmental Microbiology*, *76*, 3015–3025.

Feinstein, L. M., Sul, W. J. and Blackwood, C. B. (2009). Assessment of bias associated with incomplete extraction of microbial DNA from soil. *Applied and Environmental Microbiology*, *75*, 5428–5433.

Gans, J., Wolinsky, M. and Dunbar, J. (2005). Computational improvements reveal great bacterial diversity and high metal toxicity in soil. *Science*, *309*, 1387–1390.

Gottel, N. R., Castro, H. F., Kerley, M., Yang, Z., Pelletier, D. A., Podar, M., Karpinets, T., Tuskan, G. A., Vilgalys, R., Mitchel, J., Schadt, C. W., Uberbacher, E. and Doktycz, M. J. (2011). Distinct Microbial Communities within the Endosphere and Rhizosphere of Populus deltoides Roots across Contrasting Soil Types. *Applied and Environmental Microbiology*, 77, 5934-5944.

Hajibabaei, M., Singer, G. A. C., Hebert, P. D. N. and Hickey, D. A. (2007). DNA barcoding: how it complements taxonomy, molecular phylogenetics and population genetics. *Trends in Genetics*, *23*, 167–72.

Hamady, M., Walker, J. J., Harris, J. K., Gold, N. J. and Knight, R. (2008). Error-correcting barcoded primers for pyrosequencing hundreds of samples in multiplex. *Nature Methods*, *5*, 235–237.

Hartmann, M., Howes, C. G., VanInsberghe, D., Yu, H., Bachar, D., Christen, R., Nilsson, R. H., Hallam, S. J. and Mohn, W. W. (2012). Significant and persistent impact of timber harvesting on soil microbial communities in Northern coniferous forests. *The ISME Journal*, *6*, 2199–2218.

Hawes, M. C., Gunawardena, U., Miyasaka, S. and Zhao, X. (2000). The role of root border cells in plant defense. *Trends in Plant Science*, *5*, 128–133.

Klindworth, A., Pruesse, E., Schweer, T., Peplies, J., Quast, C., Horn, M., & Glöckner, F. O. (2013). Evaluation of general 16S ribosomal RNA gene PCR primers for classical and next-generation sequencing-based diversity studies. *Nucleic Acids Research*, *41*, e1: 1-11.

Kosch, T. A. and Summers, K. (2013). Techniques for minimizing the effects of PCR inhibitors in the chytridiomycosis assay. *Molecular Ecology Resources*, *13*, 230–236.

Lee, Z. M.-P., Bussema, C. and Schmidt, T. M. (2009). rrnDB: documenting the number of rRNA and tRNA genes in bacteria and archaea. *Nucleic Acids Research*, *37*, 489–493.

Lefever, S., Pattyn, F., Hellemans, J. and Vandesompele, J. (2013). Single-nucleotide polymorphisms and other mismatches reduce performance of quantitative PCR assays. *Clinical Chemistry*, *59*, 1470–1480.

Leplé, J.-C., Dauwe, R., Morreel, K., Storme, V., Lapierre, C., Pollet, B., Naumann A., Kang, K., Kim, H., Ruel, K., Lefèbvre, A., Joseleau, J., Grima-Pettenati, J., De Rycke, R., Andersson-Gunnerås, S., Erban, A., Fehrle A., Petit-Conil, M., Kopka, J., Polle, A., Messens, E., Sundberg, B., Mansfield, S., Ralph, J., Pilate, G. and Boerjan, W. (2007). Downregulation of cinnamoyl-coenzyme A reductase in poplar: multiple-level phenotyping reveals effects on cell wall polymer metabolism and structure. *The Plant Cell*, *19*, 3669–3691.

Leplé, J.-C., Grima-Pettenati, J., Van Montagu, M. and Boerjan, W. (1998). A cDNA encoding cinnamoyl-CoA reductase from *Populus trichocarpa*. *Plant Physiology*, 117, 1126.

Lindow, S. E. and Brandl, M. T. (2003). Microbiology of the Phyllosphere. *Applied and Environmental Microbiology*, *69*, 1875–1883.

Lundberg, D. S., Lebeis, S. L., Paredes, S. H., Yourstone, S., Gehring, J., Malfatti, S., Tremblay, J., Engelbrektson, A., Kunin, V., del Rio, T. G., Edgar, R. C., Eickhorst, T., Ley, R. E., Hugenholtz, P., Tringe, S. G. and Dangl, J. L. (2012). Defining the core Arabidopsis thaliana root microbiome. *Nature*, *488*, 86–90.

Margulies, M., Egholm, M., Altman, W. E., Attiya, S., Bader, J. S., Bemben, L. A., et al. (2005). Genome sequencing in microfabricated high-density picolitre reactors. *Nature*, *437*, 376–380.

McCully, M. E. (2001). Niches for bacterial endophytes in crop plants: a plant biologist's view. *Australian Journal of Plant Physiology*, *28*, 983–990.

Metzker, M. L. (2010). Sequencing technologies - the next generation. *Nature Reviews. Genetics*, *11*, 31–46.

Nossa, C. W., Oberdorf W.E., Yang L., Aas, J. A., Paster, B. J., DeSantis, T. Z., Brodie, E. L., Malamud, D., Poles, M. A. and Pei, Z. (2010). Design of 16S rRNA gene primers for 454 pyrosequencing of the human foregut microbiome. *World Journal of Gastroenterology*, *16*, 4135-4144.

Oksanen, J., Blanchet, G. F., Kindt, R., Legendre, P., Minchin P. R., O'Hara, R. B., Simpson G. L., Solymos, P. et al. (2013). vegan: Community Ecology Package. R package version 2.15.1. http://CRAN.R-project.org/package=vegan

Op De Beeck, M., Lievens, B., Busschaert, P., Declerck, S., Vangronsveld, J. and Colpaert, J. V. (2014). Comparison and validation of some ITS primer pairs useful for fungal metabarcoding studies. *PloS One*, *9*, e97629.

Pruesse, E., Quast, C., Knittel, K., Fuchs, B. M., Ludwig, W., Peplies, J. and Glöckner, F. O. (2007). SILVA: a comprehensive online resource for quality checked and aligned ribosomal RNA sequence data compatible with ARB. *Nucleic Acids Research*, *35*, 7188–7196.

Raven, P. H. (1970). A Multiple Origin for Plastids and Mitochondria: Many independent symbiotic events may have been involved in the origin of these cellular organelles. *Science*, *169*, 641–646.

Romero, F. M., Marina, M. and Pieckenstain, F. L. (2014). The communities of tomato (Solanum lycopersicum L.) leaf endophytic bacteria, analyzed by 16S-ribosomal RNA gene pyrosequencing. *FEMS Microbiology Letters*, *351*, 187–194.

Sagaram, U. S., DeAngelis, K. M., Trivedi, P., Andersen, G. L., Lu, S.-E. and Wang, N. (2009). Bacterial diversity analysis of Huanglongbing pathogen-infected citrus, using PhyloChip arrays and 16S rRNA gene clone library sequencing. *Applied and Environmental Microbiology*, *75*, 1566–1574.

Sakai, M., Matsuka, A., Komura, T. and Kanazawa, S. (2004). Application of a new PCR primer for terminal restriction fragment length polymorphism analysis of the bacterial communities in plant roots. *Journal of Microbiological Methods*, *59*, 81–89.

Schloss, P. D., Westcott, S. L., Ryabin, T., Hall, J. R., Hartmann, M., Hollister, E. B., Lesniewski, R. A., Oakley, B. B., Parks, D. H., Robinson, C. J., Sahl, J. W., Stres, B., Thallinger, G. G., Van Horn, D. J. and Weber, C. F. (2009). Introducing mothur: open-source, platform-independent, community-supported software for describing and comparing microbial communities. *Applied and Environmental Microbiology*, *75*, 7537–7541.

Sessitsch, A., Reiter, B., Pfeifer, U. and Wilhelm, E. (2002). Cultivation-independent population analysis of bacterial endophytes in three potato varieties based on eubacterial and Actinomycetes-specific PCR of 16S rRNA genes. *FEMS Microbiology Ecology*, *39*, 23–32.

Shade, A., McManus, P. S. and Handelsman, J. (2013). Unexpected Diversity during Community Succession in the Apple Flower Microbiome. *mBio*, *4*, 1–12.

Shendure, J. and Ji, H. (2008). Next-generation DNA sequencing. *Nature Biotechnology*, *26*, 1135–1145.

Smit, E., Leeflang, P., Gommans, S., Mil, S. V. A. N. and Wernars, K. (2001). Diversity and Seasonal Fluctuations of the Dominant Members of the Bacterial Soil Community in a Wheat Field as Determined by Cultivation and Molecular Methods. *Applied and Environmental Microbiology*, *67*, 2284–2291.

Sogin, M. L., Morrison, H. G., Huber, J. A, Mark Welch, D., Huse, S. M., Neal, P. R., Arrieta, J. M. and Herndl, G. J. (2006). Microbial diversity in the deep sea and the underexplored “rare biosphere”. *Proceedings of the National Academy of Sciences of the United States of America*, *103*, 12115–12120.

Taberlet, P. and Coissac, E. (2012). Towards next-generation biodiversity assessment using DNA metabarcoding. *Molecular Ecology*, *33*, 2045–2050.

Van Acker, R., Leplé, J.-C., Aerts, D., Storme, V., Goeminne, G., Ivens, B., Légée, F., Lapierre, C., Piens, K., Van Montagu, M., C., E., Santoro, N., Foster, C., E., Ralph, J., Soetaert, W., Pilate, G. and Boerjan, W. (2014). Improved saccharification and ethanol yield from field-grown

transgenic poplar deficient in cinnamoyl-CoA reductase. *Proceedings of the National Academy of Sciences of the United States of America*, *111*, 845–50.

Vanholme, R., Demedts, B., Morreel, K., Ralph, J. and Boerjan, W. (2010). Lignin biosynthesis and structure. *Plant Physiology*, *153*, 895–905.

Vermeer, J. and McCully, M. E. (1982). The rhizosphere in Zea: new insight into its structure and development. *Planta*, *156*, 45–61.

Supplementary Information

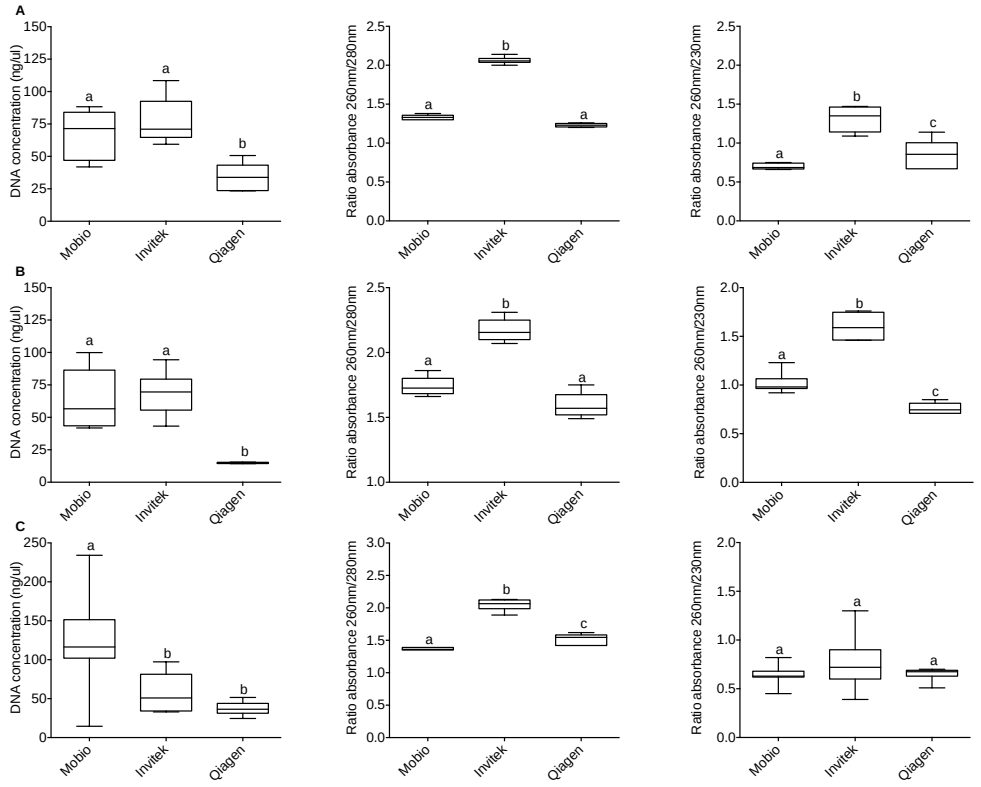

Supplementary Figure 4.1: Performance of three different commercially available DNA extraction kits (Mobio Powerplant DNA Isolation Kit, Invitek Invisorb Spin Plant Mini Kit and the Qiagen DNeasy Plant Mini Kit). DNA was extracted from roots (A), stems (B) and leafs (C) of poplar trees (Populus tremula x alba). Quantity and quality (absorbance ratios of 260nm/280 and 230nm/260nm) of extracted DNA was evaluated for each kit using a Nanodrop ND-1000 Spectrophotometer. Differences at the 95% confidence interval are displayed with lower cased letters (P < 0.05).

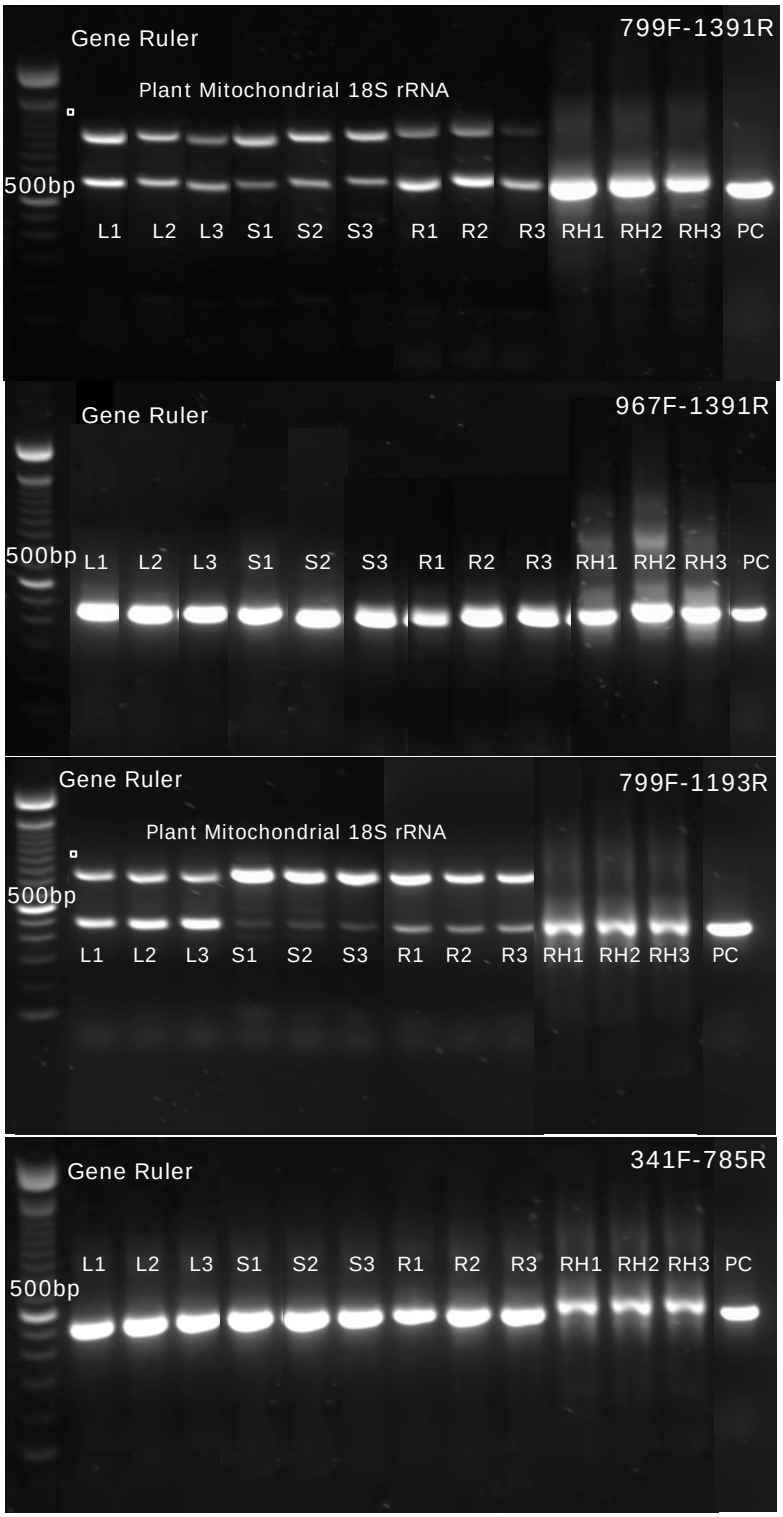
Gene Ruler
799F-1391R
Plant Mitochondrial 18S rRNA
500bp
L1 L2 L3 S1 S2 S3 R1 R2 R3 RH1 RH2 RH3 PC
Gene Ruler
967F-1391R
500bp
L1 L2 L3 S1 S2 S3 R1 R2 R3 RH1 RH2 RH3 PC
Gene Ruler
799F-1193R
Plant Mitochondrial 18S rRNA
500bp
L1 L2 L3 S1 S2 S3 R1 R2 R3 RH1 RH2 RH3 PC
Gene Ruler
341F-785R
L1 L2 L3 S1 S2 S3 R1 R2 R3 RH1 RH2 RH3 PC
500bp

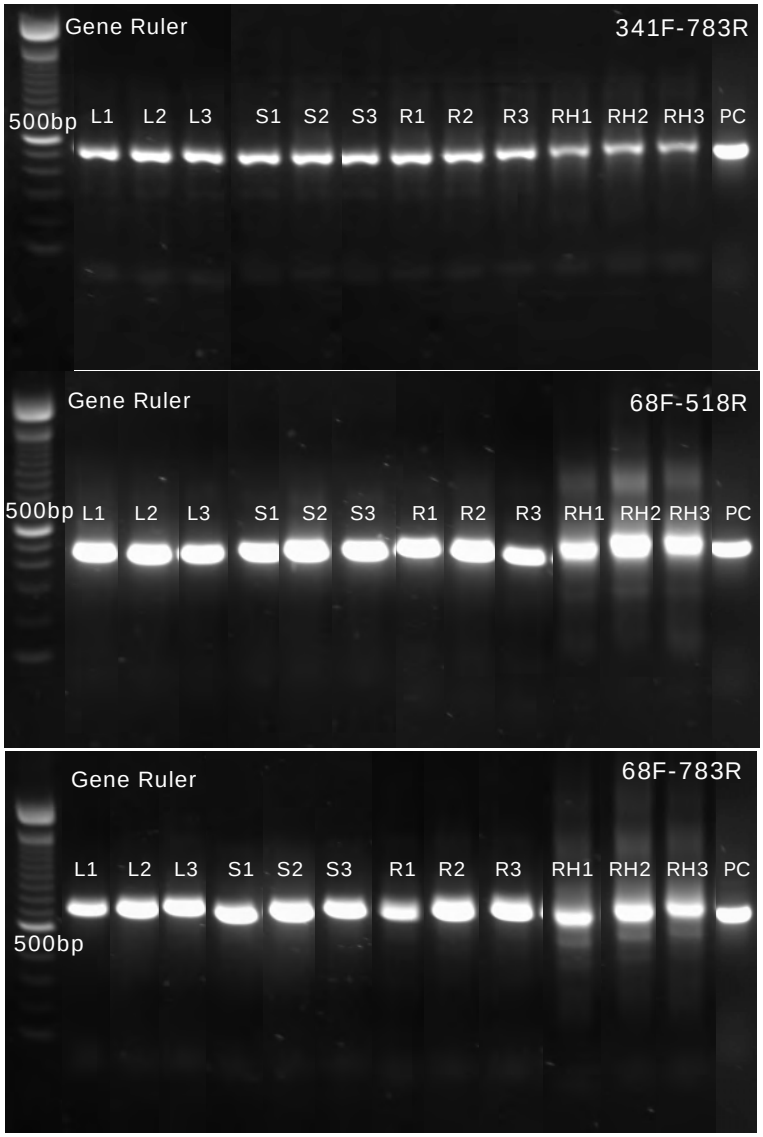

Supplementary Figure 4.2: Agarose gels (1.5%) of amplicons produced with all selected primer pairs from the different plant compartments (L = Leaf, S = Stem, R = Root, RH = Rhizosphere soil). Gels were run for 2.5 hours at 90 V and illuminated using UV-light. Positive control (PC) was the PCR product with as template pure bacterial DNA from a cultured bacterial strain (Pseudomonas putida). To check amplicon sizes, a 1kB gene ruler was used (band of 500 bp indicated).

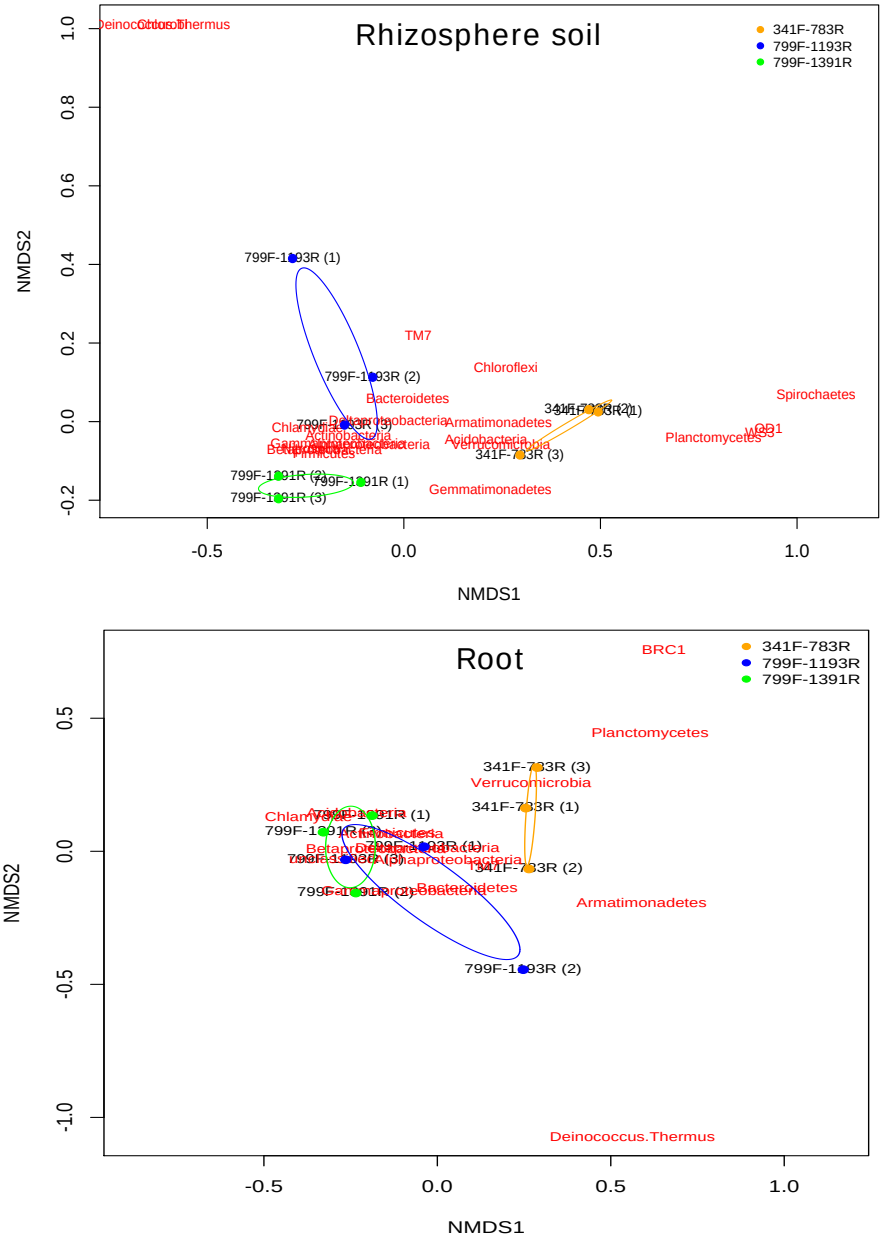

Supplementary Figure 4.3A: Comparison of phylum-level OTU abundances of replicate samples identified by the selected primer pairs (799F-1391R, 799F-1193R and 341F-783R) within every plant compartment using non-metric multi-dimensional scaling (NMDS) with Bray-Curtis dissimilarities (10,000 permutations). Bacterial phyla are displayed in red.

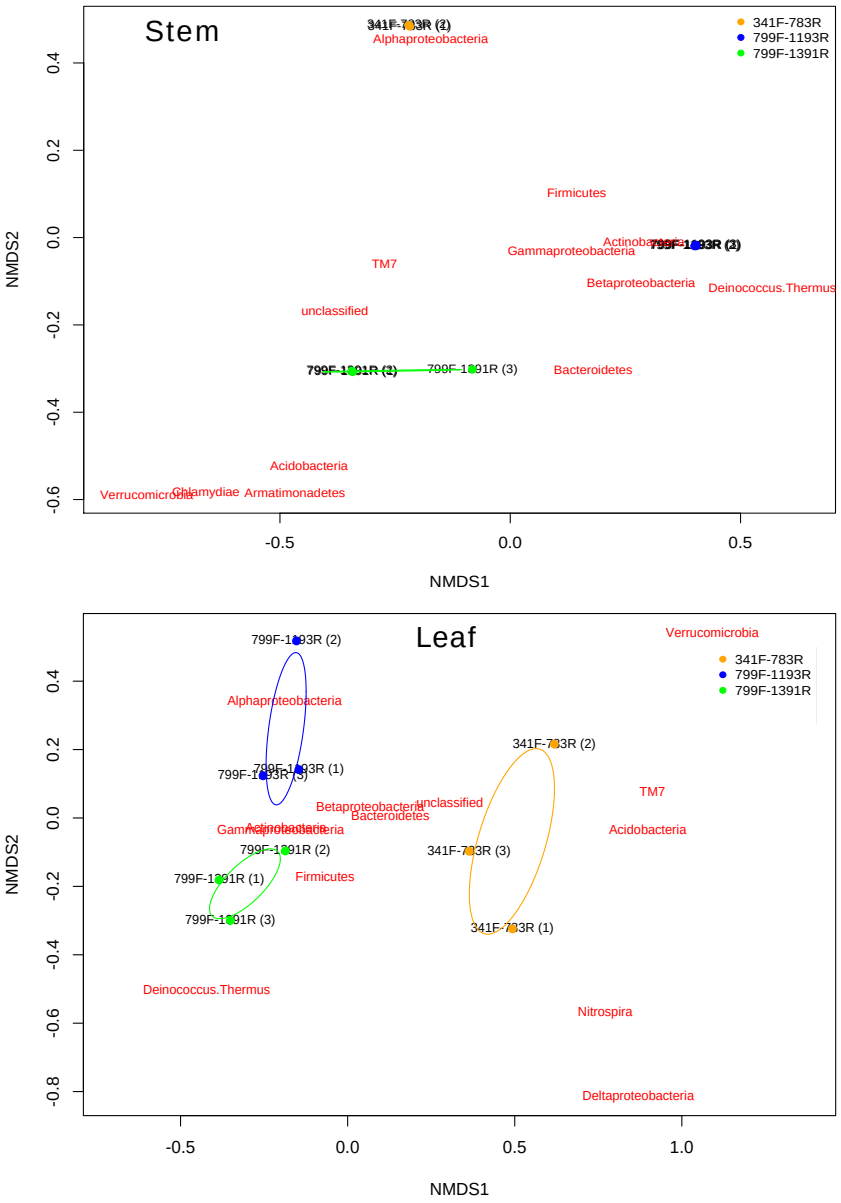

Supplementary Figure 4.3A (continued): Comparison of phylum OTU abundances of replicate samples identified by the selected primer pairs (799F-1391R, 799F-1193R and 341F-783R) within every plant compartment using non-metric multi-dimensional scaling (NMDS) with Bray-Curtis dissimilarities (10,000 permutations). Bacterial phyla are displayed in red.

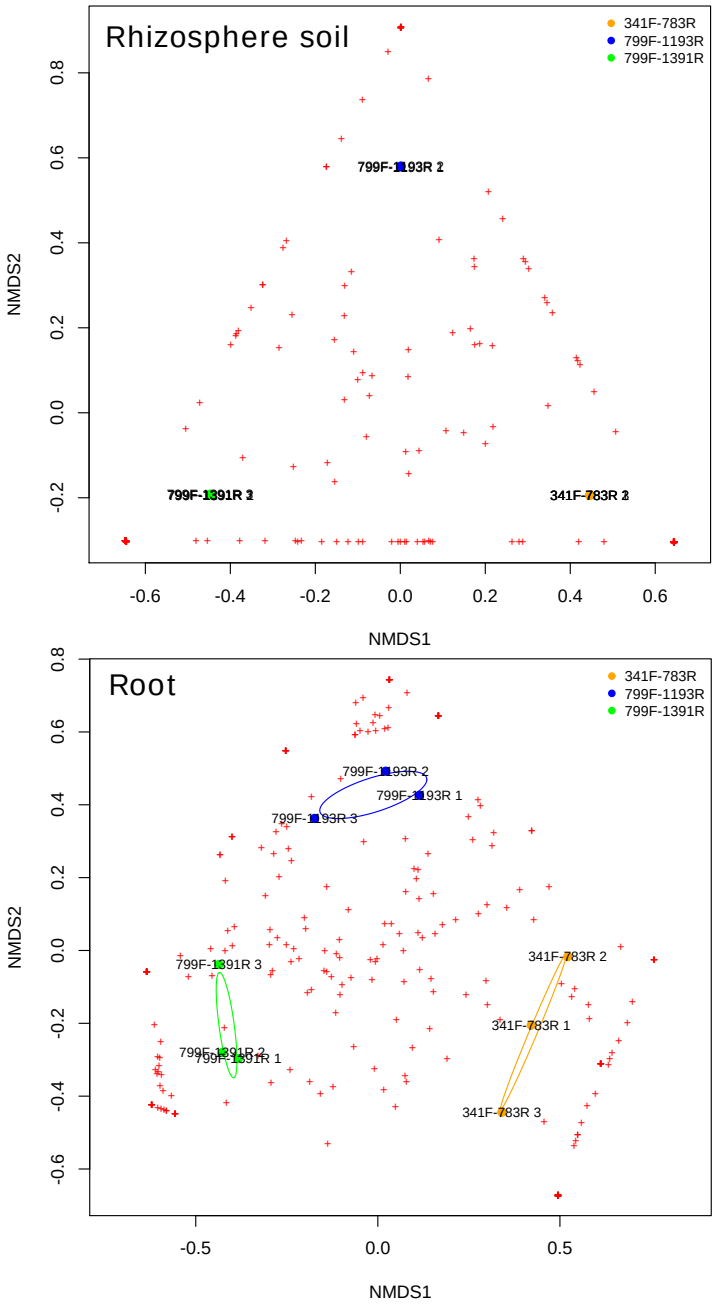

Supplementary Figure 4.3B: Comparison of genus-level OTU abundances of replicate samples identified by the selected primer pairs (799F-1391R, 799F-1193R and 341F-783R) within every plant compartment using non-metric multi-dimensional scaling (NMDS) with Bray-Curtis dissimilarities (10,000 permutations). Genus-level OTUs are displayed in red.

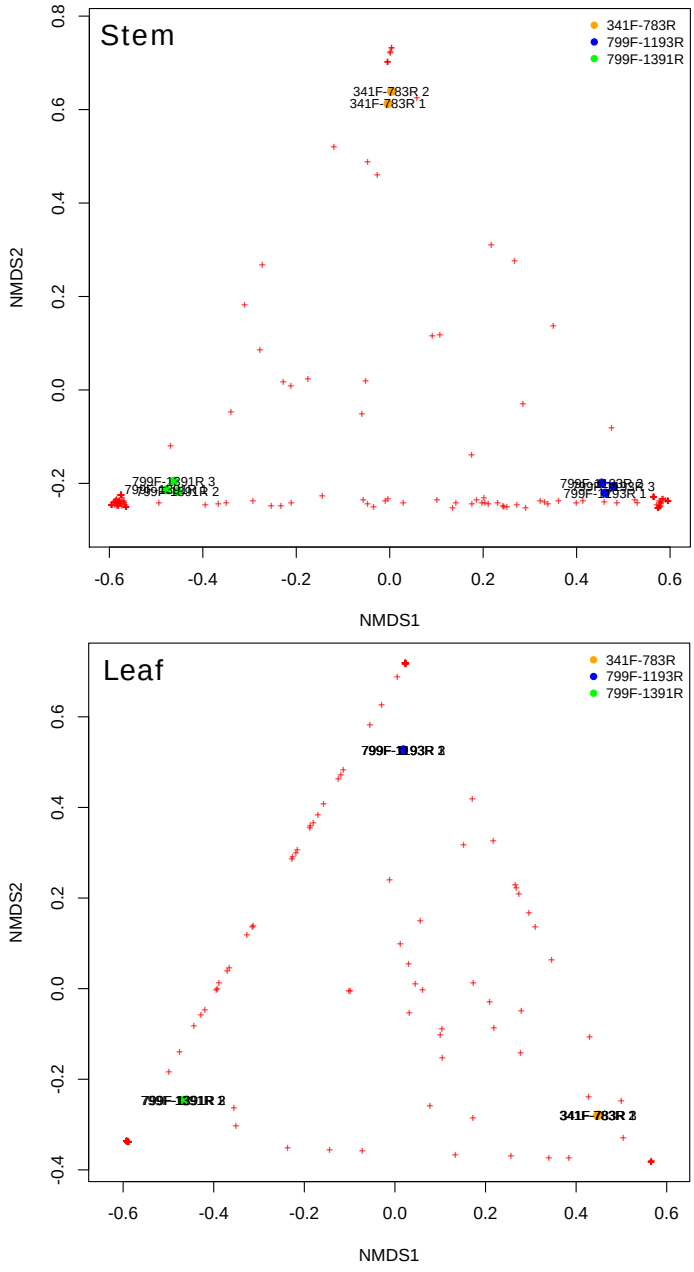

Supplementary Figure 4.3B (continued): Comparison of genus-level OTU abundances of replicate samples identified by the selected primer pairs (799F-1391R, 799F-1193R and 341F-783R) within every plant compartment using non-metric multi-dimensional scaling (NMDS) with Bray-Curtis dissimilarities (10,000 permutations). Genus-level OTUs are displayed in red.

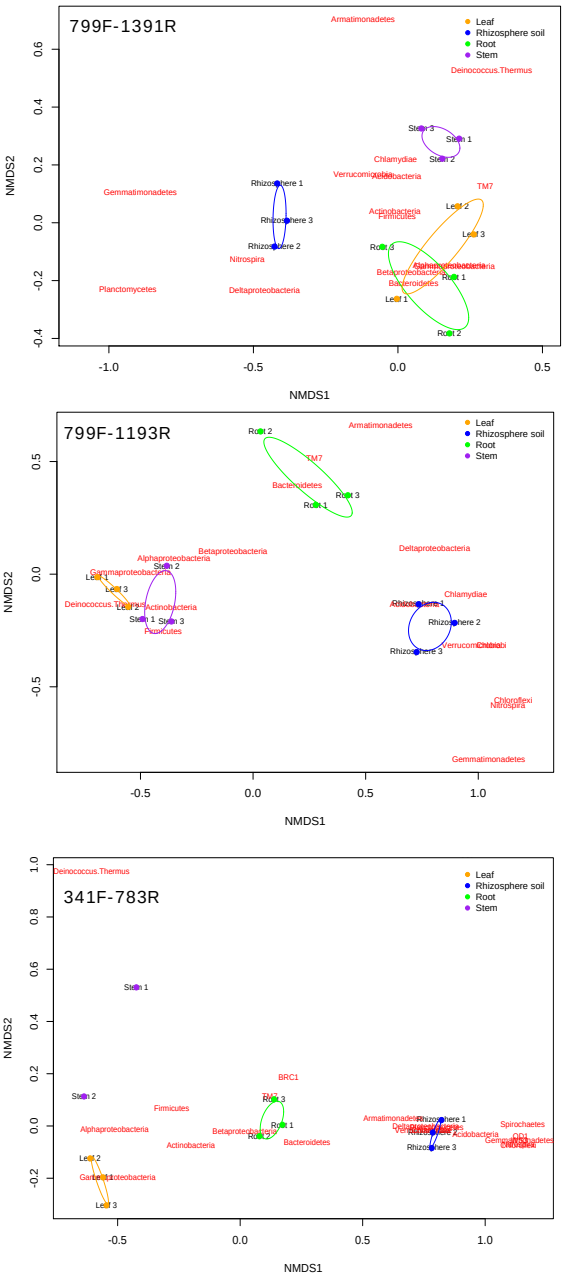

Supplementary Figure 4.4A Comparison of phylum-level OTU abundances of replicate samples identified in each plant compartment (rhizosphere soil, root, stem and leaf) by the selected primer pairs (799F-1391R, 799F-1193R and 341F-783R) using non-metric multi-dimensional scaling (NMDS) with Bray-Curtis dissimilarities (10,000 permutations). Bacterial phyla are displayed in red.

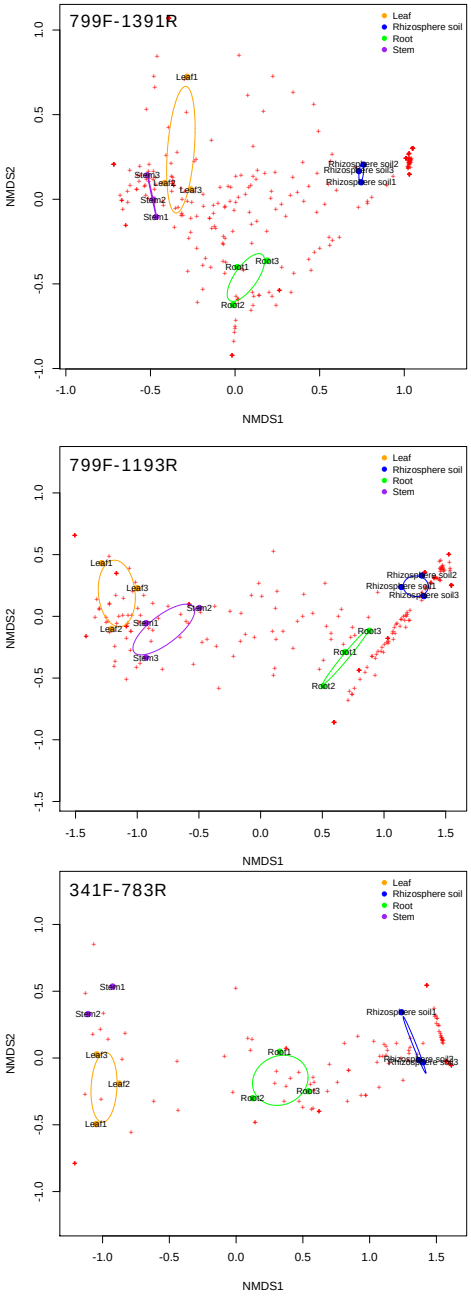

Supplementary Figure 4.4B Comparison of genus-level OTU abundances of replicate samples identified in each plant compartment (rhizosphere soil, root, stem and leaf) by the selected primer pairs (799F-1391R, 799F-1193R and 341F-783R) using non-metric multi-dimensional scaling (NMDS) with Bray-Curtis dissimilarities (10,000 permutations). Genus-level OTUs are displayed in red.

Supplementary Table 4.1A Rhizosphere core bacterial community (10 most abundant OTUs, relative abundance %) identified by each primer pair and within each plant compartment.

Genus (or higher)	Phylum	799F-1391R	799F-1193R	341F-783R
Rhizobiales	Alphaproteobacteria	1.77	11.32	8.36
Actinomycetales	Actinobacteria	9.96	8.64	7.73
Burkholderiales	Betaproteobacteria	5.97	2.97	1.68
Variovorax	Betaproteobacteria	4.33	0.00	0.11
Bacillales	Fimicutes	3.85	0.51	0.00
Chitinophagaceae	Bacteriodetes	2.65	2.23	5.65
Bradyrhizobium	Alphaproteobacteria	2.90	1.03	0.29
Arthrobacter	Actinobacteria	2.56	0.91	0.00
Pseudomonas	Gammaproteobacteria	1.93	1.11	0.33
Xanthomonadaceae	Gammaproteobacteria	1.79	1.78	0.77
Flavobacterium	Bacteriodetes	0.23	5.45	0.98
TM7_genus_incertae_sedis	TM7	0.48	5.55	2.52
Comamonadaceae	Betaproteobacteria	1.13	4.48	1.91
Myxococcales	Deltaproteobacteria	1.03	2.12	2.27
Sphingomonadaceae	Alphaproteobacteria	0.88	2.50	2.06
Ilumatobacter	Actinobacteria	0.00	2.16	0.00
Gp6	Acidobacteria	0.00	0.00	15.73
Spartobacteria	Verrucomicrobia	0.06	0.00	6.93
Planctomycetaceae	Planctomycetes	0.00	0.00	4.74
Bradyrhizobiaceae	Alphaproteobacteria	0.80	1.52	3.65
Gp4	Acidobacteria	0.03	0.00	3.64
Total amount of reads covered		42.34	54.25	69.35

Supplementary Table 4.1B Root core bacterial community (10 most abundant OTUs, relative abundance %) identified by each primer pair and within each plant compartment

Genus (or higher)	Phylum	799F-1391R	799F-1193R	341F-783R
Pseudomonas	Gammaproteobacteria	11.95	9.46	3.67
Rhizobiales	Alphaproteobacteria	11.28	7.39	38.97
Variovorax	Betaproteobacteria	8.28	0.00	1.48
Rhizobium	Alphaproteobacteria	6.70	15.88	0.00
Afipia	Alphaproteobacteria	6.13	0.00	0.00
Phenylobacterium	Alphaproteobacteria	5.88	5.25	0.22
Burkholderiaceae	Betaproteobacteria	5.52	3.95	1.48
Novosphingobium	Alphaproteobacteria	5.44	4.77	0.00
Burkholderia	Betaproteobacteria	4.72	2.14	0.62
Burkholderiales	Betaproteobacteria	3.34	1.32	2.84
Flavobacterium	Bacteriodetes	0.77	8.38	3.78
Bradyrhizobiaceae	Alphaproteobacteria	1.12	5.57	2.62
Comamonadaceae	Betaproteobacteria	1.20	4.35	1.15
TM7_genus_incertae_sedis	TM7	1.26	4.27	6.33
Erythrobacteraceae	Alphaproteobacteria	0.00	0.00	5.19
Caulobacteraceae	Alphaproteobacteria	0.17	0.68	4.85
Sphingomonadaceae	Alphaproteobacteria	1.04	1.45	3.37
Oxalobacteraceae	Betaproteobacteria	2.00	3.01	2.59
Total amount of reads covered		76.81	77.86	79.17

Supplementary Table 4.1C Stem core bacterial community (10 most abundant OTUs, relative abundance %) identified by each primer pair and within each plant compartment

Genus (or higher)	Phylum	799F-1391R	799F-1193R	341F-783R
Pseudomonas	Gammaproteobacteria	12.94	12.73	4.86
TM7	TM7	9.83	1.51	4.17
Deinococcus	Deinococcus-Thermus	7.18	5.52	0.69
Xanthomonadaceae	Gammaproteobacteria	4.70	0.14	0.00
Chlamydiales	Chlamydiae	4.49	0.00	0.00
Bradyrhizobiaceae	Alphaproteobacteria	4.46	0.11	0.00
Rhizobiales	Alphaproteobacteria	3.83	1.49	9.28
Propionibacterium	Actinobacteria	3.73	5.93	0.00
Methylobacterium	Alphaproteobacteria	3.65	5.44	1.39
Acidobacteria_Gp1	Acidobacteria	2.59	0.00	0.00
Deinococcaceae	Deinococcus-Thermus	0.00	18.22	0.00
Sphingomonas	Alphaproteobacteria	2.44	9.87	0.00
Truepera	Deinococcus-Thermus	0.00	4.55	0.00
Curtobacterium	Actinobacteria	1.17	3.89	0.00
Herbaspirillum	Betaproteobacteria	0.15	3.24	0.00
Enterobacteriaceae	Gammaproteobacteria	1.29	2.72	0.00
Sphingomonadaceae	Alphaproteobacteria	1.21	0.20	34.28
Enhydrobacter	Gammaproteobacteria	1.40	0.05	5.56
Staphylococcaceae	Firmicutes	0.08	0.28	5.56
Staphylococcus	Firmicutes	0.95	0.56	5.56
Alishewanella	Gammaproteobacteria	0.00	0.00	4.17
Actinomycetales	Actinobacteria	0.00	1.02	3.47
Microbacteriaceae	Actinobacteria	0.70	1.01	3.47
Total amount of reads covered		66.78	78.46	82.44

Supplementary Table 4.1D Leaf core bacterial community (10 most abundant OTUs, relative abundance %) identified by each primer pair and within each plant compartment

Genus (or higher)	Phylum	799F-1391R	799F-1193R	341F-783R
Pseudomonas	Gammaproteobacteria	33.95	40.13	35.97
Rhizobium	Alphaproteobacteria	8.45	0.51	0.00
Methylobacterium	Alphaproteobacteria	6.68	6.21	3.99
Rhizobiales	Alphaproteobacteria	5.47	13.65	28.77
TM7	TM7	4.79	0.00	0.00
Sphingomonas	Alphaproteobacteria	3.34	7.20	0.00
Pasteurella	Gammaproteobacteria	2.18	0.00	0.00
Burkholderiales	Betaproteobacteria	2.94	0.01	0.08
Xanthomonadaceae	Gammaproteobacteria	1.73	0.00	0.07
Actinomycetales	Actinobacteria	1.59	0.39	0.14
Rhizobiaceae	Alphaproteobacteria	0.00	6.76	0.00
Microbacteriaceae	Actinobacteria	0.37	5.43	1.26
Deinococcaceae	Deinococcus-Thermus	0.00	4.32	0.00
Aurantimonas	Alphaproteobacteria	0.47	4.26	0.00
Propionibacterium	Actinobacteria	1.37	1.67	0.00
Deinococcus	Deinococcus-Thermus	0.43	1.25	0.00
Sphingomonadaceae	Alphaproteobacteria	0.19	0.05	19.85
Clavibacter	Actinobacteria	1.22	1.02	1.89
Enhydrobacter	Gammaproteobacteria	0.42	0.01	1.13
Pseudomonadaceae	Gammaproteobacteria	0.45	0.00	0.89
Dermacoccus	Actinobacteria	0.31	0.04	0.72
Oxalobacteraceae	Betaproteobacteria	0.29	0.55	0.69
Total amount of reads covered		76.66	93.48	95.46

Chapter 5

Gene silencing of Cinnamoyl-CoA reductase (*CCR*) in field-grown poplar trees: plant compartment and host genotype effects on the total bacterial microbiome

Abstract

Plant microbiome niche differentiation, *i.e.* the occurrence of specific bacterial communities within plant microenvironments (rhizosphere, root, stem and leaf), and host genotype dependent-effects on the bacterial assemblages have been sporadically evaluated. Niche differentiation at the rhizosphere-root interface has been reported in a couple of studies, with limited focus on microbiome differentiation in the aerial plant organs. Furthermore, few studies have explored the magnitude of host genotype variation on the bacterial microbiota profiles. Therefore, we evaluated microbiome niche differentiation of bacterial communities associated with field-grown poplar trees (*Populus tremula x alba)* as well as host-genotype effects exerted by poplar trees modified in their lignin biosynthesis. Specifically, poplar trees were down-regulated for cinnamoyl-CoA reductase (*CCR*), the first enzyme in the monolignol-specific branch of lignin biosynthesis, to reduce biomass recalcitrance. *CCR* gene silencing, besides reducing lignin levels, leads to significant changes in the xylem metabolome, ultimately resulting in different carbon sources for the associated bacterial microbiome. We used 16S rRNA metabarcoding (454 pyrosequencing) to unravel the bacterial communities associated with the rhizosphere, roots, stems and leaves of wild type and *CCR* deficient poplar trees.

Our data provide convincing evidence for additional fine-tuning and niche differentiation of microbiota in the aerial plant organs and furthermore we identified significant host genotype effects on the bacterial community structure in the roots and stems of *CCR* deficient trees.

Keywords

Populus tremula x alba, bacterial microbiome, microbiome niche differentiation, host genotype effects, 16S rRNA metabarcoding, 454 pyrosequencing

5.1. Introduction

Inter-organismal associations between eukaryotic and prokaryotic organisms are one of the most studied research areas in recent years. The enormous interest in this topic is reflected by numerous studies ranging from human microbiome (Human Microbiome Project Consortium, 2012) and host-genotype associations therein (Koch, 2014; Spor et al. 2011), gut microfauna of insects (Dillon & Dillon, 2004; Hansen & Moran, 2014; Sudakaran et al. 2012) to microbiota associated with plants (Bulgarelli et al. 2013; Compant et al. 2010; Haichar et al., 2008; Hallmann & Berg, 2007; Ryan et al. 2008) (Bonito et al., 2014). In fact, most eukaryotes maintain close mutualistic relationships with microorganisms that are, in most cases, linked to their nutrient acquisition and thereby crucial for their performance and survival (Gil & Latorre, 2010; Hardoim et al. 2008). Plant-microbe interactions are of specific interest, not only to get a better understanding of their role during plant growth and development but also for the exploitation of their relationships in phytoremediation applications, sustainable crop production and the production of secondary metabolites (Brader et al. 2014; Hardoim et al., 2008; Weyens et al. 2009).

Within plant-microbiota research, intra-plant niche differentiation (or compartmentalization) within the available ecological niches in plants (rhizosphere/rhizoplane, root, stem and leaf tissues) and possible host genotype-dependent effects (ecotypes, cultivars, genetically modified genotypes) on the bacterial assemblages thriving in plants have been sporadically evaluated. Recently Bulgarelli et al. (2012) and Lundberg et al. (2012) evaluated niche differentiation at the rhizosphere soil-root interface and host genotype-dependent fine-tuning of different *Arabidopsis* ecotypes. Furthermore Weinert et al. (2011) assessed the rhizosphere soil and root microbiota of three field-grown potato cultivars. Gottel et al. (2011) analysed the microbial communities from the root endophytic and rhizospheric habitats of mature *Populus deltoides*. For all the aforementioned studies, niche differentiation between the root and rhizosphere microbiome and/or weak host genotype effects have been observed. Other than these reports, which exclusively focus on the niche differentiation and possible host-genotype effect at the rhizosphere soil-root interface, no studies, to the best of our knowledge,

have explored the magnitude of the intra-plant niche and host-genotype variation on the bacterial microbiota profiles.

In the current study, we evaluate microbiome niche differentiation of bacterial communities associated with field-grown poplar trees (*Populus tremula x alba)* as well as host-genotype effects exerted by poplar trees modified in their lignin biosynthesis. Recalcitrance of lignin polymers represents the major limiting factor in the processing of lignocellulosic biomass (*e.g.* poplar) to end-use products such as second-generation biofuels (Chen & Dixon, 2007; Studer et al., 2011). Accordingly, substantial research effort has been invested in exploring genetic engineering to tailor lignin content and/or composition to improve commercial viability of feedstocks (Leplé et al., 2007; Van Acker et al., 2014; Vanholme et al., 2012; Vanholme et al., 2008; Wilkerson et al., 2014). Specifically, gene silencing of cinnamoyl-CoA reductase (*CCR*), the first enzyme in the monolignol-specific branch of lignin biosynthesis (Boerjan et al., 2003; Vanholme et al., 2010), significantly reduces lignin levels in poplar trees (Leplé et al., 2007; Van Acker et al., 2014). However, simultaneously *CCR* gene silencing leads to significant changes in the poplar metabolome, most notably the accumulation of various extractable phenolics in xylem vessels and alterations in composition of the plant cell walls (Leplé et al., 2007).

Numerous studies describe the intimate mutualistic relationships between plants and their associated bacterial microbiome involving a plethora of reciprocal advantages. Amongst others, the host plant delivers habitation and a constant supply of energy and carbon sources to microbiota (Bulgarelli et al., 2013; Compant et al., 2010; Hardoim et al., 2008; Weyens et al., 2009). Moreover, plant cell wall features play a crucial role for endophytic competence (Compant et al., 2010) and even serve as sufficient assembly (colonization) cues for root microbiota of *Arabidopsis thaliana* (Bulgarelli et al., 2013).

Therefore, we hypothesize that modification of lignin biosynthesis (*CCR* down-regulation) in poplar trees, resulting changes in the xylem metabolome and compositional alterations in the cell-wall features may have profound effects on colonization and structural composition of plant-associated bacterial assemblages. Indeed, we previously identified significant plant compartment and host-genotype effects in the metabolic capacities of the bacterial microbiomes (cultivable fraction) of wild type poplar trees and *CCR*-down-regulated poplar

trees (Beckers et al. 2015, chapter 3). *CCR* deficient poplar trees represent prime candidates to investigate host-genotype effects since, except for the T-DNA construct, they are isogenic with the wild type poplar trees which enables direct causality between observed effects and the cause of the effect.

To investigate this hypothesis, we studied niche differentiation and host genotype effects between field-grown wild type and *CCR* deficient poplar trees (*Populus tremula x alba*) using 454 pyrosequencing with an optimized approach to reduce co-amplification of plant organellar 16S rRNA (chloroplast and mitochondrial sequences) (Beckers et al. 2015, Chapter 4).

5.2. Material and methods

5.2.1. Field trial

A poplar (*Populus tremula* x *Populus alba)* field trial located in Ghent, Belgium (property of VIB) was selected to acquire samples for this study (Custers, 2009). This field trial was established in May 2009 and contains a total of 240 *CCR* deficient (*CCR*$^{-}$) trees and 120 wild type (WT) poplar trees (all in *Populus tremula* x *Populus alba cv.* "717-1B4"). Poplar clones were transformed via an *Agrobacterium tumefaciens* procedure as described by Leplé et al. (1992). Each poplar line (WT, *CCR*-) was simultaneously micropropagated *in vitro* and 120 ramets were grown in the greenhouse for 9 months. Thereafter, the stems were cut 10 cm above soil level and plants were acclimatized for 10 days in the greenhouse. Finally, coppiced trees were transferred to the field in May 2009 (Field trial authorization: B/BE/07/V2). The trees were planted in a randomized block design (6 randomized blocks per line, 5 x 4 trees per block, for a total of 20 trees per block) in a density of 15.000 trees per hectare and with an inter-plant distance of 0.75 m. A border of WT poplar trees surrounded the field to reduce environmental effects on tree growth (Custers, 2009; Van Acker et al., 2014). The full field layout can be found in Van Acker et al. (2014).

5.2.2. Sampling

Poplar trees (WT, *CCR*-) were sampled in October 2011 after approximately 2.5 years of growth. Twelve biologically independent replicates (individual trees) were sampled for the wild type (n =12) and for the *CCR*-down-regulated poplar trees (n=12). Samples were spread, as much as possible, between different randomized blocks taking into account general appearance and preliminary data of *CCR* down-regulation (Prof. Dr Boerjan; Personal communication). Since our main interest was to investigate the influence(s) of genetic modification (*CCR* down-regulation) of poplar on plant-associated bacterial assemblages, we sampled poplar trees with the highest *CCR* down-regulation. Gene silencing of *CCR* is associated with a visible phenotype (red-brown xylem coloration), which allowed us to sample according to phenotype, and thereby somewhat bypass unequal levels of gene silencing (Léple et al., 2007). Samples included rhizosphere soil, roots, stems and leaves. Tree identification numbers can be found in Supplementary data (Supplementary Table 5.1).

Root samples were collected at a depth of 5-10 cm below ground level. Per poplar individual, a minimum of 10 g of roots was sampled. Rhizosphere soil was strictly defined as soil particles adhering to the roots. For the stem and leaf samples, one complete offshoot of every poplar individual was collected. To standardize and maximize reproducibility of stem samples, several small stem 'cores' with bark (5-7 cores; 1cm each) were collected from each offshoot from the base to the top of the offshoot to represent the stem compartment. Further, we specifically selected stem cores with high red coloration indicating high *CCR* down-regulation (Leplé et al., 2007). For the leaf samples, all leaves from the sampled offshoot were collected to represent the leaf compartment.

5.2.3. Processing of samples

Samples were processed as described by Beckers et al. (2015) (Chapter 4). Briefly, root samples were depleted from soil particles by shaking on a platform (20 min, 120 rpm). Soil particles directly dislodged from roots represented the 'rhizosphere soil' compartment. Subsequently 'root', 'stem' and 'leaf' compartments were cleared from epiphytic bacteria by sequential washing (surface-sterilization) with (a) sterile Millipore water (30 sec), (b) followed by immersion in 70% (v/v) ethanol (2 min), (c) sodium hypochlorite solution (2.5 % active Cl^-, 5 min) supplemented with 0.1% Tween 80, (d) 70% (v/v) ethanol (30 sec) and finalized by washing the samples five times with sterile Millipore water. Plant samples were portioned into small fragments using a sterile scalpel and were subsequently macerated in sterile phosphate saline buffer (PBS; 130 mM NaCl, 7 mM Na_2HPO_4, 3 mM NaH_2PO_4, pH 7.4) using a Polytron PR1200 mixer (Kinematica A6) in cycles of 2 min (4x) with cooling of the mixer on ice between cycles to reduce heating of the samples. Sterilization and homogenization of plant samples were performed under aseptic conditions in a laminar airflow. Finally, quadruplicate aliquots of each sample (1.5 mL) of the homogenized plant material (root, stem or leaf) were stored for all poplar individuals at -80°C until DNA was extracted.

5.2.4. DNA extraction

To minimize DNA extraction bias, DNA was extracted in quadruplicate from the rhizosphere soil, roots, stems and leaves samples (Feinstein et al. 2009; Op De Beeck et al., 2014). Approximately 250 mg of rhizosphere soil was used for each individual DNA extraction, performed using the Power Soil DNA Isolation Kit

following the protocol provided by the manufacturer (MoBio, Carlsbad, CA, USA). For the plant tissues (roots, stems and leaves), aliquots of homogenized plant material (1.5 mL) were first centrifuged (13,400 rpm, 30 min.) to collect all cells. Supernatants were discarded and DNA extractions were performed on pelleted plant material. DNA was extracted from plant samples using the Invisorb Spin Plant Mini Kit according to the manufacturer's protocol (Stratec Biomedical AG, Birkenfeld, Germany), which was shown to outperform other commercially available DNA extraction kits in our previous study (Beckers et al. 2015, Chapter 4).

5.2.5. PCR amplification and 454 pyrosequencing

Quadruplicate DNA samples from all compartments were individually amplified using a Techne TC-5000 thermocycler (Bibby Scientific Limited, Staffordshire, UK). We previously evaluated the performance of several 16S rRNA primer pairs in metabarcoding studies for rhizospheric and endophytic bacteria. Primer pairs were assessed based on their potential to avoid co-amplification of non-target rRNA (chloroplasts and mitochondria) and their retrieval of bacterial OTUs (Beckers et al., 2015). Based on these results, we selected primer 799F (5'-AACMGGATTAGATACCCKG-3'), with three chloroplast mismatches with the poplar chloroplast 16S rRNA, and primer 1391R (5'-GACGGGCGGTGWGTRCA-3'). A first round of PCR amplification was conducted using these primers without the Roche 454 pyrosequencing adaptors of sample-specific barcodes. Each 25 µl PCR reaction contained approximately 10 ng of DNA and was carried out using the FastStart High Fidelity PCR System (Roche Applied Science, Mannheim, Germany). Each reaction contained 2.75 µl FastStart 10 x reaction buffer, 1.8 mM $MgCl_2$, 0.2 mM dNTP mix, 0.4 µM of each primer and 2 U FastStart HiFi polymerase. Cycling conditions included: initial denaturation at 94°C for 3 min, followed by 35 cycles of denaturation at 94°C for 1 min, annealing at 53°C for 1 min and extension at 72°C during 1 min; a final extension phase was performed at 72°C during 10 min. PCR amplicon pools were cleared from residual primers and primer dimers by separating the PCR products on a 1.5% agarose gel, excising the bacterial product (amplicon length= 592 bp) and extracting the DNA from the gel slices using the QIAQuick gel extraction kit (Qiagen Benelux N.V., Venlo, The Netherlands). Mitochondrial by-products (1000 bp) were eliminated via this gel-purification. Following the

first round of PCR amplification and gel-purification of the PCR products, a second round of PCR amplification was performed with primer 967F (5'CAACGCGAAGAACCTTACC-3')-1391R(5'-GACGGGCGGTGWGTRCA-3') to reduce amplicon length (424bp) to a more suitable length for 454 pyrosequencing. The forward primer (967F) was fused to the Roche 454 pyrosequencing adaptor A including a sample-specific 10 bp barcode (multiplex identifiers, MIDs). The reverse primer (1391R) were fused to adaptor B (Roche Applied Science, Mannheim, Germany). PCR cycling conditions were identical as described above, but the number of PCR cycles, which was lowered to 25.

Subsequently, quadruplicate PCR amplicon pools from the corresponding samples were grouped together resulting in twelve samples for WT per plant compartment (12 biological replicates x 4 compartments = total of 48 samples) and twelve samples for *CCR*- per plant compartment (12 biological replicates x 4 compartments = 48 samples). PCR amplicon pools were purified to remove PCR primers and primer dimers using the QIAquick PCR purification kit (Qiagen Benelux B.V., Venlo, the Netherlands). Following purification, the quality of the amplicon pools was evaluated using an Agilent 2100 Bioanalyzer system (Agilent Technologies, Diegem, Belgium) according to the manufacturer's protocol. Finally, purified amplicon libraries were quantified with the Quant-iT PicoGreen dsDNA Assay Kit (Invitrogen, Carlsbad, CA, USA) and a Fluostar Omega plate reader (BMG Labtech, Ortenberg, Germany) and pooled in equimolar concentrations. Rhizosphere samples were pooled separately in two libraries, each consisting of 12 samples. Plant samples were grouped in three additional libraries consisting of 24 samples. Each library (total of 5) was sequenced on one eighth of a Picotiter Plate on a Roche Genome Sequencer FLX+ using Titanium chemistry (Roche Applied Science, Mannheim, Germany) by Macrogen (Seoul, Korea).

5.2.6. Sequence processing

Sequencing generated five individual standard flowgram format (SFF) files, which were analysed separately using the software package mothur (version 1.33.2) following the Standard Operating Protocol outlined in http://www.mothur.org/wiki/Schloss_SOP (Schloss et al., 2009). Briefly, the sequencing error were reduced by denoising (shhh.flows, Mothur implementation of Amplicon Noise algorithm) and quality trimming, which

removed reads shorter than 200 bases, reads with homopolymers longer than 8 bases and reads containing ambiguous bases. Unique sequences were identified, whilst archiving the abundance data of the unique sequences, and aligned using align.seqs with the SILVA reference alignment (Release 119) (Pruesse et al., 2007). Within the unique reads, chimeric sequences were identified using the Uchime tool (Edgar, 2011) followed by their removal from the dataset. Sequences matching "Chloroplast" and "Mitochondria" were identified using classify.seqs. Abundance data of these sequences were archived, and they were removed from the data sets. Finally, genus-level OTUs were defined based on a 97% sequence similarity cut-off level and OTUs were assigned a taxonomic group using classify.seqs with a 80% bootstrap cut-off value. To minimize the impact of sequencing artefacts, we removed singletons from the data sets (Tedersoo et al., 2010). Subsequently, rarefaction curves were assembled and Good's coverage scores were calculated in mothur based on 10,000 iterations. To calculate ecological indices (richness, diversity, evenness) while controlling for the sampling effort, each sample was rarefied to 2,000 sequences. OTU richness, corresponding to the number of observed OTUs per sample, Inverse Simpson diversity indices (Simpson, 1949) and Pielou's evenness indices (Pielou, 1966) were calculated in mothur based on 10,000 iterations.

5.2.7. Statistical analysis

Statistical analyses were performed in R 2.15.1 (The R Foundation for Statistical Computing, Vienna, Austria). Normal distributions of the data were checked with the Shapiro-Wilkes test and homoscedasticity of variances was analysed using either Bartlett's or the Fligner-Killeens test. Significant differences in the variance of parameter were evaluated, depending on the distribution of the estimated parameters, either with ANOVA or the Kruskal Wallis Rank Sum Test. Post-hoc comparisons were conducted by either the Tukey's Honest Significant Differences tests or Pairwise Wilcoxon Rank Sum Tests. ANOVA was used to test the effect of the plant compartment (rhizosphere soil, root, stem, leaf) and the host genotype (Wild type versus *CCR* deficient poplar trees) on the read abundances. Hierarchical clustering (based on Bray-Curtis distances) and principal component analyses (PCA) were performed in and displayed with PRIMER 7 (Clarke, 1993). To statistically support the visual clustering of the bacterial communities in the PCA analyses, the different plant compartments

were compared using permutation-based hypothesis tests: tests of the multivariate null hypotheses of no differences among *a priori* defined groups were examined using ANOSIM (an analogue of univariate ANOVA) with the Spearman rank Correlation method in PRIMER 7. Indicator species analysis was performed using the multipat function of the indicspecies package in R (version 1.7.1; Cáceres & Legendre, 2009).

5.3. Results

5.3.1. General analysis of 454 pyrosequencing data

To determine the effects of the plant compartment and the host genotype on the composition of the plant associated bacterial microbiome, we collected samples from rhizosphere soil, root, stem and leaf of wild type poplar trees and *CCR* deficient poplar trees. Bacterial communities within each plant compartment and genotype were identified using 454 pyrosequencing. Five amplicon libraries were sequenced, each on one eight of a picotiter plate. Sequencing resulted in a total of 675,802 raw reads before quality trimming and assigning the reads to their respective sample. Average read length (± standard deviation) of reads before processing was 401 bp ± 101. Sequences were processed using mothur (version 1.33.2) following the Standard Operating Protocol outlined in http://www.mothur.org/wiki/Schloss_SOP including denoising and removal of chimeras. After quality trimming and assigning reads to the different samples (12 biological replicates x 4 plant compartments x 2 genotypes = total of 96 samples) 431,189 high-quality reads remained in the dataset.

We determined the co-amplication of non-target 16S rRNA (archaeal, chloroplast and mitochondrial sequences) within each plant compartment and host genotype as well as the number of reads that could not be unambiguously classified at the phylum level (Table 5.1). Under our optimized PCR conditions (Beckers et al. 2015, Chapter 4), no mitochondrial 16S rRNA sequences were co-amplified from any of the plant compartments for any of the host genotypes. Minute fractions of chloroplast 16S rRNA sequences were co-amplified from root, stem and leaf samples (ranging from 0.01% to 0.65% of the total identified reads). Finally, in the rhizosphere, we identified a small portion of reads, which were assigned to the taxonomic domain Archaea (0.03% and 0.01% respectively for wild type poplars and *CCR* deficient poplar trees). In the rhizosphere soil, a large fraction of reads could not be unambiguously classified at the phylum level (WT: 34.07% and *CCR*-: 32.02%). In the plant compartments, we were able to classify the majority of reads and only a relatively small proportion of reads remained unclassified (ranging 1.36% to 19.05%). Unclassified reads at the phylum level were removed from the dataset for further analysis.

Table 5.1. Co-amplification of non-target 16S rRNA and unclassified reads.

Plant compartment	Rhizosphere soil		Root	
Host Genotype	WT	*CCR*	WT	*CCR*
Archaea	0.03% ± 0.01%	0.01% ± 0.01%	0% ± 0%	0% ± 0%
Chloroplast	0% ± 0%	0% ± 0%	0.01% ± 0.01%	0% ± 0%
Mitochondria	0% ± 0%	0% ± 0%	0% ± 0%	0% ± 0%
Unclassified	34.07% ± 1.10%	32.02% ± 1.11%	4.74% ± 0.32%	9.30% ± 2.02%
Plant compartment	Stem		Leaf	
Host Genotype	WT	*CCR*	WT	*CCR*
Archaea	0% ± 0%	0% ± 0%	0% ± 0%	0% ± 0%
Chloroplast	0.44% ± 0.17%	0.65% ± 0.26%	0.03% ± 0.02%	0.01% ± 0.01%
Mitochondria	0% ± 0%	0% ± 0%	0% ± 0%	0% ± 0%
Unclassified	19.05% ± 4.32%	7.51% ± 2.72%	3.59% ± 1.03	1.36% ± 0.41

Comparison of the number of non-target 16S rRNA sequences (archaeal, chloroplast and mitochondrial sequences), which were co-amplified during PCR amplification and reads that could not be unambiguously classified at the phylum level ('Unclassified'). Each plant compartment is evaluated separately and data represent relative abundances of twelve biologically independent replicates (± standard errors).

5.3.2. Alpha rarefaction curves and alpha diversity: plant-compartment and host-genotype effects

To construct alpha rarefaction curves (Figure 5.1) and estimate differences in the alpha diversity (Figure 5.2) we removed singletons (OTUs with only 1 sequence) from the dataset since these singletons could be due to sequencing artefacts (Supplementary Table 5.2). We found a distinct plant-compartment effect in the retrieval of singletons (ANOVA result). Significantly more singletons were obtained from the rhizosphere soil as compared to all other plant compartments (Supplementary Table 5.2). No host-genotype effects were observed in the number of singletons retrieved.

Rarefaction curves were constructed for each individual sample (for each genotype within each plant compartment) showing the number of observed OTUs, defined at a 97% sequence similarity cut-off in mothur, relative to the number of total identified bacterial rRNA sequences (Figure 5.1).

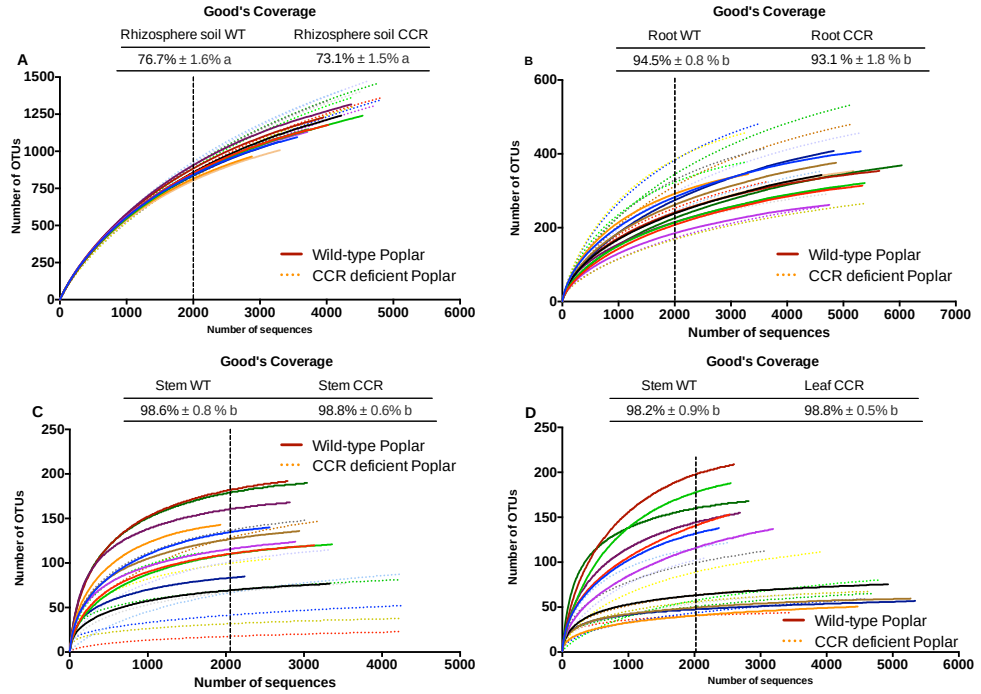

Figure 5.1. Average Good's coverage estimates (%) and rarefaction curves at the level of the individual poplar trees (per plant compartment) for each genotype (Wild type and CCR deficient). Good's coverage estimates represent averages of 12 biological replicates (± standard deviation) and were calculated in mothur based on 10,000 iterations. Lower case letters represent statistical differences (P < 0.05) Rarefaction curves were assembled showing the number of observed OTUs, defined at a 97% sequence similarity cut-off in mothur, relative to the number of total bacterial rRNA sequences. Continuous lines represent samples from wild type poplar trees and dashed lines represent samples from CCR deficient poplars. The dashed vertical line indicates the number of sequences subsampled from each sample to calculate alpha diversity estimates. A. Rhizosphere soil, B. Root, C. Stem, D. Leaf.

As expected, endophytic bacterial communities (Figure 5.1B, C, D) were much less diverse than rhizospheric communities (Figure 5.1A). Furthermore endophytic samples exhibited a higher degree of variation in the shape of their rarefaction curves as compared to rhizospheric samples. Rarefaction curves evaluating the OTU richness per sample generally approached saturation. The majority of root endophytic samples saturated around 250-300 OTUs and around 50-100 OTUs for stem and leaf samples. Rhizospheric samples only showed

saturation at about 1250 OTUs. Rarefaction curves also clearly indicate host-genotype effects. The rhizosphere soil and root rarefaction curves from *CCR* deficient trees generally indicate a slightly higher OTU richness (Figure 5.1A, B) whereas in stem and leaf samples (Figure 5.1C, D) curves of *CCR* deficient trees tended to level off faster, indicating a lower OTU richness. Statistical differences in OTU richness were inferred from alpha diversity measures (Figure 5.2).

To further assess the sequencing depth, we calculated Good's coverage estimates in mothur based on 10,000 iterations (Figure 5.1). Good's coverage scores were highly comparable for all endosphere compartments (root, stem, leaf) and host genotypes ranging from 93.1% to 98.8% indicating that sequencing depth was adequate to reliably describe the bacterial microbiome associated with these plant compartments. In rhizosphere soil, Good's coverage scores were significantly lower ($P < 0.05$) (WT: 76.7% ± 1.6%, *CCR*-: 73.1% ± 1.5%) as compared to endosphere compartments, but comparable between host-genotypes. Rarefaction curves of rhizosphere soil were starting to level off, but sequencing at a greater depth could have revealed more OTUs. However, most of the abundant OTUs should have been covered by our sequencing depth.

Alpha diversity, the microbial diversity within each sample, was analysed based on the OTU richness, the Inverse Simpson Diversity Index and Pielou's evenness (Figure 5.2). To control for differences in sampling effort across plant compartment and genotypes, we rarefied each sample to 2000 sequences per sample before calculating the diversity indices. OTU richness was highly dependent on plant compartment ($P < 0.05$), regardless of host genotype, with high richness values for rhizosphere soil (WT: 848.9 ± 7.9; *CCR*-: 872.8 ± 11.3), and consistently decreased richness estimates in root samples (WT: 243.7 ± 9.6; *CCR*-: 285.3 ± 21.8) and stem samples (WT: 126.7 ± 11.9; *CCR*-: 75.7 ± 12.2). OTU richness indices of the leaf samples (WT: 118.3 ± 17.2; *CCR*-: 70.2 ± 8.0) were comparable with the stem samples. Significant host-genotype effects were found in stem samples ($P < 0.01$) and leaf samples ($P < 0.05$) whereby *CCR* deficient trees displayed lower OTU richness.

For diversity and evenness estimates, we found a clear separation between rhizosphere soil samples and endosphere samples ($P < 0.05$), irrespective of the genotype. Higher diversity and evenness measures were observed for rhizosphere soil whereas all endosphere compartments revealed highly

comparable diversity and evenness estimates. Significant host-genotype effects for diversity and evenness estimates were observed for stem samples ($P < 0.05$) where *CCR* deficient trees showed lower diversity and evenness estimates.

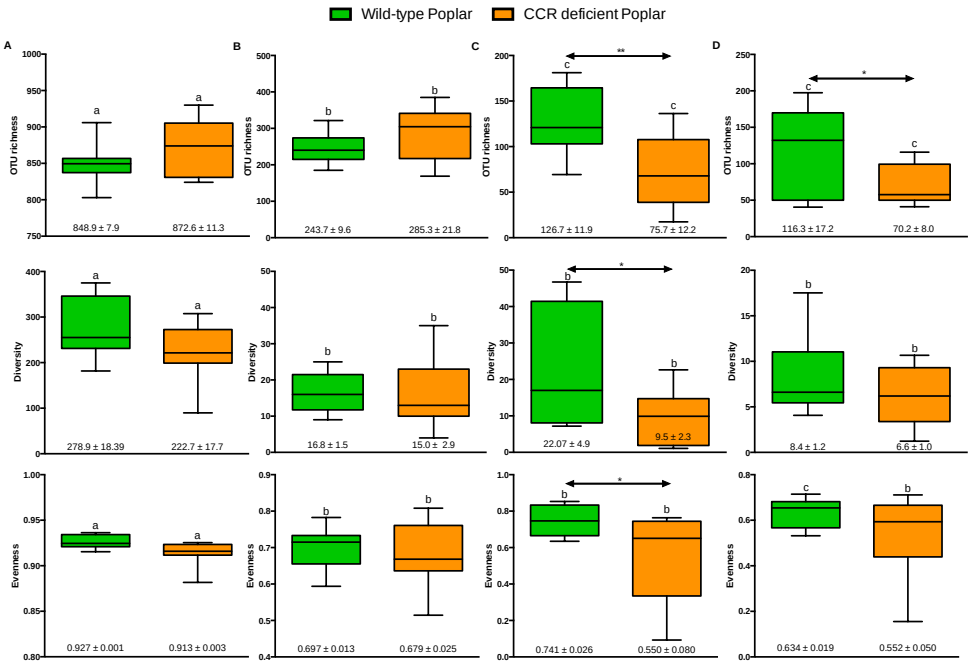

Figure 5.2. Alpha diversity estimates of the bacterial communities. A. Rhizosphere soil, B. Root, C. Stem, D. Leaf. Wild type poplar samples are displayed in green, CCR deficient poplar trees are displayed in orange. Graphs display OTU richness estimates (number of observed OTUs), Inverse Simpson Diversity Indices and Pielou's evenness estimates. Box-plots display the first (25%) and third (75%) quartile, the median and the maximum and minimum observed values within each data set. Box plots were calculated based on 12 biological replicates and alpha diversity estimates were calculated in mother with 10,000 iterations. Average values (± standard deviation) are indicated below each box plot. Data were analysed using two-way ANOVAs and Tukey Kramer post hoc comparisons. Significant differences ($P < 0.05$) across plant compartments (within each genotype) are indicated with lower-case letters and pairwise comparisons between genotypes (within each compartment) are indicated with asterisks (: $P < 0.05$, **: $P < 0.01$).*

5.3.3. Beta diversity: Plant compartment and host-genotype effects

Next, we compared beta diversity, which describes the variation in species composition. We evaluated beta diversity at two phylogenetic levels, the phylum level and the genus level (OTUs defined at a 97% similarity cut-off).

To compare the composition of identified community members within different plant compartments and host genotypes, and identify main factors driving community composition, a Bray-Curtis similarity matrix was calculated on normalized (2000 sequences per sample) and square-root transformed read abundance data. Overall similarities in bacterial community structures among samples were displayed using the unconstrained ordination technique, principal component analysis (PCA) and a hierarchical clustering based on Bray-Curtis distances. We analyzed all bacterial communities within each host genotype (wild type and *CCR* deficient poplar) (Figure 5.3, Supplementary Figure 5.1) and also made pairwise comparison between the host-genotypes within all plant compartments (Figure 5.4, Supplementary Figure 5.2).

For both host genotypes, PCA analyses revealed strong clustering of bacterial communities according to the different plant compartments (rhizosphere soil, root, stem, leaf) at each phylogenetic level (Figure 5.3 and Supplementary Figure 5.1). At genus level, PC1 explained 32.5% and 30.2% of the total variation of respectively wild type and *CCR* deficient poplar trees whereas PC2 explained respectively 17.9% and 16.0% of the total variation (Figure 5.3A,C). This pattern was recapitulated by hierarchical clustering of pairwise Bray-Curtis similarities (Figure 5.3B,D). Hierarchical clustering (at genus and phylum level) revealed strong clustering according to plant compartment for rhizosphere soil and root samples (Figure 5.3B,D and Supplementary Figure 5.1B,D). Stem and leaf samples were clearly distinguished from rhizosphere soil and roots, but did not cluster completely according to their respective plant compartment (Figure 5.3B,D and Supplementary Figure 5.1B,D).

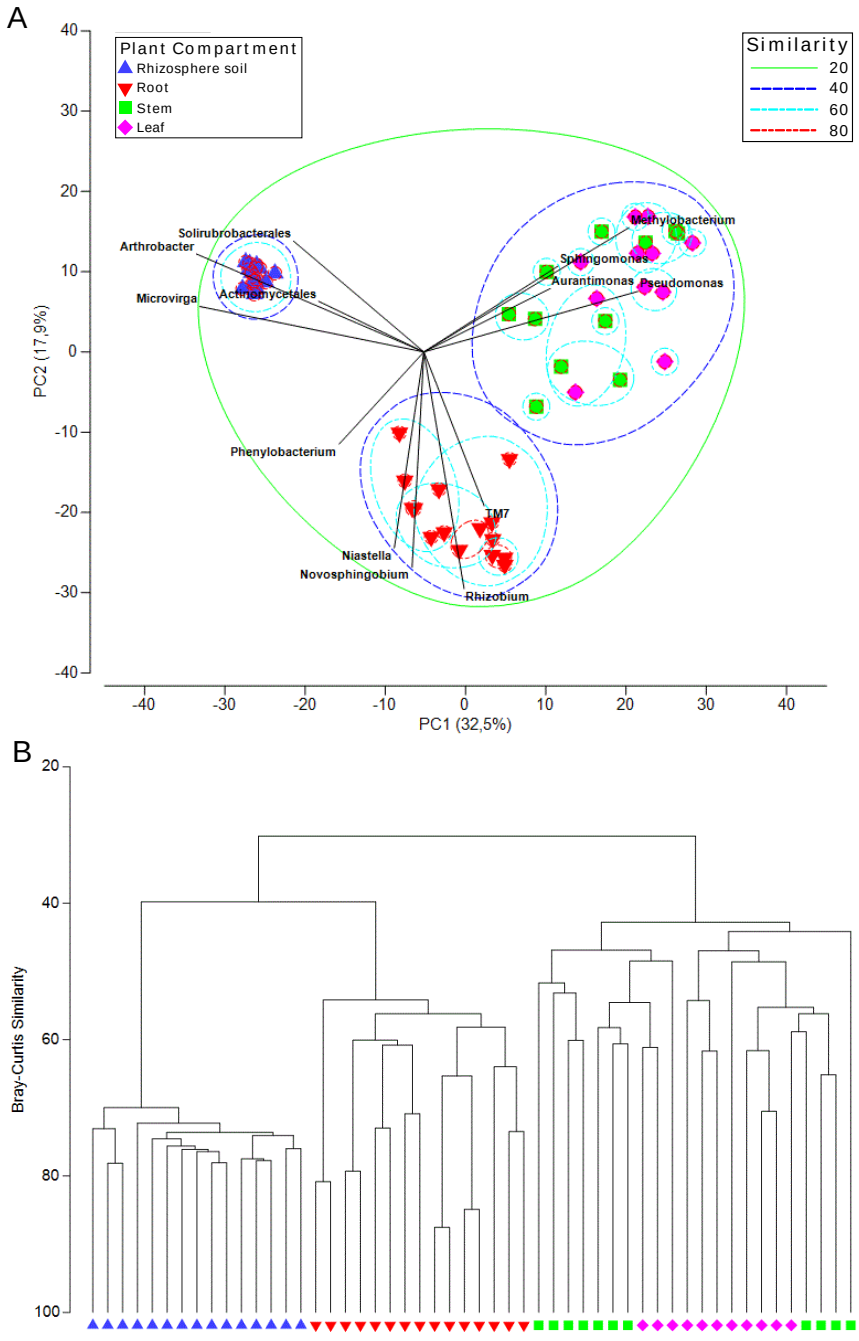

Figure 5.3. Plant compartment drives the composition of the bacterial communities at the genus-level. WT poplar trees (A, B) and *CCR* deficient poplar trees (C,D).

C

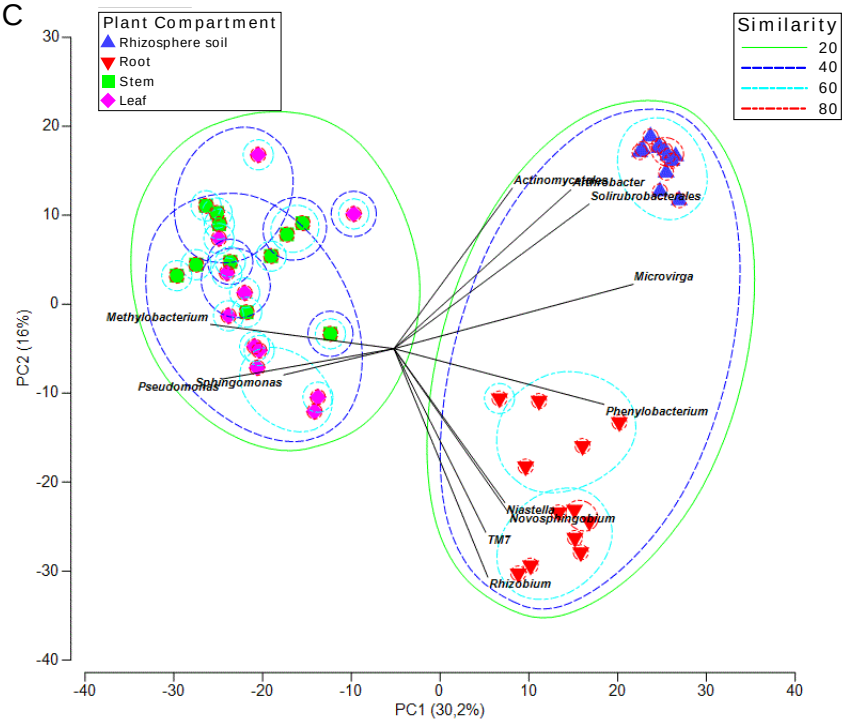
Plant Compartment
Rhizosphere soil
Root
Stem
Leaf
Similarity
20
40
60
80
PC2 (16%)
PC1 (30,2%)
Actinomycetales
Arthrobacter
Solirubrobacterales
Microvirga
Methylobacterium
Pseudomonas
Sphingomonas
Phenylobacterium
Niastella
Novosphingobium
TM7
Rhizobium

D

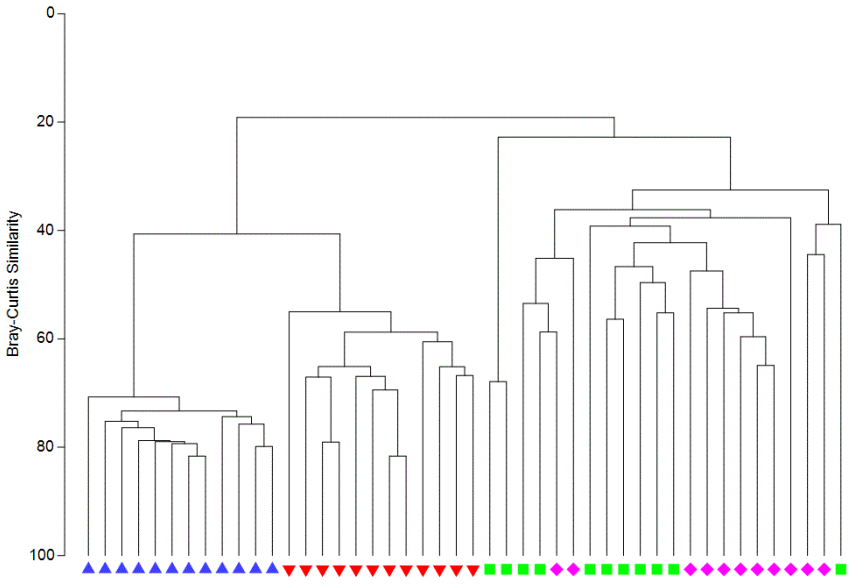
Bray-Curtis Similarity

Figure 5.3. (continued) Plant compartment drives the composition of the bacterial communities at genus-level. Principle component analysis (PCA) of square-root transformed samples based on rarefaction to 2000 reads per sample. OTUs were defined at a 97% sequence similarity cut-off in mothur (A, C). OTUs differentiating the plant compartments, are displayed as vectors on the PCA plots. Hierarchical clustering (group-average linkage) of the samples based on Bray-Curtis similarity (B, D). Similarities based on Bray-Curtis distances (B and D) were superimposed on the PCA plot (A and C). PCA and hierarchical clusters were based on 12 biological replicates and were constructed in PRIMER 7 with 10,000 iterations.

To statistically support the visual clustering of the bacterial communities in the above PCA analyses, different plant compartments were examined using ANOSIM (an analogue of univariate ANOVA) with the Spearman rank Correlation method (Table 5.2).

Table 5.2. Plant compartments effects on bacterial community composition as evaluated by ANOSIM

Host Genotype	Wild-type Poplar				*CCR* deficient poplar			
Phylogenetic level	Phylum-level		Genus-level		Phylum-level		Genus-level	
ANOSIM output	R	p-value	R	p-value	R	p-value	R	p-value
Rhizosphere soil vs root	0.580	0.0001***	0.945	0.0001***	0.852	0.0001***	0.958	0.0001***
Rhizosphere soil vs stem	0.780	0.0001***	0.965	0.0001***	0.570	0.0001***	0.760	0.0001***
Rhizosphere soil vs leaf	0.819	0.0001***	0.992	0.0001***	0.625	0.0001***	0.842	0.0001***
Root vs stem	0.437	0.0001***	0.804	0.0001***	0.538	0.0001***	0.728	0.0001***
Root vs leaf	0.370	0.0003**	0.888	0.0001***	0.317	0.0002**	0.734	0.0001***
Leaf vs stem	0.232	0.01*	0.294	0.002*	0.022	0.287	0.082	0.063

Plant compartment effects on the bacterial community structures were calculated using ANOSIM (analysis of similarities) with the Spearman Rank correlation method in Primer 7 (10,000 permutations). Plant compartments (rhizosphere soil, root, stem, leaf) were a priori defined groups within each host genotype at two phylogenetic levels: phylum-level and genus-level. Significance levels: P ≤ 0.01; P ≤ 0.001**; P ≤ 0.0001***, R: ANOSIM test statistic. Graphical results of ANOSIM are displayed in Supplementary Figure 5.3*

For wild type poplar, all plant compartments rendered bacterial microbiota significantly dissimilar from each other (P-values listed in Table 5.2) at the phylum level and genus level. For *CCR* deficient poplar trees, we observed highly similar results whereby all plant compartments displayed significantly different bacterial communities, with the single exception of the comparison between leaf

and stem compartments. At the phylum level, we observed no significant differences between these two plant compartments (R-statistic = 0.022; P = 0.287) whereas at the genus-level marginally significant results were obtained (R-statistic = 0.082, P = 0.063) (Table 5.2).

To determine the influence of host genotype on beta diversity of bacterial communities, pairwise comparisons were made between genotypes within each plant compartment and displayed using PCA ordination (Figure 5.4 and Supplementary Figure 5.2). Furthermore, pairwise comparisons within each plant compartment were statistically tested using ANOSIM (Table 5.3 and Supplementary Figure 5.4,5). We found different host-genotype effects in the four different plant compartments. Within the rhizosphere soil, we observed no clustering according to genotype (at phylum and genus level) as determined by PCA and hierarchical clustering (Bray-Curtis distances) (Figure 5.4A and Supplementary Figure 5.4A), which was confirmed by the ANOSIM results (Table 5.3, phylum-level: R-statistic = -0.014; P = 0.58 and genus-level: R-statistic = 0.036; P = 0.157). However, in roots and stems, we did observe clear effects of host genotype. In general, samples from both compartments clustered according to the host-genotype (Figure 5.4 B, C and Supplementary Figure 5.4B, C) and were significantly dissimilar from each other at the phylum level and the genus level (significance levels listed in Table 5.3). In the last endophytic plant compartment, the leaves, we again observed no distinct clustering according to genotype (Figure 5.4D and Supplementary Figure 5.4D) and also no statistical differences were detected in the bacterial community structure of this plant compartment (Table 5.3).

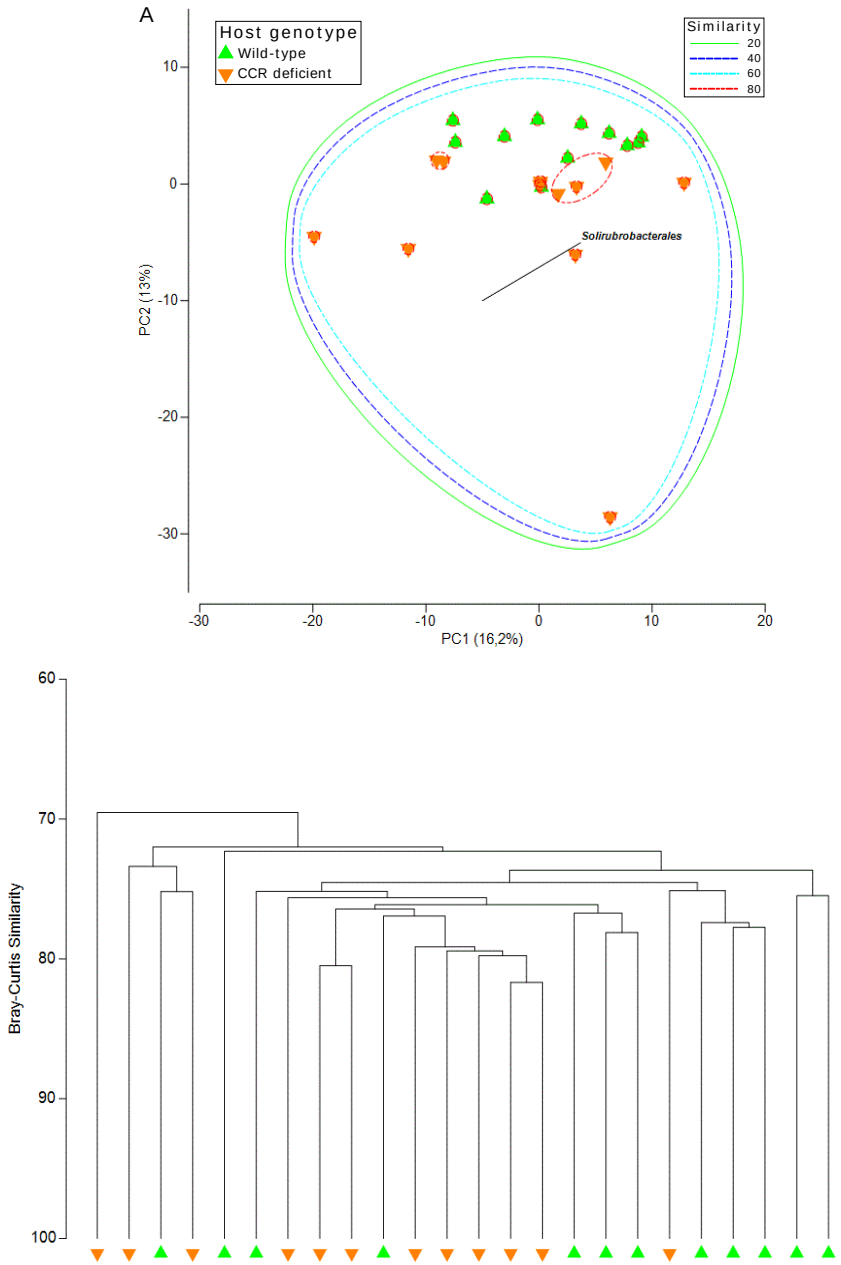

Figure 5.4. Host-genotype effects on bacterial communities (A. Rhizosphere soil, B. Root, C. Stem, D. Leaf).

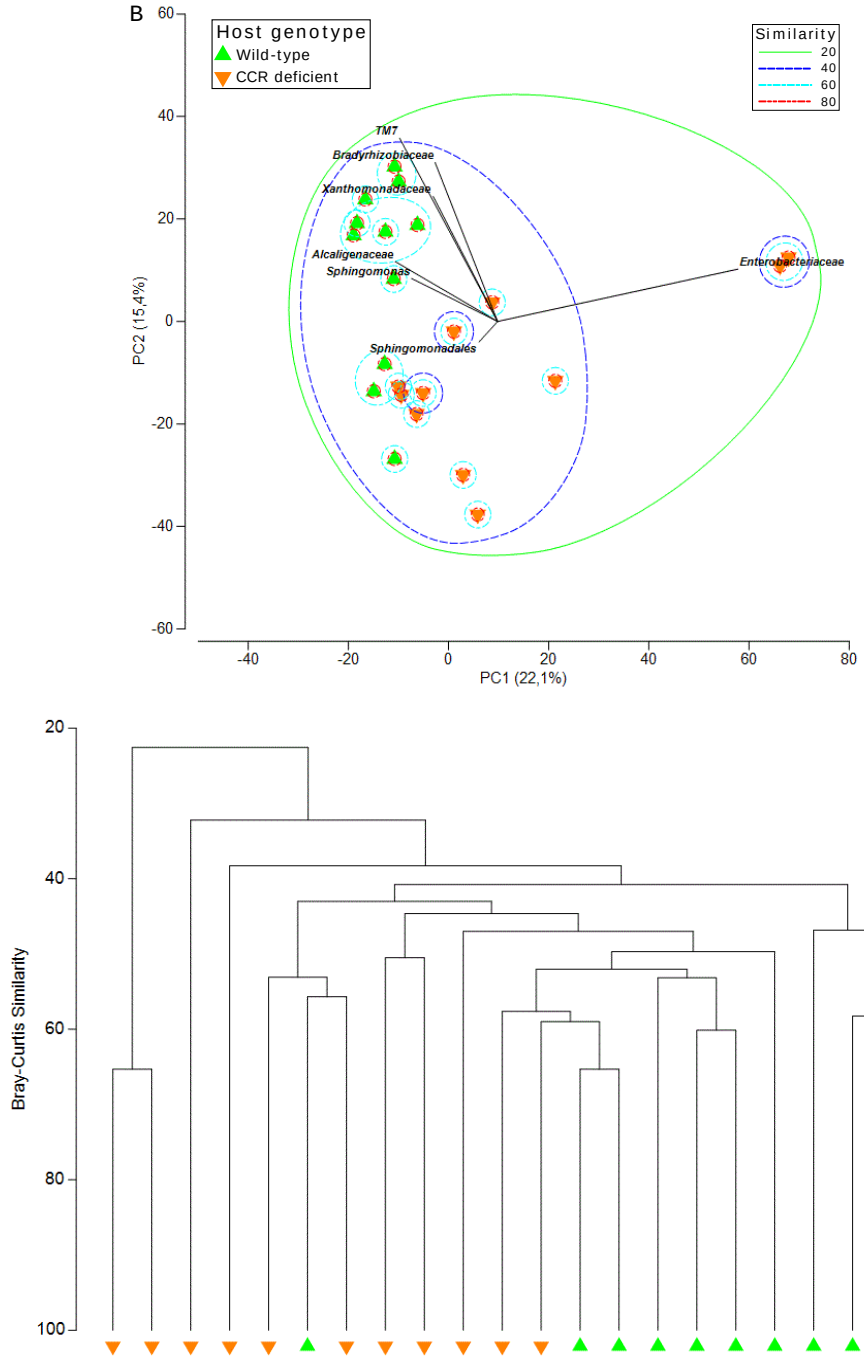

Figure 5.4. Host-genotype effects on bacterial communities (A. Rhizosphere soil, B. Root, C. Stem, D. Leaf).

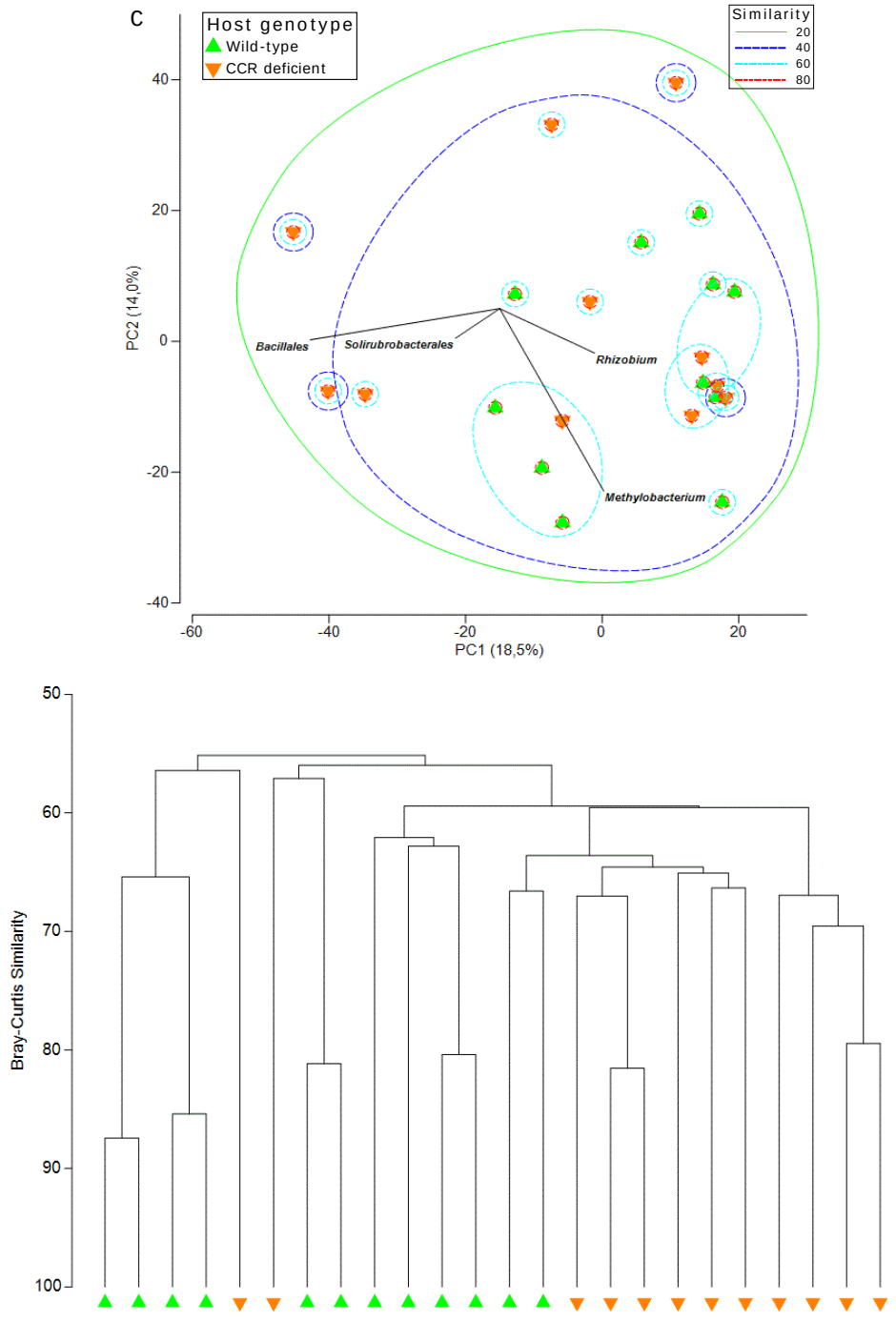

Figure 5.4. Host-genotype effects on bacterial communities (A. Rhizosphere soil, B. Root, C. Stem, D. Leaf).

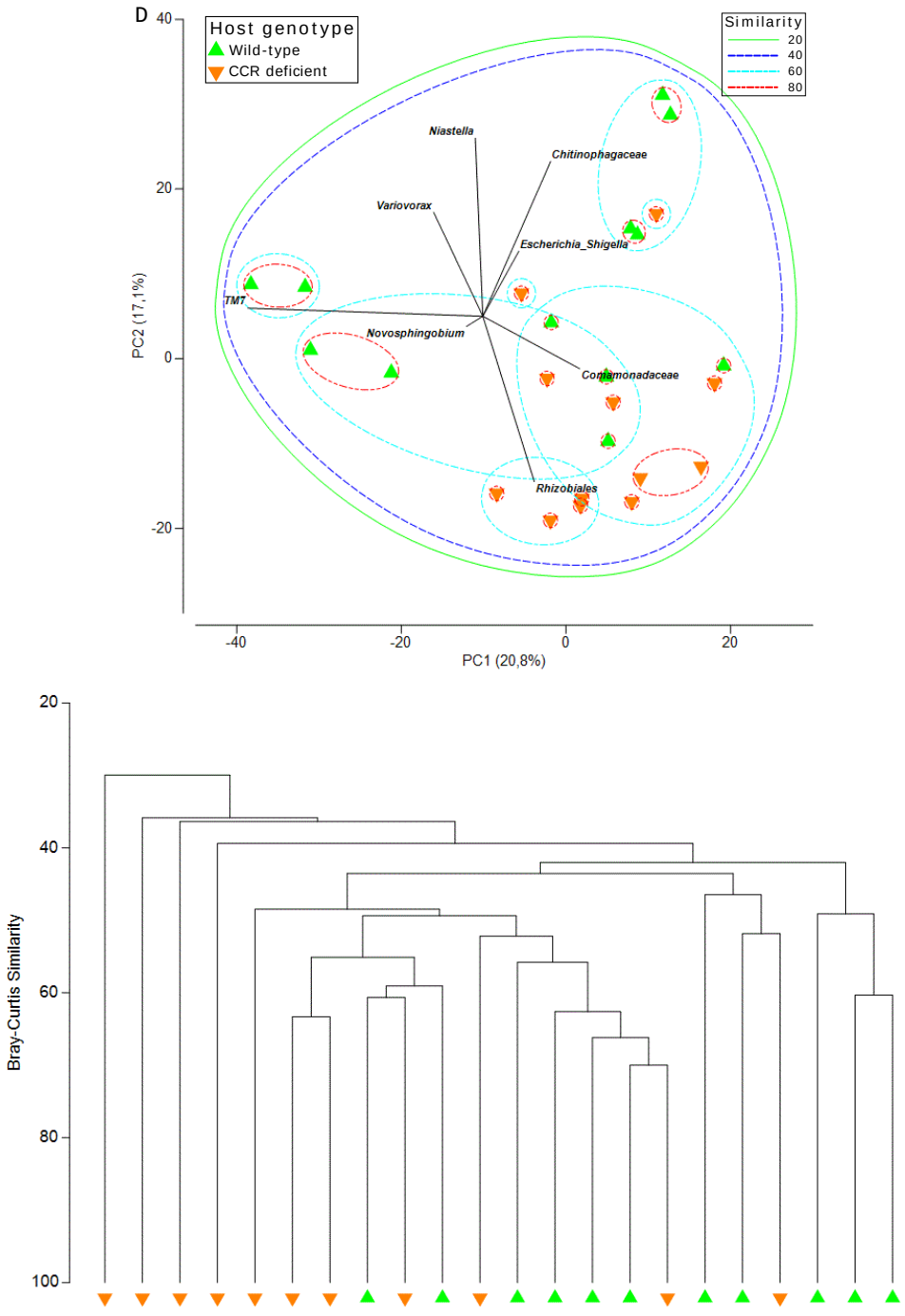
D
Host genotype
Wild-type
CCR deficient
Similarity
20
40
60
80
Niastella
Chitinophagaceae
Variovorax
Escherichia_Shigella
TM7
Novosphingobium
Comamonadaceae
Rhizobiales
PC2 (17,1%)
PC1 (20,8%)
40
20
0
-20
-40
-20
0
20
Bray-Curtis Similarity
20
40
60
80
100

Figure 5.4. Host-genotype effects on bacterial communities (A. Rhizosphere soil, B. Root, C. Stem, D. Leaf) (continued). Top panel: principle component analysis (PCA) of normalized (square-root transformed) samples based on rarefaction to 2000 reads per sample. OTUs were defined at a 97% sequence similarity cut-off in mothur. Lower panel: hierarchical clustering (group-average linkage) of the samples based on Bray-Curtis similarities. Similarities based on Bray-Curtis distances were superimposed on the PCA plot. OTUs differentiating the bacterial communities in the different plant compartments are displayed as vectors on the PCA plots. PCA and hierarchical clusters were based on 12 biological replicates and were constructed in PRIMER 7 with 10,000 iterations.

Table 5.3. Host-genotype effects on bacterial community structure as evaluated by ANOSIM

Phylogenetic level	Phylum-level		Genus-level	
ANOSIM output	R	p-value	R	p-value
Rhizosphere soil WT vs Rhizosphere soil *CCR*	-0.01399	0.57784	0.03609	0.157
Root WT vs Root *CCR*	0.1328	0.01799*	0.34490	<0.00001***
Stem WT vs Stem *CCR*	0.1772	0.00189**	0.20060	0.0009 ***
Leaf WT vs Leaf *CCR*	0.0263	0.22578	-0.01399	0.525

Host-genotype effects on the bacterial community structures were calculated using ANOSIM (analysis of similarities) with the Spearman Rank correlation method in Primer 7 (10,000 permutations). Plant compartments (rhizosphere soil, root, stem, leaf) and host-genotypes were a priori defined groups at two phylogenetic levels: phylum-level and genus-level. Significance levels: P ≤ 0.05; P ≤ 0.01**; P ≤ 0.001***, R: ANOSIM test statistic. Graphical results of ANOSIM are displayed in Supplementary figures 5.4 and 5.5*

5.3.4. Core bacterial microbiome within each plant compartment and drivers of plant compartment and host-genotype effects

Finally, we took a closer look at the individual phyla and genus-level OTUs, which differentiate the bacterial communities in the plant compartments and host-genotypes.

At the phylum level, we evaluated all observed phyla with ANOVA to test the effect of plant compartment (rhizosphere soil *vs* root *vs* stem *vs* leaf) and host-genotype (wild type *vs CCR* deficient poplar) on their abundance (Supplementary Table 5.3). For both host genotypes, Actinobacteria (Relative abundance: WT = 27.7% and *CCR* = 24.18%), Acidobacteria (WT = 1.81% and *CCR* = 1.85%) and Betaproteobacteria (WT = 24.84% and *CCR* = 25.18%) differentiated the rhizosphere soil samples from the other plant compartments.

Root samples were distinguished primarily by Alphaproteobacteria (WT = 47.05% and *CCR* = 64.6%), Betaproteobacteria (WT = 18.18% and *CCR* = 13.26%) and TM7 (WT = 11.82% and *CCR* = 5.1%). And finally stem and leaf samples were discriminated by Deinococus-Thermus and Gammaproteobacteria (Supplementary Table 5.3 and Supplementary Figure 5.1). Host-genotypes effects at the phylum level were exclusively observed in the root and stem samples, corroborating with ANOSIM results of pairwise comparisons between host-genotypes (Table 5.3). Total relative abundances of all phyla and significant effects across plant compartments and host-genotypes are listed in Supplementary Table 5.3.

For the genus-level OTUs, we defined the core bacterial microbiome as the 10 most abundant OTUs of each of the plant compartments and host-genotypes resulting in 35 OTUs altogether (Supplementary table 5.4). The percentage of sequences covered by these core OTUs are listed in Supplementary table 5.4. ANOVA was used to test the effect of plant compartment and host-genotype on the normalized sequence counts of members of the core community. In rhizosphere soil, we observed the highest relative abundance for *Rhizobiales* (WT = 12.59% and *CCR* = 10.95%), in roots for *Rhizobium* (WT = 22.80% and *CCR*= 31.18%), in stems for *Pseudomonas* (WT = 17.64%) and *Enterobacteriaceae (CCR = 20.20%)* and finally in leaves for *Pseudomonas* (WT = 26.95%, *CCR* = 26.11%). In general, rhizosphere samples were differentiated from all other plant compartments, irrespective of host-genotype, by *Actinomycetales* (WT = 10.13% and *CCR* = 7.66%), *Arthrobacter* (WT = 4.4% and CCR = 3.14%), *Microvirga* (WT = 2.68% and *CCR* = 2.44%), *Solirubrobacterales* (WT = 1.9 % and *CCR* = 6.29%) and to a lesser extent by *Xanthomonadaceae* (WT = 1.9% and *CCR* = 1.9%) and *Chitinophagaceae* (WT = 3.06% and *CCR* = 3.61%) (Supplementary table 5.4 and Figure 5.3A,B). Root samples were distinguished primarily by the abundant presence of *Rhizobium* (WT = 22.8% and *CCR* = 31.18%), *TM7* (WT = 15.77% and *CCR* = 5.83%), *Novospingobium* (WT= 3.76% and *CCR*= 1.81%), *Phenylobacterium* (WT = 2.13% and *CCR* = 0.83%), *Niastella* (WT = 2.01% and *CCR* = 0.83%), *Comamonadaceae* (WT = 0.98% and *CCR* = 4.49%) and *Bradyrhizobiaceae* (WT = 1.22% and *CCR* = 1.93%) (Supplementary Table 5.4 and Figure 5.3A, B). Finally, stem and leaf samples were discriminated most notably by

Pseudomonas, *Sphingomonas*, *Methylobacterium, Moraxellaceae* and *Paracoccus* (Supplementary table 5.4 and Figure 5.3A,B). Total relative abundances of all core OTUs and significant effects across plant compartments and host-genotypes are listed in Supplementary table 5.4. We found several host-genotype effects ($P < 0.05$) in the core OTUs, most pronounced in roots and stems of poplar trees, supporting the ANOSIM results (Table 5.3). In roots, we observed significant differences between host-genotypes for *Rhizobiales*, *Variovorax*, *TM7*, *Novosphingobium*, *Niastella*, *Escherichia shigella* and *Comamonadaceae* (Supplementary Table 5.4 and Figure 5.4B). In stems, significant differences were found for *Xanthomonadaceae*, *TM7, Bradyrhizobiaceae, Sphingomonas, Alcaligenaceae, Enterobacteriaceae and Sphinogmonadales* (Supplementary Table 5.4 and Figure 5.4C). However, some of the host-genotype effects on the core OTUs were accompanied by significant interaction effects thereby making it difficult to distinguish between plant-compartment and host-genotype effects (Supplementary Table 5.4.

To support the ANOVA results at genus level and further ascertain which OTUs are responsible for the observed community differentiation between the host genotypes, we used species indicator analyses (multipat function of the indicspecies package in R) to discover significant associations. Indicator analyses were performed on full community matrices and not only core OTUs to cover effects possibly missed by the core OTU analysis. Full lists of indicator species and their corresponding indicator values can be found in Supplementary table 5.5. Pairwise comparison of host-genotype within each plant compartment, revealed 7 indicator species in rhizosphere soil, 12 in root samples, 16 in stem samples and 5 in leaf samples (Supplementary Table 5.5). However, when we used a community matrix excluding OTUs with an average relative abundance of $< 1\%$, we found no indicator species in rhizosphere soil, 2 in root samples (WT: *Staphylococcus* and *Micromonospora*), 9 in stem samples (*CCR*: *Enterobacteriaceae, Gemella* and WT: *Alcaligenaceae, TM7, Variovorax, Bradyrhizobiaceae, Xanthomonadaceae, Rhizobacter* and *Bradyrhizobium*) and 1 in leaf samples (WT: *Variovorax*) (Supplementary table 5.5).

5.4. Discussion

The objective of this study was to unravel the specificity of bacterial assemblages for specific plant compartments (rhizosphere soil, root, stem, leaf) in *Populus tremula x alba* (niche differentiation) and furthermore determine the effect that the host-genotype (wild type versus *CCR* deficient) can exert on the *Populus* bacterial microbiome (host-genotype effects). To our knowledge this study represents the first in depth evaluation of rhizospheric and endophytic niche differentiation and host genotype effects not exclusively focussing on the rhizosphere soil-root interface. Indeed most studies describing total bacterial microbiomes and possible host-genotype interactions have been restricted to the interaction with rhizobacterial assemblages and endophytes present in the root endosphere (Bulgarelli et al., 2012; Gottel et al., 2011; Hur et al., 2011; Lundberg et al., 2012; Weinert et al., 2011). To this end, we individually sampled all plant compartments (rhizosphere soil, root, stem and leaf) of 2,5 year old field-grown wild type poplar trees *(Populus tremula x alba)* and trees with a modified, *CCR*-down-regulated, lignin biosynthesis and analysed the bacterial microbiomes using 454 pyrosequencing.

5.4.1. General analysis of the pyrosequencing data

Firstly, we took a general look at the 454-pyrosequencing data. We used an optimized PCR approach to reduce co-amplification of chloroplast and mitochondrial 18S rRNA (Beckers et al. 2015, Chapter 4). In many studies, the high homology between bacterial 16S rRNA genes, chloroplast 16S rRNA genes, plant nuclear and mitochondrial 18S rRNA genes (Dyall et al. 2004; Raven, 1970) and moreover the high abundance of chloroplast 16S rRNA genes in these environments led to undesired co-amplification of non-target sequences (Bodenhausen et al. 2013; Bulgarelli et al., 2012; Gottel et al., 2011; Lundberg et al., 2012). Our optimized PCR approach resulted in very low co-amplification of these sequences (ranging from 0% - 0.65% of the total obtained sequences) and high retrieval of bacterial 16S rRNA sequences (Table 5.1). Highest retrieval of chloroplast 16S rRNA sequences were observed in the stem samples, corroborating our results from the primer optimization, and reinforcing our view that the balance between the amount of endophytic bacterial DNA and chloroplast DNA seems to play a more important role than the absolute chloroplast concentration (Beckers et al. 2015, Chapter 4).

We also found a clear plant compartment effect in the number of reads that could not be unambiguously classified at the phylum level. Up to 34% of the reads from rhizosphere samples (regardless of host genotype) could not be classified at the phylum level. This is indicative of an insufficient database representation of the biodiversity of soil-borne bacteria and an underrepresentation of the hypervariable V6-V7 region (Bulgarelli et al., 2012; Gans et al., 2005). Indeed, the V3-V4 has been the preferred region for next-generation sequencing studies in the past (Klindworth et al., 2013).

Finally, we also considered the number of singletons (sequences only found once in the data-set) obtained from each plant compartment (Supplementary Table 5.2). Remarkably, we found high levels of singletons in rhizosphere soil (WT: 26.09% ± 0.01%, *CCR*: 27.80% ± 0.69%) and a decreasing number of singletons in other plant compartments ($P < 0.05$) (Supplementary Table 5.2). Singletons have been shown to comprise up to and beyond 60% of taxa in some surveys (Reich et al., 2009; Coddington et al., 2009) and are generally considered as being problematic since they represent inherently unreplicated data (Dickie, 2010). Most singletons arise from DNA sequencing errors (insertions, deletions, low-quality reads, inadequate clustering and formation of chimeric sequences) (Huse et al. 2007; Huse et al. 2010; Sogin et al., 2006; Tedersoo et al., 2010) creating false sequences and artificially inflating diversity estimates (Kunin et al. 2010; Quince et al., 2009; Reeder & Knight, 2010). In our experimental set-up, sequencing error (and creation of erroneous (singleton) sequences) is expected to be similar for all plant compartments, which leads us to believe that the discrepancy in the number of singletons between the plant compartments could in fact be attributable to more genuine rare (singleton) OTUs in the rhizosphere soil (Supplementary Table 5.2). Indeed, the rhizosphere soil is renowned for its vast microbial diversity (Gans et al., 2005; Roesch et al., 2007). For further analysis, we took a conservative approach and treated all singletons as potentially erroneous and removed them from the data sets (Medinger et al., 2010; Tedersoo et al., 2010). However, the involvement of this 'rare' biosphere in community dynamics and their ecological roles are largely unknown but they could contribute to community stability by allowing rapid responses to changing environmental conditions (Shade et al., 2014).

5.4.2. Plant compartment effects and niche differentiation

To unravel plant compartment effects, we initially constructed OTU rarefaction curves (97% sequence similarity cut-off) and estimated alpha diversity focussing on richness, evenness and diversity. We observed remarkably dissimilar shapes of the rarefaction curves when comparing rhizosphere and endosphere (Figure 5.1). Rhizosphere soil samples displayed highly uniform rarefaction curves (Figure 5.1A) whereas the variation in the shape of the rarefaction curves from the endophytic samples was much higher, especially for the stem and leaf samples (Figure 5.1B, C, D). High variability of endophytic OTU richness, as depicted by the rarefaction curves, could possibly be caused by sporadic and non-uniform colonization of the roots and aerial plant compartments of *Populus* (Bodenhausen et al., 2013; Gottel et al., 2011). Gottel et al. (2011) attributed some of the variation to their inability to sequence the bacterial endophytic community deeply and uniformly enough because of the high co-amplification of organellar 16S rRNA (67.000 chloroplast and 65.000 mitochondrial sequences). However our data exhibit roughly the same pattern without the co-amplification of non-target DNA (Table 5.1) and with high Good's coverage estimates (Figure 5.1). Therefore our data suggest considerable variation in endophytic colonization as a major reason for the high variability in the rarefaction curves. Indeed, whereas rhizosphere/rhizoplane colonization is primarily driven by 'inelaborate' chemo-attraction to root exudates (Bais et al. 2006; Lugtenberg & Dekkers, 1999; Lugtenberg & Kamilova, 2009; Walker et al. 2003), endophytic competence (*i.e.* ability to successfully colonize the host plant) requires specific traits and intricate interplay between rhizospheric soil-borne bacteria and the host plants innate immune system (Bulgarelli et al., 2013; Compant et al., 2010; Hardoim et al., 2008; Jones & Dangl, 2006).

Furthermore, we found that richness estimates were highly dependent on plant-compartment (regardless of host-genotype) with rhizosphere soil, root and stem compartments clearly differentiated from each other by decreasing OTU richness ($P < 0.05$, Figure 5.2). These results are in concordance with the general views of endophytic colonization. Most endophytic bacteria should originate from the rhizosphere and progressively colonize the roots, stems and leaves (Compant et al., 2010; Hardoim et al., 2008). Rhizodeposition and root exudation by the host plant in the root zone (organic acids, sugars, amino acids, root cap border cells,

etc.) fuels chemo-attraction and colonization of the rhizosphere soil and rhizoplane, thereby leading to the formation of distinctive, highly rich and diverse, rhizosphere microbiomes (Bais et al. 2006; Lugtenberg & Dekkers, 1999; Lugtenberg & Kamilova, 2009; Walker et al. 2003). After rhizoplane colonization, adaptation to an endophytic lifestyle is dependent on the ability of the soil-borne bacteria to pass (actively or passively) the endodermis and pericycle, reach the xylem vessels and finally lead to systemic colonization of the plant (Compant et al., 2010; Hardoim et al., 2008). The rhizosphere soil-root interface acts as a selective barrier and endophytic competence/colonization is limited to specific bacterial strains. The great loss of diversity and evenness (Figure 5.2A, B, C) from rhizosphere soil to endophytic compartments supports this view and indicates that only a limited number of bacteria can adapt to an endophytic lifestyle (loss of diversity) (Figure 5.2B) and these bacterial strains will therefore dominate endophytic assemblages (loss of evenness) (Figure 5.2C).

To compare beta diversity (bacterial community structures) present in the plant compartments, we clustered all samples using principal component analysis (PCA) and hierarchical clustering (Bray-Curtis distances) (Figure 5.3). At the phylum level and genus level, all samples strongly clustered according to plant compartment ($P < 0.01$) and rendered microbiota significantly dissimilar from each other, irrespective of host genotype (Figure 5.3)(Supplementary Figure 5.1)(Table 5.2). Only the separation between stem and leaf compartments in *CCR*-down-regulated poplar trees was not significant at the phylum level ($P = 0.29$) and borderline significant at genus level ($P = 0.06$) (Table 5.2). Previously, we observed the same niche differentiation for the cultivable bacteria of poplar trees in the same field study (Beckers et al. 2015, Chapter 3). Niche differentiation between rhizosphere and root endophyte microbiome has been described for mature poplar trees growing in natural ecosystems (*Populus deltoides*) (Gottel et al., 2011), for *Arabidopsis thaliana* (Bulgarelli et al., 2012; Lundberg et al., 2012) and other plant species (Berg & Smalla, 2009; Hardoim et al., 2011; Inceoğlu et al. 2010). Recently Bulgarelli et al. (2013) proposed a two-step selection model for root microbiota differentiation from the rhizosphere where rhizodeposition and host genotype-dependent fine-tuning converge to select specific endophytic assemblages. Bulgarelli et al. (2013) argue that

substrate-driven selection in the rhizosphere is expected to persist in the endosphere. Indeed, our data suggest additional fine-tuning and niche differentiation of microbiota in the aerial plant organs (both at the phylum and genus level), with the stem and leaf bacterial assemblages being remarkably dissimilar from the root and rhizosphere (Figure 5.3 and Supplementary Figure 5.1) (Table 5.2). Indeed, each of these microenvironments or ecological niches (rhizosphere soil, root, stem and leaf) provide very specific abiotic conditions such as availability of soluble organic compounds (Bulgarelli et al., 2013; Lindow & Brandl, 2003; McCully, 2001).

Furthermore, we also clearly observed more variation in bacterial community structures in the endosphere as compared to the rhizosphere communities, especially in stem and leaf endophytes (Supplementary Figure 5.3). The within group variation, as depicted by ANOSIM analysis, of rhizosphere soil bacterial assemblages is very low. This indicates that, even though the soil biome is one of the richest microbial ecosystems on Earth (Gans et al., 2005; Roesch et al., 2007) and the root exudation process is heterogeneous in space (DeAngelis et al., 2009; Grayston et al. 1997), the formation of distinctive rhizosphere bacterial communities mediated by rhizodeposition (and chemo-attraction to photoassimilates) seems to be a very consistent and stable process across different poplar individuals in the same field trial. In contrast, variation within endophytic communities is much higher (Supplementary Figure 5.3). As mentioned previously, endophytic colonization and formation of stable communities appears to be a more variable process, as suggested by our results from the alpha rarefaction curves, alpha diversity measures (Figure 5.1 and 5.2) and ANOSIM results of the bacterial community structures (Supplementary Figure 5.3). Crucial factors underlining this variability are the nature of endophytic colonization (Compant et al., 2010; Hardoim et al., 2008), interplay with the host plants innate immune system (Jones & Dangl, 2006) and furthermore acute fluctuations in abiotic conditions (temperature, humidity, access to nutrients, etc.) which differ from the buffered fluctuations in the rhizosphere (Bulgarelli et al., 2013; Hirano, 2000).

5.4.3. Host-genotype effects

We evaluated host-genotype effects between wild type poplar trees and *CCR* deficient poplar trees. Previously, *CCR* deficient poplar trees displayed different xylem compositions (Leplé et al., 2007) and are, except for the T-DNA construct, isogenic with the wild type poplar trees making them prime candidates to investigate host-genotype effects (Leplé et al., 1992).

In the rarefaction curves and alpha diversity estimates, we mainly found host-genotype differences in the stem compartment (Figure 5.2). Richness, diversity and evenness measures were significantly lower ($P < 0.05$) in *CCR*-down-regulated trees as compared to wild type trees. We previously reported that *CCR* down-regulation and accumulation in the xylem of various extractable phenolics have a profound effect on the structural composition and metabolic capacities present in cultivable endophytic communities and also influence alpha diversity measures (Beckers et al. 2015, Chapter 3). This indicates that available carbon sources present in the xylem can have a profound effect on the metabolism of endophytic bacteria and furthermore exert selective pressure on bacterial communities and alpha diversity of the endophytic microbiome (Beckers et al. 2015, Chapter 3).

Pairwise comparisons (PCA, hierarchical clustering and ANOSIM) of the beta-diversity of host-genotypes (wild type and *CCR* deficient poplar) within each plant compartment (rhizosphere soil, root, stem, leaf) revealed significant host-genotype effects. Remarkably, host-genotype effects were different for the plant compartments (Figure 5.4, Table 5.3, Supplementary Figure 5.2A, 5.4 and 5.5). In the rhizosphere soil, bacterial assemblages displayed no relevant clustering according to genotype, as visually apparent by the PCA analysis and hierarchical clustering (Figure 5.4A) and statistically supported by ANOSIM (phylum level: $P = 0.58$ and genus-level: $P = 0.15$) (Table 5.3 and Supplementary Figure 5.4 and 5.5). These results support our previous findings on the cultivable fraction (Beckers et al. 2015, Chapter 3) and the findings of Danielsen et al. (2013) who reported that transgenic poplar lines modified in the lignin biosynthesis showed a normal capacity to form ectomycorrhiza. Moreover, this also indicates that from an environmental health aspect, at least at the level of the plant-associated microbiome, genetic modification of the lignin biosynthesis evokes no significant changes in the rhizosphere soil, *i.e.* outside the trees. In the roots and stems,

we did observe significant clustering of the bacterial communities according to host-genotype (Figure 5.4B,C; Table 5.3 and Supplementary Figures 5.2B, C and supplementary figure 5.4 and 5.5). *CCR* down-regulation in poplar leads to significant changes in xylem composition and most notably to the accumulation of various extractable phenolics (Leplé et al., 2007). Accessible carbon sources are therefore obviously differential between wild type and *CCR*-down-regulated poplar trees. In the roots, lignin biosynthesis begins upon termination of primary root growth where after secondary growth commences and lignified cell walls are formed (Bulgarelli et al., 2013; Mittler & Lam, 1995). Therefore, mature root systems contain ample amounts of woody material. Indeed, we sampled the poplar trees after 2.5 years of growth and roots were therefore clearly lignified and accumulation of phenolics (as caused by *CCR* down-regulation) could explain the presence of different bacterial community structures in the wild type and *CCR* deficient poplar trees. In the stems, secondary thickening of the cell walls and lignin biosynthesis/deposition (the final stage of xylem differentiation) are well visible (Boerjan et al., 2003; Vanholme et al., 2010). Most pronounced effects of *CCR* gene silencing and changes in the xylem composition are therefore found in the stems of poplar trees. Moreover, direct contact between endophytes and increased concentrations of extractable phenolics in the xylem vessels is expected since lumen colonization of xylem vessels has been frequently reported as a route for bacterial dispersion to vegetative plant parts (Compant et al., 2010; Hardoim et al., 2008). In the leaves, we observed no clustering of samples according to genotype (Figure 5.4D, Table 5.3 and Supplementary Figures 5.2D and supplementary figure 5.4 and 5.5). Possibly intra-compartment localization of the leaf endophytes, which can also be located extracellularly (Lindow and Brandle, 2003), could explain the lack of effects in this compartment since direct contact between the endophytes and metabolites is partly avoided. However, in a previous experiment (Beckers et al. 2015, Chapter 3), we observed significant differences in the leaves. There we used a selective isolation/enrichment approach with ferulic acid to isolate the cultivable bacterial microbiome. This indicates that the effect of *CCR* down-regulation could possibly persist in the leaves, but solely affects metabolic capacities of the present leaf endophytes without altering the structural composition of the leaf microbiome, which we assessed in this approach.

Weak host-genotype effects were previously reported for different *Arabidopsis* ecotypes and different potato cultivars. Lundberg et al. (2012) evaluated the bulk soil, rhizosphere soil and the root compartment of eight *Arabidopsis* ecotypes using 16S rRNA pyrosequencing. They revealed 12 OTUs, which exhibited host genotype-dependent quantitative enrichment in the root compartment. Whereas Bulgarelli et al. (2012), in a similar approach, identified only one OTU, which was differentially abundant in two *Arabidopsis* ecotypes. Furthermore Weinert et al. (2011), using a PhyloChip analysis, examined the root microbiota of three field-grown potato cultivars in two different soils and only 9% of the detected OTUs showed quantitative cultivar dependence.

5.4.4. Drivers of plant compartment effects and host-genotype effects

In the rhizosphere soil, irrespective of genotype, Actinobacteria and Proteobacteria and to a lesser extent Bacteroidetes, Firmicutes and Acidobacteria dominated the rhizobacterial assemblages. The ratio between Proteobacteria and Acidobacteria in rhizosphere bacterial communities has previously been shown to be an indicator of soil nutrient-content where *Proteobacteria* were linked to nutrient-rich soils and *Acidobacteria* to nutrient-poor soils (Castro et al. 2010; Gottel et al., 2011; Smit et al. 2001). Proteobacteria dominated all endosphere plant compartments (Supplementary Table 5.3). In general, Proteobacteria typically dominate endophytic bacterial assemblages which suggests substantial overlap in key community members across host species (Bulgarelli et al., 2012; Gottel et al., 2011; Inceoğlu et al., 2010; Lundberg et al., 2012; Romero et al., 2014). At the genus-level, rhizosphere soil communities were dominated primarily by *Rhizobiales, Actinomycetales, Burkholderiales, Arthrobacter, Variovorax, Bacilliales, Chitinophagaceae* and *Microvirga* which are routinely isolated from soil samples (Berg & Smalla, 2009; Bulgarelli et al., 2013; Gottel et al., 2011; Haichar et al., 2008; Mongodin et al., 2006). Root endophytic assemblages were dominated by *Rhizobiales, Rhizobium and TM7*. Dominant members of the stem samples are *Pseudomonas, TM7, Methylobacterium and Deinococcus.* Finally, leaf samples mainly consisted of *Pseudomonas, Sphingomonas* and *Methylobacterium*. All of the above mentioned OTUs, which have been isolated from a variety of plant samples, may provide beneficial effects on plant health and growth (Innerebner et al., 2011; Delmotte et al., 2009; Mark et al. 2006; Patten & Glick, 2002; Wu

et al., 2011). Host-genotype effects at OTU-level in roots and stems revealed 7 OTUs in each plant compartment, which were differentially abundant ($P < 0.05$) in wild type and *CCR* deficient poplar trees (Supplementary table 5.4). However, inferring general ecological significance from these host genotype effects is difficult and speculative. One remarkable difference is the higher relative abundance of *Staphylococcus* in the stems and leaves of *CCR* deficient trees (Supplementary table 5.4). Lignin molecules, besides conferring rigidity to the cell wall for structural support and impermeability for transport (water and nutrients), also play a crucial role in the protection against biotic and abiotic stress (phytopathogens) (Boerjan et al., 2003; Miedes et al. 2014). We can therefore tentatively speculate that *CCR* deficient poplar trees are more susceptible to colonization of certain phytopathogens such as *Staphylococcus*. However, 16S rRNA metabarcoding is inherently limited to the genus-level or higher taxonomic ranks and pathogenicity is often determined by subgenus or even subspecies variation. For example *Staphylococcus* and also *Pseudomonas* contain examples of strains ranging from completely harmless bacteria (or even plant growth promoting) to pathogens and depending on the length and region of the 16S rRNA sequenced, they may appear identical (Blakney and Patten, 2011; Takahashi et al., 1998). Furthermore, Miedes et al. (2014) reviewed the role of secondary cell walls (including lignin content) in the resistance against pathogens. They concluded contra-intuitively that the effects of lignin modification in respect to resistance against pathogens is highly variable depending on the specific gene modification and resistance of modified plants against pathogens was even increased for some gene modifications (Miedes et al, 2014).

5.5. Conclusion

In conclusion, our data confirm microbiome niche differentiation reports at the rhizosphere-root interface but furthermore suggest additional fine-tuning and niche differentiation of microbiota in the aerial plant organs. Furthermore, we identified host-genotype effects, which are reminiscent of the host-genotype-dependent associations shaping the human microbiome. The host genotype was found to have a profound effect on the bacterial community structure in the endosphere of *CCR* deficient poplar trees (the roots and stems), without perceptible effects on the rhizospheric and leaf endosphere bacterial

communities. In depth metabolite profiling of all the plant environments of field-grown *CCR*-down-regulated poplar trees in comparison with the WT poplars as well as root exudate profiling could provide more insight into the main abiotic factors responsible for the microbiome differentiation between the studied genotypes.

References

Bais, H. P., Weir, T. L., Perry, L. G., Gilroy, S. and Vivanco, J. M. (2006). The role of root exudates in rhizosphere interactions with plants and other organisms. *Annual Review of Plant Biology*, *57*, 233–266.

Berg, G. and Smalla, K. (2009). Plant species and soil type cooperatively shape the structure and function of microbial communities in the rhizosphere. *FEMS Microbiology Ecology*, *68*, 1–13.

Blakney, A. J. and Patten, C. L. (2011). A plant-growth promoting pseudomonad is closely related to the Pseudomonas syringae complex of plant pathogens. *FEMS Microbiology Ecology*, *77*, 546-557.

Bodenhausen, N., Horton, M. W. and Bergelson, J. (2013). Bacterial communities associated with the leaves and the roots of Arabidopsis thaliana. *PloS One*, *8*, e56329.

Boerjan, W., Ralph, J., & Baucher, M. (2003). Lignin biosynthesis. *Annual Review of Plant Biology*, *54*, 519–546.

Bonito, G., Reynolds, H., Robeson, M. S., Nelson, J., Hodkinson, B. P., Tuskan, G., Schadt, C. and Vilgalys, R. (2014). Plant host and soil origin influence fungal and bacterial assemblages in the roots of woody plants. *Molecular Ecology*, *23*, 3356–3370.

Brader, G., Compant, S., Mitter, B., Trognitz, F. and Sessitsch, A. (2014). Metabolic potential of endophytic bacteria. *Current Opinion in Biotechnology*, *27*, 30–37.

Bulgarelli, D., Rott, M., Schlaeppi, K., Ver Loren van Themaat, E., Ahmadinejad, N., Assenza, F., Rauf, P., Huettel, B., Reinhardt, R., Schmelzer, E., Perlies, J., Gloeckner, F. O., Amann, R., Eickhorst, T. and Schulze-Lefert, P. (2012). Revealing structure and assembly cues for Arabidopsis root-inhabiting bacterial microbiota. *Nature*, *488*, 91–95.

Bulgarelli, D., Schlaeppi, K., Spaepen, S., Ver Loren van Themaat, E. and Schulze-Lefert, P. (2013). Structure and functions of the bacterial microbiota of plants. *Annual Review of Plant Biology*, *64*, 807–838.

Cáceres, M. D. and Legendre, P. (2009). Associations between species and groups of sites: indices and statistical inference. *Ecology*, *90*, 3566–3574.

Castro, H. F., Classen, A. T., Austin, E. E., Norby, R. J. and Schadt, C. W. (2010). Soil microbial community responses to multiple experimental climate change drivers. *Applied and Environmental Microbiology*, *76*, 999–1007.

Chen, F. and Dixon, R. A. (2007). Lignin modification improves fermentable sugar yields for biofuel production. *Nature Biotechnology*, *25*, 759–761.

Clarke, K. R. (1993). Non-parametric multivariate analyses of changes in community structure. *Austral Ecology*, *18*, 117–143.

Coddington, J. A., Agnarsson, I., Miller, J. A., Kuntner, M. and Hormiga, G. (2009). Undersampling bias : the null hypothesis for singleton species in tropical arthropod surveys. *Journal of Animal Ecology*, *78*,573–584.

Compant, S., Clément, C. and Sessitsch, A. (2010). Plant growth-promoting bacteria in the rhizo- and endosphere of plants: Their role, colonization, mechanisms involved and prospects for utilization. *Soil Biology and Biochemistry*, *42*, 669–678.

Custers, R. (2009). First GM trial in Belgium since 2002. *Nature Biotechnology*, 27, 506.

Danielsen, L., Lohaus, G., Sirrenberg, A., Karlovsky, P., Bastien, C., Pilate, G. and Polle, A. (2013). Ectomycorrhizal colonization and diversity in relation to tree biomass and nutrition in a plantation of transgenic poplars with modified lignin biosynthesis. *PloS One*, *8*, e59207.

DeAngelis, K. M., Brodie, E. L., DeSantis, T. Z., Andersen, G. L., Lindow, S. E. and Firestone, M. K. (2009). Selective progressive response of soil microbial community to wild oat roots. *The ISME Journal*, *3*, 168–178.

Delmotte, N., Knief, C., Chaffron, S., Innerebner, G., Roschitzki, B., & Schlapbach, R. (2009). Community proteogenomics reveals insights into the physiology of phyllosphere bacteria. *Proceedings of the National Academy of Sciences of the United States of America*, *106*, 16428-16433.

Dickie, I. A. (2010). Letters Insidious effects of sequencing errors on perceived diversity in molecular surveys. The New Phytologist, *188*, 916–918.

Dillon, R. J. and Dillon, V. M. (2004). The gut bacteria of insects: nonpathogenic interactions. *Annual Review of Entomology*, *49*, 71–92.

Dyall, S. D., Brown, M. T. and Johnson, P. J. (2004). Ancient invasions: from endosymbionts to organelles. *Science*, *304*, 253–257.

Edgar, R. C., Haas, B. J., Clemente, J. C., Quince, C. and Knight, R. (2011). UCHIME improves sensitivity and speed of chimera detection. *Bioinformatics*, *27*, 2194–2200.

Feinstein, L. M., Sul, W. J. and Blackwood, C. B. (2009). Assessment of bias associated with incomplete extraction of microbial DNA from soil. *Applied and Environmental Microbiology*, *75*, 5428–5433.

Gans, J., Wolinsky, M. and Dunbar, J. (2005). Computational improvements reveal great bacterial diversity and high metal toxicity in soil. *Science*, *309*, 1387–1390.

Gil, R., Latorre, A. and Moya, A. (2010). Evolution of Prokaryote-Animal Symbiosis from a Genomics Perspective. *(Endo)symbiotic Methanogenic Archaea*, *19*, 207-232.

Gottel, N. R., Castro, H. F., Kerley, M., Yang, Z., Pelletier, D. A., Podar, M., Karpinets, T., Tuskan, G. A., Vilgalys, R., Mitchel, J., Schadt, C. W., Uberbacher, E. and Doktycz, M. J. (2011). Distinct Microbial Communities within the Endosphere and Rhizosphere of Populus deltoides Roots across Contrasting Soil Types. *Applied and Environmental Microbiology*, 77, 5934-5944.

Grayston, S. J., Vaughan, D. and Jones, D. (1997). Rhizosphere carbon flow in trees, in comparison with annual plants: the importance of root exudation and its impact on microbial activity and nutrient availability. *Applied Soil Ecology*, *5*, 29–56.

Haichar, F. E. Z., Marol, C., Berge, O., Rangel-Castro, J. I., Prosser, J. I., Balesdent, J., Heulin, T. and Achouak, W. (2008). Plant host habitat and root exudates shape soil bacterial community structure. *The ISME Journal*, *2*, 1221–1230.

Hallmann, J. and Berg, B. (2007). Spectrum and population dynamics of bacterial root endophytes. In B. J. E. Schulz, C. J. C. Boyle, & T. N. Sieber (Eds.), *Microbial Root Endophytes* (pp. 15–31). Berlin, Heidelberg: Springer.

Hansen, A. K. and Moran, N. A. (2014). The impact of microbial symbionts on host plant utilization by herbivorous insects. *Molecular Ecology*, *23*, 1473–1496.

Hardoim, P. R., Andreote, F. D., Reinhold-Hurek, B., Sessitsch, A., van Overbeek, L. S. and Van Elsas, J. D. (2011). Rice root-associated bacteria: insights into community structures across 10 cultivars. *FEMS Microbiology Ecology*, *77*, 154–164.

Hardoim, P. R., van Overbeek, L. S. and Van Elsas, J. D. (2008). Properties of bacterial endophytes and their proposed role in plant growth. *Trends in Microbiology*, *16*, 463–471.

Hirano, S. S. (2000). Bacteria in the Leaf Ecosystem with Emphasis on Pseudomonas syringae — a Pathogen , Ice Nucleus , and Epiphyte, *64*, 624–653.

Hur, M., Kim, Y., Song, H.-R., Kim, J. M., Choi, Y. I. and Yi, H. (2011). Effect of genetically modified poplars on soil microbial communities during the phytoremediation of waste mine tailings. *Applied and Environmental Microbiology*, *77*, 7611–7619.

Huse, S. M., Huber, J. a, Morrison, H. G., Sogin, M. L., & Welch, D. M. (2007). Accuracy and quality of massively parallel DNA pyrosequencing. *Genome Biology*, *8*, R143.1-R143.9.

Huse, S. M., Welch, D. M., Morrison, H. G. and Sogin, M. L. (2010). Ironing out the wrinkles in the rare biosphere through improved OTU clustering. *Environmental Microbiology*, *12*, 1889–1898.

Inceoğlu, O., Salles, J. F., van Overbeek, L. and Van Elsas, J. D. (2010). Effects of plant genotype and growth stage on the betaproteobacterial communities associated with different potato cultivars in two fields. *Applied and Environmental Microbiology*, *76*, 3675–3684.

Innerebner, G., Knief, C. and Vorholt, J. A. (2011). Protection of Arabidopsis thaliana against leaf-pathogenic Pseudomonas syringae by Sphingomonas strains in a controlled model system. *Applied and Environmental Microbiology*, *77*, 3202–3210.

Jones, J. D. G. and Dangl, J. L. (2006). The plant immune system. *Nature*, *444*, 323–329.

Klindworth, A., Pruesse, E., Schweer, T., Peplies, J., Quast, C., Horn, M., & Glöckner, F. O. (2013). Evaluation of general 16S ribosomal RNA gene PCR primers for classical and next-generation sequencing-based diversity studies. *Nucleic Acids Research*, *41*, e1: 1-11.

Koch, L. (2014). Metagenomics: Shaping the gut microbiome. *Nature Reviews. Genetics*, *16*, 2-3.

Kunin, V., Engelbrektson, A., Ochman, H. and Hugenholtz, P. (2010). Wrinkles in the rare biosphere: pyrosequencing errors can lead to artificial inflation of diversity estimates. *Environmental Microbiology*, *12*, 118–123.

Leplé, J.-C., Brasileiro, A. C. ., Michel, M. F., Delmotte, F., & Jouanin, L. (1992). Expression of chimeric genes using four different constructs. *Plant Cell Reports*, *11*, 137–141.

Leplé, J.-C., Dauwe, R., Morreel, K., Storme, V., Lapierre, C., Pollet, B., Naumann A., Kang, K., Kim, H., Ruel, K., Lefèbvre, A., Joseleau, J., Grima-Pettenati, J., De Rycke, R., Andersson-Gunneråś, S., Erban, A., Fehrle A., Petit-Conil, M., Kopka, J., Polle, A., Messens, E., Sundberg, B., Mansfield, S., Ralph, J., Pilate, G. and Boerjan, W. (2007). Down-regulation of cinnamoyl-coenzyme A reductase in poplar: multiple-level phenotyping reveals effects on cell wall polymer metabolism and structure. *The Plant Cell*, *19*, 3669–3691.

Lindow, S. E. and Brandl, M. T. (2003). Microbiology of the Phyllosphere. *Applied and Environmental Microbiology*, *69*, 1875–1883.

Lugtenberg, B. and Dekkers, L. C. (1999). What makes Pseudomonas bacteria rhizosphere competent . *Environmental Microbiology*, *1*, 9–13.

Lugtenberg, B. and Kamilova, F. (2009). Plant-growth-promoting rhizobacteria. *Annual Review of Microbiology*, *63*, 541–556.

Lundberg, D. S., Lebeis, S. L., Paredes, S. H., Yourstone, S., Gehring, J., Malfatti, S., Tremblay, J., Engelbrektson, A., Kunin, V., del Rio, T. G., Edgar, R. C., Eickhorst, T., Ley, R. E., Hugenholtz, P., Tringe, S. G. and Dangl, J. L. (2012). Defining the core Arabidopsis thaliana root microbiome. *Nature*, *488*, 86–90.

Mark, G., Morrissey, J. P., Higgins, P. and O'gara, F. (2006). Molecular-based strategies to exploit Pseudomonas biocontrol strains for environmental biotechnology applications. *FEMS Microbiology Ecology*, *56*, 167–77.

McCully, M. E. (2001). Niches for bacterial endophytes in crop plants: a plant biologist's view. *Australian Journal of Plant Physiology*, *28*, 983–990.

Medinger, R., Nolte, V., Pandey, R. V., Jost, S., Ottenwälder, B., Schlötterer, C., and Boenigk, J. (2010). Diversity in a hidden world: potential and limitation of next-generation sequencing for surveys of molecular diversity of eukaryotic microorganisms. *Molecular Ecology*, *19*, 32–40.

Miedes, E., Vanholme, R., Boerjan, W. and Molina, A. (2014). The role of the secondary cell wall in plant resistance to pathogens. *Frontiers in Plant Science*, *5*, 358.

Mittler, R. and Lam, E. (1995). In Situ Detection of nDNA Fragmentation during the Differentiation of Tracheary Elements in Higher Plants. *Plant Physiology*, *108*, 489–493.

Mongodin, E. F., Shapir, N., Daugherty, S. C., DeBoy, R. T., Emerson, J. B., Shvartzbeyn, A., Radune, D., Vanmathevan, J., Riggs, F., Grinberg, V., Khouri, H., Wackett, L. P., Nelson, K. E. and Sadowsky, M. J. (2006). Secrets of soil survival revealed by the genome sequence of Arthrobacter aurescens TC1. *PLoS Genetics*, *2*, e214.

Op De Beeck, M., Lievens, B., Busschaert, P., Declerck, S., Vangronsveld, J. and Colpaert, J. V. (2014). Comparison and validation of some ITS primer pairs useful for fungal metabarcoding studies. *PloS One*, *9*, e97629.

Patten, C. L. and Glick, B. R. (2002). Role of *Pseudomonas putida* Indoleacetic Acid in Development of the Host Plant Root System, *68*(8), 3795–3801.

Pielou, E. C. (1966). The measurement of diversity in different types of biological collections. *Journal of Theoretical Biology*, *13*, 131–144.

Pruesse, E., Quast, C., Knittel, K., Fuchs, B. M., Ludwig, W., Peplies, J. and Glöckner, F. O. (2007). SILVA: a comprehensive online resource for quality checked and aligned ribosomal RNA sequence data compatible with ARB. *Nucleic Acids Research*, *35*, 7188–7196.

Quince, C., Lanzén, A., Curtis, T. P., Davenport, R. J., Hall, N., Head, I. M., Read, L. F. and Sloan, W. T. (2009). Accurate determination of microbial diversity from 454 pyrosequencing data. *Nature Methods*, *6*, 639–41.

R Development Core Team (2011). R: A language and environment for statistical computing. R Foundation for Statistical Computing, Vienna, Austria. ISBN 3-900051-07-0, URL http://www.R-project.org/.

Raven, P. H. (1970). A Multiple Origin for Plastids and Mitochondria: Many independent symbiotic events may have been involved in the origin of these cellular organelles. *Science*, *169*, 641–646.

Reeder, J. and Knight, R. (2010). Rapidly denoising pyrosequencing amplicon reads by exploiting rank-abundance distributions. *Nature Methods*, *7*, 668–669.

Reich, M., Murat, C., Morin, E., Nilsson, R. H., Uroz, S. and Martin, F. (2009). 454 Pyrosequencing analyses of forest soils reveal an unexpectedly high fungal diversity. The New Phytologist, *184*, 449–456.

Roesch, L. F. W., Fulthorpe, R. R., Riva, A., Casella, G., Hadwin, A. K. M., Kent, A. D., Daroub, S. H., Camaro, F. A. O., Farmerie, W. G. and Triplett, E. W. (2007). Pyrosequencing enumerates and contrasts soil microbial diversity. *The ISME Journal*, *1*, 283–290.

Romero, F. M., Marina, M. and Pieckenstain, F. L. (2014). The communities of tomato (*Solanum lycopersicum L.*) leaf endophytic bacteria, analyzed by 16S-ribosomal RNA gene pyrosequencing. *FEMS Microbiology Letters*, *351*, 187–94.

Ryan, R. P., Germaine, K., Franks, A., Ryan, D. J. and Dowling, D. N. (2008). Bacterial endophytes: recent developments and applications. *FEMS Microbiology Letters*, *278*, 1–9.

Schloss, P. D., Westcott, S. L., Ryabin, T., Hall, J. R., Hartmann, M., Hollister, E. B., Lesniewski, R. A., Oakley, B. B., Parks, D. H., Robinson, C. J., Sahl, J. W., Stres, B., Thallinger, G. G., Van Horn, D. J. and Weber, C. F. (2009). Introducing mothur: open-source, platform-independent, community-supported software for describing and comparing microbial communities. *Applied and Environmental Microbiology*, *75*, 7537–7541.

Shade, A., Jones, S. E., Caporaso, J. G., Handelsman, J., Knight, R., Fierer, N. and Gilbert, A. (2014). Conditionally Rare Taxa Disproportionately Contribute to Temporal Changes in Microbial Diversity. *American Society for Microbiology*, *5*, 1–9.

Simpson, E. H. (1949). Measurement of Diversity. *Nature*, *163*, 688–688.

Smit, E., Leeflang, P., Gommans, S., Mil, S. V. A. N. and Wernars, K. (2001). Diversity and Seasonal Fluctuations of the Dominant Members of the Bacterial Soil Community in a Wheat Field as Determined by Cultivation

and Molecular Methods. *Applied and Environmental Microbiology*, *67*, 2284–2291.

Sogin, M. L., Morrison, H. G., Huber, J. A, Mark Welch, D., Huse, S. M., Neal, P. R., Arrieta, J. M. and Herndl, G. J. (2006). Microbial diversity in the deep sea and the underexplored "rare biosphere". *Proceedings of the National Academy of Sciences of the United States of America*, *103*, 12115–12120.

Spor, A., Koren, O. and Ley, R. (2011). Unravelling the effects of the environment and host genotype on the gut microbiome. *Nature Reviews. Microbiology*, *9*, 279–290.

Studer, M. H., Demartini, J. D., Davis, M. F., Sykes, R. W., Davison, B. and Keller, M. (2011). Lignin content in natural Populus variants affects sugar release. *Proceedings of the National Academy of Sciences of the United States of America*, *108*, 6300-6305.

Sudakaran, S., Salem, H., Kost, C. and Kaltenpoth, M. (2012). Geographical and ecological stability of the symbiotic mid-gut microbiota in European firebugs, Pyrrhocoris apterus (Hemiptera, Pyrrhocoridae). *Molecular Ecology*, *21*, 6134–6151.

Takahashi, T., Satoh, I. and Kikuchi, N. (1998). Phylogenetic relationship of 38 taxa of the genus *Staphylococcus* based on 16S rRNA gene sequence analysis. International Journal of Systematic and Evolutionary Microbiology, *49*, 725-728.

Tedersoo, L., Nilsson, R. H., Abarenkov, K., Jairus, T., Sadam, A., & Saar, I. (2010). Methods 454 Pyrosequencing and Sanger sequencing of tropical mycorrhizal fungi provide similar results but reveal substantial methodological biases. *The New Phytologist*, *188*, 291–301.

The Human Microbiome Project Consortium. Structure, function and diversity of the healthy human microbiome. (2012). *Nature*, *486*, 207–14.

Van Acker, R., Leplé, J.-C., Aerts, D., Storme, V., Goeminne, G., Ivens, B., Légée, F., Lapierre, C., Piens, K., Van Montagu, M., C., E., Santoro, N., Foster, C., E., Ralph, J., Soetaert, W., Pilate, G. and Boerjan, W. (2014). Improved saccharification and ethanol yield from field-grown transgenic poplar deficient in cinnamoyl-CoA reductase. *Proceedings of the National Academy of Sciences of the United States of America*, *111*, 845–50.

Vanholme, R., Demedts, B., Morreel, K., Ralph, J. and Boerjan, W. (2010). Lignin biosynthesis and structure. *Plant Physiology*, *153*, 895–905.

Vanholme, R., Morreel, K., Darrah, C., Oyarce, P., Grabber, J. H., Ralph, J. and Boerjan, W. (2012). Metabolic engineering of novel lignin in biomass crops. *The New Phytologist*, *196*, 978–1000.

Vanholme, R., Morreel, K., Ralph, J. and Boerjan, W. (2008). Lignin engineering. *Current Opinion in Plant Biology*, *11*, 278–85.

Walker, T. S., Bais, H. P., Grotewold, E. and Vivanco, J. M. (2003). Update on Root Exudation and Rhizosphere Biology Root Exudation and Rhizosphere Biology. *Plant Physiology*, *132*, 44–51.

Weinert, N., Piceno, Y., Ding, G.-C., Meincke, R., Heuer, H., Berg, G., Schloter, M., Andersen, G. and Smalla, K. (2011). PhyloChip hybridization uncovered an enormous bacterial diversity in the rhizosphere of different potato cultivars: many common and few cultivar-dependent taxa. *FEMS Microbiology Ecology*, *75*, 497–506.

Weyens, N., van der Lelie, D., Taghavi, S., & Vangronsveld, J. (2009). Phytoremediation: plant-endophyte partnerships take the challenge. *Current Opinion in Biotechnology*, *20*, 248–54.

Wilkerson, C. G., Mansfield, S. D., Lu, F., Withers, S., Park, J.-Y., Karlen, S. D., Gonzales-Vigil, E., Padmakshan, D., Unda, F., Rencoret, J. and Ralph, J. (2014). Monolignol ferulate transferase introduces chemically labile linkages into the lignin backbone. *Science*, *344*, 90–93.

Wu, X., Monchy, S., Taghavi, S., Zhu, W., Ramos, J. and van der Lelie, D. (2011). Comparative genomics and functional analysis of niche-specific adaptation in *Pseudomonas putida*. *FEMS Microbiology Reviews*, *35*, 299–323.

Supplementary information

Supplementary Table 5.1. Field identification numbers of sampled poplar trees *(Populus tremula x alba*

Individual	Wild type	*CCR* deficient
1	K5R31	K14R12
2	K10R36	K6R22
3	K14R32	K8R23
4	K8R37	K8R24
5	K5R33	K5R19
6	K12R32	K10R25
7	K5R36	K7R19
8	K8R31	K6R8
9	K15R33	K9R15
10	K5R34	K13R10
11	K13R35	K5R23
12	K5R37	K5R25

Supplementary Table 5.2 Retrieval of singleton sequences from the different plant compartments and host genotypes.

Plant compartment	Rhizosphere soil		Root	
Host Genotype	WT	*CCR*	WT	*CCR*
Singletons	26.09% ± 0.01% a	27.80% ± 0.69% a	5.01% ± 0.55% b	6.90% ± 0.89% b

Plant compartment	Stem		Leaf	
Host Genotype	WT	*CCR*	WT	*CCR*
Singletons	2.60% ± 0.35% c	1.63% ± 0.31% c	2.21% ± 0.65% c	1.45% ± 0.35% c

Values represent relative average abundance (%) ± standard deviation of twelve biologically independent replicates. Data were analyzed using two-way ANOVA and post hoc Tukey-Kramer comparisons. Significant differences are indicated with lower case letters (P < 0.05).

Supplementary Table 5.3. *Plant compartment and host genotype effects on individual bacterial phyla.*

Plant compartment	Rhizosphere soil		Root		Stem		Leaf		Host-Genotype effect		Plant Compartment effect		Interaction	
Host-genotype	WT	CCR	WT	CCR	WT	CCR	WT	CCR	F	P	F	P	F	P
Acidobacteria	1.81 a	1.85 a	0.22 b	0.18 b	1.08 a	0.003 b	0.27 b	0.001 b	3.74	0.0564	25.96	<0.0001	2.75	0.0480
Actinobacteria	27.19 a	24.18 a	6.97 b	3.89 b	12.12 b	8.11 b	9.56 b	6.23 b	7.69	0.0068	59.00	<0.0001	0.03	0.9913
Armatimonadetes	0.02 a	0.01 a	0.003 a	0.01 a	0.009 a	0.00 a	0.00 a	0.00 a	0.01	0.9188	2.76	0.0468	1.39	0.2503
Bacteroidetes	3.38 a b	4.52 a	4.03 a	1.44 b c	1.39 c	1.3 c	0.66 c	0.19 c	1.44	0.2332	13.51	<0.0001	3.76	0.0137
Chlamydiae	0.6 a	0.59 a	0.1 a	0.08 a	1.22 a	0.00 a	0.01 a	0.005 a	1.42	0.2369	1.49	0.2232	1.27	0.2910
Chlorobi	0.00 a	0.006 a	0.00 a	0.00 a	0.00 a	0.00 a	0.00 a	0.00 a	2.12	0.1489	2.30	0.0826	2.30	0.0826
Chloroflexi	0.00 a	0.01 a	0.00 a	0.002	0.00 a	0.00 a	0.00 a	0.00 a	3.08	0.0830	1.42	0.2418	1.42	0.2418
Deinococcus-Thermus	0.003 a	0.003 a	0.02 a	0.00 a	3.37 b	4.78 b	0.77 a	0.83 a	0.20	0.6561	5.52	0.0016	0.18	0.9109
Fusobacteria	0.00 a	0.00 a	0.004 a	0.03 a	0.04 a	0.009 a	0.06 a	0.05 a	0.05	0.8348	1.79	0.1545	0.41	0.7440
Gemmatimonadetes	0.11 a	0.16 a	0.00 b	0.003 b	0.00 b	0.00 b	0.00 b	0.00 b	1.64	0.2034	57.63	<0.0001	1.43	0.2403
Nitrospira	0.69 a	0.51 a	0.00 b	0.002 b	0.00 b	0.00 b	0.03 b	0.00 b	2.20	0.1414	73.23	<0.0001	1.58	0.1992
Planctomycetes	0.03 a	0.03 a	0.00 b	0.003 b	0.00 b	0.00 b	0.00 b	0.00 b	0.22	0.6370	17.10	<0.0001	0.09	0.9671
Alphaproteobacteria	25.17 a	24.57 a	47.05 b	64.6 b	30.02 a	21.52 a	45.64 b	39.18 b	0.02	0.8816	21.12	<0.0001	3.42	0.0208
Betaproteobacteria	24.84 a	25.18 a	18.18 a	13.26 a	9.69 b	6.57 b	5.14 b	4.76 b	1.63	0.2048	31.47	<0.0001	0.63	0.5987
Deltaproteobacteria	1.9 a	1.71 a	0.43 b	0.1 b	0.12 b	0.00 b	0.03 b	0.00 b	3.79	0.0548	98.50	<0.0001	0.56	0.6407
Epsilonproteobacteria	0.00 a	0.00 a	0.00 a	0.00 a	0.00 a	0.00 a	0.001 a	0.00 a	1.16	0.2839	1.11	0.3483	1.11	0.3483
Gammaproteobacteria	9.62 a	9.99 a	9.12 a	10.79 a	23.78 b	40.79 b	32.83 b	28.06 b	1.10	0.2964	13.36	<0.0001	1.79	0.1549
Tenericutes	0.00 a	0.00 a	0.00 a	0.00 a	0.00 a	0.005 a	0.00 a	0.00 a	1.16	0.2839	1.11	0.3483	1.11	0.3483
Verrucomicrobia	0.36 a	0.32 a	0.03 b	0.008 b	0.15 b	0.00 b	0.02 b	0.00 b	3.19	0.0776	25.79	<0.0001	0.89	0.4497
BRC1	0.00 a	0.002 a	0.00 a	0.00 a	0.00 a	0.00 a	0.00 a	0.00 a	0.97	0.3277	0.98	0.4042	0.98	0.4042
Firmicutes	4.12 a	6.14 a	2.04 a	0.51 b	6.74 a	16.87 c	3.9 a	20.25 c	6.05	0.0159	3.83	0.0126	2.18	0.0964
TM7	0.17 a	0.22 a	11.82 b	5.1 c	10.29 b	0.05 a	1.09 a	0.45 a	7.14	0.0090	5.97	0.0009	2.22	0.0921

Values represent average relative abundance (%) of twelve biologically independent replicates. Data were analyzed using two-way ANOVA and post hoc Tukey-Kramer comparisons. Significant differences are indicated with lower case letters (P < 0.05).

Supplementary Table 5.4. Plant compartment and host genotype effects on core bacterial OTUs.

Plant Compartment	Rhizosphere soil		Root		Stem		Leaf		Host-Genotype effect		Plant Compartment effect		Interaction	
Host Genotype	WT	CCR	WT	CCR	WT	CCR	WT	CCR	F	P	F	P	F	P
Rhizobiales	12.59 a	10.95 a	8.48 a	17.41 b	3.85 a	2.9 a	3.22 a	1.91 a	1.918	0.1698	20.72	p<0.0001	5.391	0.0019
Actinomycetales	10.13 a	7.66 a	0.9 b	0.83 b	2.1 b	1.46 b	1.3 b	0.93 b	3.318	0.0721	56.12	p<0.0001	0.4391	0.7256
Burkholderiales	6.29 a	5.75 a	2.48 a.b	3.25 a.b	2.97 a.b	1.99 a.b	0.77 b.c	0.47 c	0.2531	0.6162	10.1	p<0.0001	0.6857	0.5632
Arthrobacter	4.4 a	3.14 a	0.06 b	0.02 b	0.05 b	0.02 b	0.02 b	0.00 b	1.771	0.1869	93.34	p<0.0001	1.177	0.3234
Variovorax	3.28 a	3.82 a	5.6 b	1.03 a.c	1.14 a.c	0.24 c	0.93 c	0.1 c	21.02	p<0.0001	16.41	p<0.0001	12.52	p<0.0001
Chitinophagaceae	3.06 a	3.61 a	1.35 a.b	0.68 b.c	0.32 c	0.01 c	0.12 c	0.02 c	1.041	0.3105	38.04	p<0.0001	3.133	0.0298
Bacillales	2.82 a.c	4.15 a.c	0.25 b	0.16 b	0.81 b	0.55 b	1.16 a.b	6.93 c	1.33	0.2521	1.526	0.2138	1.003	0.3958
Microvirga	2.68 a	2.44 a	0.26 b	0.43 b	0.03 b.c	0.00 c	0.1 b.c	<0.01 c	0.0006	0.981	140.2	p<0.0001	0.8896	0.4501
Xanthomonadaceae	1.9 a	1.9 a	0.35 b	0.35 b	1.33 a	0.02 b	0.47 b	0.03 b	3.751	0.0561	3.751	0.0139	2.108	0.1053
Solirubrobacterales	1.9 a	6.29 b	<0.01 c	0.03 c	0.00 c	<0.01 c	1.21 a	0.00 c	1.331	0.2519	13.11	p<0.0001	7.191	0.0002
Burkholderia	1.3 a	1.99 a	1.4 a	1.79 a	0.94 a	0.03 a	0.07 a	0.23 a	0.01306	0.9093	2.385	0.0749	0.6517	0.5841
Rhizobium	0.4 a	0.34 a	22.8 b	31.18 b	0.83 a	0.45 a	6.43 c	1.43 a	0.00673	0.9348	63.66	p<0.0001	2.644	0.0544
TM7	0.25 a	0.31 a	15.77 b	5.83 c	11.23 b	0.06 a	1.38 a	0.63 a	9.729	0.0025	7.398	0.0002	2.824	0.0436
Novosphingobium	0.06 a	0.13 a	3.76 b	1.81 c	0.08 a	0.02 a	0.03 a	0.03 a	2.82	0.0968	18.32	p<0.0001	2.871	0.0412
Pseudomonas	1.07 a	1.04 a	3.62 a	4.09 a	17.64 b.c	11.11 b	26.95 c	26.11 c	0.4039	0.5268	22.97	p<0.0001	0.3186	0.8119
Phenylobacterium	0.88 a	0.94 a	2.13 a	0.83 a	0.18 a	0.00 a	0.07 a	<0.01 a	0.6258	0.4311	1.915	0.1334	0.526	0.6656
Niastella	0.03 a	0.03 a	2.01 b	0.37 a	<0.01 a	0.00 a	0.00 a	0.00 a	7.487	0.0076	15.38	p<0.0001	7.591	0.0001
Staphylococcus	0.00 a	<0.01 a	1.75 a	0.13 a	3.56 a	11.14 a	1.22 a	7.46 a	2.794	0.0983	3.14	0.0295	1.484	0.2247
Escherichia_Shigella	0.00 a	0	0.04 a	4.51 b	0.24 a	1.12 a	0.07 a	0.46 a	1.434	0.2344	0.7358	0.5336	0.7494	0.5257
Comamonadaceae	1.8 a	0.04 a	0.98 a	4.49 b	0.83 a	0.57 a	0.98 a	0.36 a	1.737	0.1911	7.193	0.0002	7.49	0.0002
Bradyrhizobiaceae	0.71 a	0.57 a	1.22 b	1.93 b	1.29 b	0.00 a	0.15 a	0.01 a	1.085	0.3007	8.299	p<0.0001	3.033	0.0337
Methylobacterium	0.19 a	0.14 a	0.07 a	0.06 a	7.37 b	5.49 b.c	8.28 b	4.73 c	2.982	0.0879	22.84	p<0.0001	1.277	0.2875
Sphingomonas	0.06 a	0.05 a	0.05 a	0.15 a	3.92 b	0.94 a	5.29 b	4.64 b	0.5991	0.441	6.092	0.0008	0.3486	0.7903
Deinococcus	<0.01 a	<0.01 a	0.00 a	0.00 a	3.68 b	4.93 b	0.9 a	0.98 a	0.2046	0.6522	4.96	0.0032	0.1736	0.914
Alcaligenaceae	0.04 a	0.05 a	0.02 a	0.11 a	2.21 b	0.08 a	0.06 a	0.03 a	4.25	0.0423	4.734	0.0042	4.47	0.0058
Corynebacterium	<0.01 a	0.00 a	0.18 a	0.09 a	2.17 b	1.44 b	1.49 b	1.65 b	0.2193	0.6408	9.151	p<0.0001	0.31	0.8181
Enterobacteriaceae	0.01 a	0.11 a	0.17 a	0.26 a	0.73 a	20.2 b	0.48 a	0.11 a	3.084	0.0827	3.377	0.0221	3.093	0.0313
Moraxellaceae	<0.01 a	0.00 a	0.22 a	0.1 a	1.65 a.b	5.7 a.b	5.93 b.c	3.95 a.c	0.2292	0.6333	7.334	0.0002	1.735	0.166
Paracoccus	0.00 a	0.00 a	0.07 a.b	0.09 a.b	1.47a.b	4.39 a.b	2.85 a.b	4.69 b	2.341	0.1298	6.45	0.0006	0.8293	0.4814
Streptococcus	0.00 a	0.00 a	0.04 a	0.02 a	0.68 a	2.31 a	1.12 a	1.97 a	1.508	0.2228	3.062	0.0325	0.5981	0.618
Oxalobacteraceae	0.29 a	0.26 a	0.96 a	1.14 a	0.31 a	2.13 a	0.62 a	0.64 a	1.002	0.3198	0.8779	0.456	0.8106	0.4915
Aurantimonas	0.00 a	0.00 a	0.00 a	0.02 a	0.26 a	0.21 a	2.9 b	4.44 b	0.3814	0.5385	8.325	p<0.0001	0.3825	0.7659
Sphingomonadales	0.18 a	0.2 a	0.05 a	0.09 a	0.11 a	1.29 b	2.08 b	1.75 b	0.02335	0.8789	10.93	p<0.0001	0.123	0.9463
Dermacoccus	0.00 a	0.00 a	0.07 a	0.06 a	1.64 b	1.64 b	1.91 b	0.9 a.b	0.08352	0.7733	9.244	p<0.0001	2.098	0.1066
Rhodobacteraceae	0.24 a	0.17 a	0.27 a	0.04 a	0.07 a	0.09 a	0.74 a	4.21 a	0.7347	0.3938	1.504	0.2195	0.8416	0.4749
Percentage of reads covered	56.58	56.08	77.38	83.38	75.69	82.53	81.08	81.73						

Values represent relative average abundance (%) of twelve biologically independent replicates. Data were analyzed using two-way ANOVA and post hoc Tukey-Kramer comparisons. Significant differences are indicated with lower case letters ($P < 0.05$). Green values indicate top 10 OTUs of each plant compartment.

Supplementary Table 5.5. Indicator species analysis of bacterial OTUs within each plant compartment.

Rhizosphere soil				
OTU	Associated with	Indicator value	p-value	Relative abundance (%)
Chromatiales	Wild-type poplar	1	0.0001	0.43
Marisediminicola	Wild-type poplar	0.829	0.0058	0.16
Byssovorax	Wild-type poplar	0.686	0.0444	0.05
Caryophanon	Wild-type poplar	0.671	0.0417	0.06
Aeromonadales	CCR deficient poplar	1	0.0001	0.42
Herminiimonas	CCR deficient poplar	0.871	0.0051	0.18
Streptosporangiaceae	CCR deficient poplar	0.786	0.0194	0.06
Rhodobacter	CCR deficient poplar	0.769	0.0184	0.07
Nevskia	CCR deficient poplar	0.760	0.0478	0.06
Anaeromyxobacter	CCR deficient poplar	0.699	0.0341	0.04
Turicibacter	CCR deficient poplar	0.645	0.0368	0.02
Root				
OTU	Associated with	Indicator value	p-value	Relative abundance (%)
Staphylococcus	Wild-type poplar	0.967	0.0006	1.75
Micromonospora	Wild-type poplar	0.895	0.0043	1.39
Flavobacteriaceae	Wild-type poplar	0.817	0.0198	0.22
Myxococcales	Wild-type poplar	0.790	0.0285	0.40
Chryseobacterium	Wild-type poplar	0.782	0.0152	0.08
Thermomonosporaceae	Wild-type poplar	0.739	0.026	0.17
Sphaerotilus	Wild-type poplar	0.721	0.0212	0.07
Sinobacteraceae	Wild-type poplar	0.674	0.0347	0.05
Acetobacteraceae	CCR deficient poplar	0.856	0.0144	0.26
Labrys	CCR deficient poplar	0.785	0.0208	0.10
Rhodopseudomonas	CCR deficient poplar	0.707	0.0143	0.06
Neisseriaceae	CCR deficient poplar	0.645	0.0358	0.02
Stem				
OTU	Associated with	Indicator value	p-value	Relative abundance
Alcaligenaceae	Wild-type poplar	0.887	0.0019	2.21
TM7	Wild-type poplar	0.851	0.0031	11.23
Variovorax	Wild-type poplar	0.822	0.0188	1.14
Bradyrhizobiaceae	Wild-type poplar	0.798	0.0041	1.29
Xanthomonadaceae	Wild-type poplar	0.791	0.0318	1.33
Chitinophagaceae	Wild-type poplar	0.780	0.0038	0.32
Acetobacteraceae	Wild-type poplar	0.779	0.0208	0.29
Rhizobacter	Wild-type poplar	0.710	0.0436	0.47
Bradyrhizobium	Wild-type poplar	0.674	0.0337	1.04
Hyphomicrobium	Wild-type poplar	0.674	0.0357	0.44
Gp1	Wild-type poplar	0.672	0.0353	0.75
Enterobacteriaceae	CCR deficient poplar	0.984	0.0151	20.20
Micrococcus	CCR deficient poplar	0.794	0.012	0.36
Gemella	CCR deficient poplar	0.736	0.0377	1.00
Oceanospirillales	CCR deficient poplar	0.734	0.0493	0.77
Leaf				
OTU	Associated with	Indicator value	p-value	Relative abundance (%)
Curtobacterium	Wild-type poplar	0.884	0.0049	0.43
Variovorax	Wild-type poplar	0.805	0.0121	0.93
Kineococcus	Wild-type poplar	0.775	0.0418	0.14
Sphingomonadaceae	Wild-type poplar	0.770	0.0116	0.13
Curvibacter	Wild-type poplar	0.730	0.0184	0.22

Indicator species analysis was calculated using the multipat function of the indicspecies package (version 1.7.1).

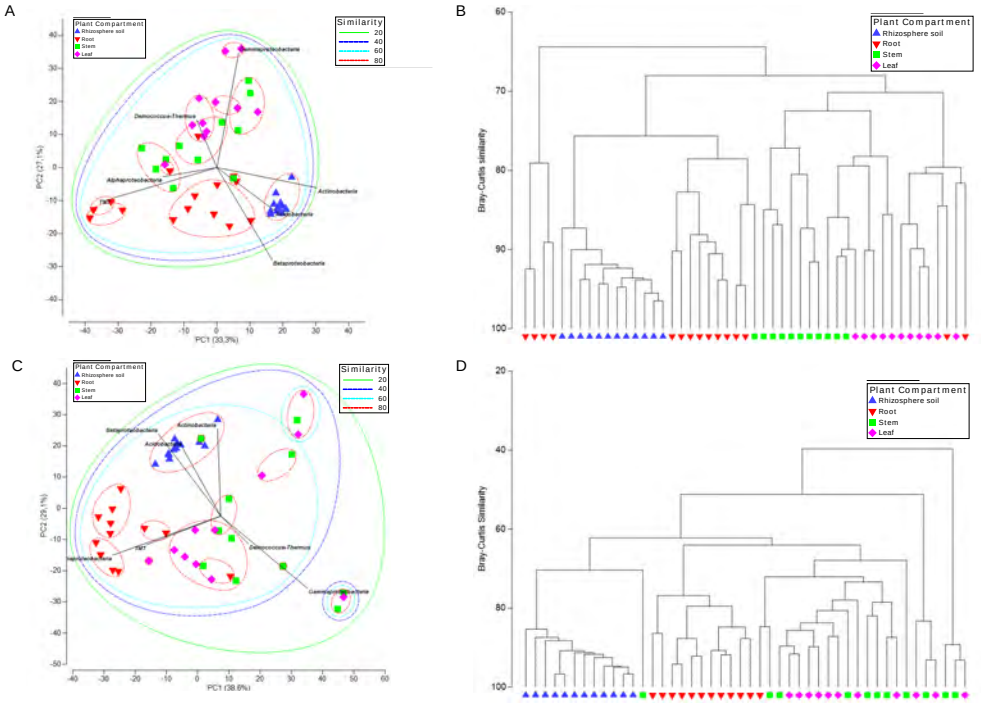

Supplementary Figure 5.1: Plant-compartments effects at phylum level. A and C: Principle component analysis (PCA) of square-root transformed samples based on rarefaction to 2000 reads per sample. OTUs were defined at a 97% sequence similarity cut-off in mothur (A,C). Phyla differentiating the plant compartments are displayed as vectors on the PCA plots. Hierarchical clustering (group-average linkage) of the samples based on Bray-Curtis similarity (B, D). Similarities based on Bray-curtis distances (B and D) were superimposed on the PCA plot (A and C).

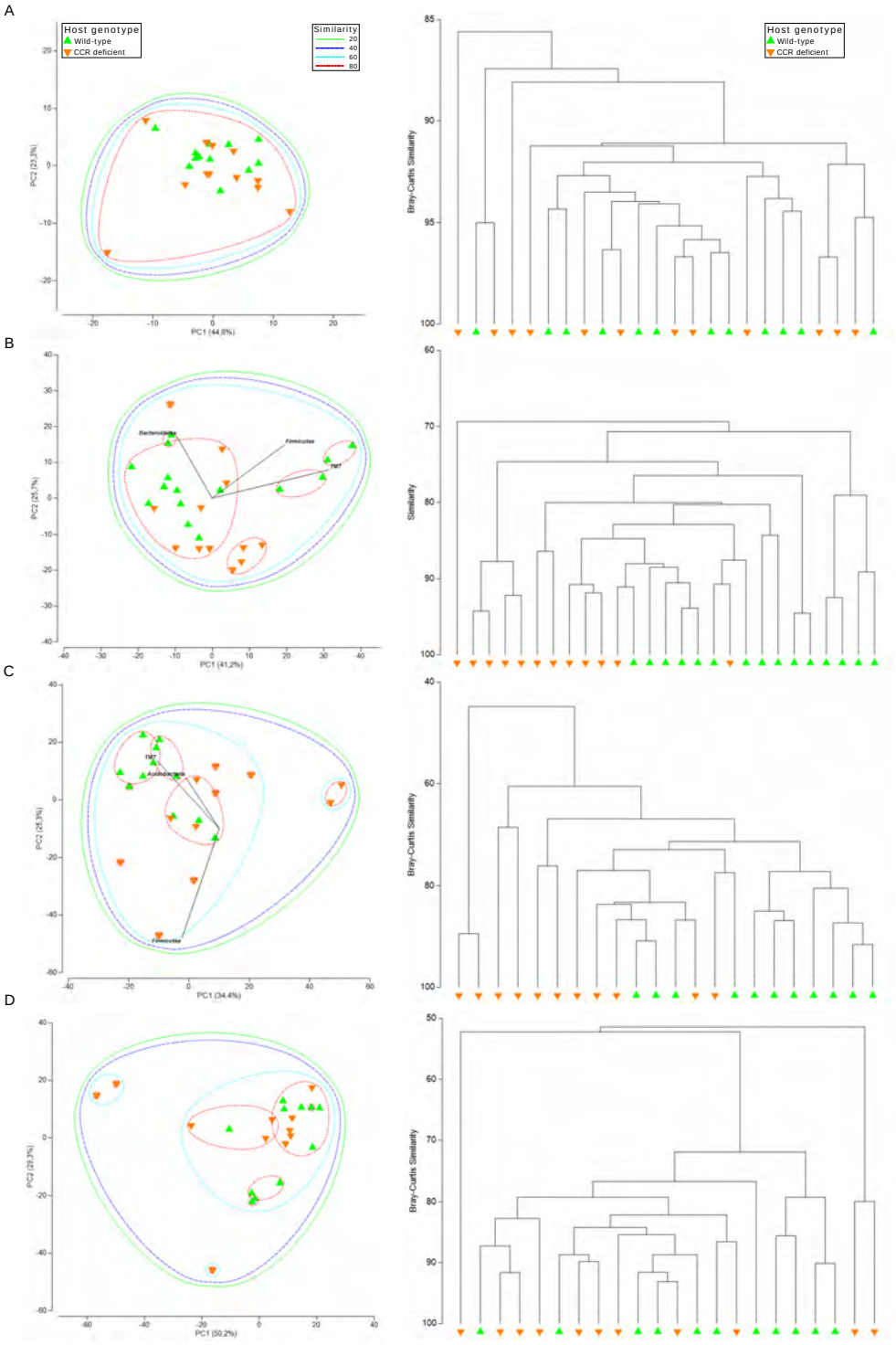
A
Host genotype
Wild-type
CCR deficient
Similarity
20
40
60
80
PC1 (44,8%)
PC2 (20,3%)
Bray-Curtis Similarity
B
Bacteroidetes
Firmicutes
TM7
PC1 (41,2%)
PC2 (25,7%)
Similarity
C
TM7
Actinobacteria
Firmicutes
PC1 (34,4%)
PC2 (25,5%)
Bray-Curtis Similarity
D
PC1 (50,2%)
PC2 (21,3%)
Bray-Curtis Similarity

Supplementary Figure 5.2 Host-genotype effects on phylum level (A. Rhizosphere soil, B. Root, C. Stem, D. Leaf). Left panels: principle component analysis (PCA) of normalized (square-root) samples based on rarefaction to 2000 reads per sample. OTUs were defined at a 97% sequence similarity cut-off in mothur. Right panels: hierarchical clustering (group-average linkage) of the samples based on Bray-Curtis similarities. Similarities based on Bray-curtis distances were superimposed on the PCA plot.

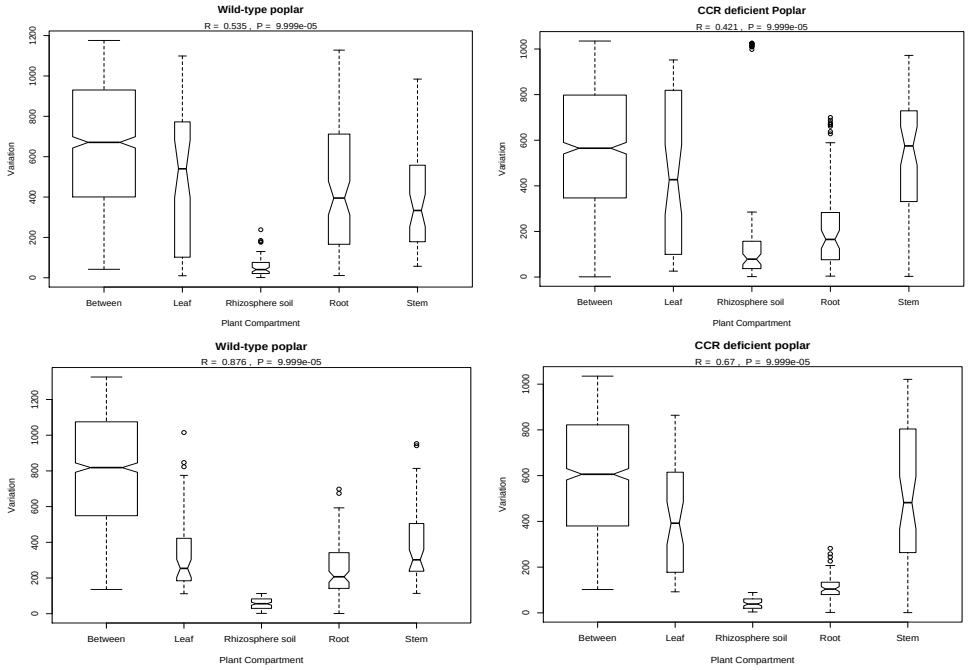

Supplementary Figure 5.3. Graphical representations of pairwise comparisons (at phylum (top) and genus level (bottom)) between host-genotypes (wild type poplar and CCR deficient poplar) within each plant compartment (rhizosphere soil, root, stem, leaf) as calculated by ANOSIM (analysis of similarities). Box-plots display the first (25%) and third (75%) quartile, the median (bold line), maximum and minimum observed values (without outliers). Outliers (more or less than 3/2 of the upper/lower quartile) are displayed as open circles. ANOSIM and resulting box plots were calculated based on 12 biological replicates in R with 10,000 iterations. Graphs display within variation of each group and variation between groups ('Between'). R-statistic and p-values are displayed on top of each individual graph.

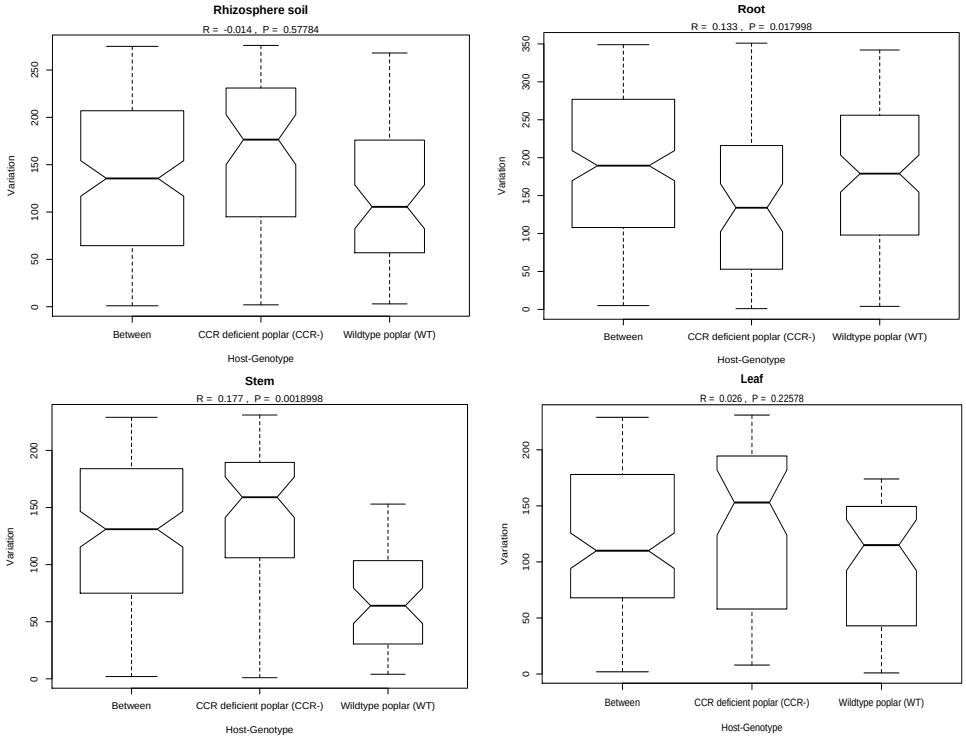

Supplementary Figure 5.4 Graphical representations of pairwise comparisons (at phylum level) between host-genotypes (wild type poplar and CCR deficient poplar) within each plant compartment (rhizosphere soil, root, stem, leaf) as calculated by ANOSIM (analysis of similarities). Box-plots display the first (25%) and third (75%) quartile, the median (bold line), maximum and minimum observed values (without outliers). Outliers (more or less than 3/2 of the upper/lower quartile) are displayed as open circles. ANOSIM and resulting box plots were calculated based on 12 biological replicates in R with 10,000 iterations. Graphs display within variation of each group and variation between groups ('Between'). R-statistic and p-values are displayed on top of each individual graph.

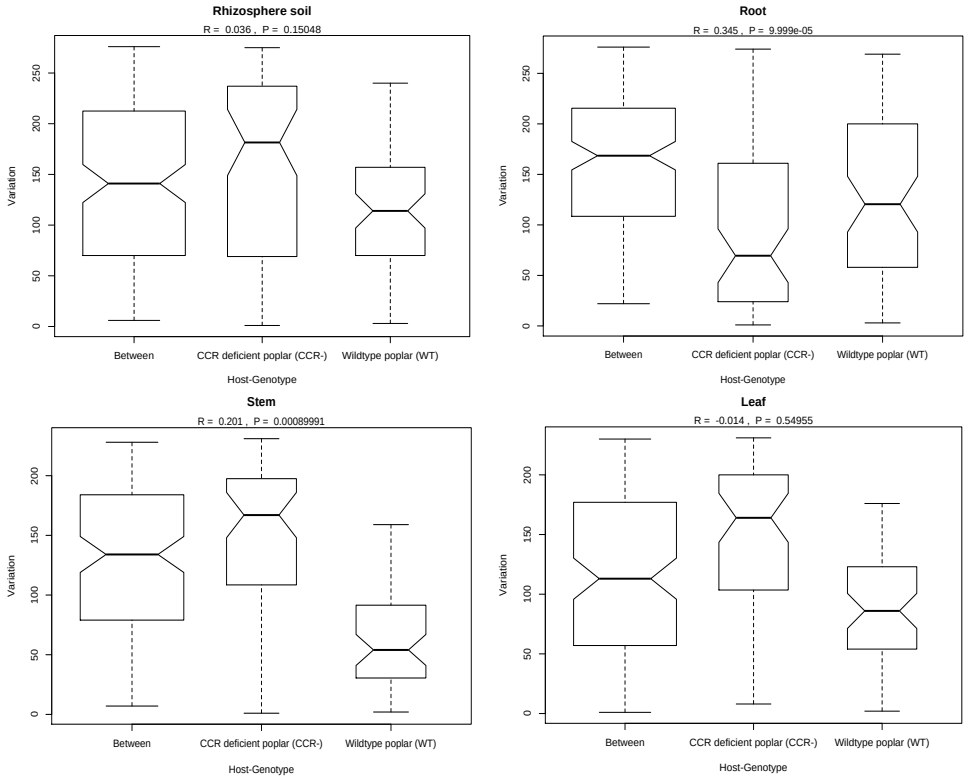

Supplementary figure 5.5. Graphical representations of pairwise comparisons (at genus level) between host-genotypes (wild-type poplar and CCR deficient poplar) within each plant compartment (rhizosphere soil, root, stem, leaf) as calculated by ANOSIM (analysis of similarities). Box-plots display the first (25%) and third (75%) quartile, the median (bold line), maximum and minimum observed values (without outliers). Outliers (more or less than 3/2 of the upper/lower quartile) are displayed as open circles. ANOSIM and resulting box plots were calculated based on 12 biological replicates in R with 10,000 iterations. Graphs display within variation of each group and variation between groups ('Between'). R-statistic and p-values are displayed on top of each individual graph.

Chapter 6

Plant growth promotion of lignin-reduced, biomass-impaired *Arabidopis thaliana* genotypes

Abstract

In the search of renewable and sustainable energy sources, the production of biofuels from biomass represents a vital component in the transition to a more bio-based economy. Second-generation biofuels produced from lignocellulosic biomass evade the competition with food crops but contain high levels of lignin, thereby reducing the commercial viability of these feedstocks. Reducing the lignin content via gene silencing of Cinnamoyl-CoA reductase (*CCR*), the first enzyme in the monolignol-specific branch of lignin biosynthesis, results in significantly reduced lignin levels and saccharification efficiency. However, *CCR* down-regulation causes the development of dwarf phenotypes in *Arabidopsis thaliana* and reduced biomass production in *Populus tremula x alba*, thereby countervailing, at least to some extent, the improved processing efficiency of these genetically engineered plants by reducing the total biomass yield. Therefore, in this work, we evaluated the potential of several plant growth promoting stress-reducing bacteria to improve plant growth of *CCR*-down-regulated *Arabidopsis thaliana* genotypes. *Arabidopsis thaliana* is widely considered to be a model plant for understanding lignin biosynthesis, deposition and function. Furthermore, during the latter stage of secondary xylem differentiation, *Arabidopsis* closely resembles the anatomy of the wood of angiosperm trees. Plant growth promotion was evaluated for two T-DNA mutants for *CCR1*, the main *CCR* isoform in *Arabidopsis thaliana* that is highly expressed in lignified tissues. And we selected promising bacterial strains using specific in vitro plant growth promotion tests and evaluated their potential to degrade lignin-derived low-molecular weight compounds.

Results from this study indicate that PGP bacteria can promote the growth of lignin-reduced *Arabidopsis thaliana* genotypes and thereby offset the biomass impairment caused by the perturbation in the lignin biosynthesis.

Keywords

Arabidopsis thaliana, Cinnamoyl-CoA reductase (*CCR*), inoculation, growth promotion

6.1. Introduction

Since the onset of the industrial revolution mankind has continuously depleted fossil energy reserves for manufacturing and transport, ultimately leading to an ever-increasing requirement for alternative and sustainable energy sources (Cassman, 2007; Hisano et al., 2009; Van Acker et al., 2013). In the impending transition to a more bio-based economy, especially the demand for biomass in the production of renewable energy and industrial feedstock applications is incessant and optimizing plant growth is required to ensure feed supply (Cassman, 2007; Vangronsveld et al., 2009; Weyens et al., 2009; Yuan et al., 2008). However, for the production of energy biomass, currently large areas of agricultural land are being used thereby endangering food supply (Cassman & Liska, 2007; Naylor et al., 2007; Weyens et al., 2009). Indeed, estimations assume that agricultural land in the European Union dedicated to biomass production for biofuel/energy will increase to 190,000 km^2 by 2030 (http://www.biofuelstp.eu/).

Second-generation biofuels, *i.e.* bioethanol derived from the sugar fraction of lignocellulosic biomass in dedicated energy crops (poplar, switchgrass, *Miscanthus* sp. and others), evade the “food versus fuel” debate (Solomon, 2010; Yuan et al., 2008). Indeed, they can be cultivated on marginal lands (contaminated and/or nutrient poor soils unsuitable for food production) with less fertilizer for multiple annual cycles (Van Acker et al., 2014). However, lignocellulosic biomass presents a challenge of a different nature. Lignin polymers, abundantly present in the walls of secondary thickened cells of vascular plants, represent a major hindrance in the enzymatic processing of lignocellulosic biomass to fermentable sugars (saccharification) (Chen & Dixon, 2007; Studer et al., 2011). Therefore genetically modified (GM) energy crops, engineered to produce less lignin or more easily degradable lignin, have been utilized to partially overcome the recalcitrance of lignocellulosic biomass and to improve the commercial viability and cost-competitiveness of second-generation biofuels (Vanholme et al., 2012; Wilkerson et al., 2014). Gene silencing of cinnamoyl-CoA reductase (*CCR*, E.C.1.2.1.44), the first enzyme in the monolignol-specific branch of lignin biosynthesis (Boerjan et al., 2003; Vanholme et al., 2010), typically results in reduced lignin content, altered cell wall metabolism and/or improved pulping characteristics, higher saccharification

and ethanol yields in for example tobacco plants, *Arabidopsis thaliana* (Mir Derikvand et al., 2008; Ruel et al., 2009; Van Acker et al., 2013) and poplar (Leplé et al., 2007; Van Acker et al., 2014). However, *CCR*-down-regulation causes the development of dwarf phenotypes in *Arabidopsis thaliana* (Mir Derikvand et al., 2008; Ruel et al., 2009; Van Acker et al., 2013) and reduced biomass production in *Populus tremula x alba* (Leplé et al., 2007; Van Acker et al., 2014), thereby countervailing, at least to some extent, the improved processing efficiency of these genetically engineered plants by reducing the total biomass yield.

Beneficial plant-associated bacteria can play a key role in supporting and/or enhancing plant health and growth (Compant et al., 2010; Hardoim et al., 2008; Weyens et al., 2009). Numerous studies describe intimate mutualistic relationships between plants and their associated bacterial microbiome involving a plethora of reciprocal advantages (Taghavi et al., 2009; Weyens et al., 2009; Yang, Kloepper, & Ryu, 2009, Taghavi et al., 2010). Plant growth promotion (PGP) activity of specific bacterial strains can be exerted by direct or indirect mechanisms. Direct PGP mechanisms may involve nitrogen fixation by diazotrophic bacteria, mobilisation/solubilisation of highly unavailable nutrients (e.g. iron, phosphorus, *etc.*), production of phytohormones (auxins, cytokinins, gibberelins) and the suppression of stress-induced ethylene production by 1-aminocyclopropane-1-carboxylic acid (ACC) deaminase activity (Bloemberg & Lugtenberg, 2001; Bulgarelli et al., 2013; Compant et al., 2010; Contesto et al., 2008; Hardoim et al., 2008; Lugtenberg & Kamilova, 2009; Mantelin & Touraine, 2004; Weyens et al., 2009; Zhang et al., 2007). Indirect PGP may occur by preventing the growth and activity of plant pathogens via competition for nutrients and space, antibiosis, production of hydrolytic enzymes, inhibition of pathogen-produced enzymes or toxins, and induction of plant defense mechanisms (Raaijmakers et al., 2008; Ryu et al., 2004, Selosse et al., 2004). In this way, plant-associated bacteria may have profound effects on biomass production and furthermore optimize plant growth on marginal or contaminated land thereby evading the unfavorable ramifications of the “food versus fuel” debate.

In this work, we evaluate the potential of several plant-associated bacteria to improve plant growth of *CCR*-down-regulated *Arabidopsis thaliana* plants.

Hereby, we combine improved processing efficiency of lignocellulosic biomass by reducing lignin content with *CCR* down-regulation and the use of specific bacterial strains to increase plant growth and optimize biomass production from lignin-reduced plants. We selected two T-DNA mutants for *CCR1* (gene At1g15950), the main *CCR* isoform that is highly expressed in lignified tissues and is considered as primordial for lignin biosynthesis (Alonso et al., 2003; Lauvergeat et al., 2001; Mir Derikvand et al., 2008; Sessions et al., 2002). Furthermore, we selected several bacterial strains with high degradation capacities for lignin-derived low-molecular weight compounds and high plant growth promotion capacities (PGP). We compared phenotypes of the lignin-reduced genotypes with the wild type *Arabidopsis thaliana* (Columbia ecotype) and evaluated the effects of the selected bacteria on primary root growth, lateral root growth and leaf surface area of the lignin-reduced genotypes.

6.2. Material and methods

6.2.1. Metabolic range of bacteria

To evaluate the metabolic potential and range to degrade specific phenolic carbon sources, all isolated bacterial strains were semi-quantitatively evaluated using Biolog MT2 plates (Biolog Inc., Hayward, CA, USA). Biolog MT2 plates utilize redox-chemistry to semi-quantitatively assess the degradation of externally added carbon sources. Each well of the Biolog MT2 microplates (96 wells) contains tetrazolium violet redox dye, which is highly sensitive to bacterial respiration, and a buffered nutrient medium optimized for a wide variety of bacteria. Bacterial respiration, *e.g.* degradation of the added carbon source, results in the reduction of tetrazolium violet to formazan, which can be spectrophotometrically quantified at 595nm.

We selected 10 phenolic carbon sources (Supplementary Figure 6.1). For the Biolog MT2 respirometric assay, pure bacterial cultures were grown overnight in liquid 869 rich medium (Mergeay et al., 1985) containing per liter of deionised water: 10 g tryptone, 5 g yeast extract, 5 g NaCl, 1 g D-glucose and 0.345 g $CaCl_2.2H_2O$ (pH 7). Subsequently, the exponentially growing cultures were washed twice (4000 rpm, 20 min) with sterile 10 mM phosphate buffered saline (PBS) buffer and optical density (600 nm) of all bacterial suspensions was adjusted to 0.20 with sterile 10 mM PBS buffer (130 mM NaCl, 7 mM Na_2HPO_4, 3 mM NaH_2PO_4, pH 7.0). Finally, the cultures were incubated at 30°C on a shaking platform (120 rpm) for 18h to deplete residual carbon nutrient content. For the Biolog MT2 assay, each well of the plates was filled with (a) 5 mM of the respective phenolic carbon source (30 µl) and (b) 115 µl of the designated bacterial suspension at optical density$_{600nm}$ = 0.20, resulting in a final concentration of approximately 1mM of carbon source per well. Each bacterial strain was tested in triplicate. Positive control wells (3) were filled with 5 mM of D-glucose. Negative control wells (3) were inoculated with 115 µl of sterile deionised H_2O. Inoculated plates were placed in self-sealing plastic bags (VWR) containing a water-soaked paper towel to minimize evaporation from the wells and incubated at 30°C. Absorbance was measured at 595 nm using an OMEGA plate reader (Fluorostar) immediately after inoculation (0 h) and at 3, 6, 18, 24, 48, 72, 144 and 288h.

6.2.2. Processing Biolog MT2 plates

Raw absorbance data for all bacterial strains from each time point (3, 6, 18, 24, 48, 72, 144 and 288 h) were collected and individually standardized by subtracting the corresponding absorbance value measured immediately after inoculation (0 h) (reaction-independent absorbance). Furthermore, to semi-quantitatively evaluate the degradation capacity of each bacterial strain in the kinetic Biolog data set, the net area under the absorbance versus time curve was calculated according to the trapezoidal approximation (Guckert et al., 1996).

$$\text{Formula: } \sum_{i=1}^{4} ((v_i + v_{i=1})/2)*(t_i + t_{i=1}) = 50$$

The resulting value calculated via the trapezoidal approximation summarizes different aspects of the measured respirometric reaction including differences in the lag phases, rates of increase, maximum optical densities, etc. (Guckert et al., 1996). Complete data of Biolog tests can be found in Supplementary Table 6.1.

6.2.3. *In vitro* plant growth promotion of bacterial strains

Siderophore production

Bacterial siderophore secretion was qualitatively evaluated by a colorimetric method using the Chrome Azurol S (CAS) reagent described by Schwyn & Neilands, 1987. Briefly, bacteria were cultivated overnight (18 h, 120 rpm) in liquid 869 rich medium. Subsequently exponentially growing cultures were harvested by centrifugation (20 min, 4000 rpm) and washed twice with 10 mM PBS buffer. Next, 20 µl of the bacterial suspensions were transferred to 800 µl of 284 minimal medium (Schlegel et al., 1991). This 284 medium contained per liter of deionised water: 6.06 g Tris–HCl; 4.68 g NaCl; 1.49 g KCl; 1.07 g NH_4Cl; 0.43 g Na_2SO4; 0.2 g $MgCl_2.6H_2O$; 0.03 g $CaCl_2.2H_2O$; 40 mg $Na_2HPO_4.2H_2O$ and 1 ml microelements solution (pH 7). The microelements solution contained per liter of deionised water: 1.3 ml 25% HCl; 144 mg $ZnSO_4.7H_2O$; 100 mg $MnCl_2.4H_2O$, 62 mg H_3BO_3; 190 mg $CoCl_2.6H_2O$, 17 mg $CuCl_2.2H_2O$, 24 mg $NiCl_2.6H_2O$ and 36 mg Na-$MoO_4.2H_2O$. Five carbon sources (C mix) were added per liter medium: 0.52 g glucose; 0.66 g gluconate; 0.54 g fructose; 0.81 g succinate and 0.35 g lactate. Finally 284 medium was supplemented with 0,

0.25 and 3 µM Fe (III)NH_4 respectively deficient, optimal and oversupply Fe conditions) (Croes et al., 2013). After five days of growth in the 284 medium, bacterial suspensions were centrifuged (20 min, 4000 rpm) and 100 µl of CAS-reagents was added to the supernatant. After 4 h orange wells were considered positive.

Production of indol-acetic acid (IAA)

Production of indole-3-acetic acid (IAA) was determined using Salkowki's reagent after incubation of the bacteria for 5 days at 30°C in the dark in liquid 1/10 869 medium supplemented with 0.5 gl^{-1} L-tryptophan. After centrifugation (4000 rpm, 15 min), 0.5 ml supernatant was mixed with 1 ml Salkowski's reagent (50 ml 35% $HClO_4$, 1 ml 0.5 M $FeCl_3$) (Gordon & Weber, 1950). After 20 min incubation, pink wells were considered positive for IAA production.

1-aminocyclopropane-1-carboxylate (ACC) deaminase activity

ACC deaminase activity was evaluated by a slightly modified protocol of Belimov et al. (2005) whereby ACC-deaminase activity was determined by monitoring the amount of α-ketobutyrate generated by enzymatic hydrolysis of ACC. Briefly, bacteria were cultured in liquid 869 medium (48h, 30°C, 120 rpm) and harvested by centrifugation (4000 rpm, 15 min). Resulting cell pellets were washed twice with 0.1 M Tris–HCl buffer (pH 7.5) and resuspended in 3 ml liquid salts minimal medium (Belimov et al., 2005) containing 5 mM ACC as a sole source of nitrogen. After 48 h of incubation (30°C, 120 rpm), bacterial suspensions were centrifuged (4000 rpm, 15 min) and resuspended in 1 ml 0.1 M Tris–HCl buffer (pH 8.5). The cells were disrupted by adding 30 µl toluene with vigorous vortexing. A 100 µl aliquot of this cell suspension was mixed with 100 µl 0.1 M Tris–HCl buffer (pH 8.5) and 10 µl 0.5 M ACC, and incubated for 30 min at 30°C. Then, 1 ml 0.56 N HCl was added and mixtures were centrifuged at 19,000 g for 5 min. Mixtures without cell suspension were used as controls. Next, 400 µl 0.56 N HCl and 150 µl 0.2% 2,4-dinitrophenylhydrazine in 2 N HCl were added to 500 µl supernatant. After incubation for 30 min at 30°C, 1 ml 2 N NaOH was added and a colour change from yellow to brown was considered positive for ACC deaminase activity.

Phosphate solubilization

National Botanical Research Institute's phosphate growth solid medium (NBRIP) was used for screening for phosphate-solubilizing bacteria (Nautiyal, 1999). Bacteria were cultured in liquid 869 medium (48 h, 30°C, 120 rpm), harvested (4000 rpm, 30 min) and pellets were washed twice with 10 mM PBS buffer. Subsequently, 50 µl aliquots of washed strains were inoculated in holes (Ø: 0.5 cm) of the NBRIP solid medium. After 1 week, the appearance of a clear zone around the colonies was considered as an indicator of phosphate solubilization.

Acetoin production

In order to detect strains that utilize the butylene glycol pathway and produce acetoin, strains were inoculated in Methyl Red-Voges Proskauer (MRVP) medium containing per liter of deionized water 17 g of MRVP medium (Sigma-Aldrich, 69150). After 48 h of incubation, a colorimetric reaction was induced according to Romick & Fleming (1998) by first adding 0.5% L-arginine to 100 µl of the bacterial supernatant. Subsequently Barrit's reagent A (5% w/v α-naphtol) and Barrit's reagent B (40% w/v KOH) were added which sequentially catalyzes the conversion of acetoin to diacetyl in the presence of oxygen (α-naphtol) whereafter diacetyl reacts with guanidine containing compounds such as arginine to produce a pinkish-red end product. During the reaction KOH acts as an oxidizing agent that accelerates the critical reaction that converts acetoin to diacetyl.

6.2.4. *In vivo* growth promotion of selected bacterial strains

Fifteen bacterial strains were selected based on their metabolic range and plant growth promotion capacities (Supplementary Table 6.1), to test their potential to improve *in vivo* plant growth (Table 6.1).

Plant material, sterilization and preparation of vertical agar plates

Arabidopsis thaliana (Columbia ecotype) wild-type (WT), *ccr1-3* (N347577) and *ccr1-6* mutant seeds (N623689) were obtained from the European *Arabidopsis* Stock Centre (NASC)(Alonso et al., 2003; Mir Derikvand et al., 2008; Sessions et al., 2002). Homozygous lines of *ccr*1-3 and *ccr*1-6 were identified using PCR (*ccr*1-3F: 5'-CCGGTCTCAAGGTACTCGTC-3'; *ccr*1-3R: 5'-GGATCATGGGACCAATTCAC-3' and *ccr*1-6F: 5'-TTGTTTTGATTGACAATTTGGA-3'; *ccr*1-6R: 5'- GGGATTAGATAACGTCACGACA-3'.

Seeds from all genotypes were surface-sterilized in 0.1 %(w/v) NaOCl and 0.1% (v/v) Tween 80 for 1 min, washed four times (5 min) with sterile distilled water and dried in a laminar air flow. Seeds were sown with a sterile toothpick on 12 x 12-cm vertical plates containing ¼ diluted Murashige-Skoog (MS) medium (Sigma Cat. No. M0404) containing macro-and micronutrients as described by Murashige & Skoog (1962) and vitamins as described by Gamborg et al. (1968). All media were supplemented with 10 g L^{-1} (1%) plant tissue culture agar (Lab-M, Bury, UK) and pH was adjusted to 5.8 with KOH. Germination plates also contained 5 g L^{-1} sucrose. Subsequently, germination plates were stored for 48 hours at 4°C (in the dark) to standardize water contents of the seeds and ensure homogenous germination. Finally, germination plates were placed vertically in a culture room at 22°C with 12/12-h light–dark cycle and a light intensity of 125–150 µmol m^{-2} s^{-1} at rosette level provided by fluorescent white lamps. After 7 days of growth, a homogeneous set of plants were transferred to treatment plates, inoculated with selected bacterial strains (see bacteria growth and inoculation), from which a 1 cm strip of agar was removed at the top with a sterile scalpel blade. From the first analysis, we selected five bacterial strains to evaluate in more detail. For the kinetic analysis, on each day of growth on vertical agar plates after transfer, the position of the primary root tip was marked on the plate. Plates were scanned on a Canoscan 4400F (Canon) at 600 d.p.i. and primary root growth of endpoint and kinetic analysis and lateral root growth were analysed using Rootnav (Pound et al., 2013). Leaf surface area was calculated using Adobe Photoshop CC (2014.2). For visualizing root hairs, roots were stained for 1 min in 0.075% Crystal-Violet in 70% ethyl alcohol and rinsed thoroughly with distilled water. Root hairs were visualized with a trinocular stereo-microscope (Nikon, SMZ 800) equipped with a CCD camera (DFK 41AF02 FC imaging source).

Co-cultivation assay: effect of the bacterial volatiles on the plant growth

Seeds from all genotypes were sterilized as described above and sown with a sterile toothpick on round Petri dishes (100 x 15 mm) containing ¼ diluted Murashige-Skoog (MS) medium supplemented with 5 g L^{-1} sucrose. Subsequently seeds were placed in the fridge (48 h, 4°C) in the absence of light where after seeds were placed in a culture room at 22°C with 12/12-h light–dark cycle and a light intensity of 125–150 µmol m^{-2} s^{-1} at rosette level provided by

fluorescent white lamps. After 2 days of growth, germinated seedlings were transferred to one side of plastic Petri dishes (100 x 15 mm) containing a center partition and filled with ¼ diluted Murashige-Skoog (MS) medium (10 seedlings per plate). The other side of the Petri dishes, which were filled with 869 rich medium, was inoculated with 100 µl of bacterial suspension or sterile PBS buffer applied dropwise onto the center of the 'half' plate. The partition of the Petri dish made sure that no direct contact between the plant and bacteria occurred. Finally, plates were sealed with Parafilm and arranged in a completely randomized design in the culture room (conditions see above). Fourteen days after inoculation, total leaf surface area was measured using Adobe Photoshop CC (2014.2).

Bacterial growth and inoculation of treatment plates

One day before inoculation experiments, bacteria were grown overnight (18 h, 30°C, 120 rpm) in 869 liquid medium and harvested in the late exponential phase. Subsequently, the exponentially growing cultures were centrifuged (4000 rpm, 20 min) and resulting pellets were resuspended in sterile phosphate saline buffer (10 mM PBS). Optical density at 600 nm of all bacterial suspensions was adjusted to 1.00 ± 0.10 (approximately 10^9 colony forming units (CFU) per mL) with sterile 10 mM PBS buffer. The obtained bacterial suspensions (10^9 CFU ml^{-1}) were further diluted to 10^8 and 10^4 CFU ml^{-1} using 10m mM PBS buffer. For inoculation of the VAPS, 400 µl of 10^4 CFU ml^{-1} was spread onto the treatment plates. For inoculation of the co-cultivation plates, 100 µl of 10^8 CFU ml^{-1} was applied dropwise on one side of the portioned Petri dishes.

6.2.5 Statistical analysis

Statistical analyses were performed in R 2.15.1 (The R Foundation for Statistical Computing, Vienna, Austria). Normal distributions of the data were checked with the Shapiro-Wilkes test and homoscedasticity of variances was analysed using either Bartlett's or the Fligner-Killeens test. Significant differences in the variance of parameters were evaluated, depending on the distribution of the estimated parameters, either with ANOVA or the Kruskal Wallis Rank Sum Test. *Post-hoc* comparisons were conducted by either the Tukey's Honest Significant Differences tests or Pairwise Wilcoxon Rank Sum Tests.

6.3. Results

6.3.1 Metabolic range and plant growth promotion capacities of selected bacteria

We previously isolated the culturable fraction from the rhizosphere soil, roots, stems and leaves of wild type and *CCR* deficient field-grown poplar trees by using a selective isolation and selective enrichment approach with ferulic acid (Beckers et al. 2015, Chapter 3). From this collection, we selected 96 bacterial strains, which displayed high ferulic acid degradation capacities (as evaluated by Biolog MT2). To determine the metabolic range of the selected bacteria to degrade a variety of specific phenolic carbon sources, we selected 10 different phenolic carbon sources (Supplementary Figure 6.1). This selection included phenolic acids (vanillic acid, *p*-coumaric acid, sinapic acid, syringic acid, p-hydroxy benzoic acid and caffeic acid), phenolic aldehydes (syrinaldehyde, coniferaldehyde and vanillin) and one phenolic alcohol (coniferyl alcohol).

Table 6.1. Selected bacterial strains for *in vivo* plant growth promotion tests

Species	Average Biolog respons	Siderophore	IAA	ACC	Phosphate	Acetoin
Microbacterium phyllosphaerae	321.41 ± 8.19	+	+	++	+	-
Nocardioides aromaticivorans	141.91 ± 5.4	+	+	-	-	-
Rhizobium radiobacter	369.8 ± 16.55	+	+	+	-	-
Bacillus simplex	280.81 ± 3.19	+	+	++	+	-
Plantibacter flavus	178.84 ± 7.93	+	+	±	-	-
Ochrobactrum cytisi	204.94 ± 2.75	-	±	±	+	-
Azospirillum oryzae	193.09 ± 14.38	-	+	±	±	-
Pseudomonas putida	267.13 ± 24.99	-	+	±	±	-
Pseudomonas congelans	248.38 ± 9.51	+	+	+	±	-
Ensifer adhaerens	269.05 ± 3.16	+	+	++	-	-
Cupravidius metallidurans	170.56 ± 13	+	+	-	-	±
Pseudomonas putida	219.35 ± 13.44	+	+	-	-	-
Starkeya koreensis	239.06 ± 18.69	+	+	+	+	-
Variovorax paradoxus	270.54 ± 8.66	+	+	-	+	-
Pseudomonas putida	212.31 ± 1.99	-	+	++	-	+

Biolog response was calculated by taking the average response of the bacteria for the 10 different phenolic carbon sources tested (Supplementary Figure 6.1 and Supplementary Table 6.1). Siderophore: Siderophore production, IAA: Indol-acetic acid production, ACC: ACC-deaminase activity, Phosphate solubilisation capacity, Acetoin: Acetoin production. Species in bold were selected for in detail evaluation of their plant growth promotion capacities (Figure 6.3 and Figure 6.5 and 6.6).

Within our collection, we found a large range of bacteria capable of degrading the selected phenolic carbon sources (Supplementary Table 6.1). Some bacterial strains showed high degradation capacities for certain carbon sources and low degradation capacities for other carbon sources. Others displayed low responses to all carbon sources. However, we were interested in those bacterial strains that showed high degradation capacities for all selected phenolic carbon sources. To facilitate further selection of suitable bacterial strains for inoculation purposes, we also evaluated the plant growth promotion capacities (focussing on siderophore production, IAA-production, ACC-deaminase activity, phosphate solubilisation capacities and acetoin production) of all 96 selected bacterial strains (Supplementary Table 6.1). Finally, based on high degradation capacities for the selected phenolic carbon sources (metabolic range) in combination with the presence of plant growth promotion characteristics, fifteen bacterial strains were selected to test their capacity to promote the plant growth of lignin-reduced *Arabidopsis thaliana* genotypes (Table 6.1).

6.3.2. Primary root growth and leaf surface areas as evaluated with vertical agar plates (VAPs): genotype-effects

Before evaluation of the possible effects of the inoculated bacterial strains on the growth of the lignin-reduced *Arabidopsis thaliana* genotypes (*ccr*1-3 and *ccr*1-6), we first assessed the genotype-effect on the primary root growth and leaf surface area (Figure 6.1). Remarkably, after 7 days of growth the lignin-reduced genotypes (*ccr*1-3 and *ccr*1-6) displayed significantly ($P < 0.001$) longer primary roots (Figure 6.1A,B top panels) and larger leaf surface area (Figure 6.1C, top panel) as compared to the wild type. Average primary root length (± standard deviation) of *ccr*1-3 and *ccr*1-6 were respectively 305 ± 37 mm and 297 ± 37 mm whereas primary root length of the wild type was 255 ± 24 mm. Average leaf surface area (± standard deviation) was also higher for the lignin-reduced genotypes (WT: 41 ± 3 mm^2, *ccr*1-3: 46 ± 4 mm^2 and *ccr*1-6: 53 ± 6 mm^2) but only significantly higher in *ccr*1-6 ($p < 0.01$). However, in the growth period between day 7 and day 14 these effects were entirely the opposite. In this growth period, the lignin-reduced genotypes showed significantly lower growth of the primary roots (Figure 6.1A,B bottom panels) and the final total leaf surface area after 14 days was also significantly lower for these genotypes (Figure 6.1C bottom panel).

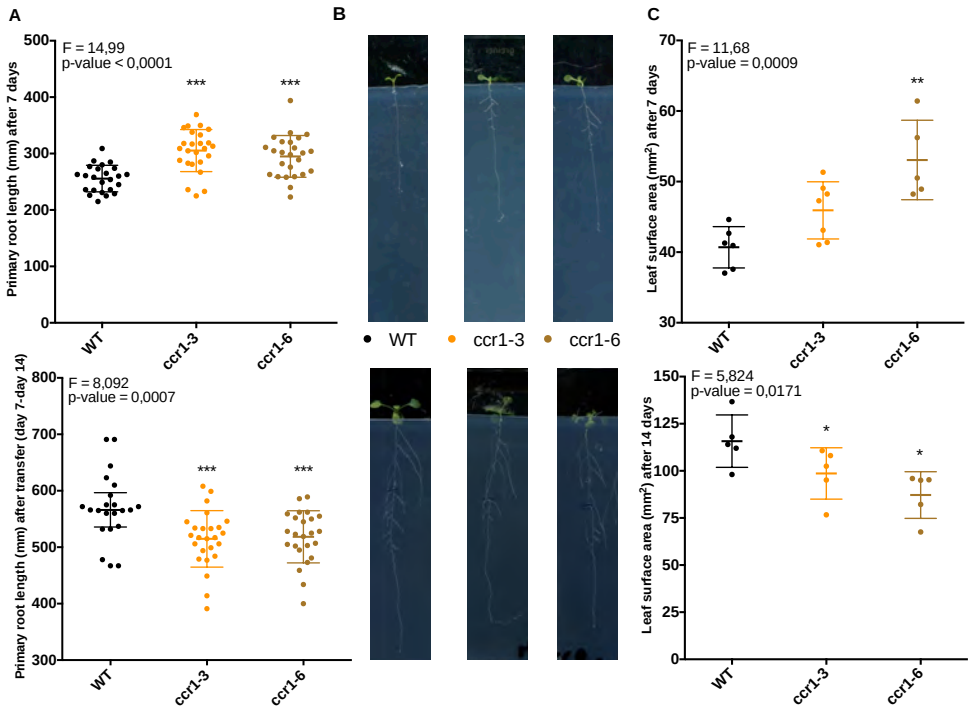

*Figure 6.1. Comparison of primary root growth of Arabidopsis thaliana genotypes (WT, ccr1-3, ccr1-6) after 7 days and 14 days of growth. A. Scatter dot-plot of primary root growth after 7 days (top panel) and in the growth period between day 7 and day 14 (bottom panel). Data represent at least 20 biologically independent replicates. B. Pictures of representative primary roots of all genotypes after 7 days of growth (top panel) and after 14 days of growth (bottom panel). C. Scatter dot-plot of the total leaf surface area after 7 days (top panel) and after 14 days of growth (bottom panel). Data represent at least five biologically independent replicates (each consisting of five seedlings). Lines within the scatter dot-plots represent means ± standard deviation. Data were analysed using one-way ANOVA and Tukey post-hoc comparisons (p-values: *P < 0.05, **P < 0.01, *** P< 0.001). Overal ANOVA results (F-value and p-value) are displayed in the bottom left corner of each graph.*

Average primary root length (± standard deviation) in this growth period of *ccr*1-3 and *ccr*1-6 were respectively 515 ± 50 mm and 518 ± 46 mm whereas primary root length of the wild type was 570 ± 59 mm. Total primary root length of all genotypes (day 0 - day 14) was comparable after 14 days of growth (data not shown). Average total leaf surface area (± standard deviation) was also lower for

the lignin-reduced genotypes (WT: 116 ± 14 mm^2, *ccr*1-3: 99 ± 14 mm^2 and *ccr*1-6: 87 ± 12 mm^2) but only significantly higher in *ccr*1-6 ($P < 0.001$).

6.3.3. Primary root growth (end-point measurement) and leaf surface area as evaluated with vertical agar plates (VAPs): bacterium-effects

To evaluate the effects of the selected bacterial strains on the primary root growth and leaf surface area of the different genotypes (WT, *ccr*1-3 and *ccr*1-6), 7-days old *Arabidopis thaliana* seedlings were transferred to treatment plates (inoculated with 400 µl of 10^4 CFU ml^{-1} of the corresponding bacterium). After an additional growth of 7 days, primary root growth and leaf surface area were evaluated (Figure 6.2 and Supplementary Figures 6.2, 6.3, 6.4 and 6.5).

For the wild type, the primary root growth (± standard deviation) was significantly increased by inoculation with *Norcardioides aromaticivorans* (6.25 ± 0.29 cm; $P < 0.05$) and *Plantibacter flavus* (6.60 ± 0.39 cm; $P < 0.01$) as compared to the non-inoculated control (5.72 ± 0.60 cm). The other bacterial inoculants had little to no effect on the primary root growth, except for the three *Pseudomonas putida* strains, which reduced the primary root growth of the wild type seedlings ($P < 0.05$) (Figure 6.2A and Supplementary Figure 6.2). For the leaf surface area, the overall effect of bacterial inoculation was significant ($F = 2.570$ and $P = 0.013$), but no significant effects were observed for the pairwise comparisons (Supplementary Figure 6.5A).

For the *ccr*1-3 genotype, we found significant increases in the primary root growth after inoculation with *Microbacterium phyllosphaerae* (5.70 ± 0.33 cm; $P < 0.05$), *Norcardioides aromaticivorans* (5.94 ± 0.47 cm; $P < 0.01$), *Plantibacter flavus* (5.83 ± 0.61 cm; $P < 0.05$) and *Variovorax paradoxus* (5.64 ± 0.47 cm; $P < 0.05$) as compared to the non-inoculated control (5.14 ± 0.51 cm) (Figure 6.2B and Supplementary Figure 6.3). For the leaf surface area, again the overall effect of bacterial inoculation was highly significant ($F = 7.846$ and $P < 0.0001$), and pairwise comparisons revealed significant increases ($P < 0.05$) in the leaf surface area for *Microbacterium phyllosphaerae*, *Norcardioides aromaticivorans* and *Variovorax paradoxus* as compared to the non-inoculated control (Supplementary Figure 6.5B).

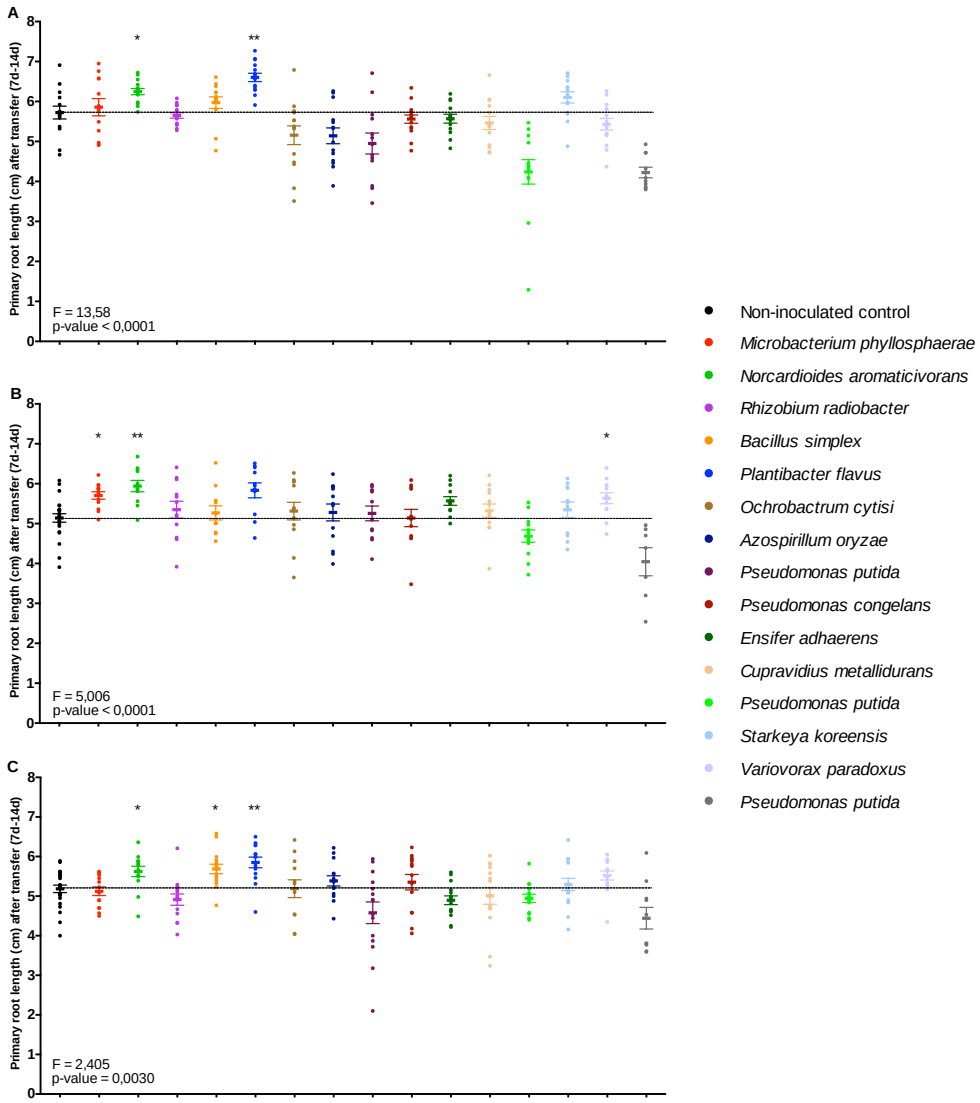

*Figure 6.2. Effect of inoculation with selected bacterial strains on the primary root growth of Arabidopsis thaliana genotypes. Aligned scatter dot-plots displaying the effect of bacterial inoculation on the primary root growth (cm) of Arabidopsis thaliana seedlings (A. Wild type, B. ccr1-3 and C. ccr1-6) after 14 days of growth (end-point measurement). To inoculate seedlings 10^4 colony-forming units (CFU) were spread onto the treatment plates. Lines within the scatter dot-plots represent means ± standard deviation. Data represent at least 12 biologically independent replicates. Non-inoculated controls are displayed in black and inoculated strains are displayed in several colours (see legend). Data were analysed using one-way ANOVA and Dunnet post-hoc comparisons (p-values: *P < 0.05, **P <*

0.01) whereby each treatment (bacteria) was compared with the control. Overall ANOVA results (F-value and p-value) are displayed in the bottom left corner of each graph.

Finally for the *ccr*1-6 genotype, the primary root growth was enhanced by inoculation with *Norcardioides aromaticivorans* (5.62 ± 0.47 cm; P < 0.01), *Bacillus simplex* (5.69 ± 0.46 cm; p < 0.05) and *Plantibacter flavus* (5.85 ± 0.50 cm; P < 0.05) as compared to the non-inoculated control (5.18 ± 0.46 cm) (Figure 6.2C and Supplementary Figure 6.4). For the leaf surface area, we found a significant overall bacterium effect (F = 3.853 and P < 0.0006) and pairwise significant differences (P < 0.05) for *Norcardioides aromaticivorans, Ochrobactrum cytisi, Azospirillium oryzae, Pseudomonas congelans* and *Variovorax paradoxus* as compared to the non-inoculated control (Supplementary Figure 6.5B).

Based on these findings of the primary root growth and leaf surface area for all genotypes, we selected *Norcardioides aromaticivorans, Variovorax paradoxus, Microbacterium phyllosphaerae, Plantibacter flavus* and *Bacillus simplex* for further analysis.

6.3.4. Kinetic analysis of primary root growth

In a next experiment, we kinetically evaluated the growth of the primary roots by marking the position of the root tip from 7-days old seedlings periodically each day from day 7 until day 15 of growth (time-points: day 7, 8, 9, 10, 12, 13, 14, 15)(Figure 6.3). For the comparison of the genotypes (Figure 6.3A), we observed significant differences (P < 0.05) at the start of the kinetic analysis of 7-days old seedlings whereby the lignin-reduced genotypes displayed longer primary roots as compared to the wild type. We made the same observation in the previous experiment (Figure 6.1A). From day 8, all genotypes showed similar growth curves through days 8, 9, 10, 12. However from day 13, the primary root growth of the lignin-reduced genotypes was slightly reduced as compared to the wild type and significantly reduced (p < 0.05) at the next two time-points (day 14 and day 15).

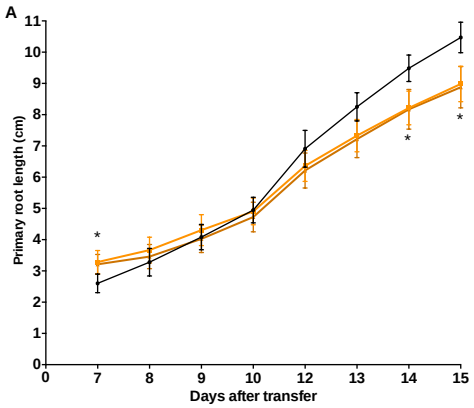

Genotype	Day 7	Day 8	Day 9	Day 10	Day 12	Day 13	Day 14	Day 15
wild-type	**2,60 ± 0,30**	**3,21 ± 0,42**	**3,98 ± 0,30**	**4,83 ± 0,27**	**6,76 ± 0,44**	**8,11 ± 0,24**	**9,36 ± 0,25**	**10,38 ± 0,45**
ccr1-3	3,21 ± 0,31*	3,46 ± 0,39	4,03 ± à,44	4,73 ± 0,47	6,22 ± 0,56	7,22 ± 0,59	8,17 ± 0,64*	8,88 ± 0,66*
ccr1-6	3,29 ± 0,37*	3,67 ± 0,41	4,31 ± 0,50	4,91 ± 0,43	6,36 ± 0,49	7,33 ± 0,52	8,22 ± 0,54*	8,98 ± 0,57*

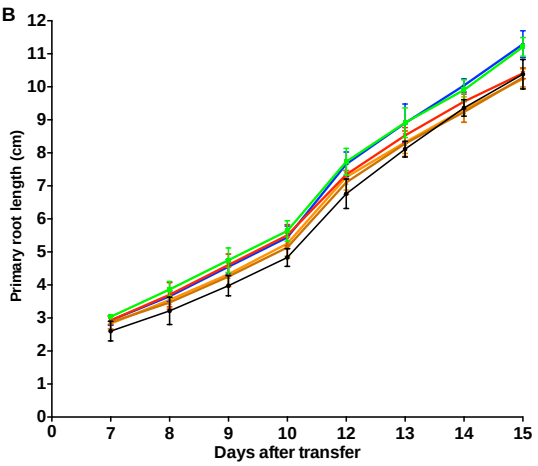

Bacterium	Day 7	Day 8	Day 9	Day 10	Day 12	Day 13	Day 14	Day 15
Non-inoculated control	**2,60 ± 0,30**	**3,21 ± 0,42**	**3,98 ± 0,30**	**4,83 ± 0,27**	**6,76 ± 0,44**	**8,11 ± 0,24**	**9,36 ± 0,25**	**10,38 ± 0,45**
Norcardoides aromaticivorans	3,04 ± 0,06	3,87 ± 0,24	4,75 ± 0,37	5,64 ± 0,31*	7,73 ± 0,40*	8,92 ± 0,45*	9,91 ± 0,31*	11,21 ± 0,28*
Variovorax paradoxus	2,87 ± 0,20	3,47 ± 0,20	4,25 ± 0,29	5,14 ± 0,32	7,10 ± 0,36	8,28 ± 0,39	9,24 ± 0,31	10,28 ± 0,28
Microbacterium phyllosphaerae	2,93 ± 0,12	3,70 ± 0,37	4,61 ± 0,33	5,5 ± 0,32	7,34 ± 0,12	8,53 ± 0,24	9,55 ± 0,23	10,41 ± 0,17
Plantibacter flavus	2,93 ± 0,15	3,66 ± 0,16	4,55 ± 0,22	5,44 ± 0,35	7,66 ± 0,37*	8,90 ± 0,58*	10,04 ± 0,20*	11,29 ± 0,41*
Bacillus simplex	2,83 ± 0,22	3,55 ± 0,29	4,33 ± 0,38	5,26 ± 0,38	7,27 ± 0,39	8,32 ± 0,34	9,32 ± 0,38	10,24 ± 0,30

Figure 6.3. Kinetic analysis of primary root growth. A. Kinetic analysis of the primary root growth of the Arabidopsis thaliana genotypes (WT, ccr1-3, ccr1-6) across eight time-points (7, 8, 9, 10, 12, 13, 14 and 15 days of growth). B. Kinetic analysis of the primary root growth of wild type Arabidopsis thaliana and the effect of 5 selected bacterial strains.

C

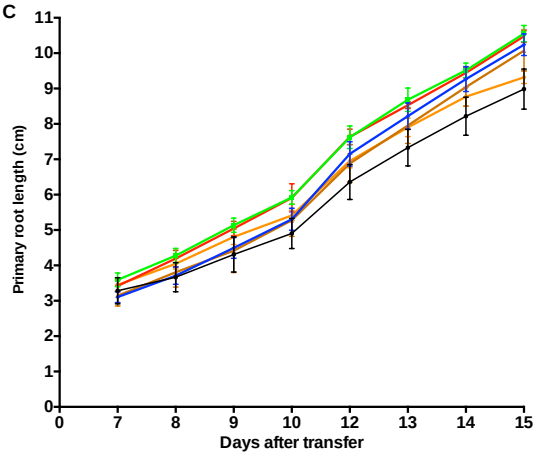

Bacterium	Day 7	Day 8	Day 9	Day 10	Day 12	Day 13	Day 14	Day 15
Non-inoculated control	**3,21 ± 0,31**	**3,46 ± 0,39**	**4,03 ± 0,44**	**4,73 ± 0,47**	**6,22 ± 0,56**	**7,22 ± 0,59**	**8,17 ± 0,64**	**8,88 ± 0,66**
Norcardoides aromaticivorans	3,59 ± 0,19	4,28 ± 0,21	5,13 ± 0,20	5,92 ± 0,19*	7,62 ± 0,32*	8,68 ± 0,33*	9,52 ± 0,21*	10,56 ± 0,23*
Variovorax paradoxus	3,14 ± 0,29	3,81 ± 0,42	4,42 ± 0,62	5,27 ± 0,46	6,88 ± 0,54	7,96 ± 0,51	9,04 ± 0,54	10,07 ± 0,56*
Microbacterium phyllosphaerae	3,42 ± 0,16	4,19 ± 0,23	5,04 ± 0,20	5,91 ± 0,40*	7,63 ± 0,22*	8,53 ± 0,10*	9,44 ± 0,14*	10,48 ± 0,18*
Plantibacter flavus	3,11 ± 0,16	3,71 ± 0,25	4,50 ± 0,29	5,30 ± 0,31	7,16 ± 0,34	8,22 ± 0,37	9,27 ± 0,35*	10,24 ± 0,31*
Bacillus simplex	3,45 ± 0,17	4,05 ± 0,15	4,81 ± 0,22	5,41 ± 0,15	6,95 ± 0,19	7,90 ± 0,26	8,77 ± 0,27	9,32 ± 0,18

D

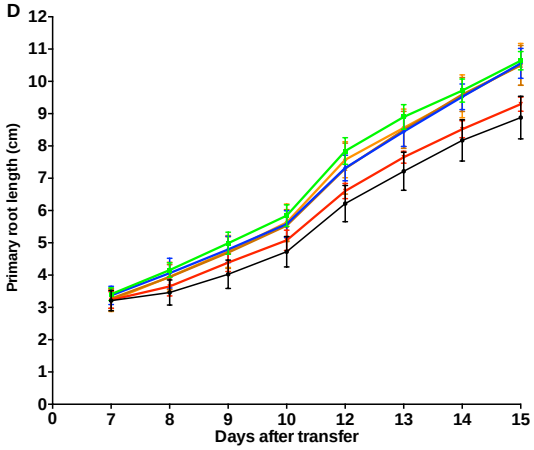

Bacterium	Day 7	Day 8	Day 9	Day 10	Day 12	Day 13	Day 14	Day 15
Non-inoculated control	**3,29 ± 0,37**	**3,67 ± 0,41**	**4,31 ± 0,50**	**4,91 ± 0,43**	**6,36 ± 0,49**	**7,33 ± 0,52**	**8,22 ± 0,54**	**8,98 ± 0,57**
Norcardoides aromaticivorans	3,41 ± 0,20	4,16 ± 0,23	4,99 ± 0,34	5,84 ± 0,34*	7,84 ± 0,41*	8,90 ± 0,38*	9,72 ± 0,36 *	10,64 ± 0,28*
Variovorax paradoxus	3,27 ± 0,31	3,94 ± 0,38	4,70 ± 0,49	5,53 ± 0,50	7,30 ± 0,79	8,50 ± 0,57	9,60 ± 0,53*	10,50 ± 0,62*
Microbacterium phyllosphaerae	3,23 ± 0,26	3,65 ± 0,29	4,39 ± 0,28	5,08 ± 0,31	6,61 ± 0,24	7,65 ± 0,19	8,52 ± 0,26	9,29 ± 0,22
Plantibacter flavus	3,37 ± 0,28	4,06 ± 0,46	4,80 ± 0,41	5,58 ± 0,42	7,32 ± 0,40*	8,45 ± 0,46*	9,52 ± 0,40*	10,56 ± 0,47*
Bacillus simplex	3,22 ± 0,35	3,95 ± 0,45	4,73 ± 0,49	5,63 ± 0,57	7,58 ± 0,56*	8,56 ± 0,58*	9,54 ± 0,66*	10,53 ± 0,65*

Figure 6.3. Kinetic analysis of primary root growth (continued). C. Kinetic effect of bacterial strains on the primary root growth of ccr 1-3. D. Kinetic effect of bacterial strains

*on the primary root growth of ccr 1-6. Data represent at least 12 biologically independent replicates and lines display average values ± standard deviation. Below each graph, tables indicate actual values used to construct the graphs and also indicate statistical differences within each time-point as compared to the control. Data were analysed using one-way ANOVA and Dunnet post-hoc comparisons (p-values: *P < 0.05) whereby each treatment (bacteria) was compared with the control within each time-point.*

Next, we kinetically evaluated the effect of the 5 selected bacterial strains on the different genotypes (Figure 6.3B, C, D). For the wild type, inoculation with *Norcardioides aromaticivorans* and *Plantibacter flavus* improved growth of the primary roots ($P < 0.05$). *Norcardioides aromaticivorans* already exerted positive effects on root growth after 10 days (3 days after inoculation) whereas *Variovorax paradoxus* started to enhance primary root growth after 12 days (Figure 6.3B). For the *ccr*1-3 genotype, all selected bacterial strains enhanced primary root growth ($P < 0.05$), with the single exception of *Bacillus simplex*, which only marginally improved root growth. Earliest effects were observed for *Norcardioides aromaticivorans* and *Microbacterium phyllosphaerae*, which started to display significant effects after 10 days whereas *Plantibacter flavus* (day 14) and *Variovorax paradoxus* (day 15) only at later time-points (Figure 6.3C). Finally for the *ccr*1-6 genotype, again all selected bacterial strains enhanced primary root growth ($P < 0.05$), with the exception of *Microbacterium phyllosphaerae*, which only very slightly improved root growth. In concordance with the results from the *ccr*1-3 genotype and wild type, *Norcardioides aromaticivorans* already exerted positive effects after day 10 whereas all other bacterial inoculants needed longer time-periods to enhance the primary root growth (Figure 6.3D).

6.3.5. Lateral root development and leaf surface area

To evaluate the lateral root development, we analysed the formation of the lateral roots (total number), the average length of the lateral roots and the total length of all lateral roots. Furthermore, we also assessed the effect on the leaf surface area (Figure 6.4 and 6.5).

Firstly we compared the lateral root development between the wild type and the lignin-reduced genotypes. Wild type seedlings (20.65 ± 3.80) formed significantly more lateral roots ($P < 0.001$) as compared to *ccr*1-3 (16.53 ± 2.84) and *ccr*1-6 seedlings (16.16 ± 3.18) (Figure 6.4A).

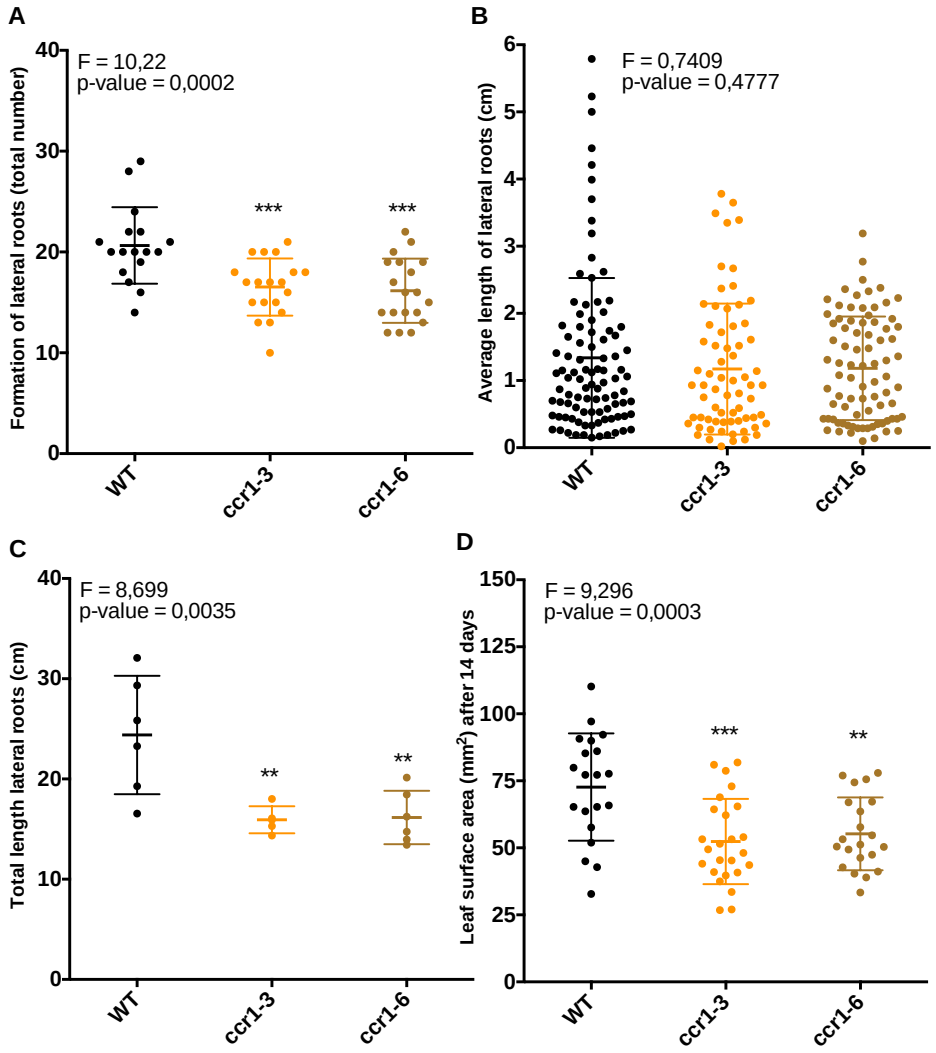

*Figure 6.4. Evaluation of lateral root development and leaf surface of Arabidopsis thaliana genotypes. A. Formation of lateral roots (total number) by Arabidopsis thaliana seedlings after 15 days of growth. B. Average length of lateral roots (cm). C. Total length of lateral roots (cm). D. Leaf surface area (mm^2) after 15 days of growth. Graphs display scatter dot-plots of at least 12 biologically independent replicates. Lines within the scatter dot-plots represent means ± standard deviation. Data were analysed using one-way ANOVA and Dunnet post-hoc comparisons (p-values: **P < 0.01, ***P < 0.001) whereby each lignin-reduced genotype (ccr1-3 and ccr1-6) was compared with the control (wild type Arabidopsis thaliana). Overall ANOVA results (F-value and p-values) are displayed in the top left corner of each graph.*

The average length of the lateral roots was highly comparable between genotypes (F = 0.7409; p = 0.4777)(Figure 6.4B). The total length of the lateral roots was significantly higher (P < 0.01) in the wild type (24.39 ± 5.91 cm) as compared to *ccr*1-3 (15.93 ± 1.34 cm) and *ccr*1-6 (16.16 ± 2.66 cm) (Figure 6.4C). Finally we again observed lower leaf surface area in *ccr*1-3 (52.38 ± 15.90 mm^2) and *ccr*1-6 (55.24 ± 13.59 mm^2) seedlings as compared to the wild type (72.68 ± 20.01 mm^2) (Figure 6.4D).

Next, we evaluated the effects of the bacterial inoculants on the lateral root development within the different genotypes (Figure 6.5A, B, C). For the wild type seedlings, we observed minimal effects of the bacterial inoculants on the lateral root growth (Figure 6.5A). The formation of lateral roots was only improved by *Microbacterium phyllosphaerae* (25.00 ± 3.50) (P < 0.01) as compared to the non-inoculated control (20.65 ± 3.80) (Figure 6.5A, first panel). The average length of the lateral roots was highly comparable (F = 1,276; p = 0,273) (Figure 6.5A, second panel) and an overall bacterium-effect was observed for the total length of the lateral roots (F = 5.085; P = 0.003) (Figure 6.5A, third panel). For the lignin-reduced genotypes, the effect of the bacterial inoculants was more pronounced. For *ccr*1-3, *Microbacterium phyllosphaerae* (19.93 ± 2.80) and *Norcardioides aromaticivorans* (20.86 ± 3.11) significantly increased the formation of lateral roots as compared to the non-inoculated control (15.93 ± 1.34) (Figure 6.5B, first panel). An overall bacterium-effect was observed for the average length of the lateral roots (F = 3.646; P = 0.003) (Figure 6.5B, second panel) and the total length of the lateral roots (F = 3.538; P = 0.019) (Figure 6.5B, third panel). Furthermore *Microbacterium phyllosphaerae* significantly increased the total length of the lateral roots (P < 0.05). For *ccr*1-6, in concordance with *ccr*1-3, *Microbacterium phyllosphaerae* (22.31 ± 3.61) and *Norcardioides aromaticivorans* (21.14 ± 2.69) significantly increased the formation of lateral roots as compared to the non-inoculated control (16.16 ± 2.66). Furthermore, *Bacillus simplex* increased the formation of lateral roots (21.92 ± 4.01) (Figure 6.5C, first panel). We again observed an overall bacterium-effect in the average length of the lateral roots (F = 3.183; P = 0.0079) but no pairwise differences (Figure 6.5C, second panel). Further, the total length of the lateral roots in *ccr*1-6 seedlings was improved by inoculation with *Microbacterium phyllosphaerae* (P < 0.01)*, Norcardioides aromaticivorans*

($P < 0.05$) and *Bacillus simplex* ($P < 0.001$) (Figure 6.5C, third panel). Finally, we evaluated the effect of the bacteria on the leaf surface area of all genotypes after 15 days of growth. Leaf surface area of wild type seedlings (72.68 ± 20.01 mm^2) was improved by inoculation with *Plantibacter flavus* (91.35 ± 21.14 mm^2; $p < 0.05$) and *Variovorax paradoxus* (109.00 ± 24.11 mm^2; $P < 0,01$) (Figure 6.5A, fourth panel). For *ccr*1-3 and *ccr*1-6 all bacterial inoculants, except *Plantibacter flavus,* enhanced the leaf surface area (Figure 6.5B, C, fourth panel).

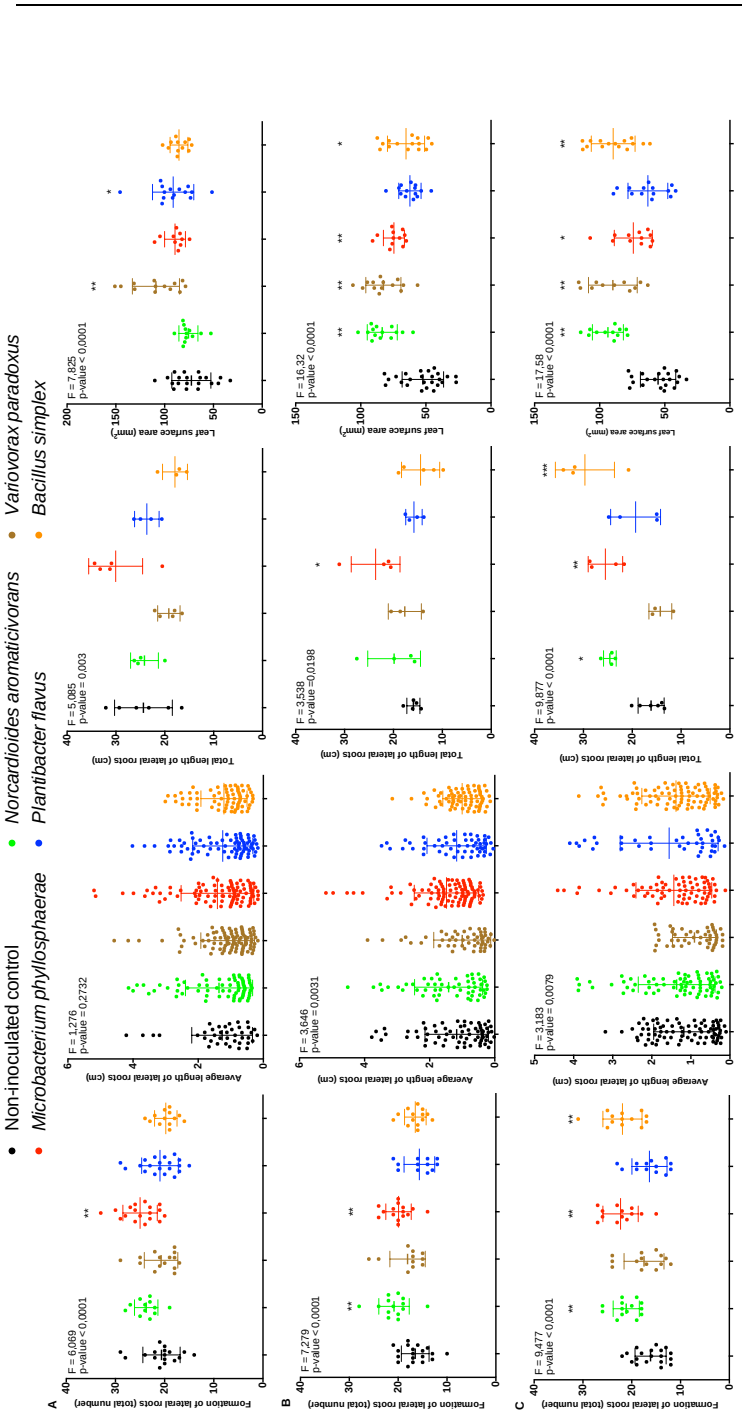

*Figure 6.5. Effect of inoculation with selected bacterial strains on the lateral root growth and leaf surface area of Arabidopsis thaliana genotypes. A. Wild type, B. ccr1-3 and C. ccr1-6. Formation of lateral roots by Arabidopsis thaliana seedlings after 15 days of growth, average length of lateral roots (cm), total length of lateral roots (cm) and leaf surface area (mm^2) after 15 days of growth. Lines within the scatter dot-plots represent means ± standard deviation. Data represent at least 12 biologically independent replicates. Non-inoculated controls are displayed in black and inoculated strains are displayed in several colours (see legend). Data were analysed using one-way ANOVA and Dunnet post-hoc comparisons (p-values: *P < 0.05, **P < 0.01) whereby each treatment (bacteria) was compared with the control. Overall ANOVA results (F-value and p-value) are displayed in the top left corner of each graph.*

6.3.6. Co-cultivation assay

To determine the effect of the bacterial volatiles on the leaf surface of all genotypes, 2-day old seedlings were co-cultivated with the bacterial strains on divided Petri dishes so that only airborne signals were allowed to be transmitted between the bacterial cultures and the plant seedlings.

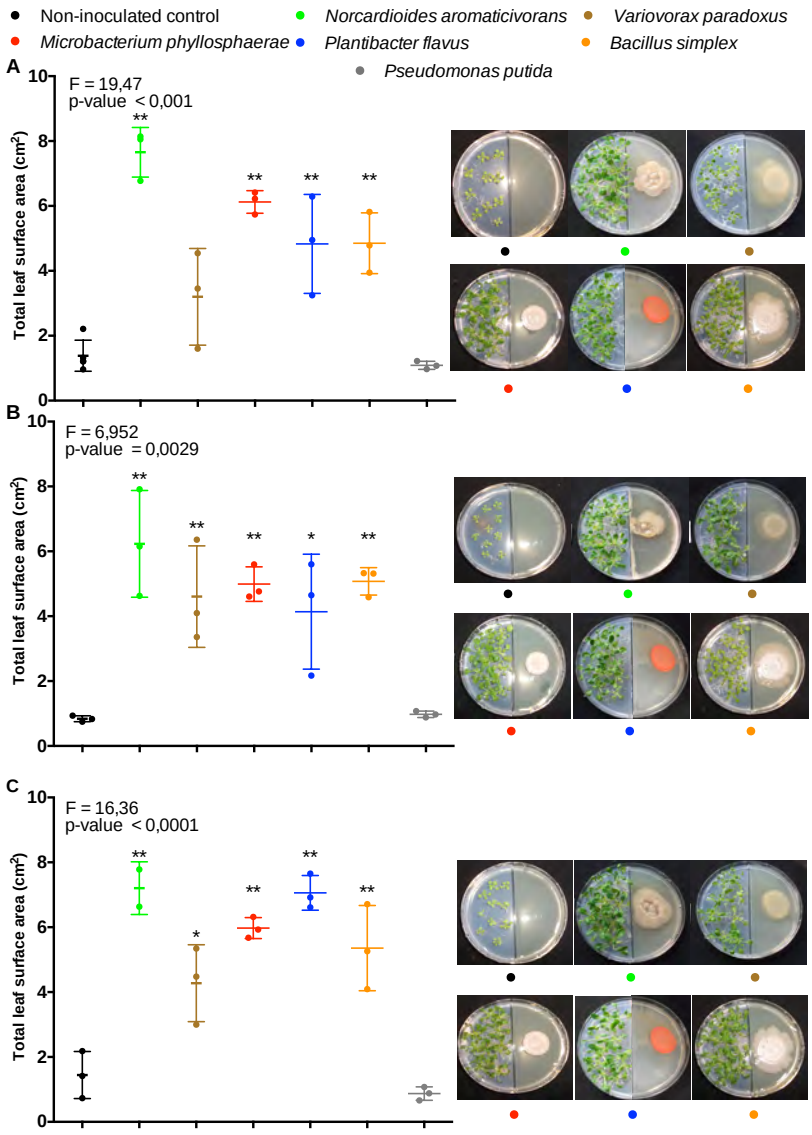

Figure 6.6. Co-cultivation assay: Effect of bacterial volatiles on the leaf surface area of Arabidopsis thaliana genotypes.

*Figure 6.6. Co-cultivation assay (continued) A. Wild type (top panel), B. ccr1-3 (middle panel) and C. ccr1-6 (bottom panel). Scatter dot-plots display total leaf surface area of 3 biologically independent replicates, each consisting of 10 seedlings. To inoculate seedlings, 10^8 colony-forming units (CFU) were applied on one side of the Petri dishes. Lines within the scatter dot-plots represent means ± standard deviation. Non-inoculated controls are displayed in black and inoculated strains are displayed in several colours (see legend). On the right side, representative pictures are shown of the bacterial effects within each genotype. Data were analysed using one-way ANOVA and Dunnet post-hoc comparisons (p-values: *P < 0.05, **P < 0.01) whereby each treatment (bacteria) was compared with the control. Overall ANOVA results (F-value and p-value) are displayed in the top left corner of each graph.*

Leaf surface area was assessed after 14 days of additional growth (16-day old seedlings) (Figure 6.6). As a control, we also included one *Pseudomonas putida* strain, which displayed negative effects on the primary root growth and leaf surface area (Figure 6.2). Irrespective of the genotype, all selected bacterial strains promoted total leaf surface after 14 days of co-cultivation as compared to the non-inoculated controls (Figure 6.6A, B, C). Only *Variovorax paradoxus* failed to improve leaf surface area in the wild type, mainly as a result of high variation in the replicates. Furthermore *Pseudomonas putida* displayed no effect on the leaf surface area.

6.4. Discussion

Arabidopsis thaliana is widely considered to be a model plant for understanding lignin biosynthesis, deposition and function (Boudet, 2000; Chaffey et al., 2002; Goujon et al., 2003; Laskar et al., 2006). Furthermore, during the latter stage of secondary xylem differentiation, *Arabidopsis* closely resembles the anatomy of the wood of angiosperm trees (Chaffey et al., 2002). The genes involved in the biosynthesis of the lignin precursors in *Arabidopsis thaliana* represent ideal candidates to (a) unravel primordial factors contributing to the recalcitrance of cell walls and (b) ultimately tailor biomass for improved cell wall deconstruction for saccharification purposes (Himmel et al., 2007; Vanholme et al., 2012). Numerous *Arabidopsis* mutants of the phenylpropanoid and monolignol biosynthetic pathways have been constructed targeting different genes, most noteworthy phenylalanine ammonia lyase (*PAL*1), *PAL* 2, cinnamate 4-hydroxylase (*C4H*), 4-coumarate-CoA Ligase (*4CL1*, *4CL2),* caffeoyl-CoA O-methyltransferase 1 (*CCOAOMT1*), cinnamoyl-CoA reductase 1 (*CCR1*), ferulate 5-hydroxylase 1 (*F5H1*), *COMT*, cinnamyl alcohol dehydrogenase and caffeoyl shikimate esterase (*CSE*) (Van Acker et al., 2013; Vanholme et al., 2012).

Here, we selected two T-DNA knockout mutants for *CCR1* (*ccr1-3* and *ccr1-6*) identified by Mir Derikvand et al. (2008). *CCR1* represents the main *CCR* isoform involved in the constitutive lignification of *Arabidopsis thaliana* and is highly expressed in lignified tissues (Lauvergeat et al., 2001; Mir Derikvand et al., 2008). Moreover, *CCR*-deficient poplar lines (*Populus tremula x alba*) have also been constructed facilitating extrapolation to commercially viable energy crops (Leplé et al., 2007; Van Acker et al., 2014). We aim to test the following concept: can we improve plant growth of biomass-impaired lignin-reduced genotypes by exploiting the metabolic and plant growth promotion capacities of selected bacterial strains? And in this way ultimately combine high processing efficiency, as delivered by the lignin-reduced genotypes, with optimized plant growth (and by extension crop biomass) with the use of PGP bacteria. For this purpose, we selected a collection of bacterial strains, isolated from wild type and *CCR*-down-regulated poplar trees, which were part of a field trial (Beckers et al. 2015, chapter 3). To limit the negative effects of the accumulation of various phenolic by-products and detoxification products (as caused by *CCR*-down-regulation)(Leplé et al., 2007; Ralph et al., 1998), we firstly evaluated the

potential of the selected bacteria to degrade aromatic lignin-related compounds, accumulated in *CCR*-deficient genotypes. We identified several bacterial strains capable of degrading a range of specific phenolic aromatic carbon sources (Table 6.1 and Supplementary Table 6.1). Indeed several bacterial degradation pathways have been elucidated for lignin-derived low-molecular weight compounds: (1) the β-aryl ether cleavage pathway reported in *Pseudomonas putida* strain FK-2 (Fukuzumi et al., 1980; Katayama and Fukuzumi, 1979), *Sphingomonas paucimobilis* SYK-6 (Masai et al., 2007), *S. paucimobilis* TMY1009 (Samejima et al., 1985) and *Delftia (Pseudomonas) acidovorans* D_3 (Vicuna et al., 1987); (2) the biphenyl catabolic pathway in *Sphingomonas paucimobilis* SYK-6 (Masai et al., 2007) and *Pseudomonas pseudoalcaligenes* (Dehmel et al., 1995); (3) the ferulate catabolic pathway whereof enzymes have been found in *Pseudomonas fluorescens* AN103 (Gasson et al., 1998), *Pseudomonas* sp. HR199 (Overhage et al., 1999; Priefert et al., 1997), *Pseudomonas putida* WCS358 (Venturi et al., 1989) and *Amycolatopsis sp*. strain HR167 (Achterholt et al., 2000); (4) the tetrahydrofolate-dependent O-demethylation systems reported in *Pseudomonas* sp., *Acinetobacter sp*. (Segura et al., 1999; Brunel & Davison, 1988; Civolani et al., 2000) and the anaerobic bacteria *Acetobacterium wooddii* (Kaufman et al., 1998), *A. dehalogenans* (Berman and Frazer, 1992) and *Moorella thermoacetica* (Naidu et al., 2001)*;* (5) the protocatechuate 4,5-cleavage pathway characterized in *Acinetobacter calcoaceticus*, *Pseudomonas putida* and *Agrobacterium tumefaciens* (Harwood & Parales, 1996); and finally (6) multiple pathways for 3-O-methylgallate catabolism (3MGA) whereof 3MGA 3,4 dioxygenase has been reported in *Acinetobacter lwoffii* (Sze and Dagley, 1987) and *Pseudomonas putida* TMC (Donnelly & Dagley, 1981). Recently, bacteria-derived enzyme systems have even been transformed in *Arabidopsis thaliana* (C α–dehydrogenase (LigD) enzyme of *Spingobium* sp. strain SYK-6) in an attempt to modify specific lignin substructures and thereby increase biomass conversion efficiency (Tsuji et al., 2015).

Furthermore, the potential of the selected plant-associated bacteria to improve plant growth was estimated by *in vitro* screening phenotypic characteristics of production of plant growth regulators (*e.g.* IAA), stress-relieving enzymes (*e.g.* ACC-deaminase) and increased nutrient uptake (*e.g.* siderophore production)

(Bulgarelli et al., 2013; Compant et al., 2010; Hardoim et al., 2008; Weyens et al., 2009). A wide range of bacteria displayed *in vitro* plant growth promotion capacities (Supplementary Table 6.1, Table 6.1), as previously observed in numerous studies (Croes et al., 2013; Truyens et al., 2013; Weyens et al., 2013). To test their *in vivo* plant growth promotion potential, 15 promising bacterial strains were selected based on their capacity to efficiently degrade the selected phenolic carbon sources and their positive results in *in vitro* plant growth promotion tests (Table 6.1). During *in vivo* plant growth tests, we firstly focussed on the effects of the host genotype (lignin-reduced genotypes (*ccr*1-3 and *ccr*1-6)) on the primary root growth, lateral root growth and the leaf surface area as compared to the wild type (Figure 6.1 and Figure 6.3A, Figure 6.4). As expected, after 14 days of growth, both lignin-reduced genotypes showed dwarfed phenotypes whereby primary root growth, lateral root development and leaf surface area was reduced as compared to the wild type. Perturbations in the lignin biosynthesis often affect plant growth and developmental effects for *ccr*1-3 and *ccr*1-6 were previously noticed by Van Acker et al. (2013) where the final heights of the inflorescence stems were reduced respectively by 83% and 34%. Also in the analysis of *CCR*-down-regulated tobacco plants and field-grown poplar trees, plants with the lowest *CCR* activity presented a dwarf phenotype accompanied with lignin alterations (Pincon et al., 2001; Chabannes et al., 2001; Leplé et al., 2007). However, remarkably, both lignin-reduced genotypes displayed faster germination rates after seven days as depicted by the length of the primary root growth and leaf surface area (Figure 6.1A and 6.1C top panels and Figure 6.3A). Possible speculative explanations of the differential germination rates of the lignin-reduced genotypes could involve several aspects: (a) lignin-reduced genotypes produced fewer seeds per plant and fewer seeds per silique which could indicate that these genotypes favour quality over quantity during seed production, (b) seeds from the lignin-reduced genotypes are also bigger which could indicate that they store more (and/or differential) reserves in the cotyledons. Aforementioned aspects could cause faster germination whereafter the effect of the mutation (perturbation in the lignin biosynthesis) sets in and ultimately leads to developmental effects. The strong reduction of the biomass by *CCR*-down-regulation counteracts, at least for some part, the improved enzymatic processing efficiency of these plants.

Therefore, we evaluated the potential of selected bacterial strains to enhance plant growth and ultimately biomass production. From our selection, especially *Norcardioides aromaticivorans, Variovorax paradoxus, Microbacterium phyllosphaerae, Plantibacter flavus* and *Bacillus simplex* promoted primary root growth and leaf surface area of the lignin-reduced genotypes (Figure 6.2, 6.3 and Supplementary Figures 6.3, 6.4 and 6.5). Indeed, *in vitro* screening of the phenotypic characteristics of these bacterial strains revealed production of siderophores, IAA, ACC-deaminase and phosphate solubilizing components to varying extents (Table 6.1). Auxin production (with the most abundant member being indol-3-acetic acid (IAA)) is a common feature of plant-associated bacteria, whereby biosynthesis is mostly mediated by the indole-3-acetamide (IAM) and indole-3-pyruvate (IPyA) pathways (Duca et al., 2014; Lambrecht et al., 2000; Spaepen et al., 2007; Spaepen & Vanderleyden, 2011). IAA-production can have profound effects on root morphology by stimulating plant cell proliferation and elongation resulting in higher total root surfaces and thus enabling the plant for more efficient uptake of nutrients and water (Glick et al., 1998; Patten & Glick, 2002; Spaepen et al., 2008). ACC-deaminase activity (encoded by the *acdS* gene) can lower the levels of stress ethylene produced by the plant. Since enhanced ethylene levels inhibit root and plant growth, metabolization of ACC (ethylene precursor) by plant associated bacteria may result in improved plant growth in stress conditions (Bulgarelli et al., 2013; Contesto et al., 2008; Glick et al., 1998; Glick et al., 2007; Tsuchisaka et al., 2009). Furthermore, bacterial inoculants *Norcardioides aromaticivorans* and *Microbacterium phyllosphaerae* also promoted lateral root development of both lignin-reduced genotypes, as measured by the formation of the lateral roots (total number) and the total length of the lateral roots (Figure 6.5). As well as providing anchorage, lateral root development contributes to more efficient usage of water and facilitates the extraction of micro- and macronutrients from the soil (Casimiro et al., 2003). Moreover, *Microbacterium phyllosphaerae* and *Bacillus simplex* also increased the formation of root hairs (Supplementary Figure 6.6). Root hairs, tubular-shaped tip-growing cells arising from specialized root epidermal cells (trichoblasts), primarily function in root anchorage and increasing the root surface area thereby enlarging the area of soil that can be exploited by the plant (Gilroy & Jones, 2000; Jungk, 2001; Schiefelbein, 1990).

Root hairs are major nutrient-uptake sites with the percentage of nutrients acquired by the root hairs varying to up to 80% of the total nutrient uptake, depending on plant species and genetic variability of root hair formation (Jungk, 2001). Bacterial IAA stimulates root hair formation while increasing the number and length of the lateral and primary roots, when it is available within an ideal concentration range (Duca et al., 2014; Spaepen & Vanderleyden, 2011). Since extrapolation to interesting bio-energy crops is desired (such as poplar (Leplé et al., 2007; Van Acker et al., 2014)), we also evaluated leaf surface area. Indeed, our selected bacterial inoculants except for *Plantibacter flavus*, increased leaf surface area of lignin-reduced genotypes to the point of completely offsetting the biomass impairment associated with *CCR* down-regulation and reaching leaf surface area of wild type *Arabidopsis thaliana* plants.

Finally, the effect of the bacterial volatile organic compounds (VOCs) (which represent an alternative plant growth promotion mechanism) was assessed on the leaf surface of the lignin-reduced genotypes and wild type *Arabidopsis thaliana*. All five PGP bacteria tested (*Norcardioides aromaticivorans, Variovorax paradoxus, Microbacterium phyllosphaerae, Plantibacter flavus* and *Bacillus simplex)* elicited, irrespective of the studied genotype, up to 8-fold promotion of the leaf surface area (Figure 6.6). However, *Pseudomonas putida* displayed no effect on the plant growth for all of the genotypes, indicating that bioactive VOCs are a strain specific phenomenon. The first report of plant growth promotion by VOCs was made by Ryu et al., (2003) whereby a blend of airborne chemicals of *Bacillus subtilis* (GB03) and *Bacillus amyloliquefaciens* (IN937a) improved plant growth. Furthermore, Ryu et al., (2004) reported the capacity of selected PGP *Bacillus* strains to emit airborne chemicals with sufficient chemical information to trigger induced systemic resistance (ISR) as measured by *Arabidopsis thaliana* seedlings ability to resist infection with the soft rot-causing pathogen *Erwinia carotovora* subsp. carotovora. This is reminiscent of the capacity of plants to release VOCs (methyl salicylate (MeSA), methyl jasmonate (MeJA), cis-jasmone and the gaseous hormone ethylene) into the environment in response to damage or infection, which evoke defence mechanisms and induce the expression of defence-related genes (Weber, 2002). Volatile profiles in these studies identified 2,3-butanediol and 3-hydroxy-2-butanone (acetoin) as major volatile chemicals of *Bacillus subtilis* (GB03) and *Bacillus*

amyloliquefaciens (IN937a) eliciting positive effects on the growth of *Arabidopsis thaliana (*Ryu et al., 2003). Acetoin and 2,3-butanediol are volatile alcohols produced from an alternative pathway for pyruvate metabolism that is favoured under low pH or anaerobic conditions (Ji et al., 2011; Ryu et al., 2003; Ryu et al., 2004). We detected no acetoin production during our *in vitro* screening of the plant growth promotion capacities of the selected bacterial strains (Table 6.1). However, as described by Ryu et al. (2003), low partial O_2 pressure in the Petri dish bioassays (which is reminiscent of the O_2 pressure in the root environment) may result in limited O_2 and may trigger the acetoin alternative pathway in bacteria. This could indicate that *in vitro* testing of bacterial acetoin production should ideally be conducted under low partial O_2 pressure. Furthermore, other bioactive VOCS may have contributed to the plant growth promotion such as 1-hexanol, indole and pentadecane (Blom et al., 2011; Ryu et al., 2003). More recently, Kai & Piechulla (2009) reported that growth promotion of *Arabidopsis thaliana* could, at least partially, be due to the privileged bacterially induced CO_2 accumulation in closed systems, which increases chlorophyll content and photosynthetic efficiency. Indeed, *Bacillus* strains usually release CO_2 via the tricarboxylic acid cycle. However growth promotion persisted, at lower rates, when CO_2 was captured from the closed systems, indicating that bacterial VOCs surely play a role in the promotion of plant growth.

6.5. Conclusion

In conclusion, we proved our hypothesis that PGP bacteria can promote the growth of lignin-reduced *Arabidopsis thaliana* genotypes and thereby offset the biomass impairment caused by the perturbation in the lignin biosynthesis. However, extrapolation of this concept to interesting bio-energy crops still needs further insights and study. Results from this study should be confirmed on a less artificial substrate such as sand. Furthermore, in depth study of the bacterial effects on the phenolic detoxification products (metabolite profiling) could provide more insight into the mechanisms of action of the PGP bacteria as well as gene expression profiles and enzyme activities of stress-related genes. Furthermore full genome sequencing of selected bacterial strains and the annotation of interesting genes (e.g. genes responsible for the degradation of

the phenolic degradation products (e.g. LIG genes) and/or genes responsible for plant-growth promotion mechanisms) could be an interesting route.

References

Achterholt, S., Priefert, H. and Steinbuchel, A. (2000). Identification of Amycolatopsis sp. strain HR167 genes , involved in the bioconversion of ferulic acid to vanillin. *Applied Microbiology Biotechnology*, *103*, 799–807.

Alonso, J. M., Stepanova, A. N., Leisse, T. J., Kim, C. J., Chen, H., Shinn, P., Stevenson, D. K., Zimmerman, J., Barajas, P., Cheuk, R., Gadrinab, C., Heller, C., Jeske, A., Koesema, E., Meyers, C. C., Parker H., et al. (2003). Genome-wide insertional mutagenesis of Arabidopsis thaliana. *Science*, *301*, 653–657

Belimov, a. a., Hontzeas, N., Safronova, V. I., Demchinskaya, S. V., Piluzza, G., Bullitta, S. and Glick, B. R. (2005). Cadmium-tolerant plant growth-promoting bacteria associated with the roots of Indian mustard (Brassica juncea L. Czern.). *Soil Biology and Biochemistry*, *37*, 241–250.

Bloemberg, G. V and Lugtenberg, B. J. (2001). Molecular basis of plant growth promotion and biocontrol by rhizobacteria. *Current Opinion in Plant Biology*, *4*, 343–350.

Blom, D., Fabbri, C., Connor, E. C., Schiestl, F. P., Klauser, D. R., Boller, T., Eberl, L. and Weisskopf, L. (2011). Production of plant growth modulating volatiles is widespread among rhizosphere bacteria and strongly depends on culture conditions. *Environmental Microbiology*, *13*, 3047–3058.

Boerjan, W., Ralph, J. and Baucher, M. (2003). Lignin biosynthesis. *Annual Review of Plant Biology*, *54*, 519–546.

Boudet, A. (2000). Lignins and lignification: Selected issues. *Plant Physiology and Biochemistry*, *38*, 81–96.

Brunel, F. and Davison, J. (1988). Cloning and Sequencing of Pseudomonas Genes Encoding Vanillate Demethylase. *Journal of Bacteriology*, *170*, 4924–4930.

Bulgarelli, D., Schlaeppi, K., Spaepen, S., Ver Loren van Themaat, E. and Schulze-Lefert, P. (2013). Structure and functions of the bacterial microbiota of plants. *Annual Review of Plant Biology*, *64*, 807–838.

Casimiro, I., Beeckman, T., Graham, N., Bhalerao, R., Zhang, H., Casero, P., Sandberg, G., and Bennett, M. J. (2003). Dissecting Arabidopsis lateral root development. *Trends in Plant Science*, *8*, 165–171.

Cassman, K. G. (2007). Climate change, biofuels, and global food security. *Environmental Research Letters*, *2*, 1-3.

Cassman, K. G. and Liska, A. J. (2007). Food and fuel for all : realistic or foolish ? *Biofuels, Bioproducts and Biorefining*, *1*, 18–23.

Chabannes, M., Barakate, A., Lapierre, C., Marita, J. M., Ralph, J. and Pean, M. (2001). Strong decrease in lignin content without significant alteration of plant development is induced by simultaneous down-regulation of cinnamoyl CoA reductase (*CCR*) and cinnamyl alcohol dehydrogenase (CAD) in tobacco plants, *28*, 257–270.

Chaffey, N., Cholewa, E., Regan, S. and Sundberg, B. (2002). Secondary xylem development in Arabidopsis : a model for wood formation. *Physiologa Plantarum*, 114, 594–600.

Chen, F. and Dixon, R. A. (2007). Lignin modification improves fermentable sugar yields for biofuel production. *Nature Biotechnology*, *25*, 759–761.

Civolani, C., Barghini, P., Roncetti, A. R. and Ruzzi, M. (2000). Bioconversion of Ferulic Acid into Vanillic Acid by Means of a Vanillate-Negative Mutant of Pseudomonas fluorescens Strain BF13. *Applied and Environmental Microbiology*, *66*, 2311–2317.

Compant, S., Clément, C. and Sessitsch, A. (2010). Plant growth-promoting bacteria in the rhizo- and endosphere of plants: Their role, colonization, mechanisms involved and prospects for utilization. *Soil Biology and Biochemistry*, *42*, 669–678.

Contesto, C., Desbrosses, G., Lefoulon, C., Béna, G., Borel, F., Galland, M., Gamet, L., Varoquaux, F. and Touraine, B. (2008). Effects of rhizobacterial ACC deaminase activity on Arabidopsis indicate that ethylene mediates local root responses to plant growth-promoting rhizobacteria. *Plant Science*, *175*, 178–189.

Berman, M., H. and Frazer, A., C. (1992). Importance of Tetrahydrofolate and ATP in the Anaerobic O-Demethylation Reaction for Phenylmethylethers. *Applied and Environmental Microbiology*, *58*, 925–931.

Croes, S., Weyens, N., Janssen, J., Vercampt, H., Colpaert, J. V, Carleer, R. and Vangronsveld, J. (2013). Bacterial communities associated with Brassica napus L. grown on trace element-contaminated and non-contaminated fields: a genotypic and phenotypic comparison. *Microbial Biotechnology*, *6*, 371–384.

Dehmel, U., Engesser, K.-H., Timmis, K. N. and Dwyer, D. F. (1995). Cloning, nucleotide sequence, and expression of the gene encoding a novel dioxygenase involved in metabolism of carboxydiphenyl ethers in Pseudomonas pseudoalcaligenes POB310. *Archives of Microbiology*, *163*, 35–41.

Donnelly, M. I. and Dagley, S. (1981). Bacterial Degradation of 3,4,5-Trimethoxycinnamic Acid with Production of Methanol. *Journal of Bacteriology 147*(2), 471–476.

Duca, D., Lorv, J., Patten, C. L., Rose, D. and Glick, B. R. (2014). Indole-3-acetic acid in plant-microbe interactions. *Antonie van Leeuwenhoek*, *106*, 85–125.

Fukuzumi, T. (1980). Microbial metabolism of lignin-related aromatics. In ‘‘Lignin Biodegradation: Microbiology, Chemistry, and Potential Applications,’’ eds. Kirk, T. K., Higuchi, T., and Chang, H.-M., CRC Press, Boca Raton, *6*, 73–94.

Gamborg, O. L., Miller, R. A. and Ojima, K. (1968). Nutrient requirements of suspension cultures of soybean root cells. *Experimental Cell Research*, *50*, 151–158.

Gasson, M. J., Kitamura, Y., Mclauchlan, W. R., Narbad, A., Parr, A. J., Parsons, E. L. H., Payne, J., Rhodes, M. J. C. and Walton, N. J. (1998). Metabolism of Ferulic Acid to Vanillin. *The Journal of Biological Chemistry*, *273*, 4163–4170.

Gilroy, S. and Jones, D. L. (2000). Through form to function: root hair development and nutrient uptake. *Trends in Plant Science*, *5*, 56-60.

Glick, B., Penrose, D. and Li, J. (1998). A model for the lowering of plant ethylene concentrations by plant growth-promoting bacteria. *Journal of Theoretical Biology*, *190*, 63–68.

Glick, B. R., Todorovic, B., Czarny, J., Cheng, Z., Duan, J. and McConkey, B. (2007). Promotion of Plant Growth by Bacterial ACC Deaminase. *Critical Reviews in Plant Sciences*, *26*, 227–242.

Gordon, S. A. and Weber, R. P. (1950). Colorimetric estimation of Indoleacetic acid. *Plant Physiology*, *1*, 192-195.

Goujon, T., Sibout, R., Eudes, A., MacKay, J. and Jouanin, L. (2003). Genes involved in the biosynthesis of lignin precursors in Arabidopsis thaliana. *Plant Physiology and Biochemistry*, *41*, 677–687.

Guckert, J. B., Carr, G. J., Johnson, T. D., Hamm, B. G., Davidson, D. H. and Kumagai, Y. (1996). Community analysis by Biolog: curve intergation for statistical analysis of activated sludge microbial habitats. *Journal of Microbiological Methods*, *27*, 183–197.

Hardoim, P. R., van Overbeek, L. S. and Van Elsas, J. D. (2008). Properties of bacterial endophytes and their proposed role in plant growth. *Trends in Microbiology*, *16*, 463–471.

Harwood, C. S. and Parales, R. E. (1996). The β-ketoadipate pathway and the biology of self-identity. *Annual Review of Microbiology*, *50*, 553–590.

Himmel, M. E., Ding, S.-Y., Johnson, D. K., Adney, W. S., Nimlos, M. R., Brady, J. W. and Foust, T. D. (2007). Biomass recalcitrance: engineering plants and enzymes for biofuels production. *Science*, *315*, 804–807.

Hisano, H., Nandakumar, R. and Wang, Z.-Y. (2009). Genetic modification of lignin biosynthesis for improved biofuel production. *In Vitro Cellular & Developmental Biology* , *45*, 306–313.

Ji, X.-J., Huang, H. and Ouyang, P.-K. (2011). Microbial 2,3-butanediol production: a state-of-the-art review. *Biotechnology Advances*, *29*, 351–364.

Jungk, A. (2001). Root hairs and the acquisition of plant nutrients from soil. *Journal of Plant Nutrition and Soil Science*, *164*, 121–129.

Katayama, Y. and Fukuzumi, T. (1979). Bacterial degradation of dimers structurally related to lignin. III. Metabolism of α-veratryl-β-guaiacylpropionic acid and D,L-pinor-esinol by *Pseudomonas putida*. *Mokuzai Gakkaishi*, *25*, 67–76.

Kai, M. and Piechulla, B. (2009). Plant growth promotion due to rhizobacterial volatiles – An effect of CO 2? *FEBS Letters*, *583*, 3473–3477.

Kaufmann, F., Wohlfarth, G. and Diekert, G. (1998). O-Demethylase from Acetobacterium dehalogenans . Cloning, sequencing, and active expression of the gene encoding the corrinoid protein. *European Journal of Biochemistry*, *257*, 515–521.

Lambrecht, M., Okon, Y., Broek, A. Vande and Vanderleyden, J. (2000). Indole-3-acetic acid : a reciprocal signalling molecule in bacteria – plant interactions. *Trends in Microbiology*, *8*, 1998–2000.

Laskar, D. D., Jourdes, M., Patten, A. M., Helms, G. L., Davin, L. B. and Lewis, N. G. (2006). The Arabidopsis cinnamoyl CoA reductase irx4 mutant has a delayed but coherent (normal) program of lignification. *The Plant Journal*, *48*, 674–686.

Lauvergeat, V., Lacomme, C., Lacombe, E., Lasserre, E., Roby, D. and Grima-pettenati, J. (2001). Two cinnamoyl-CoA reductase (*CCR*) genes from Arabidopsis thaliana are differentially expressed during development and in response to infection with pathogenic bacteria, *57*, 1187–1195.

Leplé, J.-C., Dauwe, R., Morreel, K., Storme, V., Lapierre, C., Pollet, B., Naumann A., Kang, K., Kim, H., Ruel, K., Lefèbvre, A., Joseleau, J., Grima-Pettenati, J., De Rycke, R., Andersson-Gunneråas, S., Erban, A., Fehrle A., Petit-Conil, M., Kopka, J., Polle, A., Messens, E., Sundberg, B., Mansfield, S., Ralph, J., Pilate, G. and Boerjan, W. (2007). Down-regulation of cinnamoyl-coenzyme A reductase in poplar: multiple-level phenotyping reveals effects on cell wall polymer metabolism and structure. *The Plant Cell*, *19*, 3669–3691.

Lugtenberg, B. and Kamilova, F. (2009). Plant-growth-promoting rhizobacteria. *Annual Review of Microbiology*, *63*, 541–556.

Mantelin, S. and Touraine, B. (2004). Plant growth-promoting bacteria and nitrate availability: impacts on root development and nitrate uptake. *Journal of Experimental Botany*, *55*, 27–34.

Masai, E., Katayama, Y. and Fukuda, M. (2007). Genetic and Biochemical Investigations on Bacterial Catabolic Pathways for Lignin-Derived Aromatic Compounds. *Bioscience, Biotechnology, and Biochemistry*, *71*, 1–15.

Mergeay, M., Nies, L. D., Schlegel, H. G., Gerits, J., Charles, P. and Gijsegem, F. V. A. N. (1985). Alcaligenes eutrophus CH34 Is a Facultative Chemolithotroph with Plasmid-Bound Resistance to Heavy Metals. *Journal of Bacteriology*, *162*, 328–334.

Mir Derikvand, M., Sierra, J. B., Ruel, K., Pollet, B., Do, C.-T., Thévenin, J., Buffard, D., Jouanin, L. and Lapierre, C. (2008). Redirection of the phenylpropanoid pathway to feruloyl malate in Arabidopsis mutants deficient for cinnamoyl-CoA reductase 1. *Planta*, *227*, 943–956.

Murashige, T. and Skoog, F. (1962). A Revised Medium for Rapid Growth and Bio Assays with Tobacco Tissue Cultures. *Physiologia Plantarum*, *15*, 473–497.

Naidu, D. and Ragsdale, S. W. (2001). Characterization of a Three-Component Vanillate O -Demethylase from *Moorella thermoacetica. Journal of Bacteriology*, *183*, 3276–3281.

Nautiyal, C. S. (1999). An efficient microbiological growth medium for screening phosphate solubilizing microorganisms. *FEMS Microbiology Letters*, *170*, 265–270.

Naylor, R. L., Liska, A. J., Burke, M. B., Falcon, W. P., Gaskell, J. C., Rozelle, S. D. and Cassman, K. G. (2007). The Ripple Effect: Biofuels, Food Security, and the Environment. *Environment: Science and Policy for Sustainable Development*, *49*, 30–43.

Overhage, R. G., Priefert, H. and Steinbu, A. (1999). Biochemical and Genetic Analyses of Ferulic Acid Catabolism in Pseudomonas sp. Strain HR199. *Applied and Evironmental Microbiology*, *65*, 4837–4847.

Patten, C. L. and Glick, B. R. (2002). Role of Pseudomonas putida Indoleacetic Acid in Development of the Host Plant Root System. *Applied and Evironmental Microbiology*, *68*, 3795–3801.

Pincon, G., Chabannes, M., Lapierre, C., Pollet, B., Ruel, K., Joseleau, J., Boudet, A. M. and Legrand, M. (2001). Simultaneous Down-Regulation of Caffeic / 5-Hydroxy Ferulic Acid- O -Methyltransferase I and Cinnamoyl-Coenzyme A Reductase in the Progeny from a Cross between Tobacco Lines Homozygous for Each Transgene . Consequences for Plant Development and lignin synthesis. *Plant Physiology*, 126, 145-155.

Pound, M. P., French, A. P., Atkinson, J. a, Wells, D. M., Bennett, M. J. and Pridmore, T. (2013). RootNav: navigating images of complex root architectures. *Plant Physiology*, *162*, 1802–1814.

Priefert, H., Rabenhorst, R. and Steinbuchel, A. (1997). Molecular Characterization of Genes of *Pseudomonas* sp. Strain HR199 Involved in

Bioconversion of Vanillin to Protocatechuate. *Journal of Bacteriology*, *179*, 2595–2607.

R Development Core Team (2011). R: A language and environment for statistical computing. R Foundation for Statistical Computing, Vienna, Austria. ISBN 3-900051-07-0, URL http://www.R-project.org/.

Raaijmakers, J. M., Paulitz, T. C., Steinberg, C., Alabouvette, C. and Moënne-Loccoz, Y. (2008). The rhizosphere: a playground and battlefield for soilborne pathogens and beneficial microorganisms. *Plant and Soil*, *321*, 341–361.

Romick, T. L. and Fleming, H. P. (1998). Acetoin production as an indicator of growth and metabolic inhibition of Listeria monocytogenes. *Journal of Applied Microbiology*, *84*, 18–24.

Ruel, K., Berrio-sierra, J., Derikvand, M. M., Pollet, B., Thévenin, J., Lapierre, C., Jouanin, L. and Joseleau, J. (2009). Impact of *CCR*1 silencing on the assembly of lignified secondary walls in *Arabidopsis thaliana*. *The New Phytologist, 184*, 99–113.

Ryu, C., Farag, M. A., Hu, C., Reddy, M. S., Wei, H., Paré, P. W. and Kloepper, J. W. (2003). Bacterial volatiles promote growth in *Arabidopsis thaliana*. *Proceedings of the National Academy of Sciences of the United States of America*, *100*, 4927–4932.

Ryu, C., Farag, M. A., Hu, C., Reddy, M. S., Kloepper, J. W. and Pare, P. W. (2004). Bacterial Volatiles Induce Systemic Resistance in *Arabidopsis*. *Plant Physiology*, *134*, 1017–1026.

Samejima, M., Saburi, Y., Yoshimoto, T., Fukuzumi, T. and Nakazawa, T. (1985). Catabolic pathway of guaiacyl-glycerol-β-guaiacyl ether by *Pseudomonas* sp. TMY1009. *Mokuzai Gakkaishi*, *31*, 956–958.

Segura, A., Bunz, P. V., D'Argenio, D. A. and Ornston, L. N. (1999). Genetic Analysis of a Chromosomal Region Containing vanA and vanB , Genes Required for Conversion of Either Ferulate or Vanillate to Protocatechuate in *Acinetobacter*. *Journal of Bacteriology*, *181*, 3494–3504.

Schiefelbein, J. W. (1990). Genetic Control of Root Hair Development in *Arabidopsis thaliana*. *The Plant Cell*, *2*, 235–243.

Schlegel, H. G., Cosson, J.-P. and Baker, A. J. M. (1991). Nickel-hyperaccumulating Plants Provide a Niche for Nickel-resistant Bacteria. *Botanica Acta*, *104*, 18–25.

Schwyn, B. and Neilands, J. B. (1987). Universal chemical assay for the detection and determination of siderophores. *Analytical Biochemistry*, *160*, 47–56.

Selosse, M.-A., Baudoin, E. and Vandenkoornhuyse, P. (2004). Symbiotic microorganisms, a key for ecological success and protection of plants. *Comptes Rendus Biologies*, *327*, 639–648.

Sessions, A., Burke, E., Presting, G., Aux, G., Mcelver, J., Patton, D., Dietrich, D., Ho, P., Bacwaden, J., Ko, C., Clarke, J. D., Cotton, D., Bullis, D., Snell, J., Miguel, T., Hutchison, D., Kimmerly, B., Mitzel, T., Katagiri, F., Glazebrook, J., Law, M. and Goff, S. A. (2002). A High-Throughput Arabidopsis Reverse Genetics System. *The Plant Cell*, *14*, 2985–2994.

Solomon, B. D. (2010). Biofuels and sustainability. *Annals of the New York Academy of Science*, *1185*, 119–134.

Spaepen, S., Dobbelaere, S., Croonenborghs, A. and Vanderleyden, J. (2008). Effects of *Azospirillum brasilense* indole-3-acetic acid production on inoculated wheat plants. *Plant and Soil*, *312*, 15–23.

Spaepen, S. and Vanderleyden, J. (2011). Auxin and Plant-Microbe Interactions. *Cold Spring Harbor Perspectives in Biology, 3,* 1–14.

Spaepen, S., Vanderleyden, J. and Remans, R. (2007). Indole-3-acetic acid in microbial and microorganism-plant signaling. *FEMS Microbiology Reviews*, *31*, 425–448.

Sze, I. S. and Dagley, S. (1987). Degradation of Substituted Mandelic Acids by Fission Reactions. *Journal of Bacteriology*, *169*, 3833–3835.

Ralph, J., Hatfield, R. D., Piquemal, J., Yahiaoui, N., Pean, M., Lapierre, C. and Boudet, A. M. (1998). NMR characterization of altered lignins extracted from tobacco plants down-regulated for lignification enzymes cinnamyl- alcohol dehydrogenase and cinnamoyl-CoA reductase. *Proceedings of the National Academy of Sciences of the United States of America 95*, 12803–12808.

R Development Core Team (2011). R: A language and environment for statistical computing. R Foundation for Statistical Computing, Vienna, Austria. ISBN 3-900051-07-0, URL http://www.R-project.org/.

Studer, M. H., Demartini, J. D., Davis, M. F., Sykes, R. W., Davison, B. and Keller, M. (2011). Lignin content in natural Populus variants affects sugar release. *Proceedings of the National Academy of Sciences of the United States of America 108*, 6300–6305.

Taghavi, S., Garafola, C., Monchy, S., Newman, L., Hoffman, A., Weyens, N., Barac, T., Vangronsveld, J. and van der Lelie, D. (2009). Genome survey and characterization of endophytic bacteria exhibiting a beneficial effect on growth and development of poplar trees. *Applied and Environmental Microbiology*, *75*, 748–757.

Taghavi, S., Lelie, D. Van Der, Hoffman, A., Zhang, Y. and Walla, M. D. (2010). Genome Sequence of the Plant Growth Promoting Endophytic Bacterium Enterobacter sp . 638. *PLoS Genetics*, *6*, 1-15.

Truyens, S., Weyens, N., Cuypers, A., and Vangronsveld, J. (2013). Changes in the population of seed bacteria of transgenerationally Cd-exposed Arabidopsis thaliana. *Plant Biology*, *15*, 971–981.

Tsuchisaka, A., Yu, G., Jin, H., Alonso, J. M., Ecker, J. R., Zhang, X., Gao, S. and Theologis, A. (2009). A Combinatorial Interplay Among the 1-Aminocyclopropane-1-Carboxylate Isoforms Regulates Ethylene Biosynthesis in Arabidopsis thaliana. *Genetics*, *183*, 979–1003.

Tsuji, Y., Vanholme, R., Tobimatsu, Y., Ishikawa, Y., Foster, C. E., Kamimura, N., Hishiyama, S., Hashimoto, S., Shino, A., Hara, H., Sato-Izawa, K., Oyarce, P., Goeminne, G., Morreel, K., Kikuchi, J., Fukuda, M., Katayama, Y., Boerjan, W., Ralph, J., Masai, E. and Kajita, S. (2015). Introduction of chemically labile substructures into Arabidopsis lignin through the use of LigD, the Cα-dehydrogenase from Sphingobium sp. strain SYK-6. *Plant Biotechnology Journal*, *6*, 1–12.

Vicuna, R., Gonzalez, B., Mozuch, M. D. and Kirk, T. K. (1987). Metabolism of Lignin Model Compounds of the Arylglycerol-β-Aryl Ether type by *Pseudomonas acidovorans* D_3. *Applied and Environmental Microiology*, *53*, 2605–2609.

Van Acker, R., Leplé, J.-C., Aerts, D., Storme, V., Goeminne, G., Ivens, B., Légée, F., Lapierre, C., Piens, K., Van Montagu, M., C., E., Santoro, N., Foster, C., E., Ralph, J., Soetaert, W., Pilate, G. and Boerjan, W.

(2014). Improved saccharification and ethanol yield from field-grown transgenic poplar deficient in cinnamoyl-CoA reductase. *Proceedings of the National Academy of Sciences of the United States of America*, *111*, 845–850.

Van Acker, R., Vanholme, R., Storme, V., Mortimer, J. C., Dupree, P. and Boerjan, W. (2013). Lignin biosynthesis perturbations affect secondary cell wall composition and saccharification yield in Arabidopsis thaliana. *Biotechnology for Biofuels*, *6*, 1-17.

Vangronsveld, J., Herzig, R., Weyens, N., Boulet, J., Adriaensen, K., Ruttens, A., Thewys, T., Vassilev, A., Meers, E., Nehnevajova, E., van der Lelie, D. and Mench, M. (2009). Phytoremediation of contaminated soils and groundwater: lessons from the field. *Environmental Science and Pollution Research International*, *16*, 765–794.

Vanholme, R., Demedts, B., Morreel, K., Ralph, J. and Boerjan, W. (2010). Lignin biosynthesis and structure. *Plant Physiology*, *153*, 895–905.

Vanholme, R., Morreel, K., Darrah, C., Oyarce, P., Grabber, J. H., Ralph, J. and Boerjan, W. (2012). Metabolic engineering of novel lignin in biomass crops. *The New Phytologist*, *196*, 978–1000.

Vanholme, R., Storme, V., Vanholme, B., Sundin, L., Christensen, J. H., Goeminne, G., Halpin, C., Rohde, A., Morreel, K. and Boerjan, W. (2012). A Systems Biology View of Responses to Lignin Biosynthesis Perturbations in Arabidopsis. *The Plant Cell*, *24*, 3506–3529.

Venturi, V., Zennaro, F., Degrassi, G., Okeke, B. C., & Bruschi, C. V. (1989). Genetics of ferulic acid bioconversion to protocatechuic acid in plant-growth-promoting. *Microbiology*, *144*, 965–973.

Weber, H. (2002). Fatty acid-derived signals in plants. *Trends in Plant Science*, *7*, 217–224.

Weyens, N., Beckers, B., Schellingen, K., Ceulemans, R., Croes, S., Janssen, J., Haenen, S., Witters, N. and Vangronsveld, J. (2013). Plant-associated bacteria and their role in the success or failure of metal phytoextraction projects: first observations of a field-related experiment. *Microbial Biotechnology*, *6*, 288–299.

Weyens, N., van der Lelie, D., Taghavi, S., Newman, L. and Vangronsveld, J. (2009). Exploiting plant–microbe partnerships to

improve biomass production and remediation. *Trends in Biotechnology*, *27*, 591–598.

Wilkerson, C. G., Mansfield, S. D., Lu, F., Withers, S., Park, J.-Y., Karlen, S. D., Gonzales-Vigil, E., Padmakshan, D., Unda, F., Rencoret, J. and Ralph, J. (2014). Monolignol ferulate transferase introduces chemically labile linkages into the lignin backbone. *Science*, *344*, 90–93.

Yang, J., Kloepper, J. W. and Ryu, C.-M. (2009). Rhizosphere bacteria help plants tolerate abiotic stress. *Trends in Plant Science*, *14*, 1–4.

Yuan, J. S., Tiller, K. H., Al-Ahmad, H., Stewart, N. R. and Stewart, C. N. (2008). Plants to power: bioenergy to fuel the future. *Trends in Plant Science*, *13*, 421–429.

Zhang, H., Kim, M.-S., Krishnamachari, V., Payton, P., Sun, Y., Grimson, M., Farag, M., Ryu, C., Allen, R., Melo, I. S. and Paré, P. W. (2007). Rhizobacterial volatile emissions regulate auxin homeostasis and cell expansion in Arabidopsis. *Planta*, *226*, 839–851.

Supplementary Information

Identification		Phenolic acids						Phenolic aldehydes			Phenolic alcohol	Average respons	Plant growth promotion				
Species	Origin	Caffeic acid	Sinapic acid	Vanillic acid	p-coumaric acid	p-hydroxy benzoic acid	Syringic acid	Vanillin	Coniferaldehyde	Syringaldehyde	Coniferyl alcohol	Average	SID	IAA	ACC	Phos	Aset
Azospirillum oryzae	Rhizosphere soil	296.53 ± 23.73	221.81 ± 26.85	157.78 ± 10.82	203.85 ± 34.99	171.91 ± 17.37	221.81 ± 26.85	166.57 ± 17.09	80.4 ± 15.85	154.65 ± 9.44	255.57 ± 45.33	193.09 ± 14.38	-	+	±	±	-
Ochrobactrum cytisi	Rhizosphere soil	201.3 ± 24.36	197.77 ± 17.32	287 ± 22.23	226.67 ± 14.16	132.32 ± 2.05	208.57 ± 0.94	213.68 ± 3.38	203.44 ± 4.73	165.4 ± 19.25	213.28 ± 12.72	204.94 ± 2.75	-	±	±	+	-
Mesorhizobium plurifarium	Rhizosphere soil	179.82 ± 3.35	118.92 ± 14.2	112.17 ± 27.97	201.72 ± 10.15	123.67 ± 3.98	118.92 ± 14.2	112.18 ± 9.93	59.21 ± 8.97	130.7 ± 13.74	114.77 ± 20.34	127.21 ± 6.45	-	-	-	+	+
Nocardioides aromaticivorans	Rhizosphere soil	156.4 ± 4.25	123.23 ± 9	140.69 ± 15.19	170.7 ± 2.95	142.02 ± 12.85	123.23 ± 9	158.32 ± 6.68	112.37 ± 11.36	106.93 ± 1.83	185.2 ± 1.82	141.91 ± 5.4	+	+	-	-	-
Pseudomonas putida	Rhizosphere soil	264.22 ± 48.92	155.37 ± 17.66	425.48 ± 30.95	287.57 ± 29.36	264.19 ± 0.11	155.37 ± 17.66	408.21 ± 38.5	217.04 ± 58.66	166.18 ± 39.63	327.65 ± 26.38	267.13 ± 24.99	-	+	±	±	-
Nocardioides aromaticivorans	Rhizosphere soil	133.8 ± 17.22	58.9 ± 5.58	59.14 ± 13.19	48.19 ± 5.81	52.76 ± 2.63	53.3 ± 7.36	49.99 ± 4.4	46.33 ± 11.94	41.11 ± 5.28	45.7 ± 3.26	58.92 ± 1.55	+	+	±	+	-
Ochrobactrum cytisi	Rhizosphere soil	183.1 ± 2.68	148.96 ± 16.01	114.46 ± 31.13	124.75 ± 16.78	99.2 ± 12.23	148.96 ± 16.01	161.35 ± 27.59	88.96 ± 6.35	98.91 ± 5.26	118.39 ± 13.99	128.7 ± 13.46	+	-	±	-	-
Nocardioides aromaticivorans	Rhizosphere soil	139.64 ± 6.84	92.42 ± 3.57	81.78 ± 2.21	99.77 ± 4.29	87.64 ± 6.87	92.42 ± 3.57	109.59 ± 2.78	73.35 ± 6.51	104.24 ± 10.36	96.48 ± 7.42	97.73 ± 2.04	+	-	±	-	-
Mesorhizobium plurifarium	Rhizosphere soil	197.48 ± 4.42	114.68 ± 8.34	100.52 ± 10.49	129.14 ± 10.8	96.56 ± 3.08	114.68 ± 8.34	126.11 ± 12.27	109.62 ± 13.27	119.11 ± 15.7	112.84 ± 17.22	122.08 ± 3	+	-	±	±	-
Pseudomonas putida	Rhizosphere soil	153.32 ± 11.11	122.21 ± 17.39	99.42 ± 5.22	123.89 ± 24.64	113.9 ± 18.25	122.21 ± 17.39	125.34 ± 27.83	85.68 ± 6.26	89.91 ± 10.09	156.8 ± 6.26	119.27 ± 8.79	+	-	-	-	-
Dokdonella fugitiva	Rhizosphere soil	190.38 ± 15.36	144.74 ± 19.75	100.98 ± 7.43	146.06 ± 15.47	110.33 ± 7.93	144.74 ± 19.75	132.33 ± 3.62	79 ± 7.5	144.73 ± 6.65	115.69 ± 14.64	130.9 ± 3.34	+	+	-	-	-
Bosea thiooxidans	Rhizosphere soil	301.73 ± 35.54	218.83 ± 27.71	137.87 ± 4.45	188.1 ± 36.44	147.13 ± 9.1	218.83 ± 27.71	194.43 ± 5	85.08 ± 16.38	184.25 ± 2.19	154.54 ± 19.26	183.08 ± 12.6	-	-	-	-	-
Mesorhizobium plurifarium	Rhizosphere soil	138.93 ± 20.67	154.56 ± 31.36	96.94 ± 11.97	138.22 ± 33.36	93.1 ± 14.56	154.56 ± 31.36	136.51 ± 8.8	60.44 ± 6.93	120.56 ± 14.45	136.17 ± 10.32	123 ± 11.56	+	+	±	+	-
Pseudomonas putida	Rhizosphere soil	154.81 ± 8.39	128.54 ± 17.13	98.29 ± 16.1	166.6 ± 27.92	74.55 ± 4.31	128.54 ± 17.13	111.86 ± 14.34	104.23 ± 19.27	149.48 ± 13.3	141.69 ± 30.74	125.86 ± 10.5	+	+	±	±	-
Rhizobacter spathiphylli	Rhizosphere soil	152.23 ± 12.49	116.04 ± 15.36	105.02 ± 10.94	128.1 ± 13.9	85.91 ± 6.78	116.04 ± 15.36	106.17 ± 12.26	156.4 ± 55.47	137.29 ± 19.8	128.7 ± 16.03	123.19 ± 10.4	+	+	±	±	-
Starkeya koreensis	Rhizosphere soil	369.74 ± 57.78	221.03 ± 11.35	244.04 ± 5.47	238.18 ± 32.26	250.22 ± 33.17	215.99 ± 14.79	208.96 ± 19.46	205.31 ± 51.53	310.1 ± 113.59	126.99 ± 1.62	239.06 ± 18.69	+	+	+	+	-
Rhodanobacter lindaniclasticus	Rhizosphere soil	263.17 ± 33	138.66 ± 18.97	94.98 ± 4.51	121.38 ± 26.75	101.7 ± 9.01	138.66 ± 18.97	133.11 ± 20.46	74.84 ± 9.33	119.52 ± 6.03	114.42 ± 7.16	130.04 ± 4.94	+	+	-	-	-
Microbacterium phyllosphaerae	Root	173.44 ± 11.56	118.33 ± 14.37	192.43 ± 88.91	135.06 ± 14.38	94.08 ± 18.87	83.04 ± 6.96	76.96 ± 8.68	106.06 ± 31.31	78.48 ± 3.52	111.33 ± 11.23	116.92 ± 8.26	-	+	±	-	-
Bosea thiooxidans	Root	164.94 ± 9.57	118.24 ± 4.18	126.49 ± 14.24	142.2 ± 7.75	331.64 ± 4.06	134.4 ± 4.79	141.03 ± 21.41	111.26 ± 31.21	95.64 ± 16.24	120.39 ± 19.49	148.62 ± 5.92	+	+	±	-	-
Stenotrophomonas rhizophila	Root	135.59 ± 6.96	109.99 ± 9.54	73.35 ± 2.17	93.89 ± 6.36	95.67 ± 8.87	64.4 ± 1.84	107.17 ± 7.05	108.09 ± 10.02	99.17 ± 15.64	154.32 ± 19.73	104.16 ± 2.44	+	±	++	±	-
Caulobacter vibrioides	Root	299.88 ± 2.25	171.96 ± 16.48	173.68 ± 15.54	184.74 ± 20.83	157.59 ± 9.2	150.2 ± 8.07	147.11 ± 5.51	86.96 ± 8.49	91.45 ± 10.01	129.59 ± 8.76	159.32 ± 4.42	-	-	-	-	-
Variovorax paradoxus	Root	271.97 ± 31.25	289.25 ± 14.25	684.2 ± 83.21	392.28 ± 75.67	429.91 ± 53.07	248.22 ± 12.59	503.57 ± 38.78	109.89 ± 10.5	152.77 ± 41.97	288.57 ± 9.31	337.06 ± 14.2	+	-	±	-	-
Microbacterium oxydans	Root	181.95 ± 28.68	98.62 ± 4.84	124.76 ± 12.46	95.09 ± 2.93	85.27 ± 2.28	102.3 ± 14.31	90.43 ± 6.83	96.24 ± 10.11	98.63 ± 5.81	94.96 ± 1.05	106.82 ± 2.6	+	-	±	-	-
Microbacterium phyllosphaerae	Root	164.57 ± 27.82	118.32 ± 16.05	128.91 ± 16.01	101.37 ± 7.13	131.84 ± 7.04	132.7 ± 18.04	95.95 ± 2.76	85.15 ± 7.53	89.56 ± 2.2	91.87 ± 4.37	114.02 ± 7.71	+	+	-	+	-
Variovorax paradoxus	Root	166.23 ± 5.24	164.99 ± 13.56	515.62 ± 8.14	459.65 ± 19.2	408.76 ± 20.59	97.86 ± 12.73	345.43 ± 27.08	213.96 ± 20.36	102.72 ± 26.21	183.64 ± 25.84	265.89 ± 8.55	+	-	-	+	-
Bacillus simplex	Root	401.06 ± 15.62	302.39 ± 14.45	384.34 ± 8.46	204.57 ± 19.76	416.77 ± 3.66	303.84 ± 4.03	349.85 ± 6.77	140.21 ± 12.55	123.74 ± 11.67	181.3 ± 21.07	280.81 ± 3.19	+	+	++	+	-
Microbacterium phyllosphaera	Root	430.58 ± 9.62	368.45 ± 15.44	369.93 ± 21.27	216.45 ± 9.25	469.02 ± 26.48	349.14 ± 21.32	412.72 ± 6.57	138.4 ± 2.99	201.15 ± 14.29	258.26 ± 4.59	321.41 ± 8.19	+	+	++	+	-
Stenotrophomonas rhizophila	Root	193.42 ± 9.08	100.96 ± 7.84	154.69 ± 29.23	122.68 ± 17.62	129.65 ± 10.89	107.37 ± 13.35	104.29 ± 18.92	111.36 ± 6.68	133.65 ± 14.48	130.52 ± 9.12	128.86 ± 5.04	-	-	±	-	-
Variovorax paradoxus	Root	31.59 ± 15.81	136.63 ± 15.77	134.88 ± 14.16	94.98 ± 8.23	142.04 ± 21.29	158.73 ± 23.32	105.58 ± 9.79	95.85 ± 7.22	135.21 ± 20.65	77.22 ± 6.96	111.27 ± 1.85	-	+	-	-	-
Ensifer adhaerens	Root	324.72 ± 18.02	355.14 ± 22.18	357.01 ± 29.3	184.85 ± 16.69	433.47 ± 12.3	300.39 ± 17.09	352.12 ± 4.56	131.24 ± 17.53	217.68 ± 18.86	262.44 ± 26.9	291.9 ± 2.7	+	+	+	+	-
Bacillus simplex	Root	390.77 ± 11.14	341.41 ± 16.38	341.38 ± 5.43	183.14 ± 5.92	457.41 ± 14.63	323.83 ± 5.7	328.83 ± 22.94	105.02 ± 14.19	197.01 ± 21.97	244.5 ± 25.56	291.33 ± 7.43	+	+	+	-	-
Ensifer adhaerens	Root	391.2 ± 15.94	387.34 ± 16.51	394.34 ± 18.47	207.48 ± 1.74	449.63 ± 16.32	312.56 ± 12.07	388.68 ± 31.51	119.3 ± 9.72	179.46 ± 8.86	303.37 ± 20.53	313.33 ± 11.84	+	+	+	-	-

Supplementary Table 6.1. Biolog response and plant growth promotion capacities of selected bacterial strains. Biolog responses represent data of 3 biologically independent repeats ± standard deviation

Identification		Phenolic acids						Phenolic aldehydes			Phenolic alcohol	Average respons	Plant growth promotion				
Species	Origin	Caffeic acid	Sinapic acid	Vanillic acid	p-coumaric acid	p-hydroxy benzoic acid	Syringic acid	Vanillin	Coniferaldehyde	Syringaldehyde	Coniferyl alcohol	Average	SID	IAA	ACC	Phos	Acet
Ensifer adhaerens	Root	340,44 ± 19,73	204,79 ± 33,66	345,6 ± 21,05	392,86 ± 33,7	383,39 ± 9,34	222,35 ± 46,87	296,46 ± 27,99	300,83 ± 40,03	186,75 ± 10,8	292,84 ± 32,53	296,63 ± 21,37	+	-	+	+	-
Variovorax paradoxus	Root	177,94 ± 12,05	105,53 ± 11,3	491,08 ± 24,22	406,76 ± 14,77	461,83 ± 21,47	127,05 ± 3,61	385,39 ± 21,2	198,84 ± 6,13	155,15 ± 10,11	195,87 ± 14,37	270,54 ± 8,66	+	+	-	+	-
Rhizobium huatlense	Root	231,52 ± 30,2	130,03 ± 6,46	479,19 ± 36,75	414,12 ± 10,44	481,78 ± 17,43	232,11 ± 31,58	265,92 ± 10,44	182,19 ± 24,8	96,55 ± 1,01	175,04 ± 15,92	268,84 ± 11,87	+	-	++	-	-
Ensifer adhaerens	Root	293,38 ± 30,01	363,19 ± 33,9	307,29 ± 8,11	152,03 ± 11,4	337,72 ± 32,82	364,2 ± 39,11	330,73 ± 15,94	188,33 ± 25,92	119,71 ± 3,07	233,92 ± 21,68	269,05 ± 3,16	+	+	++	-	-
Variovorax paradoxus	Root	259,51 ± 51,76	241,31 ± 21,79	356,51 ± 20,98	213,63 ± 12,14	227,17 ± 23,71	335,19 ± 12,53	207,48 ± 19,54	137,78 ± 24,51	115,45 ± 13,37	213,25 ± 12,04	230,73 ± 9,97	+	-	+	-	-
Stenotrophomonas rhizophila	Root	240,68 ± 17,26	92,75 ± 10,06	64,21 ± 3,6	94,4 ± 1,82	170,6 ± 30,73	62,78 ± 1,34	83,39 ± 11,84	97,31 ± 8,71	95,25 ± 10,8	141,15 ± 5,23	114,25 ± 4,21	+	-	++	+	-
Pseudomonas putida	Root	321,99 ± 4,62	139,39 ± 1,24	291,27 ± 10,04	333,52 ± 10,34	314,33 ± 24,83	134,56 ± 1,81	224,58 ± 16,08	271,44 ± 5,29	229,9 ± 13,74	162,3 ± 13,46	242,33 ± 6,15	+	-	++	+	-
Stenotrophomonas rhizophila	Root	184,69 ± 14,44	145,23 ± 16,07	196,33 ± 7,21	120,91 ± 16,75	104,4 ± 12,97	128,58 ± 7,96	106,86 ± 5,87	81,14 ± 16,86	119,8 ± 14,59	129,93 ± 8,04	131,79 ± 2,56	-	-	±	+	-
Rhizobium huatlense	Root	156,75 ± 29,28	92,47 ± 8,33	89,83 ± 10,06	141,85 ± 17,87	113,45 ± 36,81	90,92 ± 12,41	79,02 ± 5,02	128,97 ± 21,3	65,52 ± 8,28	155,68 ± 15,26	111,45 ± 10,12	-	±	-	-	-
Variovorax paradoxus	Root	130,28 ± 9,85	84,81 ± 10,03	67,3 ± 6,47	87,35 ± 18,9	64,98 ± 8,69	58,57 ± 3,74	60,85 ± 6,83	84,84 ± 1,66	73,64 ± 10,19	87,1 ± 13,37	79,97 ± 5,71	+	+	±	±	-
Xanthomonas sp.	Root	202,99 ± 23,12	111,65 ± 9,02	520,12 ± 11,22	327,25 ± 13,11	367,6 ± 16,48	99,54 ± 2,09	421,36 ± 2,38	220,07 ± 7,78	88,49 ± 16,41	241,78 ± 9,06	260,09 ± 3,24	+	+	±	-	-
Stenotrophomonas rhizophila	Root	145,39 ± 7,85	74,2 ± 1,92	194,48 ± 26,35	83,39 ± 8,18	177,15 ± 13,91	78,04 ± 4,18	71,56 ± 2,59	66,45 ± 1,9	119,47 ± 25,18	161,32 ± 33,91	117,14 ± 3,66	-	-	++	-	-
Starkeya korensis	Root	146,64 ± 13,42	128,25 ± 11,91	186,15 ± 9,56	139,36 ± 24,78	187,53 ± 12,9	81,51 ± 5,06	98 ± 8,15	88,27 ± 11,39	183,48 ± 9,22	157,29 ± 30,81	139,65 ± 7,64	+	±	+	-	-
Pseudomonas putida	Root	38,23 ± 22,45	120,2 ± 5,92	153,12 ± 27,79	133,37 ± 12,97	166,36 ± 34,38	173,16 ± 42,03	100,22 ± 1,46	84,93 ± 7,27	148,73 ± 14,24	83,18 ± 3,56	120,15 ± 9,58	+	±	+	-	-
Pseudomonas putida	Root	24,98 ± 14,34	120,47 ± 18,39	125,08 ± 3,31	95,86 ± 17,55	106,97 ± 16,75	112,85 ± 15,53	132,45 ± 27,76	85,49 ± 16,16	127,99 ± 9,84	100,19 ± 3,16	103,23 ± 6,4	+	-	++	-	-
Pseudomonas putida	Root	148,07 ± 8,59	77,01 ± 1,22	85,98 ± 4,16	80,09 ± 1,62	72,12 ± 5,91	71,06 ± 6,86	93,58 ± 7,84	145,1 ± 17,48	108,99 ± 16,06	103,99 ± 3,57	98,6 ± 1,98	+	-	-	-	-
Xanthomonas sp.	Root	213,09 ± 29,71	113,61 ± 7,65	168,92 ± 8,25	155,03 ± 6,39	160,73 ± 17,16	129,81 ± 18,21	135,98 ± 10,19	127,2 ± 8,25	107,21 ± 12,72	132,48 ± 10,07	144,41 ± 4,02	+	-	+	-	-
Stenotrophomonas rhizophila	Root	141,94 ± 7,75	96,35 ± 17,05	104,95 ± 24,96	150,36 ± 21,78	121,76 ± 18,53	92,84 ± 6,98	128,83 ± 24,01	144,91 ± 25,04	91,22 ± 10,06	103,11 ± 8,65	117,63 ± 9,24	+	-	-	-	-
Pseudomonas putida	Root	147,41 ± 5,64	107,69 ± 11,41	110,17 ± 24,86	83,42 ± 8,52	95,55 ± 5,23	96,99 ± 12,71	109,94 ± 14,85	96,78 ± 4,87	110,87 ± 13,35	84,41 ± 5,73	104,32 ± 5,13	+	+	-	-	-
Stenotrophomonas rhizophila	Root	135,7 ± 2,82	79,58 ± 0,96	182,43 ± 21,13	73,19 ± 1,83	167,35 ± 32,32	78,63 ± 6,14	63,37 ± 2,31	67,64 ± 1,57	110,8 ± 23,91	133,56 ± 30,98	109,22 ± 8,61	-	-	±	-	-
Pseudomonas putida	Root	176,63 ± 16,4	183,84 ± 9,11	199,83 ± 17,9	107,04 ± 11,79	120,75 ± 19,13	153,46 ± 24,85	105,58 ± 18,52	158,85 ± 25,73	136,26 ± 22,23	112,28 ± 15,68	145,45 ± 3,1	-	-	±	-	-
Pseudomonas putida	Root	262,17 ± 11,62	122,83 ± 15,28	177,8 ± 35,76	291,81 ± 18,96	296,12 ± 24,25	103,01 ± 3,6	154,9 ± 43,15	237,39 ± 14,8	145,28 ± 12,92	402,2 ± 23,22	219,35 ± 13,44	+	+	-	-	-
Pseudomonas putida	Root	327,3 ± 14,41	176,88 ± 19,11	254,42 ± 12,93	319,94 ± 13,74	291,1 ± 7,89	149,54 ± 16,88	209,05 ± 15,41	336,61 ± 10,21	220,58 ± 7,66	467,82 ± 15,36	275,32 ± 5,87	+	+	-	-	-
Cupravidius metallidurans	Root	225,07 ± 9,83	119,22 ± 12,92	195,05 ± 10,09	282,31 ± 28,91	259,63 ± 93,9	124,68 ± 7,73	100,14 ± 10,9	109,18 ± 21,46	105,87 ± 16,3	184,46 ± 11	170,56 ± 13	+	+	-	±	-
Ramlibacter sp.	Root	19,91 ± 8,95	192,6 ± 35,67	109,91 ± 18	115,67 ± 24,36	147,02 ± 40,48	114,82 ± 26,77	122,15 ± 18,19	96,84 ± 13,45	89,22 ± 14,17	85,95 ± 1,46	109,41 ± 3,81	-	-	+	-	-
Rhizobium radiobacter	Root	304,88 ± 28,07	318,61 ± 21,29	435,34 ± 6,12	431,58 ± 17,13	576,77 ± 11,61	309,24 ± 17,99	428,9 ± 38,28	190,96 ± 37,81	321,83 ± 24,14	379,92 ± 6,22	369,8 ± 16,55	+	+	+	-	-
Rhizobium hautlense	Root	163,18 ± 36,04	103,79 ± 9,32	66,25 ± 2,21	78,9 ± 15,85	55,03 ± 7,74	62,84 ± 4,07	88,77 ± 4,15	117,77 ± 16,81	57,77 ± 1,14	72,59 ± 22,85	86,69 ± 2,83	+	-	+	-	-
Achromobacter dentrificans	Root	425,04 ± 32,94	196,62 ± 20,65	308,7 ± 23,72	349,01 ± 13,34	151,6 ± 9,1	159,12 ± 18,71	243,37 ± 21,06	299,56 ± 9,63	208,25 ± 17,85	288,48 ± 28,08	262,98 ± 15,25	-	-	±	±	-
Achromobacter dentrificans	Root	534,52 ± 26,88	260,48 ± 34,28	243,47 ± 26,53	392,66 ± 49,43	293,49 ± 19,76	146,22 ± 17,75	332,47 ± 66,33	274,18 ± 33,04	198,43 ± 38,3	338,8 ± 16,23	301,47 ± 25,87	+	-	-	+	-
Rhizobium sp.	Root	365,6 ± 23,24	291,41 ± 39,43	295,46 ± 23,42	221,11 ± 40,46	448,01 ± 21,95	220,38 ± 5,74	369,81 ± 14,28	127,31 ± 15,6	211,21 ± 24,37	240,23 ± 23,25	279,05 ± 17,03	+	-	-	-	-
Rhizobium huatlense	Root	290,6 ± 42,73	289,03 ± 12,21	333,46 ± 25,86	309 ± 39,68	248,98 ± 18,96	290,14 ± 27,34	229,61 ± 15,35	173,84 ± 8,55	102,37 ± 14,73	255,02 ± 24,82	252,21 ± 13,69	+	-	±	+	-
Microbacterium oxydans	Root	181,72 ± 7,68	111,51 ± 17,05	78,01 ± 7,66	110,07 ± 12,23	87,39 ± 9,56	65,9 ± 0,54	98,51 ± 3,96	128,13 ± 19,81	71,68 ± 11,88	120,4 ± 21,28	105,33 ± 1,4	-	-	-	-	-

Supplementary Table 6.1. (continued) Biolog response and plant growth promotion capacities of selected bacterial strains. standard deviation

Identification		Phenolic acids						Phenolic aldehydes			Phenolic alcohol	Average respons	Plant growth promotion				
Species	Origin	Caffeic acid	Sinapic acid	Vanillic acid	p-coumaric acid	p-hydroxy benzoic acid	Syringic acid	Vanillin	Coniferaldehyde	Syringaldehyde	Coniferyl alcohol	Average	SID	IAA	ACC	Phos	Acet
Bosea thiooxidans	Root	217,72 ± 26,41	83,8 ± 6,67	58,35 ± 4,49	49,79 ± 8,01	54,54 ± 24,12	53,26 ± 1,99	58,88 ± 3,26	102,51 ± 13,54	59,53 ± 5,04	105,45 ± 12,09	84,38 ± 3,65	-	-	-	-	-
Achromobacter denitrificans	Root	352,26 ± 23,96	208,47 ± 26,21	158,09 ± 21,02	315,16 ± 20,57	156,27 ± 36,66	123,46 ± 1,09	221,85 ± 23,02	269,67 ± 48,94	181,66 ± 19,2	129,88 ± 8,03	211,68 ± 11,28	+	-	-	-	-
Rhizobium huatlense	Root	207,37 ± 37,55	168,48 ± 7,19	144,47 ± 38,01	313,51 ± 12,24	248,3 ± 20,08	105,85 ± 3,88	155,96 ± 14,58	170,8 ± 45,89	108,16 ± 5,36	260,33 ± 30	188,32 ± 8,34	+	-	-	-	-
Mesorhizobium plurifarium	Root	50,46 ± 18,35	126,31 ± 14,42	145,05 ± 6,72	106,61 ± 14,12	280,17 ± 143,48	135,24 ± 23,39	125,39 ± 10,72	84,1 ± 10,43	134,73 ± 12,18	70,18 ± 1,59	125,82 ± 11,69	-	-	+	-	-
Pseudomonas putida	Root	43,01 ± 14,74	119,69 ± 12,7	139,13 ± 15,02	117,82 ± 16,96	151,61 ± 23,54	186,7 ± 12,6	120,86 ± 17,9	74,01 ± 0,58	177,3 ± 9,56	83,22 ± 6,17	121,33 ± 6,01	+	±	±	-	-
Pseudomonas putida	Root	49,56 ± 23,1	112,43 ± 10,56	116,22 ± 7,79	104,13 ± 9,52	152,94 ± 14,97	95,62 ± 30,41	122,47 ± 28,45	58,41 ± 1,92	80,87 ± 3,11	65,59 ± 2,99	95,82 ± 2,13	+	-	±	±	-
Pseudomonas putida	Root	23,71 ± 5,46	114,6 ± 10,88	113,77 ± 6,36	101,54 ± 14,79	120,24 ± 22,76	166,83 ± 44,2	102,12 ± 5,87	94,95 ± 9,99	105,59 ± 14,96	88,69 ± 13,35	103,2 ± 10,14	-	-	±	+	-
Achromobacter denitrificans	Root	898,69 ± 35,49	625,43 ± 18,67	757,66 ± 74,82	806,3 ± 4,24	840,02 ± 24,8	872,34 ± 16,64	626,04 ± 23,39	647,87 ± 18,67	540,64 ± 48,5	747,24 ± 25,23	736,22 ± 9,46	+	-	-	-	-
Achromobacter denitrificans	Root	382,02 ± 25,32	289,67 ± 10,18	153,29 ± 15,79	387,99 ± 7,82	139,17 ± 27,66	105,32 ± 6,88	347,69 ± 2,96	264,06 ± 2,93	224,29 ± 6,28	264,28 ± 10,69	255,78 ± 6,21	+	-	±	-	-
Pseudomonas congelans	Stem	338,27 ± 8,74	117,58 ± 11,34	134,92 ± 17,75	437,9 ± 23,24	435,24 ± 17,46	132,16 ± 31,07	154,85 ± 4,89	308,99 ± 8,2	68,7 ± 14,66	355,15 ± 0,58	248,38 ± 9,51	+	+	+	±	-
Pseudomonas congelans	Stem	266,68 ± 24,79	122,13 ± 15,88	184,41 ± 19,93	383,51 ± 2,88	358,61 ± 16,92	88,18 ± 9,2	146,4 ± 7,2	297,73 ± 10,22	116,94 ± 8,25	329,31 ± 16,77	229,39 ± 4,01	+	+	±	±	-
Plantibacter flavus	Stem	235,5 ± 11,76	174,58 ± 13,7	169,36 ± 11,08	196,67 ± 16,57	160,34 ± 7,34	174,58 ± 13,7	225,95 ± 30,48	102,64 ± 5,62	129,07 ± 4,71	219,72 ± 17,52	178,84 ± 7,93	+	+	±	-	-
Mesorhizobium plurifarium	Stem	136,8 ± 6,99	100,99 ± 23,41	82,86 ± 2,2	163,69 ± 18,04	109,05 ± 16,74	100,99 ± 23,41	136,33 ± 24,66	84,6 ± 4,53	92,47 ± 11,92	142,16 ± 9,22	115 ± 1,3	-	-	-	-	-
Bacillus subtilis	Stem	140,16 ± 6,7	100,83 ± 8,97	114,13 ± 8,58	128,64 ± 23,85	93,48 ± 0,38	100,83 ± 8,97	110,03 ± 28,57	71,6 ± 0,79	124,03 ± 24,03	113,28 ± 19,27	109,7 ± 10,38	-	+	-	+	-
Pedobacter alluvionis	Stem	186,37 ± 7,25	226,82 ± 27,07	181,73 ± 4,07	216,05 ± 15,09	148,07 ± 17,49	226,82 ± 27,07	191,94 ± 6,76	103,11 ± 27,83	217,73 ± 18,16	187,27 ± 4,08	188,59 ± 9,34	-	-	-	±	+
Aeromicrobium ginsengisoli	Stem	113,4 ± 15,86	200,39 ± 9,19	87,43 ± 4,45	155 ± 13,31	91,79 ± 11,57	200,39 ± 9,19	147,38 ± 5,19	128 ± 38,91	157,28 ± 4,64	135,13 ± 10,51	141,62 ± 2,53	+	+	+	+	-
Bacillus subtilis	Stem	145,54 ± 18,81	91,9 ± 10,46	103,77 ± 14,72	174,32 ± 22,3	92,22 ± 18,97	91,9 ± 10,46	95,66 ± 16,26	111,46 ± 1,67	97,92 ± 8,95	121,07 ± 10,43	112,58 ± 2,22	+	+	±	-	-
Plantibacter flavus strain	Stem	175,11 ± 37,96	135,93 ± 23,31	93,33 ± 7,81	150,61 ± 6,27	101,93 ± 19,27	135,93 ± 23,31	127,46 ± 4,19	89,55 ± 7,77	158,88 ± 10,33	127,23 ± 8,48	129,6 ± 4,85	+	+	±	-	-
Curtobacterium flaccumfaciens	Stem	109,54 ± 4,62	87,98 ± 12,85	81,94 ± 3,54	120,18 ± 11,04	71,54 ± 6,53	87,98 ± 12,85	108,85 ± 18,51	83,14 ± 4,58	89,41 ± 2,93	146,71 ± 20,66	98,73 ± 7,72	+	+	±	-	-
Bacillus subtilis	Stem	183,98 ± 7,44	210,54 ± 14,24	180,03 ± 3,29	244,3 ± 12,94	151,58 ± 7,28	210,54 ± 14,24	197,89 ± 13,95	114,87 ± 46,13	203,46 ± 40,15	223,02 ± 15,29	192,02 ± 14,35	-	-	-	-	-
Pigmentiphaga litoralis	Stem	153,95 ± 53,34	97,52 ± 17,43	181,18 ± 10,1	156,07 ± 40,81	121,83 ± 12,59	97,52 ± 17,43	129,21 ± 5,99	142,48 ± 31,03	116,92 ± 3,57	135,89 ± 9,78	133,26 ± 13,38	-	-	±	-	-
Curtobacterium flaccumfaciens	Stem	121,28 ± 7,07	105,17 ± 15,76	78,4 ± 1,58	189,58 ± 9,62	80,04 ± 9,78	105,17 ± 15,76	115,23 ± 6,29	100,78 ± 14,74	108,95 ± 19,42	154,08 ± 8,75	115,87 ± 4,75	+	+	-	-	-
Phyllobacterium brassicacearum	Stem	197,89 ± 0,83	96,46 ± 18,73	94,93 ± 4,8	327,25 ± 21,78	197,9 ± 4,88	96,46 ± 18,73	153,18 ± 12,87	279,85 ± 26,38	104,86 ± 28,19	300,02 ± 21,51	184,88 ± 8,02	-	-	-	-	-
Microbacterium hydrocarbonoxyda	Stem	148,97 ± 45,25	143,69 ± 10,7	103,89 ± 9,82	195,61 ± 14,3	124 ± 32,83	143,69 ± 10,7	143,59 ± 29,82	130,53 ± 25,21	135,12 ± 29,21	190,18 ± 12,98	145,93 ± 7,53	-	-	±	±	-
Rhizobium huautlense	Stem	168,8 ± 30,14	91,5 ± 23,56	115,92 ± 7,14	159,13 ± 24,92	106,31 ± 8,52	91,5 ± 23,56	140,46 ± 9,12	136,79 ± 17,95	89,08 ± 15,12	136,52 ± 14,02	123,6 ± 8,16	-	+	++	+	-
Pseudomonas putida	Stem	296,58 ± 27,65	90,62 ± 22,47	231,3 ± 15,65	293,34 ± 12,91	232,41 ± 12,18	90,62 ± 22,47	256,41 ± 18,52	237,89 ± 22,17	222,95 ± 3,08	170,97 ± 6,52	212,31 ± 1,99	-	-	-	+	-
Pseudomonas putida	Stem	171,8 ± 61,38	156,36 ± 11,24	116,06 ± 33,94	198,58 ± 33,25	102,67 ± 33,67	156,36 ± 11,24	145,17 ± 11,15	163,9 ± 58,97	138,04 ± 10,69	136,84 ± 35,6	148,58 ± 26,77	-	-	-	+	-
Pseudomonas putida	Stem	197,02 ± 3,01	145,58 ± 12,86	115,48 ± 4,56	144,15 ± 29,08	133,9 ± 17,55	145,58 ± 12,86	137,52 ± 5,55	88,38 ± 17,7	115,09 ± 8,55	126,66 ± 8,15	134,94 ± 7,3	-	+	-	+	-

Supplementary Table 6.1. (continued) Biolog response and plant growth promotion capacities of selected bacterial strains. standard deviation

Supplementary Figure 6.1

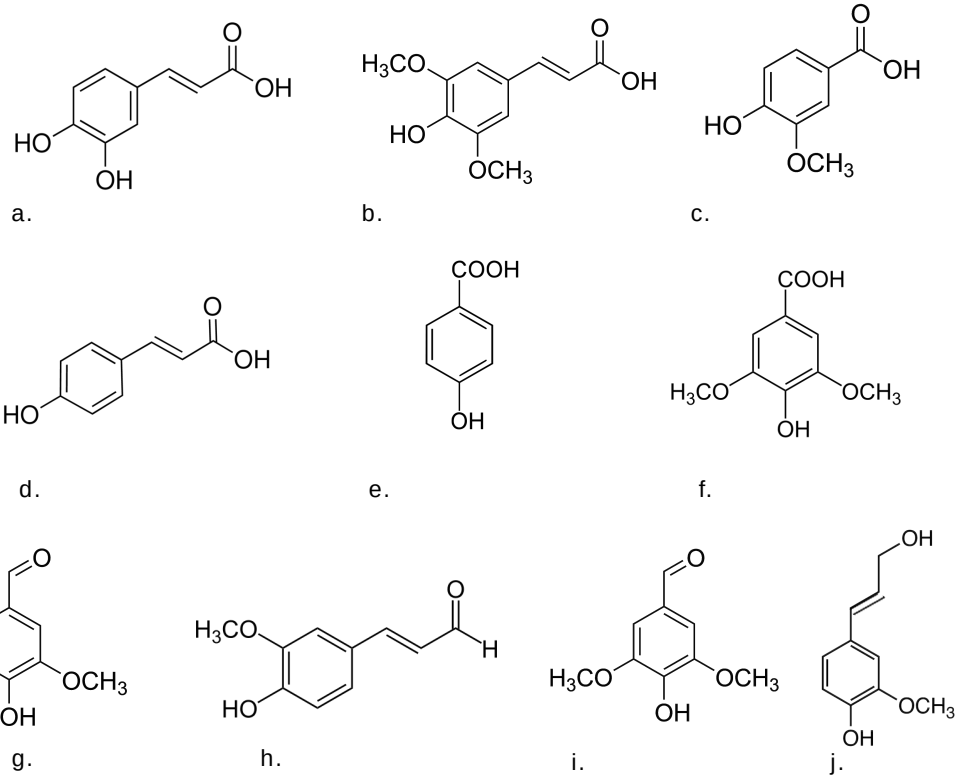

Supplemental Figure 6.1: Graphical representation of the 10 selected phenolic carbon sources. a. caffeic acid, b. sinapic acid, c.vannilic acid, d. p-coumaric acid, e. p-hydroxy-benzoic acid, f. syringic acid, g. vanillin, h. coniferaldehyde, i. syringaldehyde, j. coniferyl alcohol

Supplementary Figure 6.2

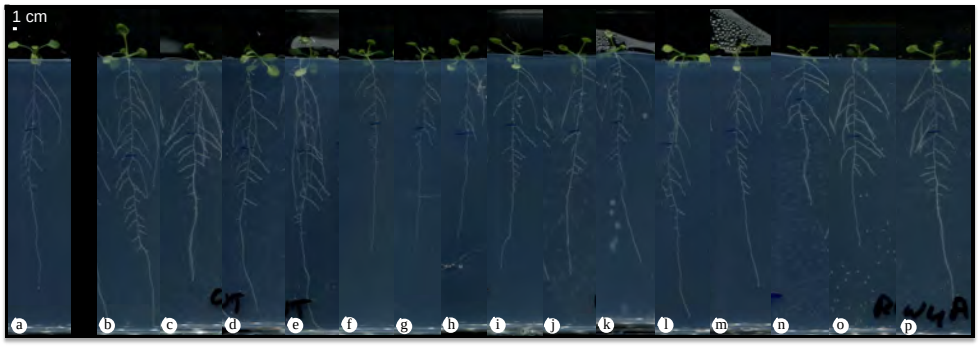

Supplemental Figure 6.2. Representative pictures of wild type Arabidopsis thaliana plants inoculated with selected bacterial strains in vertical agar plate system. Pictures were taken after 14 days of growth with a Canoscan 4400F (Canon) at 600 d.p.i. a: non-inoculated control, b: Norcardiodes aromaticivorans, c: Rhizobium huatlense, d:Bacillus simplex, e: Plantibacter flavus, f: Ochrobactrum intermedium, g: Azospirillum oryzae, h: Pseudomonas putida, i: Pseudomonas congelans, j: Ensifer adhaerens, k: Cupravidius metalludirans, l: Starkeya koorensis, m: Variovorax paradoxus, n: Pseudomonas putida, o: Pseudmonas putida, p: Microbacterium phyllosphaerae. Bold species were selected for further analysis.

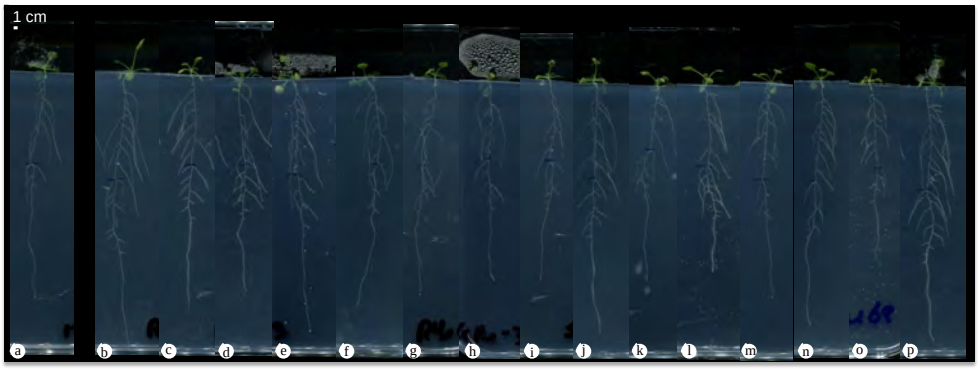

Supplemental Figure 6.3. Representative pictures of ccr1-3 Arabidopsis thaliana plants inoculated with selected bacterial strains in vertical agar plate systems. Pictures were taken after 14 days of growth with a Canoscan 4400F (Canon) at 600 d.p.i. Legend: see picture 6.2.

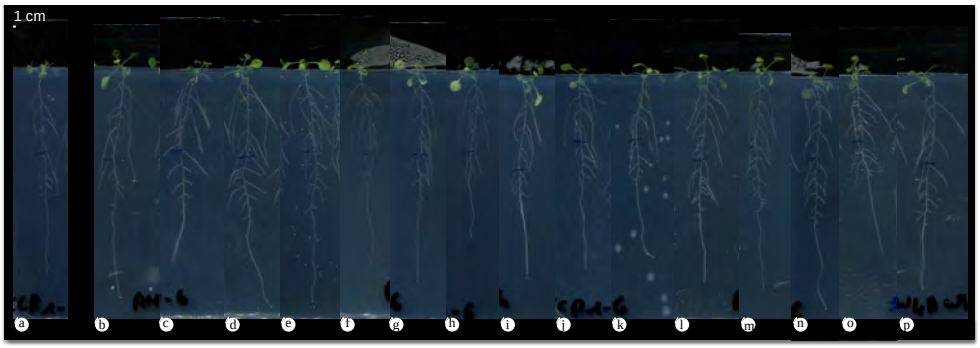

Supplemental Figure 6.4. Representative pictures of ccr1-6 Arabidopsis thaliana plants inoculated with selected bacterial strains in vertical agar plate system. Pictures were taken after 14 days of growth with a Canoscan 4400F (Canon) at 600 d.p.i. Legend: see figure 6.2.

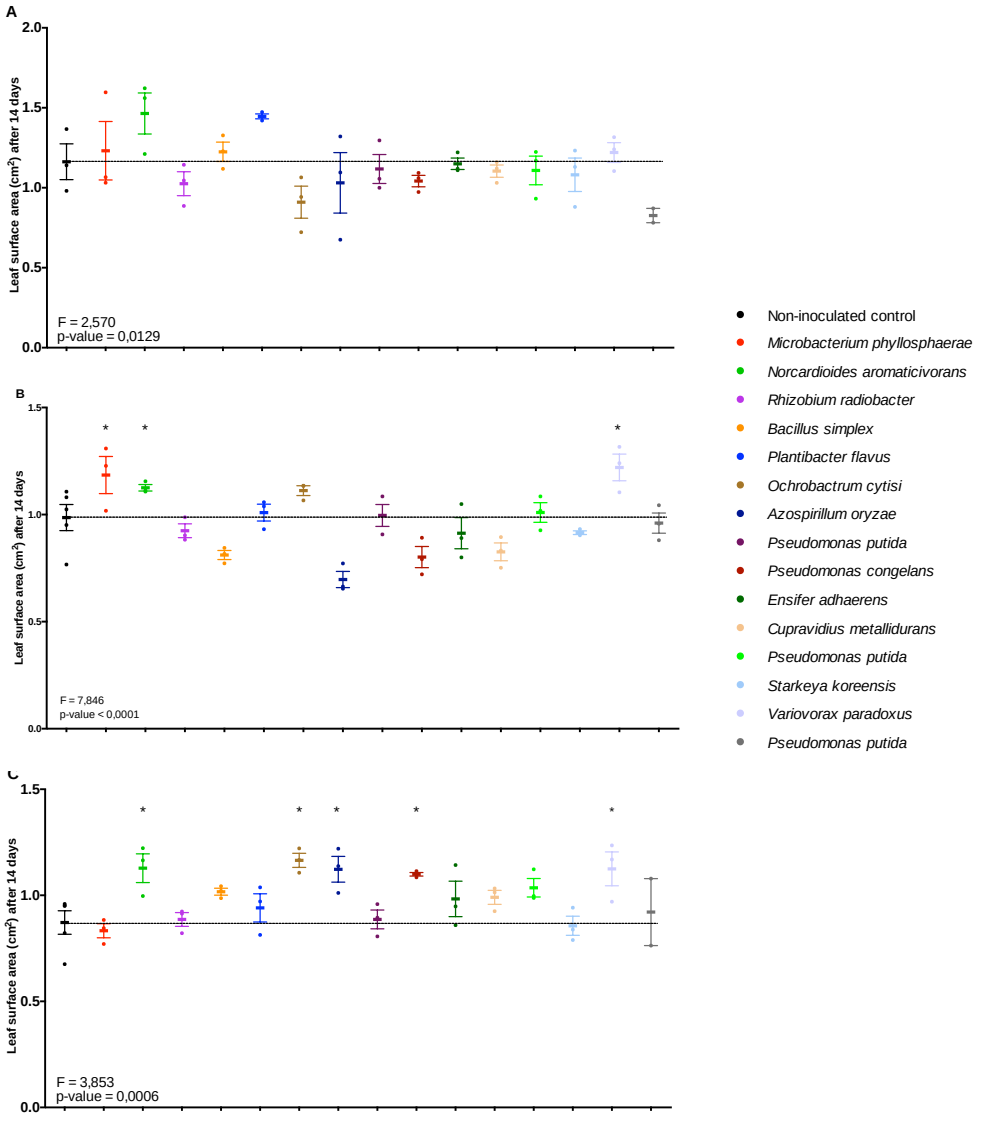

Supplementary Figure 6.5: Effect of inoculation with selected bacterial strains on the leaf surface area of Arabidopsis thaliana genotypes. Aligned scatter dot-plots displaying the effect of bacterial inoculation on the primary root growth (cm) of Arabidopsis thaliana seedlings (A. Wild type, B. ccr1-3 and C. ccr1-6) after 14 days of growth (end-point measurement). To inoculate seedlings 10^4 colony-forming units (CFU) were spread on to the treatment plates. Lines within the scatter dot-plots represent means ± standard deviation. Data represent at least 3 biologically independent replicates, each consisting of

*5 seedlings. Non-inoculated controls are displayed in black and inoculated strains are displayed in several colours (see legend). Data were analysed using one-way ANOVA and Dunnet post-hoc comparisons (p-values: *P < 0.05, **P < 0.01) whereby each treatment (bacteria) was compared with the control. Overall ANOVA results (F-value and p-value) are displayed in the bottom left corner of each graph*.

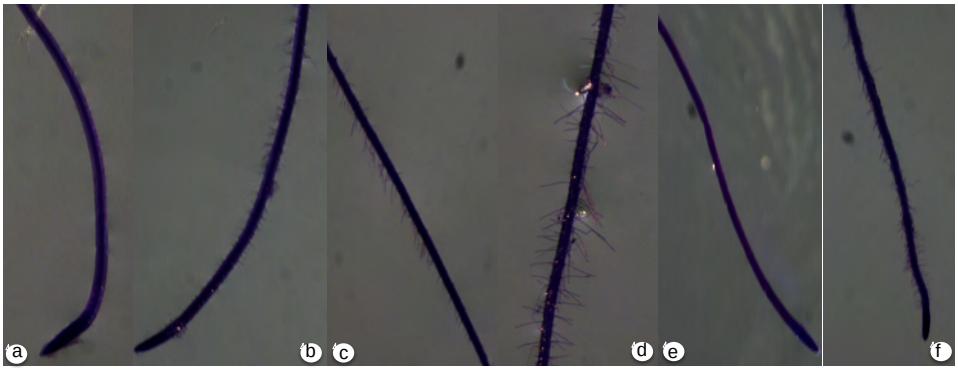

Supplemental Figure 6.6: Root hair formation of Arabidopsis thaliana seedlings in response to bacterial inoculation. For visualizing root hairs, roots were stained for 1 min in 0,075% Crystal-Violet in 70% ethyl alcohol and rinsed thoroughly with distilled water. Root hairs were visualized with a trinocular stereo-microscope (Nikon, SMZ 800) equipped with a CCD camera (DFK 41AF02 FC imaging source). a. Non-inoculated control, b. Norcardioides aromaticivorans, c. Variovorax paradoxus, d. Microbacterium phyllosphaerae, e. Plantibacter flavus, f. Bacillus simplex. Root hair formation of all genotypes was comparable, only representative pictures of wild type Arabidopsis thaliana seedlings are displayed.

Chapter 7

General discussion and perspectives

7.1 Study framework

Since their discovery and the onset of the industrial revolution fossil fuels have powered global economical development. However, the continuous depletion of fossil energy reserves for manufacturing and transport has severe economical, environmental and geopolitical ramifications underlining the need for renewable and sustainable energy sources for our industrial economies and consumer societies. Second-generation biofuels, derived from lignocellulosic biomass, represent a vital component in the impending transition to a more bio-based economy. However, their application and commercial viability is severely limited by the recalcitrance of lignin polymers present in the dedicated energy crops such as poplar. Accordingly, genetic engineering of specific genes in the lignin biosynthesis to tailor lignin content and composition can contribute to generate feedstocks with reduced recalcitrance and increased cost-competitiveness. Gene-silencing of cinnamoyl-CoA reductase (*CCR*, E.C.1.2.1.44), the first enzyme in the monolignol-specific branch of lignin biosynthesis, typically results in reduced lignin content, altered cell wall metabolism and/or improved pulping characteristics, higher saccharification and ethanol yield. Concurrently *CCR* down-regulation leads to flux changes in the phenylpropanoid and monolignol-specific pathways and accumulation of several soluble phenolics and detoxification products in the xylem vessels, ultimately providing the plant microbiome with drastically changed abiotic conditions. Moreover, perturbations in the lignin biosynthesis via *CCR* down-regulation lead to compositional alterations in the cell wall. Cell wall features represent primordial factors determining endophytic colonization potential and could potentially influence colonization by phytopathogens.

Therefore, the main objective of the current work was to explore the general and specific host genotype effects exerted by *CCR* gene silencing in field-grown poplar trees (*Populus tremula x alba*) on the plant bacterial microbiome. Furthermore we also focussed on the microbiome niche differentiation between the different plant environments. To this end, we firstly evaluated the metabolic capacities present in the culturable bacterial populations of *CCR*-down-regulated

and WT poplar trees (Chapter 3). Subsequently, to access the total plant bacterial microbiome, we optimized an approach to reduce organellar rDNA (of plastid and mitochondrial origin) co-amplification, frequently observed during 16S rRNA metabarcoding (Chapter 4). The optimized approach (Chapter 4) was ultimately applied to unravel (a) niche differentiation of the plant microbiome between the different plant environments and (b) host genotype effects as instigated by *CCR* down-regulation (Chapter 5). Single-gene modifications such as the down-regulation of *CCR* in *Populus tremula x alba* represent prime candidates to unravel host genotype effects on the plant micobiome. They are, except for the T-DNA construct, isogenic with the wild type poplar tree providing direct causality between the modification and the observed effect on the plant-associated bacterial communities.

In the last chapter we focussed on the potential of several plant-growth promoting and stress-reducing bacterial strains to increase the plant growth of lignin-reduced genotypes and thereby offset the biomass impairment caused by the perturbation in the lignin biosynthesis (Chapter 6). Most promising bacterial strains (Chapter 3) were inoculated in *Arabidopsis thaliana,* widely considered to be a model plant for understanding lignin biosynthesis, deposition and function.

7.2 Accessing the total bacterial microbiome of plants via 16S rRNA metabarcoding

In order to reliably access the plant microbiome and determine plant compartment and host genotype-effects (Chapter 5), we experimentally tested a series of commonly used primers (7 primer pairs) for the analysis of poplar-associated bacterial communities with 16S rRNA metabarcoding using 454 pyrosequencing (Table 4.1). Next-generation high-throughput sequencing technologies and their corresponding bioinformatics tools have revolutionized the methods for studying microbial ecology by enabling high-resolution community profiling (Gottel et al., 2011; Hartmann et al., 2012; Margulies et al., 2005; Metzker, 2010; Shendure & Ji, 2008; Sogin et al., 2006). However, accessing the plant microbiome using 16S rDNA metabarcoding still represents significant challenges, exclusively due to the mixed presence of eukaryotic cells, prokaryotic cells and eukaryotic plant organelles with a prokaryotic lineage (chloroplasts and mitochondria). The selection of suitable primer pairs is challenging because of the high homology between bacterial 16S rRNA,

chloroplast 16S rRNA and mitochondrial 18S rRNA (Dyall et al. 2004; Raven, 1970). Indeed several reports have struggled with the co-amplification of organellar rDNA as well as considerable primer bias (Bodenhausen et al., 2013; Bulgarelli et al., 2012; Gottel et al., 2011; Lundberg et al., 2012). To fully test the experimental performance of the selected primer pairs, we included samples with differential amounts of organellar 16S rRNA input, ranging from virtually no plastid input (rhizosphere soil), to higher plastid input (root and stem) and very high plastid input (leaves). From our initial assortment of primer pairs (Table 4.1), we selected three suitable primer pairs (799F-1391R, 799F-1193R and 341F-783R) based on (a) low co-amplification of non-target rRNA reads (Table 4.2), (b) high retrieval of bacterial rRNA reads (Table 4.3) and (c) low primer efficiency for pure poplar chloroplast DNA (Figure 4.1). The best performing primer pairs, selected for in depth study, included primer 799F and primer 783R, which possess incorporated mismatches to reduce co-amplification of chloroplast rRNA (Chelius & Triplett, 2001; Sakai et al., 2004). However, although primer 783R (Sakai et al., 2004) displayed 3 mismatches with poplar 16S rDNA during *in silico* analyses (data not shown), in an experimental set-up it failed to efficiently eliminate chloroplast 16S rDNA amplification especially in the stem and leaf samples (Table 4.2). We thereby underlined the fact that (a) *in silico* analyses may portray an incorrect image of the primer potential and experimental evaluation of primers used in metabarcoding studies is crucial and (b) that the position of the mismatches are crucial for their effectiveness in PCR amplification. Reversely, primer pairs 799F-1391R and 799F-1193R completely eliminated the co-amplification of chloroplast sequences in the root, stem and leaf samples (Table 4.2). Our sampling effort, as evaluated by the rarefaction curves and Good's coverage estimates, was very adequate for the endosphere samples (ranging from 84% to 97%) but was insufficient for the rhizosphere samples (ranging from 50.1% to 63.7%) to reliably capture the rhizosphere microbiome (Figure 4.2). Therefore, we adjusted our experimental set-up for the rhizosphere samples in the study of the plant compartment and host genotype effects on the microbiome (Chapter 5) resulting in higher Good's coverage estimates (ranging from 73% to 76%) (Figure 5.1A). Furthermore parametrical alpha diversity comparison of the three selected primer pairs revealed higher OTU richness and Inverse Simpson diversity for primer pair 799F-1391R as

compared to primer pairs 799F-1193R and 341F-783R, most pronounced in the stem and leaf samples (Figure 4.3). Our results also indicated that the choice of primer pair and the resulting bias, inherently linked to every primer pair, shapes the bacterial community observed in metabarcoding analyses (Supplementary Figure 4.3).

Based on these results (Chapter 4), we selected primer pair 799F-1391R to study the plant compartment and host genotype-effect in poplar trees with 16S rRNA metabarcoding (via 454 pyrosequencing). Indeed this approach resulted in very low co-amplification of non-target rRNA reads (Table 5.1) frequently observed in similar studies (Bodenhausen et al., 2013; Bulgarelli et al., 2012; Gottel et al., 2011; Lundberg et al., 2012), thereby reinforcing our results from the optimization study (Chapter 4).

Finally, although we performed an optimization study with a limited amount of samples (3 biological replicates per plant compartment), we did observe considerable niche differentiation of the microbiome between all the sampled plant compartments (rhizosphere, root, stem, leaf). We explored this concept, which we also observed at metabolic level (Chapter 3), in more detail in chapter 5. Up till now this concept has only been reported at the rhizosphere soil-root interface but here we present data convincingly demonstrating continued microbiome differentiation in the aerial plant compartments (Chapter 3 and Chapter 5).

7.3 Plant compartment-effects: microbiome niche differentiation

Within plant microbiota research, plant compartment effects and intra-plant niche differentiation of the bacterial microbiomes have been sporadically evaluated. Niche differentiation at the rhizosphere soil-root interface has been reported in a limited number of studies (Bulgarelli et al., 2012; Gottel et al., 2011; Inceoğlu et al. 2010; Lundberg et al., 2012; Weinert et al., 2011). To determine plant compartment-effects and unravel the specificity of bacterial assemblages for specific plant compartments (rhizosphere soil, root, stem, leaf) in *Populus tremula x alba* (microbiome niche differentiation) we used two different approaches: (1) evaluation of the culturable fraction of the plant microbiome via non-selective and selective isolation/enrichments techniques (i.e. introducing a metabolic selection factor) (Chapter 3) and (2) evaluation of the total plant microbiome via 16S rRNA metabarcoding (454 pyrosequencing)

using our optimized approach as described in chapter 4 (Chapter 5). For both approaches, we observed that bacterial cell counts (CFU/g) after non-selective isolation and OTU richness estimates (16S rDNA metabarcoding) were highly dependent upon plant compartment (regardless of the host genotype). Rhizosphere soil, root and stem compartments clearly differentiated from each other by decreasing cell counts and OTU richness estimates (Figure 3.1A; Figure 5.2A). Indeed, these results are in concordance with the general views of endophytic colonization. Most endophytic bacteria originate from the rhizosphere and progressively colonize the roots, stems and leaves (Compant et al., 2010; Hardoim et al., 2008), with minimal leaf colonization via stomata also sporadically reported. Moreover, rhizosphere/rhizoplane colonization is primarily driven by simple chemo-attraction to root exudates (e.g. organic acids, sugars, amino acids) and other rhizodeposits (e.g. root cap border cells) (Bais et al. 2006; Lugtenberg & Dekkers, 1999; Lugtenberg & Kamilova, 2009; Walker et al. 2003), whereas endophytic competence requires, in many cases, active mechanisms to cross the physical barriers (e.g. endodermis, pericyle), reach the xylem vessels and finally lead to systemic colonization of the plant. Consequently, endophytic colonization is limited to specific bacterial strains (Compant et al., 2010; Hardoim et al., 2008) as depicted by the reduced bacterial cell counts and OTU richness estimates (Figure 3.1A; Figure 5.2A). Even the introduction of a metabolic selection factor, i.e. specific phenylpropanoids (ferulic acid, sinapic acid and p-coumaric acid) as sole carbon sources in the nutrient medium, in the selective isolation/enrichments experiments of the culturable fraction did not distort these plant compartment effects (Figure 3.1B, C, D and Table 3.4A). Furthermore, the loss of diversity and evenness (Figure 5.2B, C) from rhizosphere to endophytic compartments, as evaluated by 16S rRNA metabarcoding, supports this view and indicates that only a limited amount of bacteria can adapt to an endophytic lifestyle (loss of diversity) and these bacterial strains will therefore dominate endophytic assemblages (loss of evenness) (Figure 5.2C). Moreover, in general we observed qualitatively the same results (loss of diversity and evenness) in the culturable fraction after selective enrichment with ferulic acid (Table 3.4B, C) indicating that the loss of total diversity and evenness (Figure 5.2B, C) also impacts the metabolic capacities present in the endosphere microbiomes. Obviously, less

diverse total populations intuitively harbour fewer species capable of efficiently degrading ferulic acid as sole carbon source ultimately also leading to reduced diversity and evenness estimates (Table 3.4B, C) in the endosphere compartments. Furthermore, within the bacterial community structures, we observed strong clustering according to plant compartment whereby each compartment rendered microbiota significantly dissimilar from each other, irrespective of host genotype (Figure 5.3; Supplementary figure 5.1 and Table 5.2). In this way, our data confirm microbiome niche differentiation reports at the rhizosphere-root interface (Bulgarelli et al., 2012; Gottel et al., 2011; Inceoğlu et al. 2010; Lundberg et al., 2012; Weinert et al., 2011) but furthermore suggest additional fine-tuning and niche differentiation of microbiota in the aerial plant organs, with the stem and leaf bacterial assemblages being remarkably dissimilar from the root and rhizosphere. Furthermore, even at the metabolic level after the selective enrichment with ferulic acid, samples strongly clustered according to plant compartment (Figure 3.3).

Finally, because of our extensive sampling, we were able to infer some general aspects considering rhizosphere/rhizoplane and endophytic colonization. For both approaches, we continuously observed more variation in the endosphere compartments as compared to the rhizosphere samples. Firstly, bacterial cell counts from the culturable fraction (Figure 3.1A), rarefaction curves and alpha diversity measures from the 16S rRNA metabarcoding study (Figure 5.1 and 5.2) were highly variable for the endosphere compartments (especially for the stem and leaf samples) whereas the rhizosphere samples displayed highly uniform rarefaction curves, alpha diversity measures and bacterial cell counts. Moreover, the variation in the community structures, as depicted by ANOSIM analysis, of rhizosphere soil bacterial assemblages was very low whereas, in contrast, variation within endophytic communities was much higher (Supplementary Figure 5.3). This difference in variation of the bacterial community structures was not observed for the culturable fraction, most likely because the selection factor (i.e. ferulic acid as sole carbon source) levelled off the natural variation present in the total bacterial microbiomes (Supplementary Figure 3.1). Crucial factors underlining the variability of the rhizosphere microbiome in comparison with endosphere microbiomes are the nature of endophytic colonization

(Compant et al., 2010; Hardoim et al., 2008), intricate interplay with the host plants innate immune system during plant colonization (Jones & Dangl, 2006) and furthermore acute fluctuations in abiotic conditions in the endosphere (temperature, humidity, access to nutrients, etc.) which differ from the buffered fluctuations in the rhizosphere (Bulgarelli et al., 2013; Hirano, 2000). Together these factors result in the stable formation of distinctive rhizosphere bacterial communities whereas the establishment of the endophytic communities appears to be a more variable process.

7.4 Host genotype effects exerted by the lignin-reduced genotype

Possible host genotype-dependent effects (ecotypes, cultivars, genetically modified genotypes) on the bacterial assemblages have been reported in a limited number of studies specifically for *Arabidopsis thaliana* (Bulgarelli et al., 2012; Lundberg et al., 2012) and potato cultivars (Inceoğlu et al., 2010; van Overbeek & van Elsas, 2008; Weinert et al., 2011) as well as for other organisms such as the human gut microbiome (Spor et al., 2011). Other than these, no studies have explored the magnitude of host-genotype variation on bacterial microbiota profiles. To determine host genotype dependent effects exerted by the lignin reduced (*CCR* deficient) genotype on bacterial microbiomes, we evaluated the culturable fraction of the bacterial communities at a metabolic level (Chapter 3) as well as the total bacterial microbiomes via 16S rRNA metabarcoding (Chapter 5). In the first approach, we started with the isolation and cultivation of bacterial cells from the plant compartments using a non-selective medium (carbon source mix) and selective media with using specific phenylpropanoids (ferulic acid, sinapic acid and p-coumaric acid) as sole carbon sources in the nutrient medium. Of these, ferulic and sinapic acid, and derivatives thereof, were previously shown to be upregulated in the *CCR*$^{-}$ poplar, and ferulic acid was even incorporated into the lignin polymer (Leplé et al., 2007; Ralph et al., 2008) (Figure 3.1). Bacterial cell counts (colony forming units (CFU) g^{-1}) were highly comparable between WT and *CCR*$^{-}$ poplars across all plant compartments with the non-selective isolation approach (Figure 3.1A) whereas in the selective isolation we routinely detected higher bacterial cell counts (CFU g^{-1}) in *CCR*$^{-}$ poplar as compared to the WT, except for the rhizosphere compartment (Figure 3.1B, C, D). Furthermore, qualitatively similar results were obtained after selective enrichment with ferulic acid (Figure 3.2A).

Moreover, we determined bacterial community structures after selective enrichment with ferulic acid. In the rhizosphere soil, bacterial communities showed no relevant clustering according to the genotype as visually apparent by the NMDS analysis (Figure 3.4A, Supplementary Figure 3.2) whereas in contrast the bacterial communities in the roots, stems and leaves revealed strong clustering according to the genotype (Figure 3.4B, C, D and Supplementary Figure 3.2. Moreover, respirometric analyses of the individual metabolisms of the bacterial strains supported the results at the population level (Figure 3.5). The main driver of these effects, in the root and stem endosphere, was identified as *Pseudomonas putida,* which displayed high relative abundance in the roots and stems of *CCR* deficient trees (Supplementary Figure 3.4 and 3.5) in correlation with the highest degradation capacity for ferulic acid as measured by respirometric analysis (Biolog MT2) (Figure 3.6). Indeed *Pseudomonas putida* is known for its diverse metabolic capacities and adaptation to various ecological niches including soils and sediments with high concentrations of toxic metals and complex organic contaminants (Marques & Ramos, 1993; Wu et al., 2011). Moreover, several degradation pathways have been identified in *P. putida* strains such as the ferulate catabolic pathway in *Pseudomonas putida* WCS358 (Venturi et al., 1989) and the protocatechuate 4,5-cleavage pathway (Harwood & Parales, 1996). Together these results indicate that *CCR* gene silencing and the resulting changes in xylem composition (most notably ferulic acid) drive the metabolic abilities present in the endosphere towards higher degradation potential for specific phenolics, ultimately yielding endophytic bacteria more adapted to degrade complex phenolic compounds, such as *P. putida*.

To further unravel the host genotype-dependent effects exerted by the lignin-reduced genotype, we compared the total bacterial microbiome of WT and *CCR* deficient poplar trees using 16S rRNA metabarcoding (Chapter 5). In the rarefaction curves and alpha diversity estimates, we mainly found host-genotype differences in the stem compartment whereby richness, diversity and evenness measures were lower in *CCR* down-regulated trees as compared to wild-type poplar trees (Figure 5.2). Furthermore, pairwise comparisons (PCA, hierarchical clustering and ANOSIM) of the bacterial community structure of host-genotypes (wild type and *CCR* deficient poplar) within each plant compartment revealed differential host genotype effects. In concordance with the culturable fraction

(Chapter 3), bacterial assemblages in the rhizosphere displayed no relevant clustering according to genotype (Figure 5.4A and Table 5.3) whereas in roots and stems, we observed significant clustering of bacterial communities according to host genotype (Figure 5.4B,C and Table 5.3). In contrast with the previous approach (Chapter 3), no clustering according to the genotype was observed for the leaf endosphere (Figure 5.4D and Table 5.3). This could indicate that the effect of *CCR* down-regulation could possibly persist in the leaves, but solely affects metabolic capacities of the present leaf endophytes without altering the structural composition of the leaf microbiome. Moreover, the leaf microbiome is renowned for its variability making it more difficult to ascertain specific host genotype effects (Bulgarelli et al., 2013). For both approaches, we observed plant compartment-specific host genotype effects in the rhizosphere and the endosphere compartments (Chapter 3 and Chapter 5). We consistently observed no effects in the rhizosphere environment supporting the findings of Danielsen et al. (2013) who reported that transgenic poplar lines down-regulated for *CCR* displayed a normal capacity to form ectomycorrhiza. Therefore, we can tentatively speculate that gene silencing of *CCR* evokes no changes in the root exudates profile of *CCR* down-regulated poplar trees (See 'perspectives'). In contrast, we constantly observed host genotype-effects in the root and stem endosphere. In both environments, lignin biosynthesis plays an important role: in the roots, lignin biosynthesis begins upon termination of primary root growth where after secondary growth commences and lignified cell walls are formed (Mittler & Lam, 1995) whereas in the stems secondary thickening of the cell walls and lignin biosynthesis/deposition (the final stage of xylem differentiation) is crucial for an erect growth habitat (Boerjan et al., 2003; Vanholme et al., 2012). Therefore, accumulation of phenolics (as caused by *CCR* down-regulation) could explain the differential bacterial community structure in the wild type and *CCR* deficient poplar trees (see perspectives).

In conclusion, we identified host-genotype effects, which are reminiscent of the host-genotype-dependent associations shaping the human microbiome (Spor et al., 2011). The host genotype was found to have a profound effect on the metabolic capacities and bacterial community structure in the endosphere of *CCR* deficient poplar trees (especially the roots and stems), without perceptible effects on the rhizospheric bacterial communities. Finally, it is important to

mention that 16S rRNA metabarcoding is inherently limited to the genus-level or higher taxonomic ranks, thus if subspecies genetic variation of microbiomes contributes to host colonization, the magnitude of the host genotype-dependent effect cannot be fully determined with available community fingerprinting technologies.

7.5 Biomass production from lignin-reduced genotypes

Finally, we focussed on *Arabidopsis thaliana*, the model plant in lignin biosynthesis research and the biomass impairment associated with *CCR* down-regulation. We selected two T-DNA knockout mutants for *CCR*1 (*ccr*1-3 and *ccr*1-6) identified by Mir Derikvand et al. (2008). *CCR1* represents the main *CCR* isoform involved in the constitutive lignification of *Arabidopsis thaliana* and is highly expressed in lignified tissues. We evaluated the potential of several plant-growth promoting and stress-reducing bacterial strains to offset the biomass impairment caused by the perturbation in the lignin biosynthesis (Leplé et al., 2007; Mir Derikvand et al., 2008; Ruel et al., 2009; Van Acker et al., 2013, 2014). For this purpose, we selected a collection of bacterial strains, isolated from the selective isolation/enrichment experiments displaying high ferulic acid degradation capacity (Chapter 3). Detailed phenotypic *in vitro* screening consisting of (a) evaluating the metabolic range of the bacteria to degrade aromatic lignin-related compounds, accumulated in *CCR* deficient genotypes and (b) evaluating the plant growth promotion capacities led to the selection of 15 promising bacterial strains (Table 6.1 and Supplementary Table 6.1). Subsequently, *in vivo* plant growth promotion of lignin-reduced *Arabidopsis thaliana* genotypes was observed for *Norcardioides aromaticivorans, Variovorax paradoxus, Microbacterium phyllosphaerae, Plantibacter flavus* and *Bacillus simplex* as evaluated by primary root growth and leaf surface area (Figure 6.2 and 6.3 and Supplementary figure 6.2). Moreover *Norcardioides aromaticivorans* and *Microbacterium phyllosphaerae* also promoted lateral root development of both lignin-reduced genotypes, as measured by the formation of the lateral roots (total number) and the total length of the lateral roots (Figure 6.5).

In conclusion, we underlined the potential of plant-growth promoting stress-reducing bacteria to improve plant growth and thereby offset the biomass impairment caused by the perturbation in the lignin biosynthesis.

7.6 Conclusion and perspectives

In conclusion, we provided evidence for the differentiation of the plant microbiome between different plant environments (chapter 3 and chapter 5), identified significant host genotype-effects instigated by the *CCR* down-regulation (chapter 3 and chapter 5), optimized an approach to evaluate the plant-associated microbiome using 454 pyrosequencing (Chapter 4) and finally proved the concept that inoculation with plant-growth promoting bacteria can improve the growth of lignin-reduced biomass-impaired genotypes (Chapter 6).

We optimized an efficient approach to access the plant bacterial microbiome without the co-amplification of organellar rDNA in 16S rRNA metabarcoding applications via 454 pyrosequencing (Chapter 4). Recently, the use of other 16S rRNA metabarcoding applications such as the HiSeq2000, MiSeq Illumina and Ion Torrent platforms have come to the foreground (Caporaso et al., 2012; Claesson et al., 2010; Kennedy et al., 2014; Logares et al., 2013; Metzker, 2010). However, in plant-microbiota research, the application of these platforms has been limited to the rhizosphere microbiome (Jiang et al., 2013; Sun et al., 2014). Evaluating the potential of our optimized approach, with platform-specific modifications (e.g. amplicon length), in combination with HiSeq2000, MiSeq Illumina and/or Ion Torrent could further contribute to the high-resolution 16S rRNA-based community profiling of plant-associated bacterial communities.

With the use of our optimized 16S rRNA metabarcoding approach (chapter 4) and moreover the selective isolation/enrichment of the culturable fraction (chapter 3), we built convincing evidence for the continuing differentiation of the plant microbiome (at metabolic and compositional level), not only at the rhizosphere-root interface as previously reported (Bulgarelli et al., 2012; Bulgarelli et al., 2013; Gottel et al., 2011; Lundberg et al., 2012; Weinert et al., 2011) but also in the aerial plant environments (stem and leaf endosphere) (Chapter 3 and Chapter 5). Furthermore, we identified significant host genotype-effects instigated by the *CCR*-down-regulation, which are reminiscent of the host genotype-dependent associations shaping the human microbiome (Chapter 3 and Chapter 5). Although Leplé et al. (2007) reported flux changes in the general phenylpropanoid and monolignol-specific pathways of the lignin biosynthesis of greenhouse-grown poplars, in depth metabolite profiling of all the plant environments of field-grown *CCR*-down-regulated poplar trees in

comparison with the WT poplars as well as root exudate profiling could substantially contribute to further unravel the main factors responsible for the microbiome differentiation between the studied genotypes. Moreover, to expand our knowledge concerning host genotype fine-tuning of the plant microbiome and determine crucial factors in the modulation of the communities, the study of other modified genotypes could provide interesting insights. Indeed, in the search of feedstocks with reduced recalcitrance, genotypes with lowered lignin levels and/or altered lignin composition are continuously being produced which represent ideal candidates to study.

In the final chapter (chapter 6), we focussed on *Arabidopsis thaliana* and the biomass-impairment associated with *CCR*-down-regulation (Mir Derikvand et al., 2008; Ruel et al., 2009; Van Acker et al., 2013). We proved the concept that selected bacterial strains with designated characteristics have the potential to offset, at least partially, the stunted growth of lignin-reduced genotypes. However, extrapolation of this concept to interesting bio-energy crops (e.g. poplar) requires further insights. First of all, confirmation of the results on a less artificial substrate such as sand as well as in depth study of the bacterial effects on the phenolic detoxification products (metabolite profiling) could provide more insight into the mechanisms of action of the PGP bacteria. Furthermore full genome sequencing of selected bacterial strains and the annotation of interesting genes (e.g. genes responsible for the degradation of the phenolic degradation products: FER genes, LIG genes (Masai et al., 2007) and/or genes responsible for plant-growth promotion mechanisms (Chen et al., 2007)) could be an interesting route. Interesting genes for the degradation of the phenolic detoxification products could even be transformed into *Arabidopsis thaliana* and/or poplar to reduce elevated stress levels associated with the build-up of the soluble phenolics (Leplé et al., 2007). A similar approach has very recently been employed by Tsuji et al. (2015), who used LigD (encoding an Cα -dehydrogenase enzyme), isolated from *Sphingobium* sp. strain SYK-6, to biosynthetically engineer chemically labile lignin substructures in *Arabidopsis thaliana* to improve biomass processability. Finally, extrapolation of the concept of using PGP bacteria to interesting bio-energy crops in field situations requires insights into the long-term stability and competitiveness of the inoculated strains within the natural endophytic communities as well as their potential to promote

biomass production in these situations. Moreover our data show that the effects of *CCR* down-regulation go beyond those that could have been expected from perturbation of the lignin biosynthesis as it has been described in text books: compounds that accumulate because of the perturbation in *CCR* are apparently further metabolized by the endophytic community. These new metabolites may interfere with the intended phenotype caused by the perturbation. Clearly, this type of interactions needs to be taken into account to understand the full consequences of plant metabolic pathway engineering and its relation with the final wood properties.

References

Bais, H. P., Weir, T. L., Perry, L. G., Gilroy, S. and Vivanco, J. M. (2006a). The role of root exudates in rhizosphere interactions with plants and other organisms. *Annual Review of Plant Biology*, *57*, 233–266.

Bodenhausen, N., Horton, M. W. and Bergelson, J. (2013). Bacterial communities associated with the leaves and the roots of Arabidopsis thaliana. *PloS One*, *8*, e56329.

Boerjan, W., Ralph, J., & Baucher, M. (2003). Lignin biosynthesis. *Annual Review of Plant Biology*, *54*, 519–546.Bulgarelli, D., Rott, M., Schlaeppi, K., Ver Loren van Themaat, E., Ahmadinejad, N., Assenza, F., … Schulze-Lefert, P. (2012). Revealing structure and assembly cues for Arabidopsis root-inhabiting bacterial microbiota. *Nature*, *488*(7409), 91–5. doi:10.1038/nature11336

Bulgarelli, D., Rott, M., Schlaeppi, K., Ver Loren van Themaat, E., Ahmadinejad, N., Assenza, F., Rauf, P., Huettel, B., Reinhardt, R., Schmelzer, E., Perlies, J., Gloeckner, F. O., Amann, R., Eickhorst, T. and Schulze-Lefert, P. (2012). Revealing structure and assembly cues for Arabidopsis root-inhabiting bacterial microbiota. *Nature*, *488*, 91–95.

Bulgarelli, D., Schlaeppi, K., Spaepen, S., Ver Loren van Themaat, E. and Schulze-Lefert, P. (2013). Structure and functions of the bacterial microbiota of plants. *Annual Review of Plant Biology*, *64*, 807–838.

Caporaso, J. G., Lauber, C. L., Walters, W. A., Berg-Lyons, D., Huntley, J., Fierer, N., Owens, S., Betley, J., Fraser, L., Bauer, M., Gormley, N., Gilbert, J. A., Smith, G. and Knight, R. (2012). Ultra-high-throughput microbial community analysis on the Illumina HiSeq and MiSeq platforms. *The ISME Journal*, *6*, 1621–1624.

Chelius, M. K. and Triplett, E. W. (2001). The Diversity of Archaea and Bacteria in Association with the Roots of Zea mays L. *Microbial Ecology*, *41*, 252–263. d

Chen, X. H., Koumoutsi, A., Scholz, R., Eisenreich, A., Schneider, K., Heinemeyer, I., Morgenstern, B., Voss, B., Wolfgang, H. R., Reva, O., Junge, H., Voigt, B., Jungblut, P. R., Vater, J., Sussmuth, R., Liesegang, H., Strittmatter, A., Gottschalk, G. and Borriss, R. (2007). Comparative analysis of the complete genome sequence of the plant

growth-promoting bacterium Bacillus amyloliquefaciens FZB42. *Nature Biotechnology*, *25*, 1007–1014.

Claesson, M. J., Wang, Q., O'Sullivan, O., Greene-Diniz, R., Cole, J. R., Ross, R. P. and O'Toole, P. W. (2010). Comparison of two next-generation sequencing technologies for resolving highly complex microbiota composition using tandem variable 16S rRNA gene regions. *Nucleic Acids Research*, *38*, e200.

Compant, S., Clément, C. and Sessitsch, A. (2010). Plant growth-promoting bacteria in the rhizo- and endosphere of plants: Their role, colonization, mechanisms involved and prospects for utilization. *Soil Biology and Biochemistry*, *42*, 669–678.

Danielsen, L., Lohaus, G., Sirrenberg, A., Karlovsky, P., Bastien, C., Pilate, G. and Polle, A. (2013). Ectomycorrhizal colonization and diversity in relation to tree biomass and nutrition in a plantation of transgenic poplars with modified lignin biosynthesis. *PloS One*, *8*, e59207.

Dyall, S. D., Brown, M. T. and Johnson, P. J. (2004). Ancient invasions: from endosymbionts to organelles. *Science*, *304*, 253–257.

Gottel, N. R., Castro, H. F., Kerley, M., Yang, Z., Pelletier, D. A., Podar, M., Karpinets, T., Tuskan, G. A., Vilgalys, R., Mitchel, J., Schadt, C. W., Uberbacher, E. and Doktycz, M. J. (2011). Distinct Microbial Communities within the Endosphere and Rhizosphere of Populus deltoides Roots across Contrasting Soil Types. *Applied and Environmental Microbiology*, 77, 5934-5944.

Hardoim, P. R., van Overbeek, L. S. and Van Elsas, J. D. (2008). Properties of bacterial endophytes and their proposed role in plant growth. *Trends in Microbiology*, *16*, 463–471.

Hartmann, M., Howes, C. G., VanInsberghe, D., Yu, H., Bachar, D., Christen, R., Nilsson, R. H., Hallam, S. J. and Mohn, W. W. (2012). Significant and persistent impact of timber harvesting on soil microbial communities in Northern coniferous forests. *The ISME Journal*, *6*, 2199–2218.

Harwood, C. S. and Parales, R. E. (1996). The β-ketoadipate pathway and the biology of self-identity. *Annual Review of Microbiology*, *50*, 553–590.

Hirano, S. S. (2000). Bacteria in the Leaf Ecosystem with Emphasis on Pseudomonas syringae — a Pathogen , Ice Nucleus , and Epiphyte, *64*, 624–653.

Inceoğlu, O., Salles, J. F., van Overbeek, L. and Van Elsas, J. D. (2010). Effects of plant genotype and growth stage on the betaproteobacterial communities associated with different potato cultivars in two fields. *Applied and Environmental Microbiology*, *76*, 3675–3684.

Jiang, X.-T., Peng, X., Deng, G.-H., Sheng, H.-F., Wang, Y., Zhou, H.-W. and Tam, N. F.-Y. (2013). Illumina sequencing of 16S rRNA tag revealed spatial variations of bacterial communities in a mangrove wetland. *Microbial Ecology*, *66*, 96–104.

Jones, J. D. G. and Dangl, J. L. (2006). The plant immune system. *Nature*, *444*, 323–329.

Kennedy, K., Hall, M. W., Lynch, M. D. J., Moreno-Hagelsieb, G. and Neufeld, J. D. (2014). Evaluating bias of illumina-based bacterial 16S rRNA gene profiles. *Applied and Environmental Microbiology*, *80*, 5717–5722.

Leplé, J.-C., Dauwe, R., Morreel, K., Storme, V., Lapierre, C., Pollet, B., Naumann A., Kang, K., Kim, H., Ruel, K., Lefèbvre, A., Joseleau, J., Grima-Pettenati, J., De Rycke, R., Andersson-Gunneråas, S., Erban, A., Fehrle A., Petit-Conil, M., Kopka, J., Polle, A., Messens, E., Sundberg, B., Mansfield, S., Ralph, J., Pilate, G. and Boerjan, W. (2007). Down-regulation of cinnamoyl-coenzyme A reductase in poplar: multiple-level phenotyping reveals effects on cell wall polymer metabolism and structure. *The Plant Cell*, *19*, 3669–3691.

Logares, R., Sunagawa, S., Salazar, G., Cornejo-Castillo, F. M., Ferrera, I., Sarmento, H., Hingamp, P., Ogata, H., de Vargas, C., Lima-Mendez G., Raes, J., Poulain, J., Jaillon, O., Wincker, P., Kandels-Lewis, L., Karsenti, E., Bork, P. and Acinas, S. G. (2013). Metagenomic 16S rDNA Illumina tags are a powerful alternative to amplicon sequencing to explore diversity and structure of microbial communities. *Environmental Microbiology*, *16*, 2659-2671.

Lugtenberg, B. and Dekkers, L. C. (1999). What makes Pseudomonas bacteria rhizosphere competent . *Environmental Microbiology*, *1*, 9–13.

Lugtenberg, B. and Kamilova, F. (2009). Plant-growth-promoting rhizobacteria. *Annual Review of Microbiology*, *63*, 541–556.

Lundberg, D. S., Lebeis, S. L., Paredes, S. H., Yourstone, S., Gehring, J., Malfatti, S., Tremblay, J., Engelbrektson, A., Kunin, V., del Rio, T. G., Edgar, R. C., Eickhorst, T., Ley, R. E., Hugenholtz, P., Tringe, S. G. and Dangl, J. L. (2012). Defining the core Arabidopsis thaliana root microbiome. *Nature*, *488*, 86–90.

Margulies, M., Egholm, M., Altman, W. E., Attiya, S., Bader, J. S., Bemben, L. A., ... Rothberg, J. M. (2005). Genome sequencing in microfabricated high-density picolitre reactors. *Nature*, *437*, 376–80.

Marques, S. and Ramos, J. L. (1993). Transcriptional control of the Pseudomonas putida TOL plasmid catabolic pathways. *Molecular Microbiology*, *9*, 923–929.

Masai, E., Katayama, Y. and Fukuda, M. (2007). Genetic and Biochemical Investigations on Bacterial Catabolic Pathways for Lignin-Derived Aromatic Compounds. *Bioscience, Biotechnology, and Biochemistry*, *71*, 1–15.

Metzker, M. L. (2010). Sequencing technologies - the next generation. *Nature Reviews. Genetics*, *11*, 31–46.

Mir Derikvand, M., Sierra, J. B., Ruel, K., Pollet, B., Do, C.-T., Thévenin, J., Buffard, D., Jouanin, L. and Lapierre, C. (2008). Redirection of the phenylpropanoid pathway to feruloyl malate in Arabidopsis mutants deficient for cinnamoyl-CoA reductase 1. *Planta*, *227*, 943–956.

Mittler, R. and Lam, E. (1995). In Situ Detection of nDNA Fragmentation during the Differentiation of Tracheary Elements in Higher Plants. *Plant Physiology*, *108*, 489–493.

Ralph, J., Kim, H., Lu, F., Grabber, J. H., Leplé, J.-C., Berrio-Sierra, J., Derikvand, M. M., Jouanin, L., Boerjan, W. and Lapierre, C. (2008). Identification of the structure and origin of a thioacidolysis marker compound for ferulic acid incorporation into angiosperm lignins (and an indicator for cinnamoyl CoA reductase deficiency). *The Plant Journal : For Cell and Molecular Biology*, *53*, 368–79.

Raven, P. H. (1970). A Multiple Origin for Plastids and Mitochondria: Many independent symbiotic events may have been involved in the origin of these cellular organelles. *Science*, *169*, 641–646.

Ruel, K., Berrio-sierra, J., Derikvand, M. M., Pollet, B., Thévenin, J., Lapierre, C., Jouanin, L. and Joseleau, J. (2009). Impact of *CCR*1

silencing on the assembly of lignified secondary walls in Arabidopsis thaliana. *The New Phytologist, 184*, 99–113.

Sakai, M., Matsuka, A., Komura, T. and Kanazawa, S. (2004). Application of a new PCR primer for terminal restriction fragment length polymorphism analysis of the bacterial communities in plant roots. *Journal of Microbiological Methods*, *59*, 81–9.

Shendure, J. and Ji, H. (2008). Next-generation DNA sequencing. *Nature Biotechnology*, *26*, 1135–1145.

Sogin, M. L., Morrison, H. G., Huber, J. A, Mark Welch, D., Huse, S. M., Neal, P. R., Arrieta, J. M. and Herndl, G. J. (2006). Microbial diversity in the deep sea and the underexplored “rare biosphere”. *Proceedings of the National Academy of Sciences of the United States of America*, *103*, 12115–12120.

Spor, A., Koren, O. and Ley, R. (2011). Unravelling the effects of the environment and host genotype on the gut microbiome. *Nature Reviews. Microbiology*, *9*, 279–290.

Sun, J., Zhang, Q., Zhou, J. and Wei, Q. (2014). Illumina amplicon sequencing of 16S rRNA tag reveals bacterial community development in the rhizosphere of apple nurseries at a replant disease site and a new planting site. *PloS One*, *9*, e111744.

Tsuji, Y., Vanholme, R., Tobimatsu, Y., Ishikawa, Y., Foster, C. E., Kamimura, N., Hishiyama, S., Hashimoto, S., Shino, A., Hara, H., Sato-Izawa, K., Oyarce, P., Goeminne, G., Morreel, K., Kikuchi, J., Fukuda, M., Katayama, Y., Boerjan, W., Ralph, J., Masai, E. and Kajita, S. (2015). Introduction of chemically labile substructures into Arabidopsis lignin through the use of LigD, the Cα-dehydrogenase from Sphingobium sp. strain SYK-6. *Plant Biotechnology Journal*, *6*, 1–12.

Van Acker, R., Leplé, J.-C., Aerts, D., Storme, V., Goeminne, G., Ivens, B., Légée, F., Lapierre, C., Piens, K., Van Montagu, M., C., E., Santoro, N., Foster, C., E., Ralph, J., Soetaert, W., Pilate, G. and Boerjan, W. (2014). Improved saccharification and ethanol yield from field-grown transgenic poplar deficient in cinnamoyl-CoA reductase. *Proceedings of the National Academy of Sciences of the United States of America*, *111*, 845–50.

Van Acker, R., Vanholme, R., Storme, V., Mortimer, J. C., Dupree, P. and Boerjan, W. (2013). Lignin biosynthesis perturbations affect secondary

cell wall composition and saccharification yield in Arabidopsis thaliana. *Biotechnology for Biofuels*, *6*, 1-17.

Van Overbeek, L. and van Elsas, J. D. (2008). Effects of plant genotype and growth stage on the structure of bacterial communities associated with potato (Solanum tuberosum L.). *FEMS Microbiology Ecology*, *64*, 283–96.

Venturi, V., Zennaro, F., Degrassi, G., Okeke, B. C., & Bruschi, C. V. (1989). Genetics of ferulic acid bioconversion to protocatechuic acid in plant-growth-promoting. *Microbiology*, *144*, 965–973.

Vanholme, R., Morreel, K., Darrah, C., Oyarce, P., Grabber, J. H., Ralph, J. and Boerjan, W. (2012). Metabolic engineering of novel lignin in biomass crops. *The New Phytologist*, *196*, 978–1000.

Walker, T. S., Bais, H. P., Grotewold, E. and Vivanco, J. M. (2003). Update on Root Exudation and Rhizosphere Biology Root Exudation and Rhizosphere Biology. *Plant Physiology*, *132*, 44–51.

Weinert, N., Piceno, Y., Ding, G.-C., Meincke, R., Heuer, H., Berg, G., Schloter, M., Andersen, G. and Smalla, K. (2011). PhyloChip hybridization uncovered an enormous bacterial diversity in the rhizosphere of different potato cultivars: many common and few cultivar-dependent taxa. *FEMS Microbiology Ecology*, *75*, 497–506.

Wu, X., Monchy, S., Taghavi, S., Zhu, W., Ramos, J. and van der Lelie, D. (2011). Comparative genomics and functional analysis of niche-specific adaptation in Pseudomonas putida. *FEMS Microbiology Reviews*, *35*, 299–323.

Scientific output

International Journals

Weyens, N., Beckers, B., Schellingen, K., Ceulemans, R., Croes, S., Janssen J., Haenen, S. and Vangronsveld, J. (2013). Plant-associated bacteria and their role in the success or failure of metal phytoextraction projects: first observations of a field-related experiment. *Microbial Biotechnology*, 6, 288-299.

Weyens, N., Schellingen, K., Beckers, B., Janssen, J., Reinhart, C., van der Lelie, D., Taghavi, S., Carleer, R. and Vangronsveld, J. (2013). Potential of willow and its genetically engineered associated bacteria to remediate mixed Cd and toluene contamination. *Journal of soils and Sediments*, 13, 176-188.

Weyens, N., Gielen, M., Beckers, B., Boulet, J., van der Lelie, D., Taghavi, S., Carleer, R. and Vangronsveld, J. (2014). Bacteria associated with yellow lupine grown on a metal-contaminated soil: *in vitro* screening and *in vivo* evaluation for their potential to enhance Cd phytoextraction. *Plant Biology*, 16, 988-996.

Weyens, N., Beckers, B., Schellingen, K., Ceulemans, R., van der Lelie, D., Newman, L., Taghavi, S., Carleer, R. and Vangronsveld, J. (2015). The potential of the Ni-resistant TCE-degrading *Pseudomonas putida* W619-TCE to reduce phytotoxicity and improve phytoremediation efficiency of poplar cuttings on a Ni-TCE co-contamination. *International Journal of Phytoremediation*, 17, 40-48.

Janssen, J., Weyens, N., Croes, S., Beckers, B., Meiresonne, L., Van Peteghem, P., Carleer, R. and Vangronsveld, J. (2015). Phytoextraction of metal contaminated soils using willow: a role for plant-associated bacteria to improve biomass production and metal uptake? *International Journal of Phytoremediation*, accepted.

Beckers, B., Op De Beeck, M., Weyens, N., Boerjan, W. and Vangronsveld, J. (201x). Gene silencing of cinnamoyl-coA reductase (*CCR*) in field-grown poplar trees influences the bacterial microbiome present in the endosphere. Submitted.

Beckers, B., Op De Beeck, M., Thijs, S., Truyens, S., Weyens, N., Boerjan, W. and Vangronsveld, J. (201x). Performance of 16S rRNA primer pairs in the study of rhizosphere and endosphere bacterial microbiomes in metabarcoding studies. In preparation.

Beckers, B., Op De Beeck, M., Weyens, N., Boerjan, W. and Vangronsveld, J. (201x). Gene silencing of cinnamoyl-coA reductase (*CCR*) in field-grown poplar trees: Plant microbiome niche differentiation and host genotype effects on the total bacterial microbiome. In preparation.

Beckers, B., Gielen, M., Weyens, N., Boerjan, W. and Vangronsveld, J. (201x). Plant growth promotion of lignin-reduced biomass-impaired Arabidopsis thaliana genotypes. In preparation.

Abstracts

Weyens, N., Truyens, S., Saenen, E., Croes, S., Beckers, B., van der Lelie, D. and Vangronsveld, J. (2010) Modified endophytes for improving phytoremediation of mixed contaminations of toxic metals (Ni) and organic contaminants (toluene or TCE). Phytotechnologies in the 21st century: challenges after Copenhagen 2009. Remediation-Energy-Health-Sustainability, 26-29 september Parma, Italy. Abstract of oral presentation.

Weyens, N., Truyens, S., Saenen, E., Croes, S., Beckers, B., van der Lelie, D., Taghavi, S. and Vangronsveld, J. (2011). Modified endophytes for improving phytoremediation of mixed contaminations of toxic metals (Ni) and organic contaminants (toluene or TCE). 5th European Bioremediation Conference July, 4-7, 2011, Chania, Crete, Greece. Abstract of oral presentation.

Weyens, N., Beckers, B., van der Lelie, D., Taghavi, S. and Vangronsveld, J. (2011). Bioaugmentation with Engineered Endophytic Bacteria improves Phytoremediation. Microbial Diversity 2011, Environmental Stress and Adaptation, 26-28 October Milan, Italy. Abstract of poster presentation.

Beckers, B., Weyens, N., Gielen, M., Boerjan, W. and Vangronsveld, J. (2011) The influence of reduced lignin levels on the cultivable bacterial population associated with *Arabidopsis thaliana* and field-grown *Populus tremula x alba.* Microbial Diversity 2011, Environmental Stress and Adaptation, 26-28 october Milan, Italy. Abstract of poster presentation.

Gielen, M., Weyens, N., Beckers, B., Croes, S., Truyens, S., Boerjan, W. and Vangronsveld, J. (2012) Comparison of *Arabidopsis thaliana* with normal and reduced lignin: differences in growth, bacterial population and cadmium responses. 9th International Phytotechnologies Conference September 11-14 2012, Hasselt University, Diepenbeek, Belgium. Abstract of poster presentation.

Beckers, B., Weyens, N., Gielen, M., Boerjan, W. and Vangronsveld, J. (2012) The influence of CCR-downregulation (reducing lignin levels) on the bacterial communities associated with field grown Populus tremula x alba. 9th International Phytotechnologies Conference September 11-14 2012, Hasselt University, Diepenbeek, Belgium. Abstract of poster presentation.

Eevers, N., Beckers, B., Gielen, M., Weyens, N., White, J. and Vangronsveld, J. (2014). Isolation, cultivation, and characterization of endophytes in function of phytoremediation of DDE-contaminated soils. 11th International Phytotechnologies conference, Heraklion (Crete), Greece, Sept 30 – Oct 3 2014. Abstract of oral presentation.